UNIVERSITÄTSKLINIKUM HAMBURG-EPPENDORF

Zentrum für Molekulare Neurobiologie Hamburg
Institut für Molekulare und Zelluläre Kognition

Prof. Dr. Dietmar Kuhl

Developmental and adult expression of Arc/Arg3.1 in corticolimbic structures determines memory and emotional control

Dissertation

zur Erlangung des Doktorgrades Dr. rer. biol. hum.
an der Medizinischen Fakultät der Universität Hamburg.

vorgelegt von:

Dr. med. Mario Sergio Castro Gómez
aus Aranzazu – Caldas – Kolumbien

Hamburg, 2016

(wird von der Medizinischen Fakultät ausgefüllt)

Angenommen von der
Medizinischen Fakultät der Universität Hamburg am: 02.11.2016. . . . . .

Veröffentlicht mit Genehmigung der
Medizinischen Fakultät der Universität Hamburg.

Prüfungsausschuss, der/die Vorsitzende: Prof. Dr. Dietmar Kuhl. . . . . .

Prüfungsausschuss, zweite/r Gutachter/in: Prof. Dr. Stefan Kindler . . . . . .

Table of Contets

Figures

Tables

Abbreviations

ACC Anterior cingulate cortex
AAP Assembly activating protein
adBNST Anterodorsal bed nucleus of the stria terminalis
ADHD Attention deficit hyperactivity disorders
AMPARs α-amino-3-hydroxy-5-methyl-4-isoxazolepropionic acid receptors
Amy Amygdala
ANOVA Analysis of variance
Arc/Arg3.1 Activity regulated cytoskeletal protein / activity-regulated gen of 3.1 kb
AS Angelman syndrome
ASD Autism spectrum disorders
ATP Adenosine triphosphate
b.w. Body weight
BA Basal amygdala
BCA Bicinchoninic acid assay
BDNF Brain-derived neurotrophic factor
BLA Basolateral amygda
BOLD Blood oxygen level dependent signal
BSA Bovine serum albumin
CaMKIIα Calcium calmoduling kinase II alpha
CBP Creb-binging protein
CeA Central nucleus of the amygdala
CeL Lateral central amygdala
CeM Medial central amygdala
CG Citocyn guanine
Cl Claustrum
CNS Central nervous system
CPu Dorsal striatum (caudate nucleus and putamen)
CREB cAMP response element-binding protein
CS Conditioned stimulus
CSD Current source density
CSF Cerebral spinal fluid
Ct Threshold cycle value
CTA Conditioned taste aversion
CTAB Cetyltrimethyl ammonium bromide
CTP Cytidine triphosphate
DAB 3,3'-diaminobenzidine
DAPI 4′,6-diamidin-2-phenylindol
dCA3 Dorsal cornus ammonis 3
DEPC Diethylpyrocarbonate
DG Dentate gyrus
dHpc Dorsal hippocampus
DIV Days *in vitro*

dLS Dorsal lateral septum
DMEM Dulbecco's modified eagle medium
DNA Deoxyribonucleic acid
dNTPs Deoxynucleotides
DTE Dendritic targeting element
DTT Dithiothreitol
EDTA Ethylenediaminetetraacetic acid
EF Endotoxin free
E/I Excitatory/inhibitory
EJC Exon-junction complex
EOM Elevated O-maze
EPM Elevated plus-maze
ERK extracellular signal–regulated kinases
ES Embryonic stem
FBS Fetal bovine serum
FC Fear conditionong
FMRP Fragile x syndrome protein
GAPDH Glyceraldehyde 3-phosphate dehydrogenase
GluA1 Glutamate receptor subunit A1
GRIA1 Glutamate receptor 1 gene
GTP Guanosine triphosphate
HEK Human embryogenic kidney cell
HEPES 4-(2-hydroxyethyl)-1-piperazineethanesulfonic acid
hnRNP Heterogeneous nuclear ribonucleoprotein
HPA Hypothalamic-pituitary-adrenal axis
Hpc Hippocampus
Hyp Hypothalamus
Iba-1 Ionized calcium binding adaptor molecule 1
IC Inferior colliculus
IEGs Inmediate early-genes
IL Infralimbic cortex
ITR Inverted terminal repeats
KO Knockout
KO-GFP KI Knockout - green fluorescent protein knock-in
LA Lateral amygdala
LB Lysogeny broth
LFP Local field potential
LS Lateral septum
LSD Least significant difference
LTD Long-term depression
LTP Long-term potentiation
M1 Primary motor cortex
MAPK Mitogen-activated protein kinase
MB Mammillary bodies
MEF2 Myocyte enhancer factor-2

mEPSC Miniature excitatory postsynaptic currents
mGluR Metabotropic glutamate receptors
mPFC Medial prefrontal cortex
MRI Magnetic resonance imaging
MS Medial septum
MWM Morris water maze
N2A Neuro-2a cells
NMD Nonsense-mediated decay
NMDAR N-methyl-D-aspartate receptor
NR Nucleus reuniens
NR2A NMDA receptor 2A subunit
ODNs Antisense oligonucleotides
ORF Open reading frame
PAGE Polyacrylamide gel electrophoresis
PB Parabraquial nucleus
PBS Phosphate buffered saline
PCR Polymerase chain reaction
PEI Polyethylenimine
PFA Paraformaldehyde
PFC Prefrontal cortex
PKA Protein kinase A
PML Promyelocytic leukemia tumor suppressor protein
PML-NBs PML-nuclear bodies
PNN Perineural nets
prAAV Recombinant adeno-associated viral vectors plasmid
PrCm Medial precentral cortex
PrL Prelimbic cortex
PSD-95 Postsynaptic density protein 95
PSTD Posttraumatic stress disorder
PVDF Polyvinylidene fluoride
rAAV Recombinant adeno-associated viral vector
REM Rapid eye movements
Rep Replication proteins
RM Repeated measurement
ROIs Regions of interest
rsfMRI Resting state funtional magnetig resonace imaging
RT Room temperature
SEM Standar error of the mean
S1 Somatosensory cortex
SARE Synaptic activity-responsive element
SDS Sodium dodecyl sulfate
SHN Septal hippocampal nucleus
shRNA Short harpine RNA
SOC Super optimal broth
SRE Serum response element

SRF Serum response factor
SSC Saline sodium citrate buffer
STET Sucrose-triton-EDTA-tris
SWS Slow wave sleep
TAE Tris acetate
TARPγ2 Transmembrane ampar regulatory protein γ2
tPA Tissue-type plasminogen activator
Ube3A Ubiquitin-protein ligase E3A
UPF1 Regulator of nonsense transcripts 1
US Unconditioned stimulus
UTR Untranslated region
UV Ultraviolet
V1 Primary visula cortex
vBNST Ventral bed nucleus of the stria terminalis
vCA3 Ventral cornus ammonis 3
vHpc Venral hippocampus
VOI Volumen of interes
vPAG Ventral periaqueductal gray matter
vmPFC Ventromedial prefrontal cortex
VTA Ventral tegmental area
WT Wild-type
YT Yeast extract / tryptone

Abstract

The corticolimbic circuitry plays a central role in memory and emotions, two strongly interlinked functions of the brain. While plasticity in this circuitry is considered essential for memory consolidation, its role in emotion regulation remains unclear. Moreover, synaptic plasticity during early postnatal development shapes the connectivity within this circuit, yet its impact on either of these functions remains elusive. In this thesis, I sought to address these questions by disrupting plasticity in the corticolimbic circuitry, mediated by the activity-regulated cytoskeleton-associated protein / activity-regulated gene of 3.1 kb (Arc/Arg3.1), in a time and location dependent manner.

Arc/Arg3.1 is rapidly induced by acquisition of experience and synaptic plasticity-producing stimuli and is in turn essential for consolidation of long-term memories and synaptic plasticity. Strong upregulation of Arc/Arg3.1 in the corticolimbic circuitry of adult mice subjected to fearful experience and its presence during early postnatal development make it a strong candidate for disrupting plasticity mechanisms in the developing, as well as in the adult brain. In this study, I employed an Arc/Arg3.1 floxed mouse line (Arc/Arg3.1$^{f/f}$), engineered in our lab, together with Cre-mediated recombination to achieve spatio-temporal removal of Arc/Arg3.1. By *in situ* radioactive hybridization and immunohistochemistry, I analyzed Arc/Arg3.1 expression in wild-type and mutant animals, and assessed memory and emotional behaviors with specialized behavioral tests. *In vivo* field recordings and magnetic resonance imaging (MRI) were used to study functional and structural modifications of corticolimbic networks.

In the first part of this thesis, I quantified the expression profile of Arc/Arg3.1 mRNA in the brain across the first postnatal month and evaluated the impact of removing the gene within this developmental period. Arc/Arg3.1 mRNA expression begins early during postnatal development in the cornus ammonis 3 (CA3) region of the hippocampus and in the olfactory bulb, increases sharply after the second week in the rest of corticolimbic and sensory structures and diminishes slowly in cortical regions to low levels in the nonstimulated adult brain. Thus, Arc/Arg3.1 bears the potential to impact postnatal brain development and thereby its loss might cause a later disturbance of long-term memory consolidation and emotion regulation. To address this possibility, Arc/Arg3.1$^{f/f}$ mice were bred with CaMKIIα-iCre carrying mice to obtain progeny in which the Arc/Arg3.1 gene was ablated in principal neurons during the second postnatal week (Early-cKO). Behavioral assessment confirmed a strong impairment in the consolidation of explicit and implicit long-term memories and *in vivo* local field recordings showed strong deficits in memory-linked activity, alteration of hippocampal sharp-wave ripples and of oscillatory activity in the prefrontal cortex (PFC). Additionally, and unlike constitutive KO mice, Early-cKO mice exhibited a significantly

enhanced learning of aversive stimuli and strong anxiolytic-like phenotype. MRI analysis demonstrated an altered morphology of the CA3, fimbria and lateral septum. Resting state funtional (rs-fMRI) revealed specific disruption of the functional connectivity in cortico-PFC and hippocampal-diencephalic circuits, both of which play a central role in memory, decision making and emotional control. These results demonstrate, for the first time, the participation of Arc/Arg3.1 in shaping developmental connectivity of corticolimbic networks and also suggest that emotional dysregulation might arise from an imbalance in the Arc/Arg3.1-mediated plasticity among structures that express the gene at different time points during early postnatal development.

In the second part of this thesis, I evaluated the importance of Arc/Arg3.1 expression in specific hubs of the corticolimbic circuitry for fear memory and anxiety, by employing stereotactic delivery of Cre-carrying viral vectors to the brain of Arc/Arg3.1$^{f/f}$ adult mice. Behavioral assessment showed that Arc/Arg3.1 expression in the basolateral amygdala is essential for the consolidation of auditory fear conditioning, thus confirming its role in memory formation. In contrast, removal of Arc/Arg3.1 from the hippocampus and the anterior cingulate cortex (ACC) only modulated the acquisition of fear and unconditioned avoidance, respectively. These results confirm that Arc/Arg3.1 plays an essential role in the consolidation of long-term implicit fear memory and modifies anxiety in adulthood. Furthermore, imbalanced Arc/Arg3.1-mediated plasticity among regions participating in this circuitry might cause an emotional dysregulation even in adulthood.

This work provides new evidence that reaffirms the essential participation of the synaptic plasticity gene Arc/Arg3.1 in the consolidation of long-term fear memory. It highlights for the first time its contribution to sensitive periods of emotional behavior and to functional connectivity within the corticolimbic circuitry. This novel role of Arc/Arg3.1 implies its importance in the pathophysiology of neurodevelopmental and fear-related disorders, and paves the way to study the interaction of Arc/Arg3.1 with environmental risk factors during sensitive periods for neuropsychiatric disorders.

Zusammenfassung

Das neuronale Netzwerk der cortico-limbischen Hirnareale spielt eine zentrale Rolle für die Generierung von Gedächtnis und Emotionen, zwei stark miteinander verbundene Gehirnfunktionen. In diesem Netzwerk wird die synaptische Plastizität als essentieller Bestandteil zur Konsolidierung des Langzeitgedächtnisses angesehen. Es ist jedoch unbekannt, ob diese zelluläre Funktion auch für die Emotionsregulation notwendig ist. Darüber hinaus formt die synaptische Plastizität während der frühen postnatalen Entwicklung die Konnektivität innerhalb dieses Netzwerkes, ihre Notwendigkeit während dieser Phase zur Ausbildung der Gehirnfunktionen ist bisher jedoch unklar. In dieser Doktorarbeit adressiere ich diese Fragen mit Hilfe der gezielten, zeit- und ortsabhängigen, konditionalen Störung der Arc/Arg3.1-vermittelten Plastizität im cortico-limbischen System.

Die Expression des aktivitätsregulierten Gens Arc/Arg3.1 wird durch plastizitätsinduzierende Stimuli und das Erlernen neuer Erfahrungen schnell hochreguliert. Die konstitutive Deletion des Arc/Arg3.1 Gens in Mäusen verursacht schwere Störungen in der Konsolidierung hippocampaler synaptischer Plastizität und führt zur Beeinträchtigung des expliziten und impliziten Langzeitgedächtnisses. Während der frühen postnatalen Entwicklung und nach dem Erfahren von Angst in erwachsenen Mäusen kommt es zur starken Hochregulation von Arc/Arg3.1 im cortico-limbischen System. Daher erscheint die konditionale Ausschaltung der Arc/Arg3.1-Expression neue Erkenntnisse über die Plastizitätsmechanismen im sich entwickelnden und im adulten Gehirn zu erlauben. In dieser Dissertation verwende ich eine, in unserem Labor generierte, LoxP-flankierte Arc/Arg3.1 Mauslinie (Arc/Arg3.1$^{f/f}$) in Kombination mit Cre-vermittelter Rekombination, um eine orts- und zeitabhängige Entfernung des Arc/Arg3.1 Gens zu erzielen. Der Verlust der Arc/Arg3.1-Expression im Gehirn wurde mittels *in situ*-Hybridisierung und Immunohistochemie nachgewiesen. Zur Analyse des Gedächtnisses und des Emotionalverhaltens habe ich spezifische Verhaltensexperimente durchgeführt. Des Weiteren wurden *in vivo* Feldpotenzialmessungen und die Magnetresonanztomographie (MRT) angewendet, um funktionelle und strukturelle Modifikationen im cortico-limbischen System zu identifizieren.

Im ersten Teil meiner Dissertation habe ich die Expression der Arc/Arg3.1 mRNA während des ersten postnatalen Monats quantifiziert und die Auswirkung des Verlustes von Arc/Arg3.1 ab dieser Entwicklungsphase evaluiert. Die Expression der Arc/Arg3.1 mRNA beginnt während der frühen postnatalen Entwicklung in der Cornu Ammonis 3 (CA3)-Region des Hippocampus und dem Bulbus Olfaktorius. Nach der zweiten Woche steigt sie in den restlichen cortico-limbischen und sensorischen Arealen stark an und pendelt sich letztlich in kortikalen Regionen langsam auf

einem schwachen Niveau ein. Daher besitzt Arc/Arg3.1 das Potential, die postnatale Entwicklung des Gehirns zu beeinträchtigen und dadurch die Konsolidierung des Langzeitgedächtnisses und die Regulation von Emotionen im adulten Tier zu stören. Um diese Möglichkeit zu erforschen, wurde die Arc/Arg3.1$^{f/f}$ Mauslinie mit einer CaMKII-iCre Mauslinie gekreuzt, wodurch Arc/Arg3.1 in der zweiten Woche der postnatalen Entwicklung ausschließlich in prinzipalen Neuronen entfernt wurde (Early-cKO). Mithilfe von Verhaltensversuchen konnte ich die schweren Konsolidierungsstörungen des expliziten und impliziten Langzeitgedächtnisses in diesen Mäusen bestätigen. *In vivo* Messungen der Feldpotentiale zeigen darüber hinaus starke Veränderungen der Gedächtnis-assoziierten Aktivität, der *sharp wave-ripple* Komplexe sowie der Oszillationen im Präfrontalen Cortex (PFC). Zusätzlich, und im Unterschied zur konstitutiven KO-Mauslinie, zeigen die Early-cKO Mäuse ein signifikant verbessertes Lernen nach aversiven Stimuli und ein stark vermindertes Angstverhalten. Die Magnetresonanzanalyse zeigt Veränderungen der grauen Substanz in der CA3-Region, der Fimbria, des lateralen Septums und der funktionellen Konnektivitäten zwischen Arealen des PFCs sowie Hippocampus und Habenula, die beide mit Gedächtnis, Emotionsregulation und Entscheidungsprozessen in Verbindung gebracht werden. Diese Befunde zeigen zum ersten Mal, dass Arc/Arg3.1 in einer sensitiven Periode der Entwicklung an der Ausbildung der funktionalen Konnektivität von cortico-limbischen Netzwerken beteiligt ist. Dies weist darauf hin, dass diese Emotionsdysregulation aus einem gestörten Gleichgewicht der Arc/Arg3.1-vermittellten Plastizität zwischen Regionen des cortico-limbischen Systems folgen könnte, in denen das Gen während der postnatalen Entwicklung in einem differenzierten zeitlichen Muster exprimiert wird.

Im zweiten Teil dieser Dissertation habe ich die Rolle von Arg/Arg3.1 für das emotionale Gedächtnis und das Angstverhalten im Zusammenhang mit den zuvor identifizierten, zentralen cortico-limbischen Schnittstellen untersucht. Zu diesem Zweck wurde Viren zur Expression der Cre-Rekombinase und damit zum Ausschalten von Arc/Arg3.1 stereotaktisch in zentrale Areale des neuronalen Angstnetzwerks injiziert. Die anschließende Untersuchung des Verhaltens zeigte, dass die Expression von Arg/Arg3.1 in der basolateralen Amygdala für die Konsolidierung der auditorischen Angstkonditionierung notwendig ist. Darüber hinaus hat die Arc/Arg3.1-Expression im Hippocampus und anterioren cingulären Cortex (ACC) nur eine modulierende Funktion beim Erlernen der Angstkonditionierung, beziehungsweise des Angstverhaltens. Diese Ergebnisse zeigen, dass Arc/Arg3.1 eine zentrale Rolle bei der Konsolidierung des impliziten Langzeitangstgedächtnisses spielt und das Angstverhalten in erwachsenen Tieren modulieren kann.

Diese Arbeit untermauert die entscheidende Rolle des synaptischen Plastizitäts-Gens Arg/Arg3.1 bei der Konsolidierung des Langzeitgedächtnisses und zeigt zum ersten Mal seine Beteiligung an

einer sensitiven Phase der Entwicklung des Emotionalverhaltens und der funktionalen Hirnkonnektivität des cortico-limbischen Netzwerks. Diese neue Funktion von Arc/Arg3.1 deutet auf dessen Bedeutung bei der Pathophysiologie von Entwicklungsstörungen des Nervensystems und bei Angststörungen hin. Diese Befunde ebnen den Weg für weitere Analysen der Funktion von Arc/Arg3.1 in Entwicklungsprozessen und zeigen die entscheidende Rolle der Wechselwirkungen von Arc/Arg3.1 mit Umweltrisikofaktoren während der für neuropsychiatrische Störungen sensitiven Entwicklungsphase.

Part I:
Arc/Arg3.1 expression during early postnatal development determines memory and emotional processes

1. Introduction

In 1967 the Colombian Nobel laureate Gabriel García Márquez published the literature masterpiece One Hundred Years of Solitude. In the third chapter of this splendid book, the writer describes Rebeca, a little girl of an unknown origin that was adopted by the Buendía family and who brought with her a dreadful malady: "one night about the time that Rebeca was cured of the vice of eating earth… Visitación (The Indian woman who took care of her) saw Rebeca … sucking her finger and with her eyes lighted up in the darkness like those of a cat. Terrified, exhausted by her fate, Visitación recognized in those eyes the symptoms of the sickness whose threat had obliged her and her brother to exile themselves forever from an age-old kingdom where they had been prince and princess. It was the insomnia plague... the lethal sickness ... that had been scourging their tribe for several years" (García Márquez 1967). This disorder according to Garcia Márquez was tremendously devastating because its "most fearsome part was not the impossibility of sleeping, but its inexorable evolution toward a more critical manifestation: a loss of memory" (García Márquez 1967) in which the person who suffers the condition: "the recollection of his childhood to be erased from his memory, then the name and the notion of things, and finally, the identity of people and even the awareness of his own being, until he sinks into a kind of idiocy that had no past"(García Márquez 1967).

In his splendid novel, García Márquez described in an extremely vivid manner, how important memories are for the proper and independent functioning of a person, for the construction of the autobiographic identity and the notion of self. In a similar and remarkable manner, he depicted without prior scientific knowledge the importance of brain rhythms (sleep) in the maintenance of mnemonic and cognitive functions. After more than 60 year of study, it has been possible to understand some of the anatomical and physiological bases of memory and confirm some of the García Marquez's "fictional descriptions" by the study of healthy organisms and dementia syndromes such as the Fatal Familial Insomnia or the more prevalent Alzheimer's type (Sweatt 2016). The study of memory has become a priority for our modern society not only because of our intrinsic interest of knowing ourselves but also due the high burden of neuropsychiatric and neurological disorders in the contemporary world that frequently involves impairments in mnemonic functions (Budson & Price 2001).

In the first part of this dissertation, I describe how Arc/Arg3.1 – a gene essential for consolidation of learning, memory and synaptic plasticity – affects memory by modulating the developmental emergence of neuronal oscillatory activity and functional brain connectivity.

1.1. Learning and memory consolidation

Learning is defined as the ability to acquire new information and knowledge, and memory refers to the process of storing and later evoking this information. These brain functions are therefore fundamental for survival because they allow the organism to respond and adapt to the continuous changes in the environment. Memory is not a single mental process but adopts different forms and relies on different neuronal systems. Categorically, memory can be classified by its duration as short or long-term memories, and by its content as explicit (declarative) or implicit (nondeclarative) memories depending on how the recall process is performed, consciously or unconsciously, respectively (Squire & Dede 2015).

Explicit memory contains stored information related to events and facts. This type of memory is at the same time subdivided into: (i) episodic memories, that address the questions what, where and when, and (ii) semantic memories, which correspond to the general knowledge or facts. It is accepted that the consolidation of explicit memories takes place in structures of the temporal lobe since the original description by Scoville and Milner of a patient who underwent a bilateral temporal lobectomy and developed severe anterograde amnesia only for explicit memories after surgery (Scoville & Milner 1957). On the other hand, implicit memory covers all the information related to procedures, skills, habits, and emotional behaviors. The implicit memories are allocated mostly in local and phylogenetically old circuits such as cerebellum (motor memories) (Krakauer & Shadmehr 2006), basal ganglia (procedural memory) (Kreitzer & Malenka 2008) and amygdaloid complex (classical conditional) (LeDoux 2000).

During the formation of long-term memory, it is necessary that the recently acquired information, which at the beginning is fragile and can be affected by behavioral or molecular disturbances, becomes stronger and resistant to disruption. The process by which memories strengthen and stabilize, and therefore transforms from short-term into longer-term memories, is known as consolidation. The standard consolidation model usually conceives two levels, cellular and systemic consolidation. Cellular consolidation (also known as synaptic or local consolidation) refers to all cellular modifications necessary to encode information into synaptic and cellular nodes in the neural circuit, whereas the systemic consolidation denotes the post-encoding process that reorganizes representations over distributed brain circuits (Dudai *et al* 2015).

The synapse is the functional unit of communication in the brain, and consists of a highly specialized cell-cell junction that mediates transmission of signals (action potentials) between neurons and surrounded by astrocytes (tripartite synapses). The most common type of synapses in the

central nervous system (CNS) is the chemical one; this type operates through exocytosis of neurotransmitters from the presynaptic terminal that are released into the synaptic cleft and thereby activate receptors on an enriched surface in the post-synapse; either propagating or blocking the electrical signal. Certain components in the presynaptic or postsynaptic compartments during the process of neurotransmission are malleable and adaptable in order to increase or decrease the efficacy of transmission at specific synaptic contacts. This ability to adapt the synaptic response is known as synaptic plasticity, and it has been proposed as one of the main substrates of cellular consolidation.

In his synaptic plastic and memory hypothesis, Richard Morris and colleagues proposed that "activity-dependent synaptic plasticity is induced at appropriate synapses during memory formation, and is both necessary and sufficient for the information storage underlying the type of memory mediated by the brain area in which that plasticity is observed" (Martin *et al* 2000). This hypothesis arose from the initial theoretical constructions of pioneer neuroscientists such as Ramón y Cajal, Hebb and Konorski, who proposed that the growth of new neuronal connections in the brain would provide the substrate for the storage of new information in specific brain areas. A hypothesis later supported by experimental evidences of simple implicit learning paradigms (sensitization and habituation) in the marine mollusk *Aplysia Californica* (Bailey *et al* 1996), and followed by Bliss and Lømo's discovery of the long-term potentiation (LTP) in the dentate gyrus (DG) in the rabbit hippocampus (Bliss & Lomo 1973).

Cellular consolidation in mammals has been extensively studied in synapses of the dorsal hippocampus (anterior hippocampus in humans), a structure in the medial temporal lobe in which it is believed that fast synaptic plasticity takes place as one of the first stages in the consolidation of episodic memories. It is also thought to comprise plastic changes such as LTP and long-term depression (LTD), two electrophysiological paradigms known as Hebbian plasticity. LTP is a long-lasting strengthening of synaptic currents/potentials of a single neuron or a population of neurons induced by specific patterns of stimuli applied to the synpases or their inputs (*e.g.* theta burst or high-frequency stimulation). In contrast, LTD refers to the reduction in the strength and weakening of synaptic connection (Stent 1973). Similar to what was found during acquisition of memory in animal models; LTP and LTD share some common molecular mechanisms with this process such as N-Methyl-D-aspartate receptor (NMDAR) activation (Dudek & Bear 1992, Harris *et al* 1984), calcium-dependent intracellular signaling (Mulkey & Malenka 1992, Wang & Stelzer 1996), regulation of genomic transcription (Frey *et al* 1993, Kemp *et al* 2013) and translation of new proteins (Kauderer & Kandel 2000, Stanton & Sarvey 1984). For synaptic strength maintenance, it is assumed that LTP induces the enhancement of α-amino-3-hydroxy-5-methyl-4-isoxazolepropionic

acid receptor (AMPAR) exocytosis, whereas the LTD increases their endocytosis (Malenka & Bear 2004). Along with Hebbian plasticity, scaling of synaptic activity, a form of homeostatic plasticity where synaptic strength is up- or down-regulated to restore neurons averaged firing rates, is thought to contribute to the network stability and specificity of synaptic modifications underlying information encoding (Turrigiano 2012).

In contrast to cellular consolidation, systems consolidation is less well understood and is a slower process. It is thought to occur over time via recurrent waves of synaptic consolidation that reiterate and relocate the gist of information in different brain regions; and thus serve as a long-term memory storage mechanism. Through this process, the memory is thought to become independent from the hippocampal circuitry (Dudai 2012). In human studies using functional MRI (fMRI) (Tambini *et al* 2010) and in animals using the detection of immediate early genes (IEGs), it has been shown that a few minutes or hours after encoding the information (Tanaka *et al* 2014), distinct neocortical regions are engaged together with the hippocampus, suggesting that memory information is distributed across cortico-hippocampal circuits even at early time point of consolidation.

Sleep has been suggested as one of the main requirements for systems consolidation over longer time periods, shown by the fact that periods of sleep prevent forgetting and sleep deprivation deteriorates the ability to remember (Rasch & Born 2013). Furthermore, during sleep and rest, reactivation and replay of firing patterns of similar sequences are observed in place cells of the hippocampus and neocortex after spatial exploration, especially during periods of slow-wave sleep (SWS) (Kudrimoti *et al* 1999). In the hippocampus, this neuronal replay occurs during events of high-frequency oscillatory activity (around 180 Hz) called ripples that usually co-occur in association with a sharp waves (together SPW-Rs) (Diba & Buzsaki 2007),. Ripples are effectively coupled and triggered by neuronal bursts in deep cortical layers during sleep-associated spindles and delta waves (slow frequency oscillations) (Clemens *et al* 2007). The latter phenomena raise the hypothesis that such coupled activity may represent a state of transferring and consolidation of information between the hippocampus and neocortical areas. Since rapid eye movements (REM) sleep always follows SWS, it is believed that spindles during this sleep phase stimulate the induction of synaptic plasticity-like events in REM and thereby induces a massive transcription of IEGs in waves of synaptic consolidation to complete system consolidation processes initiated in SWS (Ribeiro 2012). REM sleep seems to be particularly beneficial for memories that are supposed to be independent of cortico-hippocampal networks such as procedural skills and delay cued fear conditioning (Popa *et al* 2010). Recently, Boyce *et al*. using optogenetic silencing of GABAergic neurons in the medial septum showed that the suppression of theta (ϑ) rhythm in the

hippocampus (network oscillations at ~4-10 Hz) exclusively during REM sleep impairs contextual and spatial memory consolidation (Boyce *et al* 2016).

Currently, memory is used as an umbrella term referring to a group of complex physiological processes in the brain that aim at storing information and require the use of high amounts of cellular and network resources during the time. Memory is constantly reprocessed and transformed in order to guide the behavior of the organism and change the conduct in specific environments for increasing finally all chances of survival.

1.2. Memory and emotions

From a very Darwinistic point of view, information is stored and retrieved in most of the cases as survival signals that serve to identify and recognize in future situations safety, pleasure or danger. Hence, information is always associated with a valence that strengthens or weakens the necessity and priority for its consolidation. Thus, the processes of consolidation are dramatically influenced by environmental stimuli and closely connected to the emotional content. It is not surprising that circuits used by the brain for mnemonic processing are in tight connection or in some types of memory are the same as the ones used for generating and processing emotional states.

In the neuroscience literature, there is no consensus about the definition of emotions, because some fields that deal with this concept are centered on anthropomorphic definitions or in the subjective appreciation of feelings without taking into account behavioral readouts of neuronal systems. A working and very useful definition of emotions adopted by Rolls and other (Rolls 2000) is that "they are internal states elicited by rewards and punishment; a reward is anything for which an animal will work. A punishment is anything that an animal will work to escape or avoid". These states trigger unconscious autonomic, behavioral and cognitive responses that aim at escaping, avoiding or persevering at certain actions that will lead the organism to survive and thrive. Feelings are defined according to Damasio and colleagues (Damasio & Carvalho 2013), as the conscious perception resulting from emotional states, and although they are always triggered by emotions, their study has been only possible in humans without negating their probable existence in other organisms.

Among emotions, one can count all the "action programmes" that aim at satisfying basic instinctual needs such as hunger, thirst, libido, exploration and play, care of progeny and attachment to mates (Damasio call them "drives"); they respond in some extent to rewards. Additionally, emo-

tional states that are elicited by punishment or extereoceptive stimuli include disgust, fear, anger, sadness, contempt, pride, compassion, and admiration. Emotions are manifested by certain and specific behavioral and physiological actions that include changes in visceral and internal milieu (e.g. autonomic responses and hormonal secretion), striated muscle (e.g. facial expression, startle, immobility or running) and cognition (e.g. increase attention and favoring ideas or way of thinking) (Damasio & Carvalho 2013).

The most extensively studied emotion in experimental neuroscience is fear. Fear is an emotional state that is caused by the exposure to a real threat, or to stimuli or situations previously associated with threats. Consequently, fear is an emotion that contains nonassociative and associative components that usually elicits a behavioral readout produced by a pattern of physiological actions such as the acute activation of the sympathetic nervous system (including increased heart and respiratory rate, mydriasis, urination, defecation, sweating, secretion of cortisol and adrenaline from the suprarenal glands), and aversive behavioral responses such as running, hiding, hypervigilance or immobility (in case of some rodents) (LeDoux 2014). Fear has been extensively investigated in both animals and humans through Pavlovian fear conditioning (FC). In this procedure, a neutral conditioned stimulus (CS, often a tone, light or a context) is presented together with a noxious or harmful unconditioned stimulus (US, typically a mild footshock), as result, an association US-CS is acquired (fear learning) and consolidated, and when the neutral stimulus is presented alone, the retrieval of the fear (fear memory) is elicited together with all the emotional responses and outcomes (autonomic and behavioral responses).

It has been repeatedly shown that synaptic plasticity mechanisms in the lateral amygdala (LA) mediates fear associations (Pape & Pare 2010),. Other components of the amygdaloid complex such as the central nucleus (CeA), that is tightly connected with the hypothalamus (Hyp) and periaqueductal gray matter (PAG), participate directly in the expression of fear. Furthermore, changes in CS responses have been observed in auditory and multimodal nuclei in the thalamus, auditory cortex, prefrontal cortex (PFC), and the hippocampus (Hpc) (Tovote *et al* 2015). Interestingly, during fear expression and innate avoidance, entrainment in a specific oscillatory activity at a range of 4-10 Hz (θ rhythm) has been observed between the amygdala and the medial PFC (mPFC) (Likhtik *et al* 2014), and amygdala and the Hpc (Seidenbecher *et al* 2003), suggesting a functional and cellular long-range connectivity that participates in the consolidation of fear associations and contextual modulation of fear and unconditioned avoidance.

A feeling that is related but yet very frequently confused with fear is anxiety, and although the neurobiological circuits of anxiety may overlap with fear, clear distinctions have been made between

them. Anxiety is defined as the feeling of uneasiness, unprovoked worries and apprehension over potential threats or expected negative events (Davis *et al* 2010). A possible readout of such a feeling in experimental animals is perhaps the autonomic responses, innate unconditioned avoidance and risk assessment shown by rodents in innocuous but confounding environments with bright open and dark enclosed compartments (such as elevated plus-maze and light-dark box). If normal anxiety in humans is defined as a feeling (conscious emotional perception), and despite similar neuronal circuits in animals may control related behavioral outcomes showing that is very likely that other species experience these feelings (Panksepp 2005); due to the impossibility of communication through language with the experimental animal models, it is still debatable to call anxiety to the behavior observed in ethological paradigms. Hence, in most of the modern literature, expressions such as anxiety-like or anxiety-related behavior are used, and they are adapted in the present thesis.

Different to fear, anxiety-like behaviors elicit milder autonomic and defensive responses including muscle tension and vigilance in preparation to future danger and cautious or avoidant behaviors that last longer than those elicited by fear. The latter includes strong autonomic arousal necessary for fight or flight, thoughts of immediate danger and escape behaviors; the latter used to decline fast and disappeared once the threat is absent (Davis *et al* 2010). Fear and anxiety neural circuits will be explained and expanded in the second part of this thesis.

Although fear and anxiety are innate emotional states mediated by genetically coded neural circuits, these circuits are tremendously plastic and tightly interconnected with mnemonic networks. Fear for example is mainly studied as a learned behavior through Pavlovian conditioning, whereas anxiety-like behavior is investigated in most of the cases as an innate behavior because the pre-training or pre-exposure to ethological paradigms is rarely performed. It is however well known that anxiety-related behaviors are enhanced when the animals are re-exposed to the testing environment (Lamprea *et al* 2000) or by fear conditioning (Botta *et al* 2015), leading to a state of sustained anxiety-like behavior which may account for a closer model of anxiety disorders.

1.3. Development of neural circuits involved in memory and emotions

Emotions and memory are brain functions that develop and shape with time during the entire lifespan after birth, in close modulation or dependence on novel experiences. Prenatal brain development is mainly determined by a fixed set of highly conserved genes that establish the neural plate, the formation of the neural tube and its subsequent anatomical organization. In rodents by the

late gestation (E18), most the neurons that constitute the so-called corticolimbic system (neuroanatomical structures related with mnemonic and emotional processing) have migrated to their final destination, with the exception of the granule cells in the DG and a subset of interneurons in the olfactory bulb that differentiate and migrate throughout the lifetime (Marin & Rubenstein 2003).

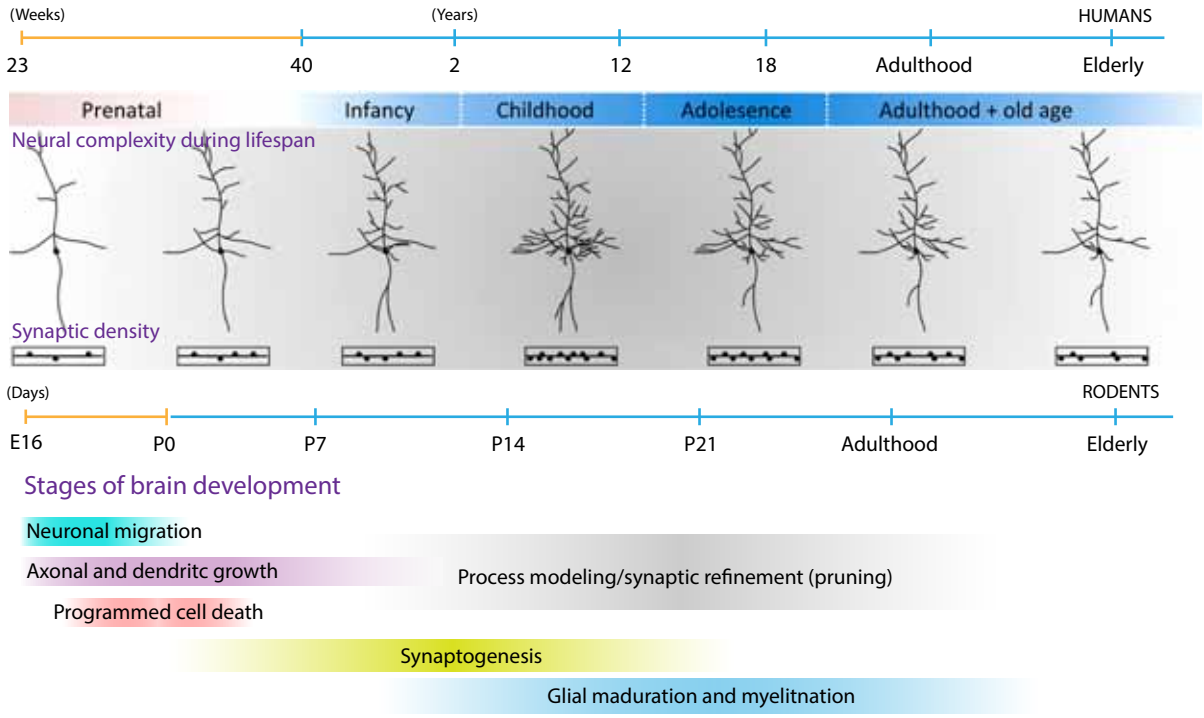

Figure 1. Temporal profile of neurodevelopmental sequences
Modified after (Borre et al., 2014).

In rodents, the postnatal development of corticolimbic structures has been divided into 3 stages: (i) P0 to P10, is characterized by extensive growth; the cell volume expands, and axons and dendrites finalize their development (Caley & Maxwell 1968a). (ii) Between P11 and 20, the growth and extracellular space reduce and blood vessels, astrocytes and oligodendrocytes mature and myelination begins (Caley & Maxwell 1968b, Caley & Maxwell 1970). (iii) After P21 (weaning), cortical growth is minimal and the pruning of exuberant synapses is the predominant process, the generation of synapses and spines reaches a steady level. Synapse adjustment and pruning are processes that extend until puberty together with the addition of myelin and maturation of glial cells (Huttenlocher & Dabholkar 1997). Notably, an accelerated increase in the number of cortical synapses is observed in the first half of the second postnatal phase (around P14), co-occurring with hearing onset and eyes opening, as well as an increase in cortical connectivity (Figure 1) (Ashby & Isaac 2011).

The influence that new sensory and social experiences have in guiding the final maturation of neu-

ral circuits and behavior has been extensively investigated in the last decades, especially in these accelerated synaptic periods, giving rise to the hypothesis of critical periods of synaptic plasticity.

1.3.1. Critical periods of postnatal development

Sensitive periods are defined as the time during development in which experiences potentiate or inhibit neuronal plasticity and connectivity that in turn shape the final network functions and behavior. If the presence or abscess of experience results in an irreversible change in the network function, this sensitive period is then defined as critical (Nabel & Morishita 2013). One of the best characterized examples of critical periods for network development is the visual system; where inputs from both eyes compete with each other on when to converge to the primary visual cortex (V1) onto individual neurons, this process depends entirely on binocular visual experiences. For example, in the absence of visual stimulus, children that born with dense bilateral cataracts or experimental deprivation of vision in rodents, the visual circuits do not complete their development and the normal increase in visual acuity do not occur. Similarly, if only one of the eyes is deprived of early visual experiences; in case of refractive defects, strabismus o monocular cataracts; a strong amblyopia is established due to the lack of maturation of visual circuits of the affected visual field and is accompanied by a strong reduction of binocular vision (Maurer *et al* 1999, Wiesel 1982).

Critical periods during cortical development (*e.g.* V1) are opened by an increase in inhibitory signaling in a developing network that is mainly excitatory, an optimal trigger of excitatory/inhibitory balance (E/I balance) is then necessary to engage enhanced levels of neuronal plasticity that involves several cellular and molecular events, including experience-dependent activation of the NMDARs, neurotropic factors (*e.g.* Brain derived neurotrophic factor- BDNF) and proteases (*e.g.* tissue-type plasminogen activator - tPA) secretion, and intracellular signaling cascade activation (i.e. ca^{2+}/calmodulin-dependent protein kinase II - CaMKII, protein kinase A - PKA, extracellular signal–regulated kinases - ERK) leading to protein synthesis, transcriptional and epigenetic modifications in chromatin structure, and changes in structural plasticity. Interestingly, these mechanisms are autoregulated, given that these critical periods are closed by the appearance of molecular "breaks" that limit adult plasticity. These breaks include the maturation of perineural nets (PNN) -extracellular macromolecular aggregates associated with sulfate proteoglycans-, myelin-related inhibitory signaling (*e.g.* Nogo receptors), paired immunoglobulin-like receptor B expression, and functional factors such as the expression of Lynx1 (nicotinic receptor binding protein Lynx1) that acts by regulating E/I balance within local circuits (Takesian & Hensch 2013).

Similar to sensory functions, it has been proposed that other cerebral functions such as language, emotions and memory capacities have sensitive periods during postnatal development. A classic example of a postnatal critical period for social behavior and recognition was described as filial imprinting by Konrad Lorenz (Lorenz 1935). Lorenz observed in several species of birds a period of few hours after hatching (13-16 h) when the fledglings are imprinted on their mother or first suitable moving stimulus, which they will closely follow around. Another more controversial example is the proposed critical period for the acquisition of certain aspects of language. It is suggested that phonetic learning occurs prior to the end of the first year, whereas syntactic learning has a peak of learning between 18 and 36 moths, while vocabulary items can be learned at any age. Such a theory explains why although people in their adulthood that can learn fluently foreign languages, will not easily acquire some phonemes that are inexistent in their native languages (Kuhl 2010). Additionally, for more than four decades, it is known that rearing children or nonhuman primates in deprivation of social stimuli and parental care (but with adequate nutrition) is associated with devastating behavioral development delays and changes in functional and anatomical brain connectivity (Eluvathingal *et al* 2006).

The theories of critical periods of development have brought an immense impact in education and public health measurements. The interventions during these periods could influence the prevention or treatment not only of visual or language disorders but some of the neurodevelopmental and psychiatric conditioning that are believed to appear as disturbances during sensitive periods of brain development (Pratt & Tsitsika 2007).

1.3.2. Developmental emergence of memory and emotional learning

The study of the development of memory and emotions is an important matter for education and pediatric mental health. The advance in effective pedagogic methods cannot be achieved by educators and relatives if learning capacities during infancy and adolescence are not well understood. Similarly, in child and adolescent psychiatry and psychology, effective management strategies for neurodevelopmental disorders could be accomplished only if the normal development of these brain functions is understood.

The development of fear and associative fear learning is determined by the sequential emergence of sensory functions, functional maturation of the amygdala and hippocampus. The first type of learning observed in neonates is the emotional attachment to their mothers or caregivers that in rodents is based on odor cues (Galef & Kaner 1980). Until P10, amygdala responses to aversive stimuli are attenuated, thereafter conditioned odor aversion can be induced, reflecting the emer-

gence of cued fear memory and the onset of learning-induced plasticity in the amygdala (Thompson *et al* 2008). The amygdala's functional maturation seems to be experience-dependent since maternal presence delays cued fear conditioning onset, while maternal separation promotes a premature maturation of this type of learning (Moriceau & Sullivan 2006). Although cued fear memories are acquired after P10, their persistence for more than 10 days is observed only after P17. This phenomenon has been call infantile amnesia and seems to be dependent on experience because early stress abolishes this amnesic effect (Callaghan & Richardson 2012).

In contrast, the developmental emergence of contextual fear conditioned memories seems to reflect the functional maturation of the hippocampus and its connections with the amygdala, appearing after weaning in an adult-like fashion at P23. These types of memories in the juvenile and pre-adolescent phase are labile presenting a fast forgetting. It has been hypothesized that anterograde amnesia for fear contextual and spatial memories during this phase correlates with enhanced developmental neurogenesis in the DG (Akers *et al* 2014). Contextual fear memory acquired during the adolescence (around P29) is not expressed during this developmental period, but reemerges during the transition to adulthood (after P45). This suppression in the contextual fear recall is proposed to be necessary for the transitional phase between parental care and independence in adulthood.

Interestingly, other types of learning paradigms that are thought to be dependent on the hippocampal function have a rather late onset in development. For example, learning of spatial navigation in the water maze emerges first at P17-P18 but is based on directional cues and is labile, lasting less than one day. Stable spatial representations emerge in the following weeks together with reference based navigation (P30 – P42) (Akers *et al* 2009, Schenk 1985). Other hippocampal-dependent paradigms such as auditory trace fear conditioning and passive avoidance seem to emerge only after functional hippocampal development after P21.

1.3.3. Oscillatory activity in adult and developing networks

Brain rhythms are oscillatory fluctuations of neural activity produced by multiple groups of neuronal populations in specific brain regions; this activity is usually measured using local field potential (LFP) recordings and represents the synchronized activity of a large number of neurons that fire periodically in a similar manner. Since a single neuron activity could not explain cognitive operations, it is thought that synchronous neural activity is the underlying property of neural circuits that supports complex cognitive operations such as memory processing and consolidation, where ensembles of neurons must communicate for information transfer and later reactivate to

evoke the stored traces.

The hippocampus is a structure that shows oscillatory activity during behavioral activation, rest and sleep, and it has been constantly linked with the consolidation of episodic memories. The CA1 region of the hippocampus is especially characterized in LFP recordings for its relatively simple access and morphology. CA1 pyramidal cell layer contains principal neurons that have receptive fields codifying specific locations in space, and hence they are known as place cells. These cells fire in specific sequences within a particular rhythmic activity called theta (ϑ); ϑ is a low-frequency oscillation (~4-12 Hz) and one of the three types of oscillations that can be recorded in the hippocampus. It has been proposed that this sequential activity of place cells in ϑ cycle is important for spatial processing and acquisition of spatial information (Colgin 2013).

In the hippocampus, additionally to ϑ oscillations, it is possible to record faster oscillatory events in the gamma (γ) band (~25 -100 Hz) and SPW-Rs (~100-250 Hz ripples superimposed on ~0.01-3 Hz sharp waves) during rest and slow wave sleep. Oscillations in the ϑ and γ frequency bands are considered essential for synchronizing cortico-hippocampal networks during navigation, spatial learning and memory retrieval (Lisman & Jensen 2013). SPW-Rs are considered to be important in memory consolidation, especially during the transferring of labile information from the hippocampus to the neocortex (Ego-Stengel & Wilson 2010, Girardeau *et al* 2009).

During postnatal development, studies in the hippocampus of rodents have reported a period of intense modulations between P7 and P30, starting with a sharp increase in γ oscillations around P5 (Lahtinen *et al* 2002), followed by an increase in ϑ power at P9-10 (Mohns & Blumberg 2008) and the sudden emergence of ripples at P13. ϑ, γ and ripples oscillations are believed to be important for spatial navigation and memory consolidation. They emerge just before the onset of active exploration at the end of the second postnatal week (P13-P14) and mature in parallel with the ontogeny of these behaviors (Buhl & Buzsaki 2005). In contrast to the hippocampus, the emergence of oscillatory activity occurs later in the development of the PFC (Brockmann *et al* 2011, van Eden *et al* 1991). Interestingly, the oscillatory and functional activity of the cortico-hippocampal networks appears by modulation of sensorial experience and its development finishes before any mnemonic process is possible.

1.4. Arc/Arg3.1

Arc/Arg3.1 is an IEG whose expression is rapidly and tightly regulated upon neuronal and plas-

ticity-inducing stimuli exclusively in principal neurons of the CNS. Arc/Arg3.1 was independently discovered and initially characterized in the laboratories of Dietmar Kuhl (Link *et al* 1995) and Paul Worley (Lyford *et al* 1995). Arc/Arg3.1 is a single copy gene located in the chromosome 8q24.3 in humans and 15qD3 in mice, and consists of 3 exonic regions that codify for a single mRNA. The 5' untranslated region (UTR) and open reading frame (ORF) are codified by the first exon, whereas the 3' UTR is codified in the three exons (Figure 2, 6a, 10a, 49a and 50a). Arc/Arg3.1 is a highly conserved gene in mammals and is proposed to have arisen through domestication of a transposon from the Ty3/Gypsy family. The crystal structure of the so-called Arc GAG domain (portions from 207-278 and 278-37 amino acids) has been recently described, sharing some structural homology to the C-terminal domain capsid proteins of the Human Immunodeficiency and Raus Sarcoma viruses (Zhang *et al* 2015). Arc/Arg3.1 is a protein of 396 amino acids with only an additional coil-coiled domain in the N-terminus and a PEST [Proline (P), Glutamate (E), Serine (S) and threonine (T)] sequence motif at the end of the protein; no additional similarities to other proteins have been described in the literature (Figure 2). In the adult brain, Arc/Arg3.1 is only expressed in principal neurons of regions that have been engaged in neural activity after behavioral tasks and it is believed that Arc/Arg3.1 positive neurons have a higher probability to undergo plastic chances in their synapses (Gouty-Colomer *et al* 2016). Arc/Arg3.1 expression in the adult brain remains low in the absence of activity and however is expressed early in the postnatal development, the expression profile of Arc/Arg3.1 mRNA and protein during this period has not yet been fully investigated.

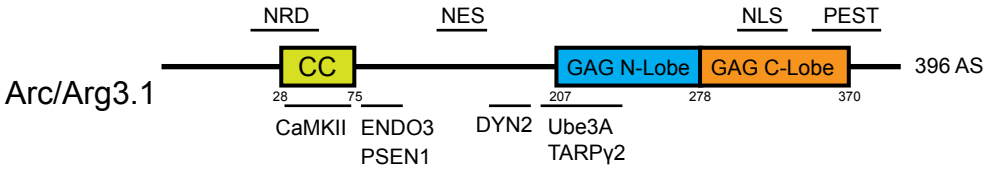

Figure 2. Arc/Arg3.1 structural domains and sites for interaction partners
Arc/Arg3.1 is a protein of 396 amino acids that exhibits in the N-terminus a coiled-coil helix (CC) domain (green); GAG (or capsid-related retrotranspon-related proteins domain) N-lobe and C-lobe are colored in blue and orange, respectively (Zhang *et al*., 2015); NRD; nuclear retention motif; NES, Nuclear export signal; NLS, Nuclear localization signal (Korb *et al*., 2013); PEST sequence, Proline (P), Glutamate (E), Serine (S) and threonine (T). Described interation partners: CaMKII, Ca^{2+}/calmodulin-dependent protein kinase II (Okuno *et al*., 2012); Ube3A, Ubiquitin-protein ligase E3A (Greer *et al*., 2010); TARPγ2, Transmembrane AMPAR regulatory protein γ2, also known as voltage-dependent calcium channel γ2 (CACNG2), MRD10, or stargazing (Zhang *et al*., 2015); ENDO 2, Endopholin 2; DYN2, Dynamin 2 (Chowdhury *et al*., 2006) ; PSEN1, Presiniling 1(Wu *et al*., 2011). [Modified after (Binkle, 2014)]

Arc/Arg3.1 mRNA is rapidly transcribed upon synaptic plasticity-inducing stimuli and trafficked to activated dendrites where it accumulates and undergoes local translation (Steward & Worley 2001). Arc/Arg3.1 gene possess a promoter of approximately 7 kb that contains two serum response elements (SRE) (Waltereit *et al* 2001), a "Zeste-like" element (Pintchovski *et al* 2009), and a synaptic activity-response element (SARE) that present a unique cluster of binding sites for

CREB, Serum Response Factor (SRF) and myocyte enhancer factor-2 (MEF2) proteins (Kawashima *et al* 2009). The intracellular cascade that induces and regulates Arc/Arg3.1 transcription has not been completely investigated but some studies demonstrated that intracellular influx of Ca^{+2} through activation of NMDAR (Steward & Worley 2001), voltage-sensitive calcium channels (Adams *et al* 2009) and activation of group 1 metabotropic glutamate receptor (mGluRs) (Brackmann *et al* 2004) could activate, via incresed level of cyclic adenosine monophosphate (cAMP), PKA, mitogen-activated protein kinases (MAPK) (Waltereit *et al* 2001) and CaMKII cascades (Kumar *et al* 2012), which finally contribute to Arc/Arc3.1 promoter activation.

Upon transcription, Arc/Arg3.1 mRNA is transported to distal dendrites by heterogeneous nuclear ribonucleoprotein (hnRNP) that recognizes 11 consensus nucleotides in the coding regions called A2 response element (Gao *et al* 2008). Additionally, Arc/Arg3.1 mRNA 3'UTR contains a *cis*-acting region with dendritic targeting element (DTE) activity, which may control the dendritic level of mRNA expression (Kobayashi *et al* 2005). Furthermore, the fragile X syndrome protein (FMRP) and Purα interacts with Arc/Arg3.1 mRNA and inhibit its translation while being transported to dendrites (Zalfa *et al* 2003).

A distinct feature of Arc/Arg3.1 transcript is that it is a natural target for nonsense-mediated decay (NMD) (Giorgi *et al* 2007). NMD is a special type of cytoplasmic post-transcriptional control mechanism that identifies and degrades RNAs harboring premature stop codons, produced by nonsense and frameshift mutations or incorrect pre-mRNA splicing. NMD substrates are very diverse and include transcripts with introns in the 3'-untranslated regions (3'UTR) and long 3'-UTR in which physiological stop codons are recognized as premature (Eberle & Visa 2014). Since Arc/Arg3.1 contains two intronic regions in the 3'UTR, the exon-junction complex (EJC) proteins assembles downstream of its stop codon and thereby inhibits its ribosomal entry and degradation after regulator of nonsense transcripts 1 (UPF1) recruitment. In neurons, NMD appears to be essential for the tight control of normal levels and localization of mRNAs in dendrites and is essential for normal neuronal function (Yap & Makeyev 2013).

1.4.1. Arc/Arg3.1 in synaptic plasticity

Arc/Arg3.1 is IEG that in the brain is expressed exclusively in principal cells, and its mRNA and proteins are rapidly and precisely upregulated in neurons that are engaged in response to neuronal activity during a broad range of behavioral and learning paradigms. Currently, Arc/Arg3.1 is considered the best molecular marker for tagging neurons in whole-brain mapping (Vousden *et al* 2015), identification of memory ensembles (Denny *et al* 2014) or neurons which experience

memory-related synaptic plasticity (Gouty-Colomer *et al* 2016).

Arc/Arg3.1 is a very important molecular tool for neuroscientific studies and its cellular function has been extensively linked to diverse forms of synaptic plasticity and consolidation of long-term memories. Guzowski *et al* showed for the first time *in vivo* that the infusion of antisense oligonucleotides (ODNs), that hybridize with the Arc/Arg3.1 mRNA, in the rat DG decreased the translation of the protein and impaired the consolidation of LTP and spatial reference memory in the hidden version of the Morris Water Maze (MWM), without affecting the acquisition of this navigational task (Guzowski *et al* 2000b). In addition to this study, our laboratory generated a constitutive Arc/Arg3.1 knockout (KO) mouse (as previously described by Dammermann 1999, Plath 2004, Plath *et al* 2006) that displayed a dramatic impairment in the consolidation of LTP in the DG, LTP and LTD in CA1 and consolidation of long-term memories.

Moreover, several studies have shown that Arc/Arg3.1 is necessary for the maintenance of at least three types of long-term synaptic plasticity: LTP, LTD and homeostatic synaptic scaling (Table 1). Although many other molecules have been implicated in the physiology of synaptic and experience-dependent plasticity, so far Arc/Arg3.1 has shown to have a precise regulation and functional impact in these phenomena. This is the reason why some current literature has proposed Arc/Arg3.1 as the master regulator of synaptic plasticity (Shepherd & Bear 2011).

How Arc/Arg3.1 participates in the maintenance of these forms of synaptic plasticity is still a matter of debate and continued research. Unlike most other IEG products, Arc/Arg3.1 mRNA encodes for an effector protein that is not a transcription factor but a cytosolic protein that is also found in the post-synaptic density and co-purified with NMDA receptor complexes (Husi *et al* 2000). While HFS and BDNF-induced LTP in the DG, the blockage of Arc/Arg3.1 mRNA by ODNs destabilizes the maintenance of this type of plasticity and induces a rapid dephosphorylation of cofilin and subsequent destabilization of F-actin, suggesting that the induction of Arc/Arg3.1 during LTP induces polymerization of F-actin via associated proteins like cofilin (Messaoudi *et al* 2007); which have been shown to be essential for spine structural changes and consolidation of LTP *in vivo* (Fukazawa' *et al* 2003).

In cultured neurons and hippocampal slices, the overexpression of Arc/Arg3.1 downregulates the surface expression of α-amino-3-hydroxy-5-methyl-4-isoxazolepropionic acid receptors (AMPARs). Conversely, neurons that lack Arc/Arg3.1 exhibit an abnormally high level of surface GluA1 (AMPAR receptor A1 subunit) and slower receptor endocytosis, which strongly suggests that Arc/Arg3.1 expression is involved in the endocytosis/exocytosis cycle of AMPARs (Figure

Table 1. Arc/Arg3.1 in synaptic plasticity

Type	Protocol	Synapes	Method	Model	Effect	Reference
LTP	HFS	PP-DG	ODN	*in vivo* - Rat	Impaired maintenance	(Guzowski et al., 2000b)
LTP	BDNF - LTP, HFS	PP-DG	ODN	*in vivo* - Rat	Impaired consolidation	(Messaoudi et al., 2007)
BDNF-induced LTP	BDNF - LTP	PP-DG	ODN	*in vivo* - Rat	Lack of induction	(Kuipers et al., 2016)
mGluR-dependent LTP	HFS + APV	SC-CA1	KO	Hpc slices	Impaired consolidation	(Wang et al., 2016)
LTP	TBS	PP-DG	KO	*in vivo* - Mouse	Enhanced E-LTP and impaied L-LTP consolidation	(Plath et al., 2006)
LTP	HFS	SC-CA1	KO	Hpc slices		(Plath et al., 2006)
LTD	LFS	SC-CA1	KO	Hpc slices	Impaired induction and maintenance	(Plath et al., 2006)
LTD	PP-LFS	SC-CA1	KO	Hpc slices	Impaired maintenance	(Park et al., 2008)
mGluR-dependt LTD	DHPG	SC-CA1	KO	Hpc slices	Impaired maintenance	(Park et al., 2008)
mGluR-dependt LTD	DHPG	Hippocampal neurons / SC-CA1	shRNA / ODN	Primary cultures / Hpc slices	Impaired expression and maintenance	(Waung et al., 2008)
Cerebelar LTD	Glutamate/ depolarization	Purkinje neurons	KO	Primary cultures	Impaired consolidation	(Smith-Hicks et al., 2010)
Cerebelar LTD	Chemical PDA aplication	Purkinje neurons	KO	Primary cultures	Impaired late phase	(Smith-Hicks et al., 2010)
Homeostatic synaptic scaling	TTX or Bic incubation	Hippocampal neurons	KO	Primary cultures	Abolished AMPARs scaling	(Shepherd et al., 2006)
Synapse-specific homeostatic plasticity	Uncaging of MNI-Glu	Cortical neurons	KO	Primary cutures	Abolished AMPARs insertion	(Beique et al., 2011)
Experience-induced homeostatic plasticity	Dark rearing per 2 d at P21	L2/3 Visual cortex	KO	Cortical slices	Absence of homeostatic plasticity of mEPSCs	(Gao et al., 2010)
Ocular dominance plasticity	Monocular deprivation	Visual cortex	KO – GFP KI	*in vivo* – Mouse	Reduced open-eye and selective response potentiation	(McCurry et al., 2010)

Abbreviations: E-LTP and L-LTP, Early- and Late-long-term potentiation; LTD, Long-term depression; HFS, High-frequency stimulation; BDNF, Brain derived neurotrophic factor; ODN; oligonucleotides, PP; performant path of the entorhinal cortex; DG, Dentate Gyrus; APV, (2R)-amino-5-phosphonovaleric acid; (2R)-amino-5-phosphonopentanoate; SC, Schaffer collaterals of CA3; TBS, theta burst stimulation; DHPG, Dihydroxyphenylglycine; PDA, PKC-activating phorbol ester phorbol-12,13-diactate; TTX, Tetrodotoxin; Bic, Bicuculline; MNI-Glu, 4-methoxy-7-nitroindolinyl-caged-L- glutamate; AMPARs, α-amino-3-hydroxy-5-methyl-4-isoxazolepropionic acid receptor; mEPSCs, miniature excitatory postsynaptic currents.

3). It has been proposed that Arc/Arg3.1 can modulate AMPAR trafficking to the neuronal surface via its interaction with proteins of the endocytic machinery such as dynamin 2 and endophilin 2/3 (Chowdhury *et al* 2006) or by its interaction with Stargazing/Transmembrane AMPAR regulatory protein γ2 (TARPγ2) (Zhang *et al* 2015). This regulatory effect of Arc/Arg3.1 on AMPARs trafficking could partially explain its importance during homeostatic synaptic scaling (Shepherd *et al* 2006) and LTD (Waung *et al* 2008) but cannot explain how upregulation of Arc/Arg3.1 mediates LTP.

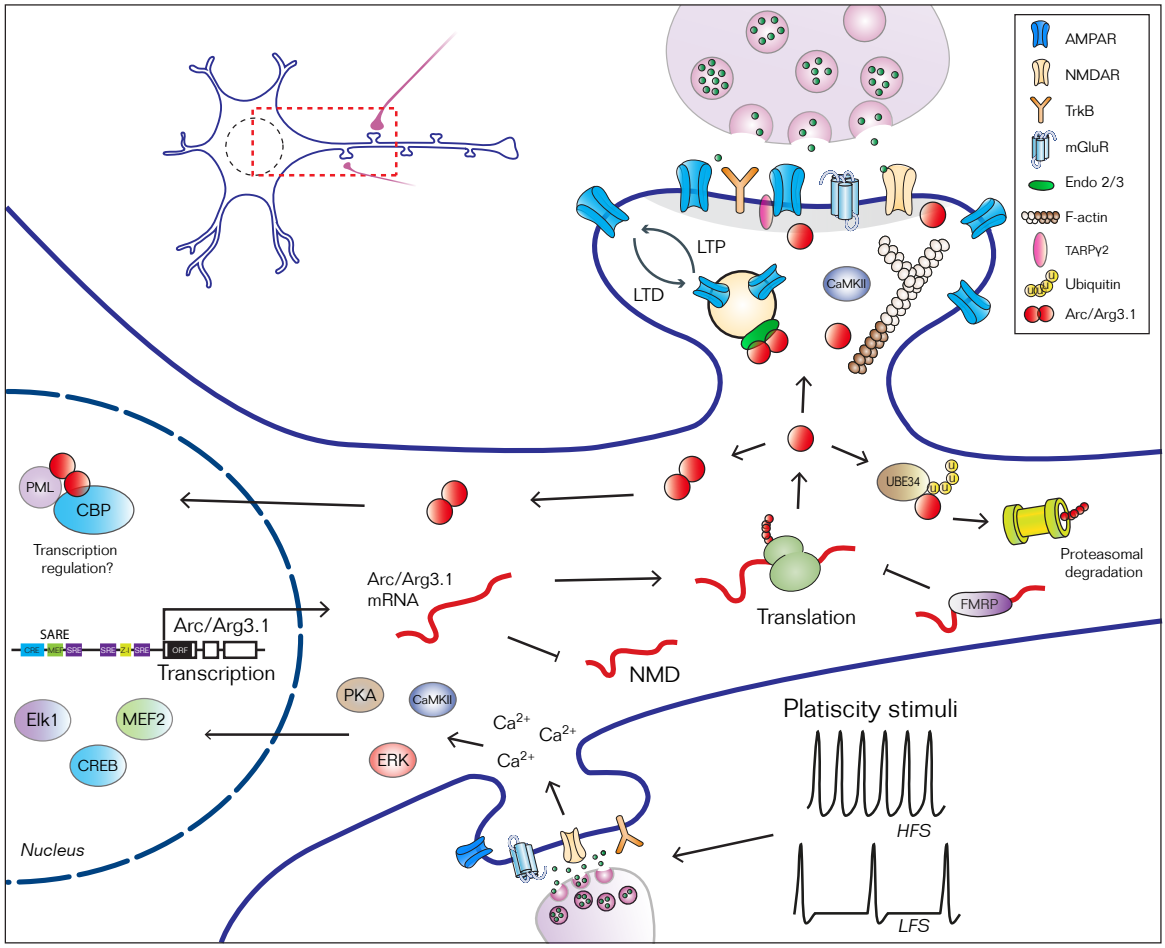

Figure 3. Hypothetical model of molecular events in Arc/Arg3.1-dependent plasticity
Neuronal stimulation-inducing plasticity activates NMDARs, calcium channels, neurotrophic factors or metabotropic glutamate receptors, and thereby intracellular cascades (PKA, MAPK and CaMKII) that control rapid transcription of Arc/Arg3.1 mRNA. The mRNA is transported to dendrites near to activated spines and local translation takes place. In spines, Arc/Arg3.1 protein could interact with the endocytic machinery and control AMPARs trafficking and polymerization of F-actin. After plastic changes Arc/Arg3.1 may be transported back to the nucleus where it is localized to PML nuclear bodies and regulates transcriptional processes. Abbreviations: HFS; High-frequency stimulation, LFS; low-frequency stimulation, CaMKII, Ca^{2+}/calmodulin-dependent protein kinase II, PKA, protein kinase A; ERK , Extracellular signal–regulated kinases; Elk-1; ETS domain-containing protein Elk-1; CREB, cAMP response element-binding protein; SARE, synaptic activity-responsive element, NMD, nonsense-mediated decay; FMRP, fragile X mental retardation protein; Ube3A, Ubiquitin-protein ligase E3A; TARPγ2, Transmembrane AMPAR regulatory protein γ2, also known as voltage-dependent calcium channel γ2 (CACNG2), MRD10, or stargazing; AMPARs, α-amino-3-hydroxy-5-methyl-4-isoxazolepropionic acid receptor; NMDAR, N-Methyl-D-aspartate receptor, TrKB, Tropomyosin receptor kinase B; mGlurR, metabotropic glutamate receptors; Endo 2/3, Endopholin 2/3.

Okuno and colleges have proposed the "inverse synaptic tagging" hypothesis showing that Arc/Arg3.1 is enriched in inactive synapses where low concentrations of Ca^{+2} induce its high-affinity interaction with CaMKII-β; this hypothesis reconciles the role of Arc/Arg3.1 in different forms of synaptic plasticity and proposes that in case of the late-LTP, Arc/Arg3.1 prevents weak synapses from amplifying AMPARs transmission (Okuno *et al* 2012), while stronger synapses can be potentiated.

In addition to the described function at the synapse, Korb *et al*. have described in mice that 8 hours after novel spatial exploration, Arc/Arg3.1 protein is mainly detected in the nucleus of granule cells in the DG, suggesting a crosstalk function from synaptic to the nucleus. In the same report, it was shown that Arc/Arg3.1 protein might interact with the promyelocytic leukemia tumor suppressor protein (PML) and CREB-binding protein (CBP) in PML-Nuclear bodies (PML-NBs) and thereby directly regulates GRIA1 (Glutamate receptor 1-GluA1 coding gene) transcription (Korb *et al* 2013). The function of Arc/Arg3.1 in the nucleus might account for the remote regulation and maintenance of plasticity during systems consolidation.

1.4.2. Arc/Arg3.1 in learning, memory and emotions

The induction of Arc/Arg3.1 mRNA after different behavioral paradigms and brain regions has been extensively studied by using ODNs or RNA interference (*e.g.* short harping RNAs – shRNAs) (Table 2), and the constitutive lack of Arc/Arg3.1 in the KO or Knockout –green fluorescent protein knock-in (KO-GFP KI) mice, suggesting that the behavioral or developmental induced-expression of Arc/Arg3.1 is essential for consolidation of diverse forms of memory, not only in hippocampal subfields but in other brain regions that may use Arc/Arg3.1-related plasticity as mechanism for memory storage (Table 2).

Notably, the Arc/Arg3.1 KO mice present a profound impairment in the consolidation of implicit and explicit memories without significant changes in anxiety-like behavior. These animals exhibit a normal short-term memory in novel object recognition and acquisition of delay fear conditioning (FC), but they show a strong deficit in the consolidation long-term memory of contextual and cued fear conditioning, novel object recognition and conditioned taste aversion (CTA). During the hidden version of the Morris water maze (MWM), Arc/Arg3.1 KO mice have impairments in learning of spatial strategies and show a deficit in long-term spatial reference memory (Plath *et al* 2006).

Moreover, similar learning deficits in the MWM task were found in the Arc/Arg3.1 KO-GFP KI mice (Peebles *et al* 2010); and during rotarod task, these animals exhibited a deficiency in learn-

ing of a precise motor skills (Ren *et al* 2014). It is nevertheless intriguing whether these behavioral phenotypes arise from the lack of Arc/Arg3.1 or as a side effect of the GFP and neomycin cassette transgenes that were inserted in this KI model.

Arc/Arg3.1 expression is also modulated by acute and chronic stress, but there is only consensus that acute restraint stress induces Arc/Arg3.1 significantly in the PFC and amygdala, an effect that seems to be mediated by glucocorticoid receptors (GR) (Molteni *et al* 2008). The role of Arc/Arg3.1 in emotional processes different to fear memory consolidation remains to be investigated. It is known however that antidepressants can modulate Arc/Arg3.1 gene and protein expression in brain regions linked to emotional control such as the PFC, orbitofrontal cortex (OFC) and Hpc, suggesting that Arc/Arg3.1 plays a role in the regulation of emotional states (Li *et al* 2015).

1.4.3. Arc/Arg3.1 during postnatal development and neurodevelopmental disorders

It was previously reported that IEGs such as Arc/Arg3.1, c-fos and zif268 were naturally and differentially upregulated during early postnatal development in the rat brain (Kosofsky *et al* 1995, Sanders *et al* 2008). Additionally, it was proposed that expression of Arc/Arg3.1 in the visual cortex postnatally reflects experience-dependent synaptic changes that underlie maturation of ocular dominance and orientation selectivity (Tagawa *et al* 2005). McCurry *et al*. demonstrated that the Arc/Arg3.1 KO-GFP KI mice lacked plastic mechanism for shifting ocular dominance after monocular deprivation, suggesting that Arc/Arg3.1 is necessary for the critical period of ocular dominance but not for the normal development of the visual sensory function since Arc/Arg3.1 KO-GFP KI presented normal visual acuity, visual responsiveness and organization of retinotopic maps (McCurry *et al* 2010). The requirement of Arc/Arg3.1 during the critical period of binocular dominance is mediated by changes in the homeostatic scaling of excitatory but not inhibitory synapses (Gao *et al* 2010). Additionally and supporting this idea, Arc/Arg3.1 is only necessary for those developmental changes that are related with experience-depend plasticity, because the Arc/Arg3.1 KO-GFP KI mice showed an increased number of cells with low orientation specificity and broader tuning (Wang *et al* 2006); developmental phenotypes similarly found in NR2A and PSD-95 KO mice (Fagiolini *et al* 2003). Moreover, Mikuni *et al* investigated the role of Arc/Arg3.1 in the postnatal development of cerebellar circuits and described that after P11, an activity-dependent mechanism mediated by Arc/Arg3.1 expression in Purkinje cells leads to the elimination of redundant climbing fiber synapses (Mikuni *et al* 2013).

In addition to the role of Arc/Arg3.1 during the critical period of synaptic plasticity in the visual cortex and cerebellum, some studies showed changes in Arc/Arg3.1 expression or function in

Table 2. Arc/Arg3.1 in learning and memory paradigms

Behavioral paradigm	Region	Method	Model	Impairment	Reference
Contextual and cued FC	Whole brain	KO	Mouse	Consolidation of LTM	(Plath et al., 2006)
Contextual fear memory	BLA	ODN	Mouse	Memory persistence	(Nakayama et al., 2016)
Contextual fear memory	DHpc	ODN	Mouse	Memory persistence	(Nakayama et al., 2015)
Auditory fear conditioning	LA	ODN	Rat	Consolidation of LTM	(Ploski et al., 2008)
Trance and contextual FC	DHpc/VHpc	ODN	Rat	Consolidation of LTM	(Czerniawski et al., 2011)
Trance fear conditioning	VHpc	ODN	Rat	Reconsolidation of LTM	(Chia and Otto, 2013)
Cue fear extinction	BLA	ODN	Mouse	Extinction memory	(Onoue et al., 2014)
Inhibitory avoidance	DHpc	ODN	Rat	IGF-II memory enhancement	(Chen et al., 2011)
Inhibitory avoidance	ACC	ODN	Rat	Consolidation of LTM	(Holloway and McIntyre, 2011)
Step-down Inhibitory avoidance	DHpc	ODN	Rat	Persistence of LTM	(Tomaiuolo et al., 2015)
Inhibitory avoidance	mPFC	ODN	Rat	Consolidation of LTM	(McReynolds et al., 2014)
Inhibitory avoidance	DHpc	ODN	Rat	Consolidation of LTM	(Martinez et al., 2012)
Open Field	DHpc	ODN	Rat	Long-term habituation	(Martinez et al., 2012)
Conditioned taste aversion	Whole brain	KO	Mouse	Consolidation of LTM	(Plath et al., 2006)
Hidden version of MWM	DG	ODN	Rat	Consolidation of LTM	(Guzowski et al., 2000a)
Hidden version of MWM	Whole brain	KO	Mouse	Learning of spatial strategies	(Plath et al., 2006)
	Whole brain	KO – GFP-KI			(Peebles et al., 2010)
Rotaroad			Mouse	Leaning of precise motor skills	(Cao et al., 2015)
Novel object recognition	Whole brain	KO	Mouse	Consolidation of LTM	(Plath et al., 2006)
Estradiol-induced lordosis behavior in female rats	Arcuate nuclei	KO	Mouse	Unrestrained sexual receptivity	(Christensen et al., 2015)
Morphine-induced conditioned place aversion.	NAc	ODN	Rat	Acquisition, expression and reinstatement	(Lv et al., 2011)
Morphine-induced conditioned place aversion.	BLA	ODN	Rat	Consolidation of morphine withdrawal	(Liu et al., 2012)
Cocaine-seeking	dlCPu	shRNA	Rat	Extinction of drug-seeking	(Hearing et al., 2011)

Abbreviations: FC, Fear conditioning; OF, open field; LTM, Long-term memory; BLA, Basolateral amygdala; DHpc, Dorsal Hippocampus; NAc, Nucleus Accumbes; ACC, Anterior Cingulate Cortex; dlCPu, dorsolateral Caudate Putamen; LA; Lateral Amygdala; DG, Dentate Gyrus; ODN, antisense oligonucleotides; KO - GFP-KI; Knockout –green fluorescent protein knock-in

relation to physiopathological processes of neurodevelopmental disorders such as Fragile X and Angelman syndrome. This suggests a possible role of Arc/Arg3.1 in the normal early development of cognitive functions.

Fragile X syndrome is the most common inherited form of intellectual disability and the second most prevalent cause after Down syndrome (Hunter *et al* 2014). It is a genetic syndrome inherited through the X chromosome and caused in most of the cases by an abnormal epigenetic inactivation through aberrant methylation of the promoter, causing an expansion in the number of CGG repeats that are located in the 5' UTR in the fragile mental retardation 1 gene (FMR1) that encodes for the FMRP (Saldarriaga *et al* 2014). FMRP is an RNA-binding protein that regulates dendritic mRNA stability and translation. FMRP interacts with Arc/Arg3.1 mRNA and regulates Arc/Arg3.1 protein levels in dendrites by inhibition of its local translation. Fmr1 KO mice (Fragile X syndrome model) exhibit abnormalities in synaptic plasticity dependent on dendritic protein synthesis. Especially, mGluR-LTD is enhanced and independent of new protein synthesis. It was proposed that abnormal levels of Arc/Arg3.1 and the lack of fine control of translation by FMRP contribute to the synaptic abnormalities present in Fmr1 KO mice (Niere *et al* 2012).

Another neurodevelopmental disorder linked to Arc/Arg3.1 disregulation is the Angelman syndrome (AS). AS is characterized by severe cognitive disability, motor dysfunction, speech impairment, hyperactivity, epilepsy and developmental delay, and is usually observed postnatally in the first year of life. AS is caused by the disruption of the maternally expressed and paternally imprinted UBE3A gene, which encodes an E3 ubiquitin ligase (Margolis *et al* 2015). Ube3A KO mice display AS-like phenotypes, abnormalities in LTP (Jiang *et al* 1998), and impaired experience-dependent synaptic development in the neocortex (Yashiro *et al* 2009). Furthermore, it has been showed that Arc/Arg3.1 protein is abnormally expressed in these mutants, mediating aberrant low AMPAR synaptic transmission. Physiologically, Ube3A targets Arc/Arg3.1 protein in an activity-regulated manner and induces its degradation in the proteasome (Greer *et al* 2010). Recently, abnormal levels of Arc/Arg3.1 protein have been also found in a model of intellectual disability and autism spectrum disorder caused by microdeletion of the chromosome 16p11.2 (Tian *et al* 2015), and elevated levels of Arc/Arg3.1 protein in the plasma of a small group of children diagnosed with Autism (Alhowikan 2016).

In addition to these monogenic models, synaptic genes clustered by Arc/Arg3.1 signaling complex and those genes that present N-lobe consensus binding sequences such as CYFIP1, DLG1, DLG2, BAIAP2, SYNGAP1, ABLIM and ANKS1B (Zhang *et al* 2015) have been found to present deletions, *de novo* mutations or recurrent genomic copy number variants (CNVs) in a large

cohorts of patients with Schizophrenia (Fromer *et al* 2014, Kirov *et al* 2012, Purcell *et al* 2014). Aditionally, single nucleotide polymorphisms in the Arc/Arg3.1 gene have been associated with schizophrenia risk (Huentelman *et al* 2015) and its expression has been found to be reduced in the dorsolateral PFC of people with this disorder (Guillozet-Bongaarts *et al* 2014). These findings support the hypothesis that although genetic changes in the Arc/Arg3.1 locus have yet to be identified as cause of disease, Arc/Arg3.1 is a molecular hub that contributes to normal neurodevelopment, as well as neuropsychiatric disorders. Therefore, it might have a role in the normal establishment of synaptic networks during postnatal development.

1.5. Hypothesis and aims of the first part

Because Arc/Arg3.1 is expressed early after birth and its function has been linked to several forms of developmental plasticity and neurodevelopmental disorders, as well as adult plasticity and long-term memory consolidation; Arc/Arg3.1 is in the position of affecting the development of corticolimbic networks and their later function in memory consolidation in the adulthood. In the first part of this dissertation, the main hypotheses are:

- The expression of Arc/Arg3.1 during early postnatal development influences the emergence of functional networks that sustain mnemonic functions in the adult brain. Therefore, a conditional deletion of the Arc/Arg3.1 early during postnatal development will lead to impairments in long-term memory consolidation in the adult mice when compared to WT controls.

- Alternatively, the expression of Arc/Arg3.1 is only necessary pre or perinatally for the development of corticolimbic circuits, thus a postnatal conditional deletion of this gene would not affect the emergence of networks for memory, and the mnemonic performance of the adult animals would be comparable to WT mice.

1.5.1. Specific goals

- To investigate Arg/Arg3.1 expression during early postnatal development and identify developmental windows of Arg/Arg3.1-related plasticity.

- Characterization of the conditional Arc/Arg3.1$^{f/f}$ mouse line and generation of an early postnatal conditional KO mouse line.

- To address the impact of a early postnatal ablation of Arc/Arg3.1 on mnemonic and emotional proceses thorough behavioral assessment.

- To investigate changes in network activity and brain connectivity resulting from early postnatal removal of Arc/Arg3.1.

2. Results

2.1. Arc/Arg3.1 mRNA upregulation during postnatal development

Arc/Arg3.1 participates in the stabilization of diverse forms of synaptic plasticity that are observed not only in adult animals, but also during the development of neuronal circuits. Nonetheless, the role of Arc/Arg3.1 in normal postnatal development of brain networks for memory or emotional processing has not yet been investigated. I first examined the natural spatio-temporal pattern of Arc/Arg3.1 mRNA expression during postnatal development in sagittal slices from brains of young WT mice using radioactive *in situ* hybridization (rISH) at different time points (Figure 4). Across the brain, Arc/Arg3.1 mRNA was present at very low levels from postnatal day 0 (P0) to P7, but highly increased in the forebrain and subcortical structures during the third and fourth postnatal weeks, and finally diminished to low levels in nonstimulated adult brain.

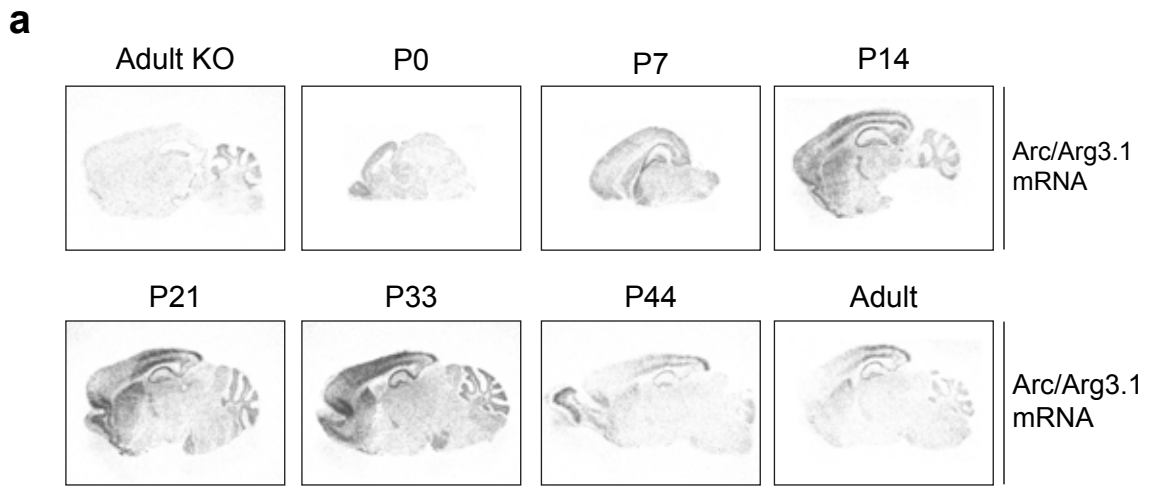

Figure 4. Arc/Arg3.1 mRNA expression in sagittal slices of brains during postnatal development and adulthood
a. *in situ* hybridization with Arc/Arg3.1 antisense probe indicates a natural upregulation of Arc/Arg3.1 mRNA across postnatal development with a high expression during the third and fourth postnatal week and low levels in the adult nonstimulated brain.

I performed 3 additional *in situ* hybridization experiments in coronal slices at 5 different time points (P0, P7, P14, P21 and P28) to semi-quantify Arc/Arg3.1 mRNA expression in different anatomical areas of the mouse brain during the first postnatal month (Figure 5 and Table 3). The radiomicrographs displayed a heterogeneous spatial pattern of Arc/Arg3.1 mRNA expression with some regions strongly upregulated while others only weakly or not at all. Signal intensity in each region was measured and converted to an arbitrary scale by a linear standard microscale, allowing the averaging across several series of sections that were hybridized and exposed separately. I classified and displayed these regions in three functional categories:

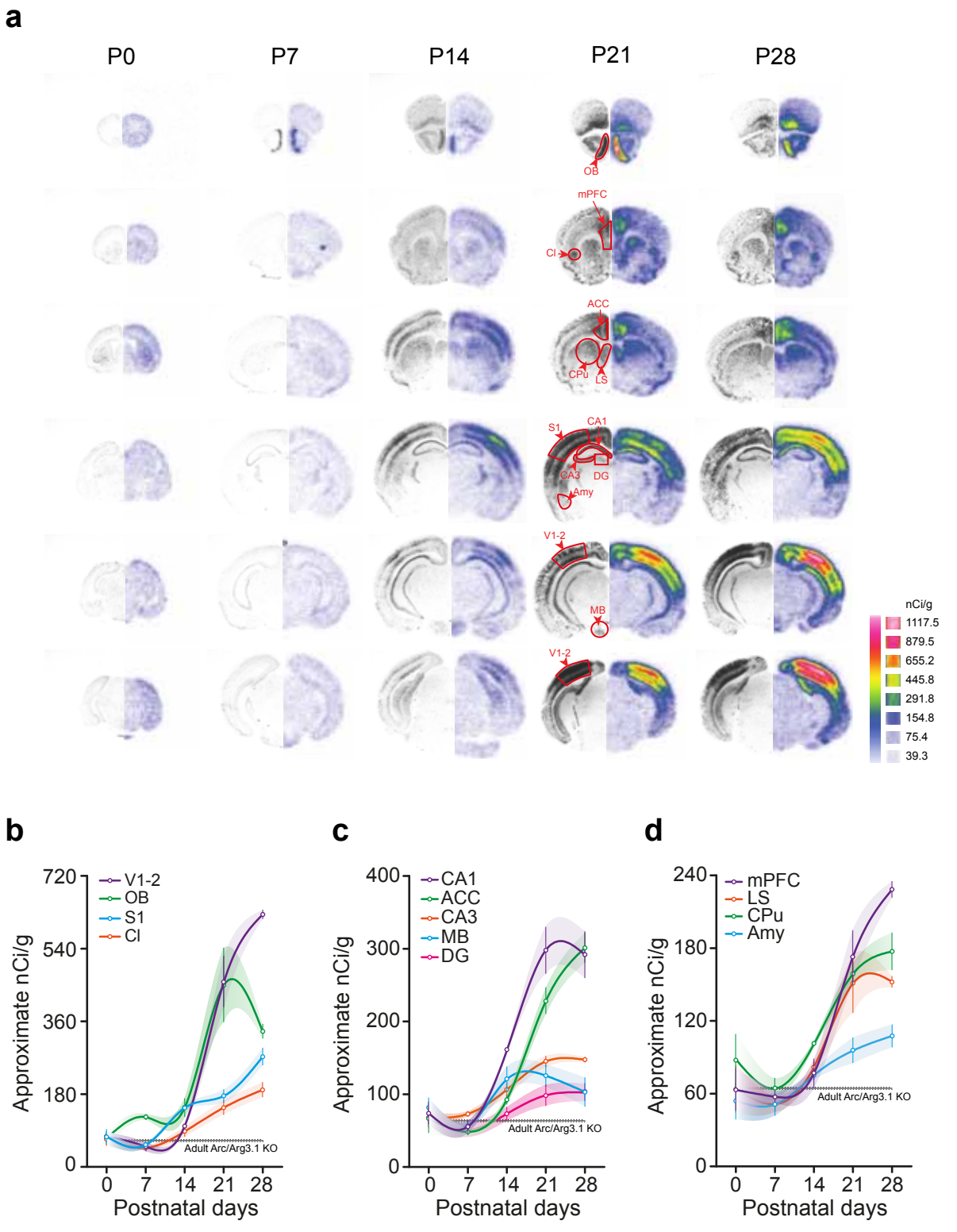

Figure 5. Arc/Arg3.1 mRNA level in coronal slices of brains during the first month of postnatal development
in situ hybridization with Arc/Arg3.1 antisense probe, performed in parallel from 3 brains (per time point) of WT mice. **a.** Autoradiograms (left hemisphere, gray scale) were normalized to a standard ^{14}C scale (right hemisphere, colored) at 5 different time points across the first postnatal month. Examples of measured regions of interest (ROIs) are depicted in red lines. Representative image of a ^{14}C microscale (low right) - exposed in parallel with the samples - illustrates the conversion of main gray level into nCi/g of tissue equivalents. Quantification Arc/Arg3.1 mRNA levels in structures related to: **b.** sensory processing **c.** spatial and episodic memories and **d.** emotional and executive funtions. Lines and shades represent the polynomially interpolated means ± SEM values, respectively.

Table 3. Arc/Arg3.1 mRNA levels in coronal slices of brains during the first month of postnatal development

	P0		P7		P14		P21		P28		Adult KO	
ROI	**nCi/g**	**SEM**	**nCi/g**	**SEM**	**nCi/g**	**SEM**	**nCi/g**	**SEM**	**nCi/g**	**SEM**	**nCi/g**	**SEM**
CA1	73.71	15.90	55.35	9.03	160.15	2.64	298.10	33.18	291.62	32.18	66.06	9.51
CA3	67.58	7.19	72.76	3.93	106.23	9.68	144.91	7.88	147.45	3.74	67.38	13.51
DG	68.26	13.97	50.89	9.53	73.25	9.53	98.75	14.58	102.82	12.15	78.43	10.43
MB	77.08	13.72	52.10	5.44	115.93	17.56	120.96	15.24	98.76	20.02	57.99	8.95
ACC	66.62	19.97	48.27	4.86	92.48	6.70	227.94	18.25	301.29	20.61	62.66	13.20
mPFC	62.99	17.55	57.41	4.73	76.76	12.21	172.85	22.69	228.26	6.86	70.19	13.12
Amy	54.25	15.32	51.08	9.13	75.15	3.77	95.44	10.73	107.54	9.43	65.24	10.65
LS	63.74	19.89	51.00	6.28	81.60	4.92	150.55	24.63	152.00	4.70	52.70	11.62
CPu	88.29	23.03	64.21	8.40	100.82	2.88	158.67	9.13	177.24	15.54	70.38	19.33
OB	70.45	19.18	123.18	7.08	146.53	25.00	449.45	92.66	334.49	18.60	62.67	15.14
Cl	68.97	16.78	47.13	3.90	87.38	13.39	146.38	17.24	190.71	18.67	56.43	16.72
S1	74.88	18.15	53.94	5.62	146.00	5.90	175.30	16.37	272.70	21.64	64.57	13.04
V1-2	75.63	11.03	49.95	11.74	100.77	4.08	455.81	65.66	624.43	11.04	54.90	8.10
IC	47.71	8.49	44.42	7.12	56.80	7.38	78.25	14.91	96.74	16.54	59.56	8.70

Abbreviations: ROI: Regions of interest; CA1: Cornus Ammonis area 1; CA3: Cornus Ammonis area 3; DG: Dentate Gyrus; MB: Mammillary Bodies; ACC: Anterior Cingulate Cortex; mPFC: medial Prefrontal Cortex; Amy: Amygdala; LS: Lateral Septal nucleus; CPu: Dorsal striatum (caudate nucleus and putamen); OB: Olfactory Bulb; Cl: Claustrum; S1: Somatosensory cortex; V1-2: Visual cortex; IC: Inferior Colliculus.

I. Sensory processing (Figure 5b): In sensory structures, Arc/Arg3.1 mRNA is rapidly upregulated from P14 without showing an apparent peak in the first postnatal month, supporting the idea that cortical areas have experience-dependent synaptic development that will end at the early adult period (around P40). In contrast to cortical development, the OB expresses Arc/Arg3.1 from P0 and peaks at P21, after which it declines, reflecting the natural peak in the synaptic density of the glomerular layer around P15-P20 (Matsutani & Yamamoto 2004).

II. Mnemonic processes (Figure 5c): In mnemonic regions, the upregulation of Arc/Arg3.1 mRNA appears earlier in the hippocampal area CA3 followed by CA1, and later in the prefrontal cortices (ACC). The mammillary bodies, a subcortical diencephalic structure classically linked with amnesic manifestations in Korsakoff's syndrome (Oudman *et al* 2015), shows a clear developmental expression of Arc/Arg3.1 peaking at P14. In contrast, the dentate gyrus expressed Arc/Arg3.1 mRNA only weakly between P21 and P28.

III. Emotional and executive functions (Figure 5d): Furthermore, I identified prominent Arc/Arg3.1 mRNA expression in structures related to emotional and executive processing such as the mPFC, Striatum (CPu) and Lateral Septum (LS). They shared a sharp increase of mRNA levels during the third postnatal week, after which LS and CPu seem to peak in the fourth week whereas mPFC maintained a high expression. The Arc/Arg3.1 mRNA expression once again resembles the described dynamics in the development of synaptic density, where the LS and CPu (Tepper *et al* 1998) show synaptic structural stability at the end of the 3rd week whereas the mPFC finalized the synaptic development in the early adult period (Benes *et al* 2000). In contrast and similar to the DG, the amygdala (Amy) expresses Arc/Arg3.1 mRNA only weakly between P21 and P28.

Based on the expression profile across development, it is reasonable to hypothesize that Arc/Arg3.1 plays a role in the early postnatal development of brain structures that show a sharp upregulation of the gene in this period and its genetic removal at this time would cause functional and behavioral changes in the adult life.

2.2. Conditional ablation of Arc/Arg3.1 during early postnatal development

To investigate the role of Arc/Arg3.1 during early postnatal development, I employed conditional ablation as the main strategy. The conditional deletion of this gene during a specific time of development, or specific anatomical region can be achieved with the implementation of Cre-*LoxP* systems and the Arc/Arg3.1$^{f/f}$ mouse line.

2.2.1. Validation of Arc/Arg3.1$^{f/f}$ mouse line for conditional knockout

I tested behavior and biochemistry of the Arc/Arg3.1$^{f/f}$ mouse line (Figure 6, 7 and 8) as the basis of these projects and as the main tool for investigating the role of Arc/Arg3.1 during postnatal development or in the adult brain. Arc/Arg3.1$^{f/f}$ mutants can be bred and maintained according to Mendelian laws; appeared normal and reached the same age and body weight as their wild-type (WT) littermates. Because the *LoxP* sequences in the Arc/Arg3.1$^{f/f}$ mice are located in noncoding genomic regions that could interfere with normal levels and proper control of mRNA expression (promoter and intronic regions), I subjected the Arc/Arg3.1$^{f/f}$ mice to a series of biochemical and behavioral assays to investigate whether they differed from WT littermates.

2.2.1.1. Arc/Arg3.1$^{f/f}$ mice present normal brain morphology and activity-regulated Arc/Arg3.1 expression.

Arc/Arg3.1$^{f/f}$ mice and their WT littermates were subjected to strong neural activity by inducing seizures through intraperitoneal injection of kainate. The animals were anesthetized and intracardially perfused 90 min after the onset of generalized convulsive seizures, and their brains were sectioned and stained for Arc/Arg3.1 protein.

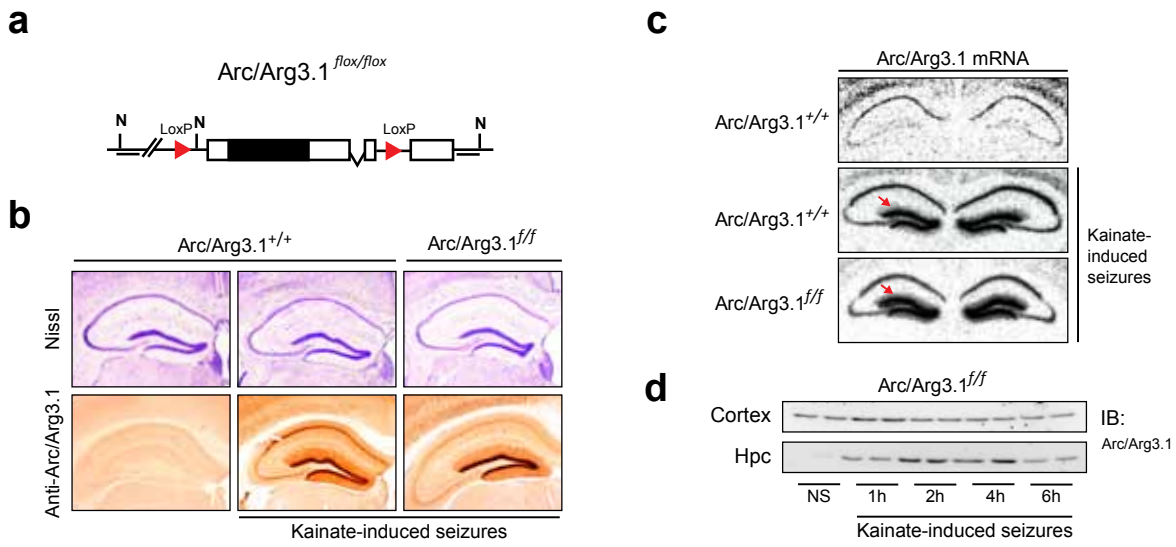

Figure 6. Arc/Arg3.1$^{f/f}$ mice show normal brain morphology and activity-regulated expression of Arc/Arg3.1 mRNA and protein
a. Genomic organization of the mouse Arc/Arg3.1$^{f/f}$ locus with *loxP* sites (red triangles) [Modified from Plath, N. (Plath 2004)]. **b.** Nissl staining reveals similar hippocampal and cortical morphology and layering of WT and Arc/Arg3.1$^{f/f}$ mice. Immunostaining analysis of Arc/Arg3.1 protein displays similar spatial expression pattern and dendritic localization in the hippocampus of WT and Arc/Arg3.1$^{f/f}$ mice after kainate-induced seizures. **c.** Upregulation of Arc/Arg3.1 mRNA in the dHpc of adult mice subjected to kainate-induced seizures. rISH on coronal sections of WT and Arc/Arg3.1$^{f/f}$ brains, red arrows mark dendritic mRNA localization in DG. **d.** Normal upregulation of Arc/Arg3.1 protein and transient time course that peaks within 2 hours and decays after 6 hours in cortex and hippocampus lysates of Arc/Arg3.1$^{f/f}$ mice under control conditions and 1, 2, 4, and 6 hr after kainate-induced seizures (n=1 per each time point).

Compared to WT mice, Nissl stained brain sections of Arc/Arg3.1$^{f/f}$ mice show a similar layering and cellular density, and the Arc/Arg3.1 immunostaining shows identical levels of Arc/Arg3.1 and dendritic distribution (Figure 6b). Radioactive *in situ* hybridizations of WT and Arc/Arg3.1$^{f/f}$ after kainate-induced seizures confirmed that the mRNA is effectively upregulated and located in dendrites where it can be locally translated (Figure 6c).

Additionally, I performed protein analysis from brain lysates using SDS-PAGE and immunoblotting to test Arc/Arg3.1 protein expression in the cortex and hippocampus at different time points after kainate-induced seizures. Arc/Arg3.1$^{f/f}$ mice showed a typical transient time course that peaks within 2 hours and decays after 6 hours (Figure 6d). Hence, I concluded that the spatial-temporal pattern and levels of Arc/Arg3.1 expression are intact in the Arc/Arg3.1$^{f/f}$ mice.

2.2.1.2. Arc/Arg3.1$^{f/f}$ mice show normal locomotor, exploratory and anxiety-like behavior

To test locomotor and exploratory activity, WT and Arc/Arg3.1$^{f/f}$ mice were placed in an open field arena for 5 min (Figure 7a-c). Both genotypes showed similar path lengths (WT, 27.31±1.92 m; Arc/Arg3.1$^{f/f}$, 28.63±1.28 m; t_{22} = - 0.57; p=0.57) and time spent in the center (WT, 8.30±1.34%; Arc/Arg3.1$^{f/f}$, 5.75±0.84%; Mann Whitney U=48; p=0.17, NS; n=12 per group).

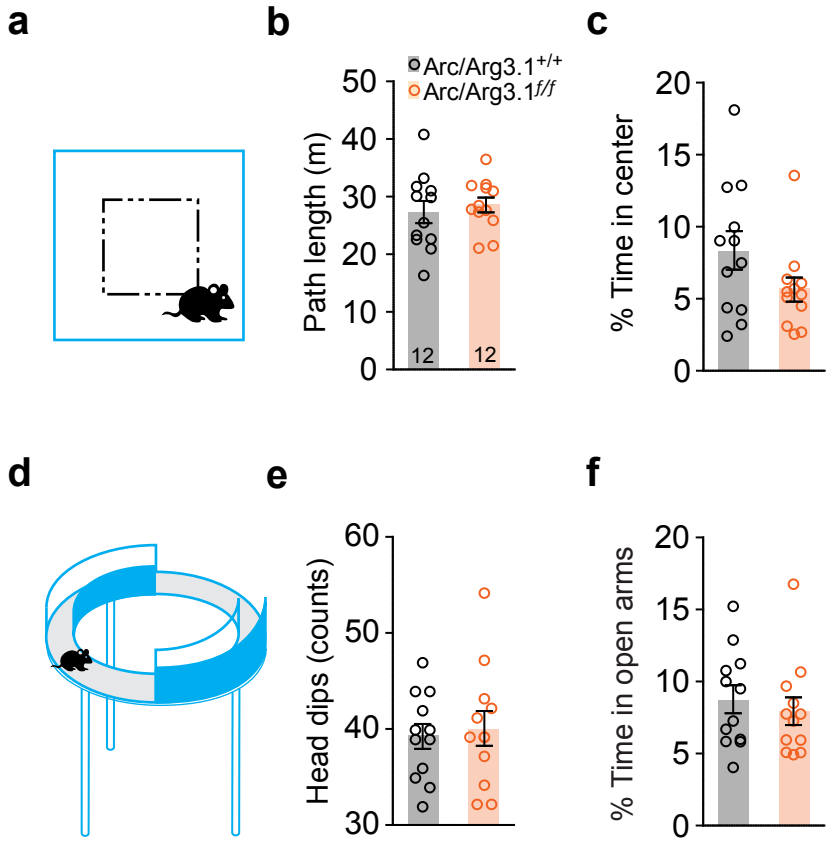

Figure 7. Arc/Arg3.1$^{f/f}$ mice show normal locomotor, exploratory and anxiety-like behavior
a. Exploratory activity in the open field test was similar in WT and Arc/Arg3.1$^{f/f}$ mice
b. Path length in m; WT, 27.31 ± 1.92; Arc/Arg3.1$^{f/f}$, 28.63 ± 1.28; t_{22}=-0.57, p=0.57, NS; and
c. Percent of time spent in the center: WT, 8.30±1.34; Arc/Arg3.1$^{f/f}$, 5.75±0.84; Mann Whitney U=48, p=0.17, NS.
d. Risk assessment and unconditioned avoidance in the Elevated-O maze were similar for WT and Arc/Arg3.1$^{f/f}$ mice.
e. Number of head dips beyond the open arms edges was 39.33±1.30 and 39.92±1.82, respectively, (t_{22}=-0.26, p=0.8, NS) and
f. Percent time spent in the open arms was 8.74±0.97 and 7.95±0.96; Mann Whitney U=60.5, p=0.53, NS.
All error bars show mean ± SEM. n=12 per group.

I next tested the mice in the elevated O-maze, a test to examine anxiety-like behavior (Section 8.7.2). Mice (12 per genotype) were introduced in one of the closed arm and allowed to move freely for 5 min. Head dips were counted as an indication of risk assessment, and the time spent in the open arms as measure of unconditioned avoidance (Figure 7d-f). I found no significant differences in number of head dips beyond the open arms edges (WT, 39.33±1.30; Arc/Arg3.1$^{f/f}$, 39.92±1.82, t_{22}=-0.26; p=0.8) or in percent of time spent in the open arms (WT, 8.74±0.97%; Arc/Arg3.1$^{f/f}$, 7.95±0.96%; Mann Whitney U=60.5, p=0.53; n=12 per group). Arc/Arg3.1$^{f/f}$ mice were identical in exploratory, locomotor and unconditioned avoidance behavior to their WT littermates.

2.2.1.3. Arc/Arg3.1$^{f/f}$ mice exhibit a normal nociceptive threshold, and acquire and consolidate long-term fear memories.

Behavioral paradigms for investigating mnemonic and emotional processes rely on normal sensory function. For example, conditioning procedures depend on normal sensitivity to nociceptive stimuli. Accordingly, the nociceptive threshold was investigated using flinch-jump procedure (Figure 8a). In this test, mice were subjected to increasingly stronger electrical currents while their behavior was closely monitored. The lowest shock intensity eliciting flinch or jump was taken as threshold (Section 8.7.7).

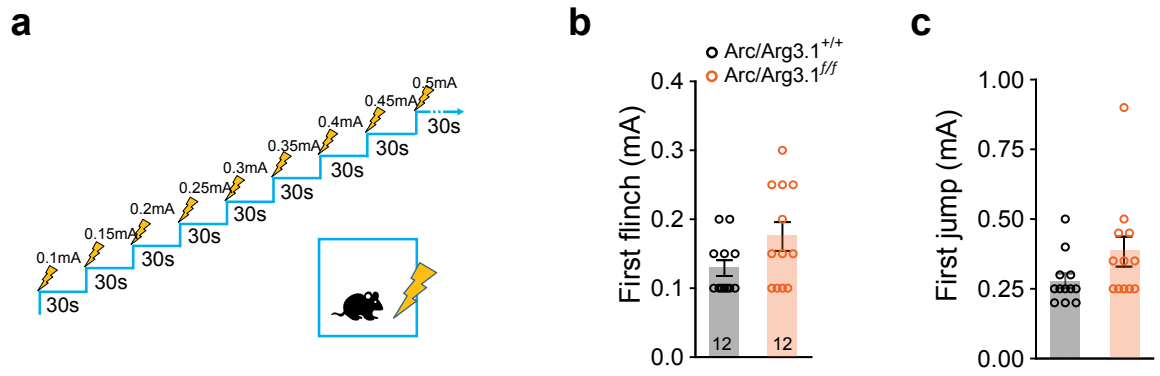

Figure 8. Arc/Arg3.1$^{f/f}$ mice exhibit a normal nociceptive threshold
a. Sensitivity to the electrical thresholds (mA) to elicit stereotypic responses were measured for Arg/Arg3.1 WT (n=12) and Arc/Arg3.1$^{f/f}$ mice (n=12). No differences were found in **b.** the first flinch (in mA; WT, 0.13±0.01; Arc/Arg3.1$^{f/f}$, 0.18±0.02; Mann–Whitney U=45.50, p=0.11, NS) or **c.** the first jump (WT, 0.28±0.03; Arc/Arg3.1$^{f/f}$, 0.38±0.05; Mann–Whitney U=41, p=0.07, NS; WT). All error bars show ± SEM.

The first flinch response in WT ranged from 0.1 to 0.2 mA (0.13 ± 0.01 mA, Mdn=0.1, IQR=0.1-0.15), and in Arc/Arg3.1$^{f/f}$ from 0.1 to 0.3 mA (0.18 ± 0.02 mA, Mdn=0.15, IQR=0.1-0.25), I found no significant differences in the flinch threshold between genotypes (U Mann-Whitney = 45.50, p=0.11). WT showed the first jump in a range from 0.2 to 0.5 mA (0.28 ± 0.03 mA, Mdn=0.25,

IQR=0.21-0.30), and the Arc/Arg3.1$^{f/f}$ from 0.25 to 0.9 mA (0.38±0.05 mA, Mdn=0.35, IQR=0.25-0.45), the genotypes did not differ in the jump threshold (U Mann-Whitney= 41.0, p=0.07). These experiments provide evidence that Arc/Arg3.1$^{f/f}$ show similar nociception for electrical stimuli when compared to WT littermates (Figure 8b-c).

On the basis that the Arc/Arg3.1$^{f/f}$ mice display normal nociception to electrical stimuli, I used Fear Conditioning (FC) as a behavioral paradigm to investigate long-term fear memory. I conditioned 18 mice per genotype using FC - protocol 1 (description in section 8.7.8, Figure 9a and 61d), and tested contextual fear memory retrieval across 3 different delays (1, 7 and 28 days) in groups of 6 mice per genotype and delay. Similar levels of immobility (expressed in % of freezing) were observed during baseline (BL: Arc/Arg3.1 WT, 6.72±1.48%; Arc/Arg3.1$^{f/f}$, 6.49±1.53%) and after conditioning (Post: WT, 15.90±3.75; Arc/Arg3.1$^{f/f}$ 20.04±4.72). As expected, a significant effect for time was found for both genotypes (Conditioning: $F_{(1,34)}$=30.82; ***p<0.001) confirming that the conditioning protocol was effective in inducing fear learning. Moreover, I observed no significant differences in genotype ($F_{(1,34)}$=0.43, p=0.52, NS) or in the interaction between conditioning and genotype ($F_{(1,34)}$=0.65, p=0.43, NS), confirming that Arc/Arg3.1$^{f/f}$ mice possess a intact fear behavior and acquisition of fear associations (Figure 9b).

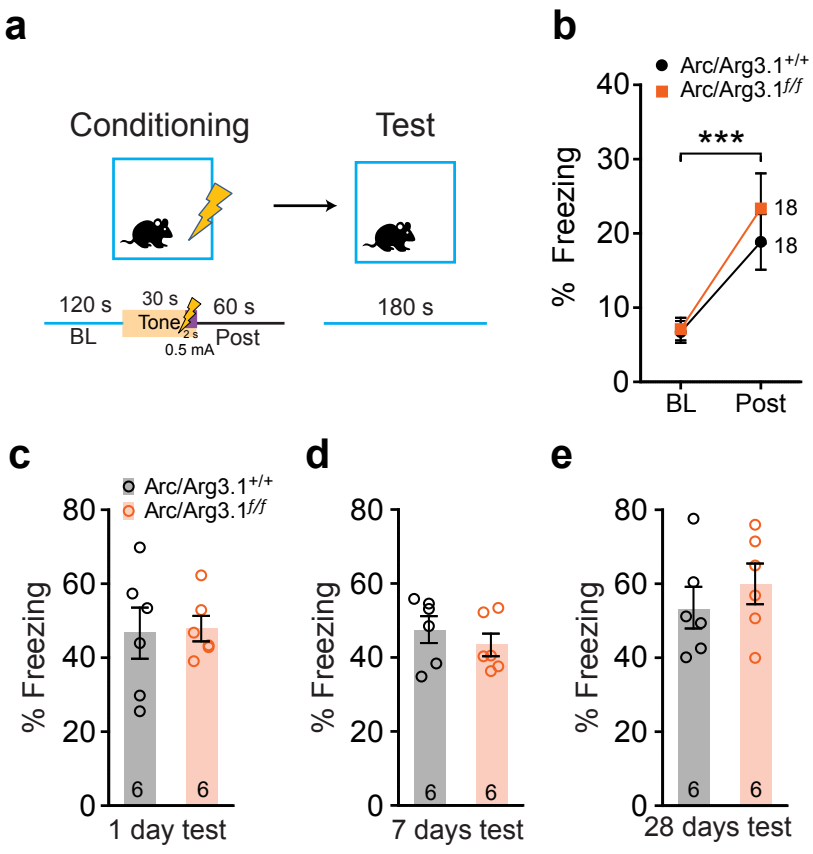

Figure 9. Arc/Arg3.1$^{f/f}$ mice acquire and consolidate long-term fear memories
a. Schematic representation of fear conditioning protocol. **b.** Conditioning was comparable in Arg/Arg3.1 WT and Arc/Arg3.1$^{f/f}$ mice (Freezing in baseline [BL]: WT, 6.72± 1.48; Arc/Arg3.1$^{f/f}$, 7.11±1.53%; Post-conditioning [Post]: WT, 18.85±3.75; Arc/Arg3.1$^{f/f}$ 20.04±4.72%; 2-way RM ANOVA: Conditioning $F_{(1,34)}$=30.82; ***p<0.001; Genotype $F_{(1,34)}$=0.43, p=0.52, NS; Interaction $F_{(1,34)}$=0.65, p=0.43, NS; WT, n=18; Arc/Arg3.1$^{f/f}$, n=18.
Long-term and remote memory in fear conditioning **c.** 1-day test: WT, 47.01 ± 6.92; Arc/Arg3.1$^{f/f}$, 47.81 ± 3.45%; t_{10} = 0.10; p=0.91, NS; WT, n=6; Arc/Arg3.1$^{f/f}$, n=6; **d.** 7 days test: WT, 47.45 ± 3.63; Arc/Arg3.1$^{f/f}$, 43.49 ± 3.05%; t_{10} = 0.83; p=0.42, NS; WT, n=6; Arc/Arg3.1$^{f/f}$, n=6; **e.** 28 days test: WT, 53.26 ± 5.63; Arc/Arg3.1$^{f/f}$, 59.84 ± 5.50%; t_{10} = 0.84; p=0.42, NS; WT, n=6; Arc/Arg3.1$^{f/f}$, n=6). All error bars show mean ± SEM.

WT and Arc/Arg3.1$^{f/f}$ mice showed similar immobility when contextual memory was tested at 1 day (WT, 47.01±6.92%; Arc/Arg3.1$^{f/f}$, 47.81±3.45%; t_{10}=0.10, p=0.91; NS; n=6 per group), 7 days (WT, 53.26±5.63%; Arc/Arg3.1$^{f/f}$, 59.84±5.50%; t_{10}=0.84; NS; p=0.42, NS; n=6 per group) and 28 days after conditioning (WT, 53.26±5.63%; Arc/Arg3.1$^{f/f}$, 59.84±5.50%; t_{10}=0.84, p=0.42, NS; n=6 per group); indicating that both genotypes acquired and consolidated fear memories for prolonged periods.

Taken together, the results suggest that expression of the floxed Arc/Arg3.1 allele in Arc/Arg3.1$^{f/f}$ mice is comparable to the endogenous allele in WT mice. The amount of Arc/Arg3.1, its expression pattern in the brain, dendritic localization and temporal expression pattern were all indistinguishable from WT. Furthermore, Arc/Arg3.1$^{f/f}$ mice have a comparable nociceptive sensitivity, locomotor, exploratory, unconditioned avoidance and fear behavior, and retain contextual memory for similarly prolonged periods of time. Hence, this mouse line is suitable to investigate the role of Arc/Arg3.1 using Cre-*LoxP* systems in a tissue and/or time specific manner without evident off-target effects from *LoxP* sequences.

2.2.2. Generation and validation of an early postnatal Arc/Arg3.1 conditional KO (Early-cKO).

To evaluate the function of Arc/Arg3.1 and its upregulation during postnatal development, I bred the Arc/Arg3.1$^{f/f}$ mice with mice expressing iCre recombinase under the CaMKIIα promoter (Tg[CaMKIIα-cre]1Gsc) (Casanova *et al* 2001) (Figure 10a). Arc/Arg3.1$^{+/+,iCre+}$ (hereafter named WT-Control) and Arc/Arg3.1$^{-/-,iCre+}$ (hereafter named Early-cKO) progeny were obtained. To test iCre activity, I additionally bred the Arc/Arg3.1$^{f/f}$ and Arc/Arg3.1$^{-/-,iCre+}$ with the ROSA26 Cre reporter mouse line (Soriano 1999) in a triple transgenic approach (Figure 10b).

In the F3 generation, *in situ* hybridizations and lacZ staining were performed at 3 different time points across postnatal development (P0, P7 and P14), in order to investigate the efficacy and time of Cre-mediated Arc/Arg3.1 ablation. Albeit positive LacZ staining product of an earlier iCre activity at P0 (Figure 10c, lower panel), I observed a complete lack of Arc/Arg3.1 mRNA at P14 in Early-cKO brain coronal or sagittal slices when compared with age-matched WT-control littermates.

Even though the *in situ* hybridization experiments in Early-cKO brain tissues of first postnatal month showed an apparent complete inactivation of Arc/Arg3.1 loci during the second postnatal week, I examined Arc/Arg3.1 mRNA and protein expression after kainate-induced seizures in

adult mice to assess whether any residual expression of the gene was present following maximal neuronal activation.

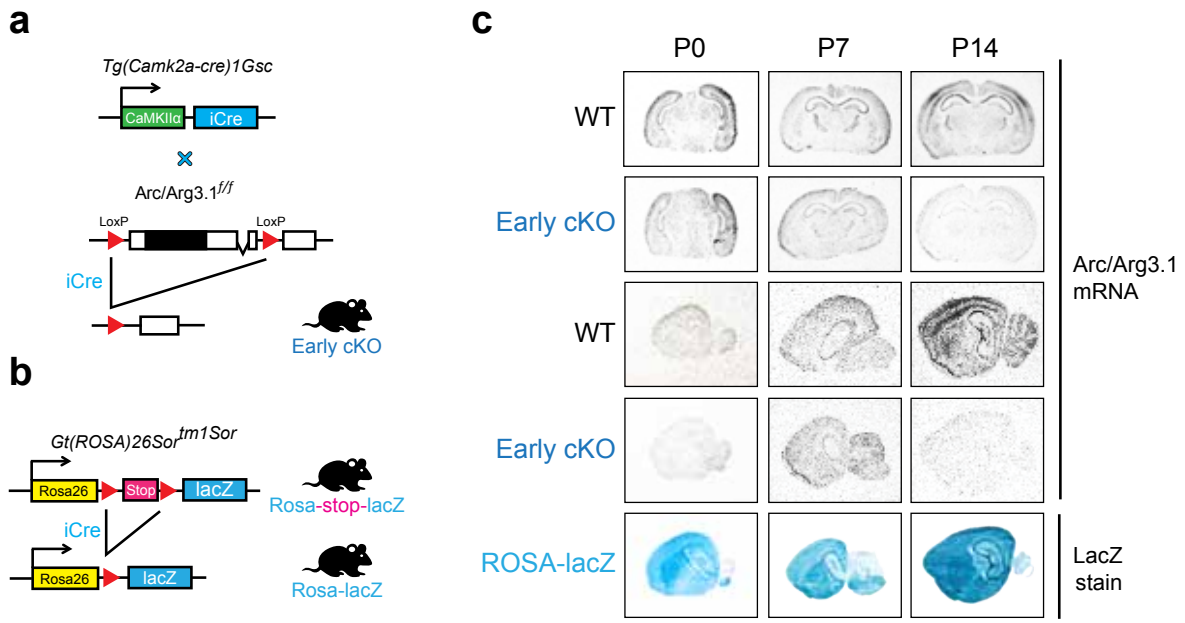

Figure 10. Generation and validation of an early postnatal Arc/Arg3.1 conditional KO (Early-cKO)
a. Genomic organization of the mouse Arc/Arg3.1$^{f/f}$ locus with *LoxP* sites (red triangles) before and after Cre recombination. [Modified from Plath N (Plath 2004)]. **b.** iCre transgenic line (Tg[CaMKIIα-cre]1Gsc) was bred with Arc/Arg3.1$^{f/f}$ mice to generate an early postnatal Arc/Arg3.1 conditional KO (Early-cKO in dark blue). **b.** Gt[ROSA]26Sor^{tm1Sor} indicator mouse line, when crossed with a Cre transgenic strain, lacZ is expressed in cells where Cre expressed. **c.** Albeit an earlier detection of iCre activity at P0 in the same tissue by LacZ staining (lower panel), rISH in coronal and sagittal slices shows that a complete ablation of Arc/Arg3.1 in Early-cKOs takes place between P7-P14.

For this purpose, I performed *in situ* hybridization and immunostaining in coronal slices, and immunoblotting of brain lysates from the cortex (Ctx), hippocampus (Hpc) or amygdala (Amy) dissected from brains of adult WT, constitutive KO and Early-cKO mice subjected to kainate-induced seizures (Figure 11).

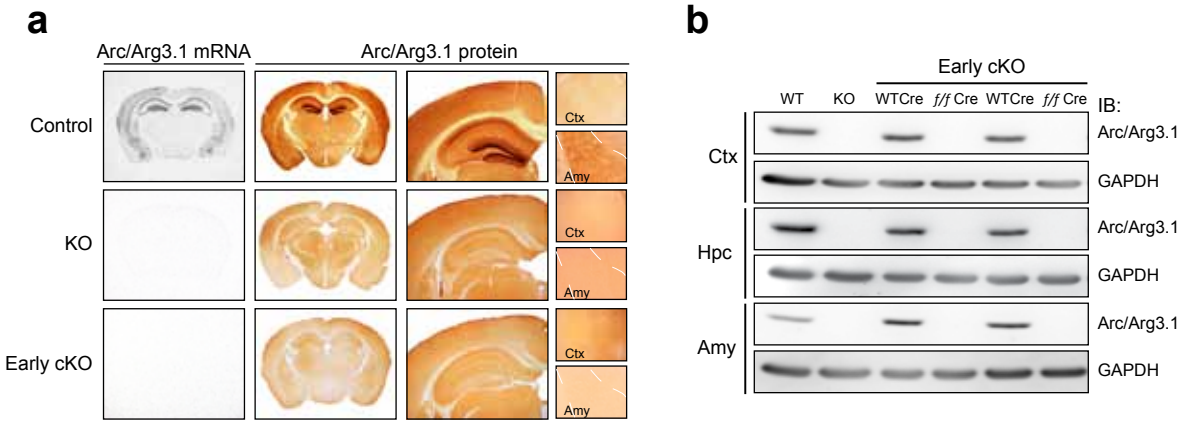

Figure 11. Spatial pattern of ArcArg3.1 mRNA and protein expression in adult Early-cKO
a. Adult Early-cKO mice lack Arc/Arg3.1mRNA and protein expression following kainate-induced seizures. Brain tissues were examined by rISH and immunostaining. **b.** Arc/Arg3.1 protein in brain lysates from cortex (Ctx), hippocampus (Hpc) or amygdala (Amy) is not detected by immunoblotting in adult brains of constitutive KO or Early-cKO mice subjected to kainite-induced seizures.

The results of these experiments confirm that in Early-cKO mice Arc/Arg3.1 is completely removed in the brain and are in agreement with previous reports that show Arc/Arg3.1 mRNA expression only in CaMKIIα positive neurons (Tagawa *et al* 2005, Vazdarjanova *et al* 2006).

2.3. Arc/Arg3.1 expression during early postnatal development sculpts the function of networks for explicit and implicit memory

2.3.1. Early-cKO display impaired consolidation of explicit memories

2.3.1.1. Early conditional ablation of Arc/Arg3.1 impairs long-term object recognition memory in adult mice

To evaluate the impact of Arc/Arg3.1 loss during early postnatal development on cognitive abilities of adult mice, I performed a series of behavioral assays. First, explicit memory in the novel object recognition task (NOR) was examined. NOR is a non-fear motivated behavioral task that requires no reward or punishment, but short habituation and training, and is based on the natural preference of rodents for novelty (Antunes & Biala 2012). It is accepted that the acquisition and consolidation of NOR memory requires structures located in the medial temporal lobe such the perirhinal, entorhinal and inferior temporal cortices, and the hippocampus (Hammond *et al* 2004).

In this behavioral paradigm, mice are habituated to an open field arena for 2 days. In the third day two identical objects are placed in the arena and mice explore them for 10min (acquisition phase). A day later, mice are presented with a replica of the familiar object and a novel object for 10 min (24 h test). Typically, WT mice remember the familiar object and distinguish it from the novel one, and therefore spend a longer time exploring the novel object (Figure 12a). The time in close proximity (2.5 cm around the object) to each object was analyzed for the first 5 min. A preference index (time novel/total time of exploration x 100) and a discrimination index (time with novel – familiar object/total exploration time) were calculated (Section 8.7.4).

WT-control and Early-cKO mice moved similar distances in the open field arena during habituation (WT-control: 30.42±2.07 m; Early-cKO: 27.74±2.49 m; t_{13}=0.76; p=0.46, NS). They also spent similar amount of time exploring the objects during acquisition (WT-control, 26.89±7.63 s; Early-cKO, 18.31±3.89 s; t_{13}=1.10; p=0.29, NS) and test phases (WT-control, 32.34±9.85 s; Early-cKO, 28.21±4.48 s; t_{13}=0.43; p=0.68, NS); suggesting that Early-cKO have normal locomotor activity and response novel objects.

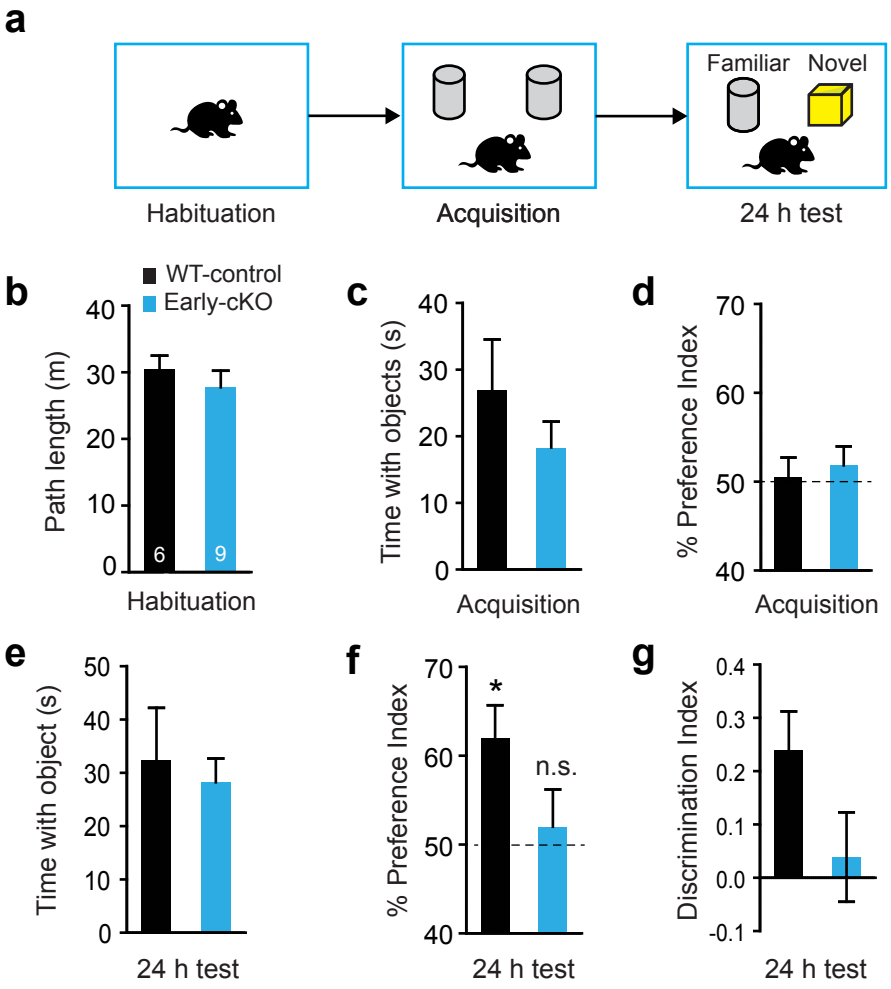

Figure 12. Early conditional ablation of Arc/Arg3.1 impairs long-term object recognition memory in adult mice
a. Schematic representation of the novel object recognition (NOR) task. **b.** WT-controls and Early-cKO walked comparable distances in the open field arena on the first day of habituation (Path length: WT-control, 27.46±2.61 m; Early-cKO, 30.42±2.07 m; t_{13}=0.76; p=0.55, NS) **c.** Total exploration time of objects was not different for WT-control and Early-cKO mice (WT-control: 26.89±7.63 m; Early-cKO: 18.31±3.89 m; t_{13}=1.10; p=0.3, NS) **d.** Both genotypes show a Preference Index (%PI) in the chance level range (50%) for each identical object during the acquisition phase (PI: WT-control, 51.84±2.14 %, t_5=0.86; p=0.43, NS; Early-cKO, 50.55±2.17%; t_8=0.26; p=0.81, NS; one sample t-test) **e.** No differences in the total object-exploration time were observed between the genotypes during the test phase (Time in s: WT-control, 32.34±9.85 m; Early-cKO, 28.21±4.48 m; t_{13}=0.43; p=0.68, NS). **f.** WT-control but not Early-cKO mice preferentially explored the novel object (WT-control: 62.00±3.69 %, t_5=3.25, *p<0.05, n=6 and Early-cKO; 52.02±4.19 %, t_8=0.48; p=0.64, NS, n=9, respectively). **g.** Nonsignificantly reduced discrimination index in Early c-KO (WT-control, 0.24±0.07; Early-cKO, 0.04±0.08; t_{13}=1.67, p=0.12, NS).

When presented with the replica of the familiar object and a novel object, WT-control mice recognized the replica, and preferentially explored the novel object for times significantly longer than chance level (50%) (62.00±3.69%, t_5=3.25, *p<0.05, n=6, one sample t-test). In contrast, Early-cKO mice displayed no preference for novel or familiar objects (52.02±4.19%, t_8=0.48, p=0.64, NS, n=9, one sample t-test). Moreover, a nonsignificant reduction in the discrimination index in Early cKO compared to the WT-control was found (WT-control, 0.24±0.07; Early-cKO, 0.04±0.08; t_{13}=1.67, p=0.12, NS).

The NOR task results suggest that Early-cKO lack the ability to recognize familiar over novel objects after 1-day delay, and therefore imply that the long-term object recognition might be impaired. It is intriguing if this memory deficit is due to an impaired acquisition of the task, and hence short-term object recognition memory remains to be tested in these mice. Nonetheless, the constitutive Arc/Arg3.1 KO mice displayed intact short-term recognition for novel objects (Plath *et al* 2006), suggesting that it is likely that Early-cKO mice acquire similarly this type of memory.

2.3.1.2. Adult Early-cKO mice exhibit impaired spatial reference memory

Spatial learning and memory was next investigated using the Morris water maze (MWM) as a task to examine explicit learning and memory that rely on hippocampal functions (Morris *et al* 1982). The MWM consisted of a training phase (acquisition), in which the mice were introduced daily into a circular pool filled with opaque water. Animals were required to find a hidden platform for escaping the water using distant visual cues around the pool. If unable to find the platform, they were guided to it. With time and multiple repetitions, the mice learned to locate the platform using spatial strategies. Once the learning curve reached an asymptotic and steady state, memory was assessed at different time points by removing the platform and re-introducing the animal into the pool (probe test). If the consolidation of the spatial information was optimal, mice swim directly towards the platform location and if not present persistently look for its original location. At the end, as a control procedure, an additional set of training sections with a flag signaling the platform (visible - cued version) was given to test the visual and motor function of the animals (Figure 13a).

I trained a cohort of Early-cKO mice and compared them with matched WT-controls in the MWM task. During the acquisition, WT-control mice improved their escape strategy as reflected in shorter path lengths and latencies to the platform (Figure 13 b-c). Early-cKO mice show a mild imperment at the beginning of the learning curve (2-way RM ANOVA for path length to the platform: genotype $F_{(1,17)}$=3.81; p=0.7, NS; Blocks $F_{(9,153)}$=19.83, ***p<0.0001; interaction $F_{(9,153)}$=2.04, *p<0.05; Fisher LSD post hoc analysis *p<0.05); especially at earlier time points in training (blocks 1 and 3) but reached similar scape latencies after intensive training (2-way RM ANOVA; genotype $F_{(1, 17)}$=1.49, p=0.24, NS; Blocks $F_{(9,153)}$=23.80, ***p<0.0001; interaction $F_{(9,153)}$ =1.84, p=0.07, NS)

The mild deficit in Early-cKO mice was observed only in parameters related to the spatial learning (path length to the platform and escape latency). No impairments in motor function or motivation were found as shown by comparable swim speeds (Figure 13 d) (2-way RM ANOVA Velocity in cm/s; genotype $F_{(1, 17)}$=0.01, p=0.91, NS; blocks $F_{(9,153)}$=2.38, *p<0.05; interaction $F_{(9,153)}$=1.48,

p=0.16, NS) or the time to swim or float in an area of 20 cm near to the walls (Figure 13 e) (2-way RM ANOVA Thigmotaxis in s; genotype $F_{(1,17)}$=0.22, p=0.64, NS; block $F_{(9,153)}$=31.50, ***p<0.001; interaction $F_{(9,153)}$=0.52, p=0.86, NS).

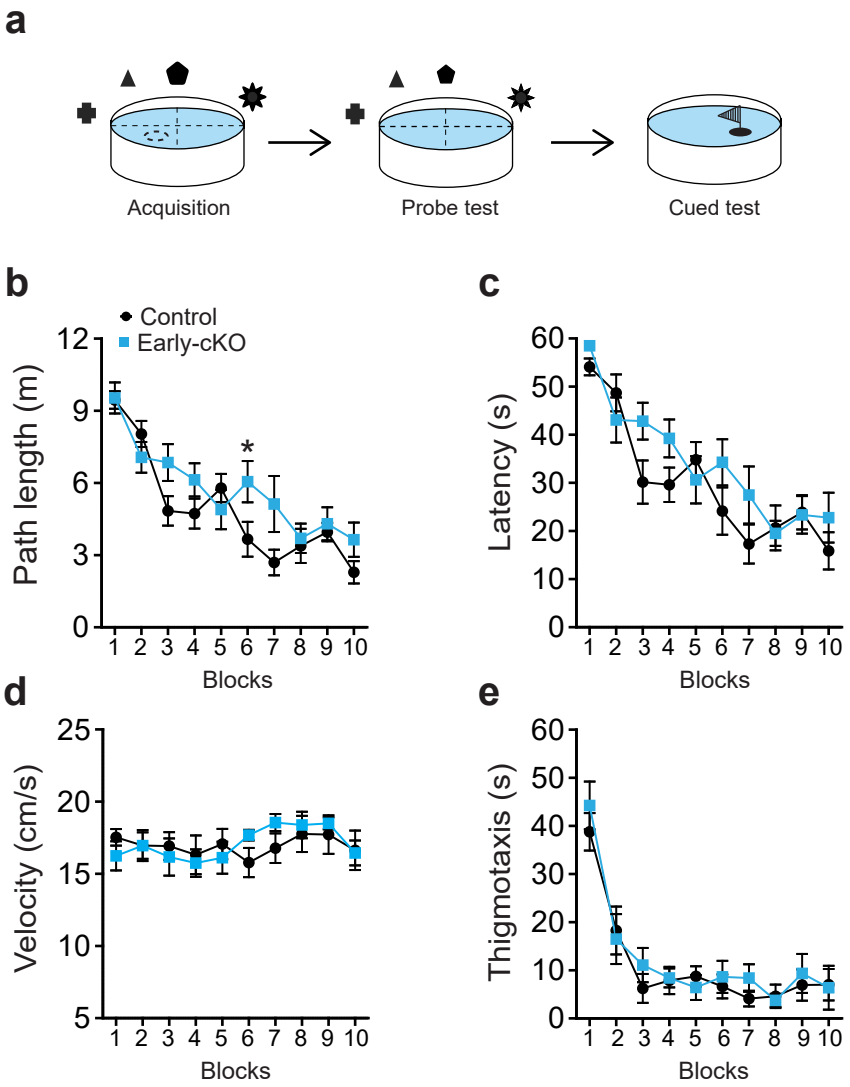

Figure 13. Spatial learning in adult Early-cKO mice
a. Schematic representation of the Morris water maze (MWM) navigation task. **b.** Early-cKO mice show mild impairment at the beginning of the learning curve (Path length to the platform: genotype $F_{(1,17)}$=3.81, p=0.07, NS; blocks $F_{(9,153)}$=19.83, ***p<0.001; interaction [genotype*blocks] $F_{(9,153)}$=2.04, *p<0.05). **c.** Early-cKO learn to locate the hidden platform more slowly (blocks 1 and 3) than WT-control littermates but reach similar escape latencies after intensive training (genotype $F_{(1,17)}$=1.49, p=0.24, NS; block $F_{(9,153)}$=23.80, ***p<0.001; interaction $F_{(9,153)}$=1.84, p=0.07, NS). **d.** No differences in swim speed (Velocity in cm/s: genotype $F_{(1,17)}$=0.01, p=0.91, NS; blocks $F_{(9,153)}$=2.38, *p<0.05; interaction $F_{(9,153)}$=1.48, p=0.16, NS) or **e.** Thigmotatic behavior (genotype $F_{(1,17)}$=0.22, p=0.64, NS; block $F_{(9,153)}$=31.50, ***p<0.001; interaction $F_{(9,153)}$ = 0.52, p=0.87, NS). All error bars represent the mean ± SEM. Significance was assessed with a 2-way RM ANOVA and post hoc Fisher LSD test; *p<0.05. WT-control, n=10; Early-cKO, n=9.

The consolidation of long-term spatial reference memory was tested by performing two probe trials, 1 day after the 9th and before 10th block of training and 7 days after the last training block (Figure 14). In the first probe trial, both WT-control and Early-cKO spent significantly more time exploring the target quadrant (T) (Figure 14b) (2-way ANOVA: Genotype $F_{(1,68)}$=0, p=1, NS;

Quadrants $F_{(3,68)}$=10.22; ***p<0.001; Interaction $F_{(3,68)}$=0.78, p=0.78; NS). Although Early-cKO mice acquired information about the location of the platform as reflected in the quadrant occupancy, they exhibited an imprecise 1 day memory as depicted by the averaged density plots (Figure 14 a) and a significantly decreased number of crossings in the area around the platform (annulus crossings) when compared to homologous areas in other quadrants (Figure 14c) (1way-ANOVA for WT-Control, $F_{(3,39)}$=9.15, ***p<0.001; Early-cKO, $F_{(3,35)}$=2.08, p=0.12, NS). Thus, Early-cKO mice display a less accurate spatial reference memory even 1 day after last training block. Taken together these results, it is reasonable to hypothesize that the removal of Arc/Arg3.1 in Early-cKO affects off-line consolidation of precise spatial information.

To evaluate if the observed spatial memory in Early-cKO mice deteriorates with time, an additional training block was performed the same day after the first memory test and the persistence of long-term memory was evaluated 7 days later performing an additional probe trial (Figure 14d-f). Remarkably, the averaged density plot from Early-cKO depicted a complete lack of spatial bias for the platform when compared to WT-controls' plot (Figure 14 d). Moreover, a highly significant difference between WT-control and Early-cKO was found in the percentage of time spent in the target quadrant (2-way ANOVA: Genotype $F_{(1,68)}$=2.57^{-14}, p=1, NS; Quadrants $F_{(3,68)}$=11.18; ***p<0.001; Interaction $F_{(3,68)}$=11.75, ***p<0.001; Bonferroni post hoc test T:$^{###}$p<0.001, L: $^{##}$p<0.01) and annulus crossing to target zones (2-way ANOVA: Genotype $F_{(1,68)}$=2.23, p=0.13, NS; Quadrants $F_{(3,68)}$=12.82; ***p<0.001; Interaction $F_{(3,68)}$=4.96, ***p<0.01; Bonferroni post hoc test T: $^{###}$p<0.001). These probe trials confirmed that the expression of Arc/Arg3.1 during early postnatal development interferes with long-term consolidation of spatial reference memory.

After memory tests, the same groups were additionally trained in a visible platform version of the MWM to evaluate whether this severe impairment in consolidation of spatial memory arose from motor, visual or emotional deficits. In this procedure, all visual cues around the pool were removed and the mice located the platform in a different position for each trial by a flag that signaled its location (Figure 15a). Interestingly, Early-cKO outperformed WT-controls gauged from path length (Figure 15b) (Genotype $F_{(1,17)}$=5.87, $^{#}$p<0.05; trial block $F_{(2,34)}$=11.58, ***p<0.001; interaction $F_{(2,34)}$=0.26, p=0.77, NS), latency to the platform (Figure 15c) (Genotype $F_{(1,17)}$=3.60, p=0.075, NS; block $F_{(2,34)}$=13.01, ***p<0.001; interaction $F_{(2,34)}$=0.07, p=0.9, NS) or immobility (Genotype $F_{(1,17)}$=3.93, p=0.064, NS; block $F_{(2,34)}$=11.88, ***p<0.001; interaction $F_{(2,34)}$=0.03, p=0.98, NS); suggesting that Early-cKO mice have normal visual perception and an apparent better cued learning. These results may be explained by the assumption that WT-control are confounded with old memories of previous procedures and therefore learn the new procedure slowly, or it is possible that Early-cKO present a faster extinction that allow a more efficient cue learning.

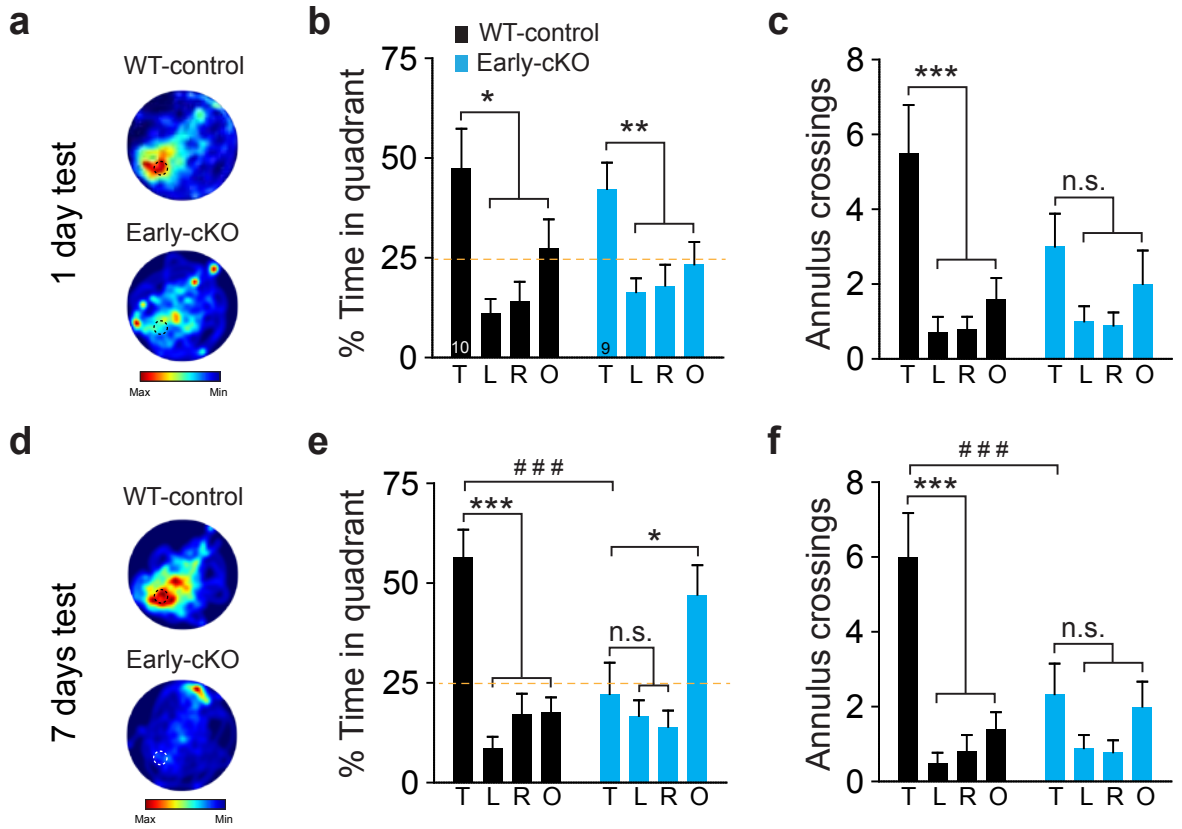

Figure 14. Impaired long-term spatial reference memory in Early-cKO adult mice
a. Spatial memory test 1 day after last training block. Density plots show that Early-cKO performed an imprecise search strategy compared to the WT-control mice. **b.** WT-control and Early-cKO spent significantly more time exploring the target quadrant (T) (WT-Control T: 47.38±9.96 ; L: 11.07±3.60; R: 14.15±4.84; O: 27.4 ±7.23%, 1way-ANOVA $F_{(3,39)}$=5.81, **p<0.01, Dunnett's multiple comparison test T vs L: **p<0.01; T vs R: **p<0.01 T vs O, NS; Early-cKO T: 42.23±6.61; L: 16.39±3.47; R: 18.04±5.23; O: 23.34±5.63, 1way-ANOVA $F_{(3,35)}$=4.90, **p<0.01, Dunnett's test T vs L: **p<0.01; T vs R: **p<0.01 T vs O, *p<0.05) **c.** Early-cKO show imprecise memory with nonsignificant crossings to the target zone when compared to other zones (Early-cKO T: 3.00±0.88; L: 1.00 ± 0.41; R: 0.89±0.35; O: 2.00±0.90, 1way-ANOVA $F_{(3,35)}$=2.08, p=0.12, NS). **d.** 7 days spatial memory test. Density plots show that Early-cKO lack spatial bias for the platform position compared to the WT-control mice. **e.** High significant difference between WT-control and Early-cKO in % time spent in target quadrat (2-way ANOVA: Genotype $F_{(1,68)}$=2.57^{-14},p=1, NS; Quadrants $F_{(3,68)}$=11.18; ***p<0.001; Interaction $F_{(3,68)}$=11.75,***p<0.001; Bonferroni post hoc test T: $^{###}$p<0.001, L: p<0.01; R: NS, O: NS. WT-control but not Early-cKO displayed a significant occupancy in target quadrant when compared to other quadrants (WT-Control T: 59.47 ± 6.92; L: 8.62±2.87; R: 17.14±5.14; O: 17.77±3.60%, 1way-ANOVA $F_{(3,39)}$=19.17, ***p<0.0001, Dunnett's multiple comparison test T vs L: ***p<0.001; T vs R: ***p<0.001 T vs O, ***p<0.001; Early-cKO T: 22.20±7.85; L: 16.71±3.92; R: 14.00±4.05; O: 47.09±7.41%, 1way-ANOVA $F_{(3,35)}$=6.16, **p<0.01, Dunnett's test T vs L: NS; T vs R: NS; T vs O, *p<0.05;). **f.** High significant difference between WT-control and Early-cKO in annulus crossing of the target zone (2-way ANOVA: Genotype $F_{(1,68)}$=2.23, p=0.13, NS; Zone $F_{(3,68)}$=12.82; ***p<0.001; Interaction $F_{(3,68)}$=4.96, ***p<0.01; Bonferroni post hoc test T: $^{###}$p<0.001, L: NS; R: NS, O: NS). Morover, WT-control but not Early-cKO crossed significantly more times the annulus area around the platform when compared to other annulus areas (WT-Control T: 6±1.17; L: 0.5±0.27; R: 0.8±0.44; O: 1.40±0.45, 1way-ANOVA $F_{(3,39)}$=14.36, ***p<0.0001, Dunnett's test T vs L: ***p<0.001; T vs R: ***p<0.001 T vs O, ***p<0.001. Early-cKO T: 2.33±0.82; L: 0.88±0.35; R: 0.78±0.32; O: 2±0.67, 1way-ANOVA $F_{(3,35)}$=1.83, p=0.16, NS). All error bars represent mean ± SEM. WT-control, n=10; Early-cKO, n=9.

Early-cKO and WT-controls swam comparably similar time in the vicinity of walls (2-way RM ANOVA thigmotaxis: Genotype $F_{(1,17)}$=0.82, p=0.38, NS; block $F_{(2,34)}$=6.92, **p<0.01; interaction $F_{(2,34)}$=0.68, p=0.51, NS) with similar speed (Velocity cm/s: Genotype $F_{(1,17)}$=0.82, p=0.58, NS; block $F_{(2,34)}$=6.92, p=0.85, NS; interaction $F_{(2,34)}$=0.68, p=0.66, NS), demonstrating that Early-cKO display normal motor activity and motivation for novel cued learning.

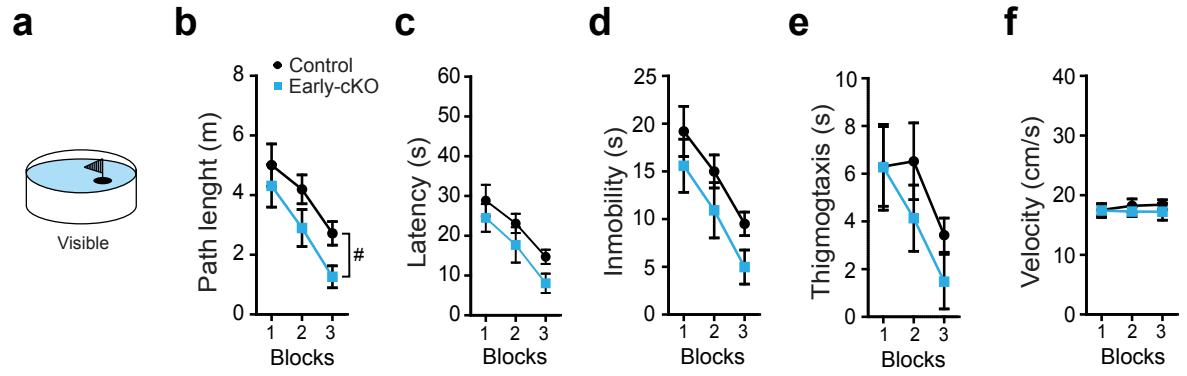

Figure 15. Enhanced cued learning in adult Early-cKO
a. Schematic representation of visible version of MWM. Early-cKO outperformed WT-controls in cued learning curves gauged from **b.** Path length (Genotype $F_{(1,17)}$=5.87, $^{\#}p<0.05$; trial block $F_{(2,34)}$=11.58, $^{***}p<0.001$; interaction $F_{(2,34)}$= 0.26, p=0.77, NS); **c.** Latency to the platform (Genotype $F_{(1,17)}$=3.60, p=0.07, NS; trial block $F_{(2,34)}$=13.01, $^{***}p<0.001$; interaction $F_{(2,34)}$=0.07, p=0.9, NS) and **d.** Immobility (Genotype $F_{(1,17)}$=3.93, p=0.06, NS; trial block $F_{(2,34)}$=11.88, $^{***}p<0.001$; interaction $F_{(2,34)}$ =0.03, p=0.97, NS). **e.** Both genotypes display comparable thigmotaxis (Genotype $F_{(1,17)}$ = 0.82, p=0.37, NS; trial block $F_{(2,34)}$=6.92, $^{**}p<0.01$; interaction $F_{(2,34)}$=0.68, p=0.5, NS) and **f.** Velocity (Genotype $F_{(1,17)}$=0.31, p=0.85, NS; trial block $F_{(2,34)}$=0.49, p=0.85; interaction $F_{(2,34)}$=0.42, p=0.66, NS). Significance was assessed with a 2-way RM ANOVA. All error bars represent mean ± SEM. WT-control, n=10; Early-cKO, n=9.

Altogether, MWM in Early-cKO demonstrates that the removal of Arc/Arg3.1 during the second postnatal week disturbed consolidation of spatial reference memory, without affecting motivation, motor or visual processing.

2.3.2. Early-cKO display disrupted implicit memory in conditioned test aversion

In contrast to explicit memories, it has been proposed that implicit or nondeclarative memories rely partially on different brain areas and circuits such as amygdala, striatum or cerebellum (Henke 2010). As described earlier, some of these structures also naturally upregulate Arc/Arg3.1 expression during early postnatal development, suggesting that developmental Arc/Arg3.1 expression may participate also in the establishment of circuits for implicit memories and emotional processing.

To evaluate this possibility, I used the conditioning taste aversion (CTA) as a model of implicit associative learning. In CTA, the consumption of a solution with a sweet taste (usually saccharin, as a conditioned stimulus [CS]) is followed by the induction of malaise and visceral illness (achieved by intraperitoneal injection of LiCl, as unconditioned stimulus [US]), this paired stimulation induces aversive learning that can be evaluated by presenting the taste together with a neutral solution (water). If CTA memory is acquired and consolidated mice will normally prefer to consume the neutral solution and avoid the conditioned taste (Figure 16a). CTA involves diverse areas such as the pontine parabrachial nuclei, amygdala, insular cortex, supramammillary nucleus, nucleus accumbens, ventral pallidum, gustatory and insular cortices (Yamamoto 2007).

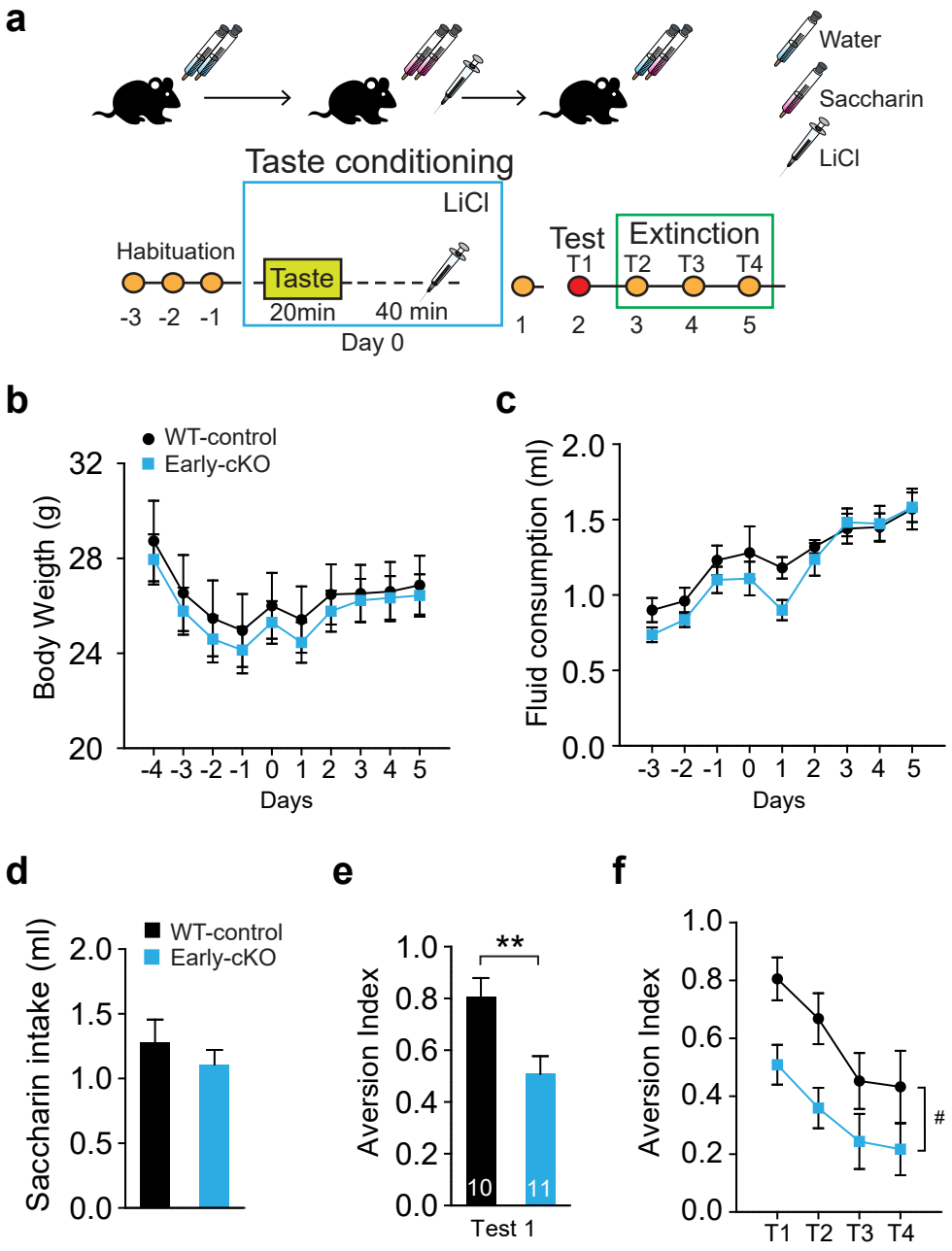

Figure 16. Conditioned taste aversion memory and extinction in adult Early-cKO
a. Schematic representation of CTA protocol. **b.** Comparable variation in body weight through CTA procedures (Genotype $F_{(1,19)}$=0.16, p=0.69, NS; Time $F_{(9,171)}$=55.95, ***p<0.001; Interaction $F_{(9,174)}$=0.71, p=0.70, NS). **c.** Early-cKO show comparable liquid consumption during CTA (Genotype $F_{(1,19)}$=1.31, p=0.27, NS; Time $F_{(9,171)}$=20.90, ***p<0.001; Interaction $F_{(9,174)}$=0.86, p=0.55, NS). **d.** Comparable saccharin intake in both genotype at condition day (WT-control, 1.28±0.17; Early-cKO 1.11±0.11 ml; t_{19}=0.84, p=0.41, NS). **e.** Early cKO exhibit impaired CTA memory retrieval (WT-control, 0.81±0.07; Early-cKO 0.51±0.10 ml; t_{19}=2.95, **p<0.01). **f.** WT-control and Early cKO extinguish CTA memory (Genotype $F_{(1,19)}$=5.39, #p<0.05; Time $F_{(9,57)}$=19.75, ***p<0.001; Interaction $F_{(9,57)}$=0.56, p=0.64, NS). Significance was assessed with a two-tailed unpaired t-test and 2-way RM ANOVA. All error bars represent ±SEM. WT-control, n=10; Early-cKO, n=9.

I performed CTA in Early-cKO adult mice and tested CTA memory retrieval 2 days after conditioning and CTA extinction for 3 additional days (Figure 16a). The CTA procedure requires water restriction, strict control and monitoring of liquid consumption and weight loss. I observed similar and nonsignificant variations in body weight (Figure 16b) between Early-cKO and their

WT-control littermates (2-way RM ANOVA Genotype $F_{(1,19)}$=0.16, p=0.69, NS; Time $F_{(9,171)}$=55.95, ***p<0.001; Interaction $F_{(9,174)}$=0.71, p=0.70, NS). Furthermore, both genotypes consumed similar amounts of saccharin before conditioning (Figure 16d) (WT-control, 1.28±0.17 ml; Early-cKO 1.11±0.11; t_{19}=0.84, p=0.41, NS).

Interestingly, I observed that both Early-cKO and WT-control littermates consumed similar amounts of liquid throughout the whole procedure, except for day 1 after conditioning (Figure 16c) (2way-RM ANOVA Genotype $F_{(1,19)}$=1.31, p=0.27, NS; Time $F_{(9,171)}$=20.90), ***p<0.001; Interaction $F_{(9,174)}$=0.86, p=0.55, NS), suggesting that Early-cKO mice have an enhanced aversion after conditioning that disappears at the testing day with a significantly impaired retrieval of CTA memory, showed by a normal liquid intake but decreased aversion index for saccharin consumption (ml water/ml water + ml saccharin) (Figure 16e) (WT-control, 0.81±0.07 ml; Early-cKO 0.51±0.10; t_{19}=2.95, **p<0.01).

Moreover, I assessed CTA extinction by performing 3 additional tests in consecutive days, both WT-control and Early-cKO mice displayed rapid CTA extinction (Figure 16f) (2way-RM ANOVA Genotype $F_{(1,19)}$=5.39, #p<0.05; Time $F_{(9,57)}$=19.75; ***p<0.001; Interaction $F_{(9,57)}$=0.56; p=0.64, NS). Extinction in Early-cKO appeared to be more complete probably due to their impairment in consolidation and continuous forgetting.

CTA procedures demonstrate that the ablation of Arc/Arg3.1 in principal neurons during early postnatal development not only impairs the consolidation and retrieval of implicit memories, but enhances the aversive responses after acquired conditioned associations, since Early-cKO mice displayed lower consumption of water a day after CTA despite the water restriction regimen.

2.3.3. Early postnatal inactivation of Arc/Arg3.1 alters fear acquisition, memory and extinction

2.3.3.1. Enhanced fear acquisition, but impaired fear memory consolidation

Implicit and explicit memories are also investigated by Pavlovian fear conditioning (FC). In adulthood, fear conditioning depends on the normal function of structures such as Amy, Hpc and the PFC (mPFC and ACC) (Orsini & Maren 2012); which exhibit a natural upregulation of Arc/Arg3.1 after the second postnatal week, leading to the hypothesis that this gene may interfere with their normal functional development and future function in the adult brain.

I performed delay FC in a group of 19 Early-cKO mice and 20 matched WT-controls using proto-

col 1 (Figure 17a, c, f and 61d) and tested their contextual (explicit) and cued (implicit) memories at 1 day (WT-control, n=10; Early-cKO, n=10) or 7 days delay (WT-control, n=10; Early-cKO, n=9). Remarkably, Early-cKO displayed significantly higher immobility after the CS-US presentation than WT-control during fear conditioning acquisition (Figure 17b) (2way-RM ANOVA Genotype $F_{(1,37)}$=2.76, ###p<0.001; Time $F_{(2,74)}$=95.28; ***p<0.001; Interaction $F_{(2,740)}$=11.53; ***p<0.0001; post hoc Fisher LSD test; ***p<0.0001), suggesting that early postnatal expression of Arc/Arg3.1 may participate in the postnatal development of structures that control fear acquisition and expression conferring these mice an enhanced fear learning.

I tested retrieval of long-term explicit and implicit memories in two independent groups across two time points (1 and 7 days), by placing the animals in the conditioning environment (contextual test, figure 17c) and in a novel environment where the tone was presented after a period of habituation (cued test, Figure 17f), respectively. WT-control and Early-cKO exhibited a comparable retrieval of explicit memory when reintroduced to the context 1 day after conditioning (Figure 17d and i) (2-way RM ANOVA for 1 min bin: Genotype $F_{(1,17)}$=0.37, p=0.55, NS; Time $F_{(2,34)}$=4.22; *p<0.05; Interaction $F_{(2,34)}$=1.11, p=0.34, NS. In Figure 17i: Freezing during context: WT-control 47.15±3.71; Early-cKO 43.27±4.00, t_{17}=0.71, p=0.49, NS).

Furthermore, I found a significant difference in retrieval of implicit memory during the second minute bin of the cued test 1 day after conditioning (Figure 17g and i) (2-way RM ANOVA for 1 min bin: Genotype $F_{(1,17)}$=1.34, p=0.26, NS; Time $F_{(1,17)}$=30.56; ***p<0.001; Interaction $F_{(1,17)}$=6.08, *p=0.03. post hoc Fisher LSD test: *p<0.05; In Figure 17i, freezing in altered: WT-control 17.95±4.45; Early-cKO 15.15±3.59, t_{17}=0.48, p=0.63, NS; freezing during cue: WT-control 44.43±7.04%; Early-cKO 36.45±5.96%, t_{17}=0.85, p=0.41, NS), indicating a significantly faster cued extinction (Figure 17g).

To evaluate the persistence of fear memory, I tested 7 days after conditioning a separate group of WT-control (n=10) and Early-cKO (n=10) mice. Strikingly, Early-cKO showed a highly significant reduction of freezing during the entire duration of the contextual test (Figure 17h and j) (2-way RM ANOVA for 1 min bin: Genotype $F_{(1,18)}$=12.72, ##p<0.01; Time $F_{(2,36)}$=7.71; **p<0.01; Interaction $F_{(2,36)}$=0.28, p=0.75, NS; In figure 17 i: Freezing during context: WT-control 52.90±3.33; Early-cKO 21.07±6.35, t_{18}=4.439, ***p<0.001). During cued test Early-cKO mice froze significantly less than their WT-control especially in the first minute of cue retrieval (2-way RM ANOVA for 1 min bin: Genotype $F_{(1,18)}$=1.62, p=0.22, NS; Time $F_{(1,18)}$=58.96;***p<0.001; Interaction $F_{(1,18)}$ = 3.62, *p<0.05 , post hoc Fisher LSD test; *p<0.05. In Figure 17j freezing in altered: WT-control 7.30±1.81; Early-cKO 8.71±3.72, t_{18}=0.34, p=0:74; NS; freezing during cue: WT-control

49.64±5.73; Early-cKO 30.52±5.80 %, t_{18}=2.35, *p<0.05).

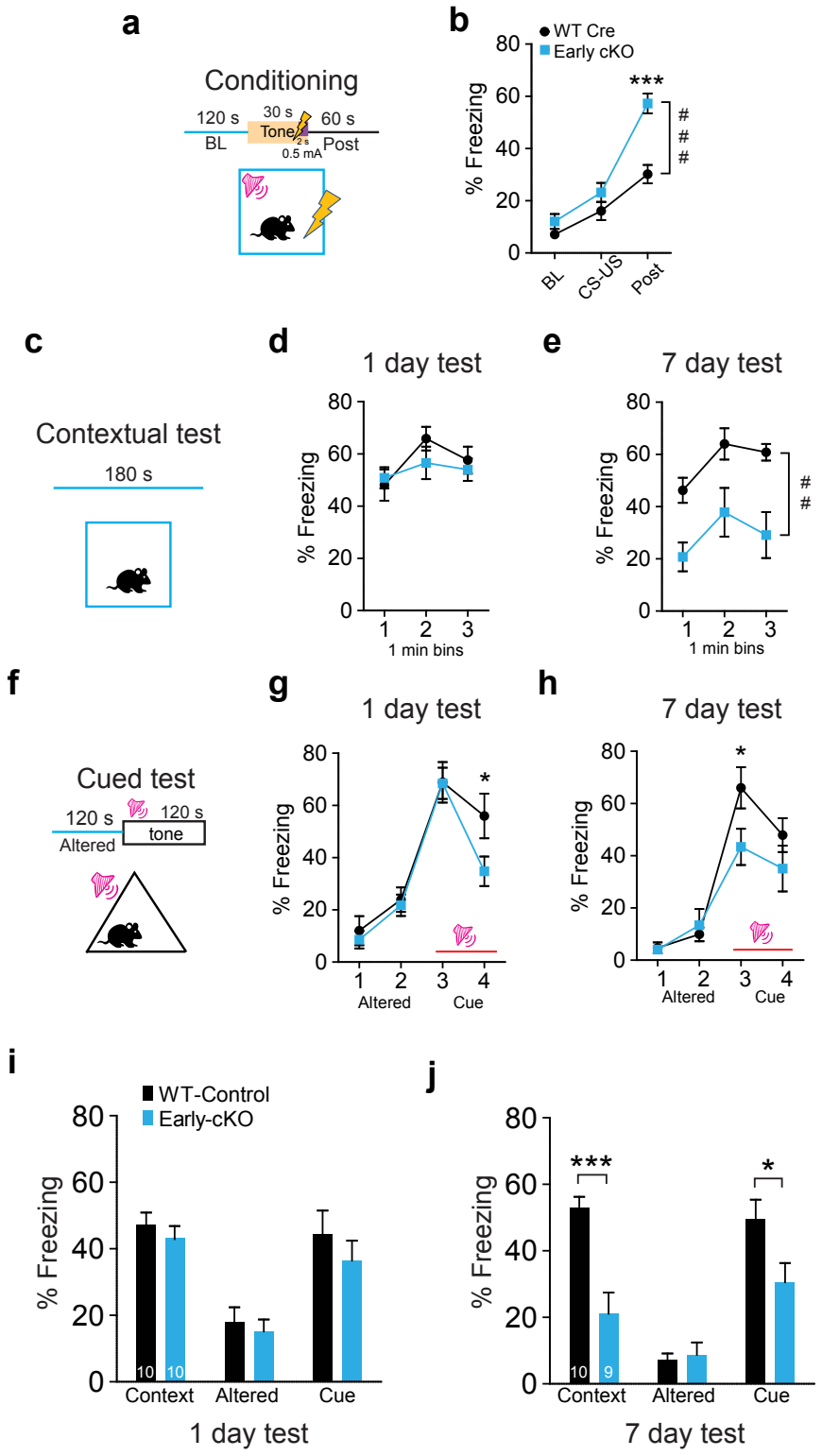

Figure 17. Early-cKO display enhanced learning but disrupted fear memory
a. Schematic representation of fear conditioning protocol **b.** Early-cKO display enhanced fear response after the CS-US presentation (2way-RM ANOVA Genotype $F_{(1,37)}$=2.76, ###p<0.001; Time $F_{(2,74)}$=95.28; ***p<0.001; Interaction $F_{(2,74)}$=11.53; ***p<0.0001; post hoc Fisher LSD test; ***p<0.001). **c.** Schematic representation of contextual test. **d.** Comparable contextual retrieval in WT-control and Early-cKO 1 day after conditioning (Genotype $F_{(1,17)}$=0.37, NS; Time $F_{(2,34)}$=4.22; *p<0.05; Interaction $F_{(2,34)}$ = 1.11, NS). **e.** Early-cKO display impaired contextual retrieval 7 days after conditioning (Genotype $F_{(1,18)}$=12.72, ##p<0.01; Time $F_{(2,36)}$=7.71;**p<0.01; Interaction $F_{(2,36)}$ = 0.28, NS). **c.** Schematic representation of cued test. **d.** Comparable cue retrieval in WT-control and Early-cKO 1 day after conditioning but enhanced extinction (2-way RM ANOVA for 1 min bin: Genotype $F_{(1,17)}$=1.34, p=0.26, NS; Time $F_{(1,17)}$=30.56; ***p<0.001; Interaction $F_{(1,17)}$=6.08, *p=0.03, Fisher LSD test: *p<0.05). **e.** Early-cKO exhibit impaired cue retrieval 7 days after conditioning (1 min bin: Genotype $F_{(1,18)}$=1.62, NS; Time $F_{(1,18)}$=58.96;***p<0.001; Interaction $F_{(1,18)}$=3.62, *p<0.05 , Fisher LSD test; *p<0.05). **i.** Comparable 1 day explicit and implicit memory retrival in WT-Control and Early-cKO (% freezing in context: WT-control 47.15±3.71; Early-cKO 43.27±4.00, t_{17}=0.71, NS; % freezing in altered: WT-control 17.95±4.45; Early-cKO 15.15±3.59, t_{17}=0.48, NS; freezing during cue: WT-control 44.43±7.04%; Early-cKO 36.45±5.96%, t_{17}=0.85, NS). **j.** Impaired 7 days explicit and implicit memory in Early-cKO (%freezing during context: WT-control 52.90±3.33; Early-cKO 21.07±6.35, t_{18}=4.439, ***p<0.001; % freezing in altered: WT-control 7.30±1.81; Early-cKO 8.71±3.72, t_{18}=0.34, NS; %freezing during cue: WT-control 49.64±5.73; Early-cKO 30.52±5.80, t_{18}=2.35, *p<0.05). All error bars represent mean ± SEM.

FC experiments not only demonstrate the necessity of Arc/Arg3.1 expression for the consolida-

tion of implicit and explicit fear memories, but confirm that removal of Arc/Arg3.1 early during postnatal development interferes the control and acquisition of fear. As observed in the CTA (increased aversion for liquids shortly after condition), I found a highly significant enhancement of fear responses immediately after CS-US presentation in fear conditioning and enhanced extinction.

2.3.3.2. Early-cKO display enhanced extinction of contextual fear memory

Fear conditioning paradigm allows not only the evaluation of explicit and implicit fear memories, but also the evaluation of a type of new inhibitory learning called extinction. Extinction occurs when the CS (tone or context) is repeatedly presented without US pairing leading to reduction in conditioned fear responses. Due to the enhanced learning of fear and persistence of fear memory during the first week post-conditioning in Early-cKO mice, I hypothesized that these mice may have an enhanced extinction of learned fear. To test this hypothesis, I designed a fear conditioning protocol for evaluating contextual fear extinction. In this protocol, mice were fear conditioned without the use of tone to avoid interferences with auditory stimuli, and 3 US stimuli were delivered with an inter-trial interval (ITI) of 60 s. Mice were tested for 5 minutes one day after conditioning and subsequently exposed to the same context across 5 consecutive days in order to evaluate extinction of contextual fear (Figure 18a).

Confirming the previous observations in CTA and cued FC test, I found that during acquisition of fear (conditioning phase), Early-cKO mice displayed a significantly higher conditioned response (% of freezing) after each US presentation when compared their littermates WT-controls (Figure 18b) (2-way RM ANOVA each min bin: Genotype $F_{(1,13)}=5.46$, $^{\#}p<0.05$; Time $F_{(4,52)}=43.44$; $^{***}p<0.001$; Interaction $F_{(2,52)}=3.11$; $^{*}p<0.05$; post hoc Fisher LSD test; $^{**}p<0.01$). This result suggests once again that Arc/Arg3.1 removal during early postnatal development leads to an enhancement in learning of fear and conditioned stimuli.

Contextual fear memory was tested 1 day after conditioning during 5 min and each minute bin was analyzed. Surprisingly, I observed that Early-cKO mice showed a enhanced freezing in the context during the first min of retrieval, this response was stable in the second and third minutes but diminished significantly in the 4th and 5th minute compared to WT-control littermates (2way-RM ANOVA each min bin: Genotype $F_{(1,13)}=1.73$, $p=0.21$, NS; Time $F_{(4,52)}=2.93$; $^{*}p<0.05$; Interaction $F_{(4,52)}=3.78$, $^{**}p<0.01$; post hoc Fisher LSD test; $^{*}p<0.05$, $^{**}p<0.01$).

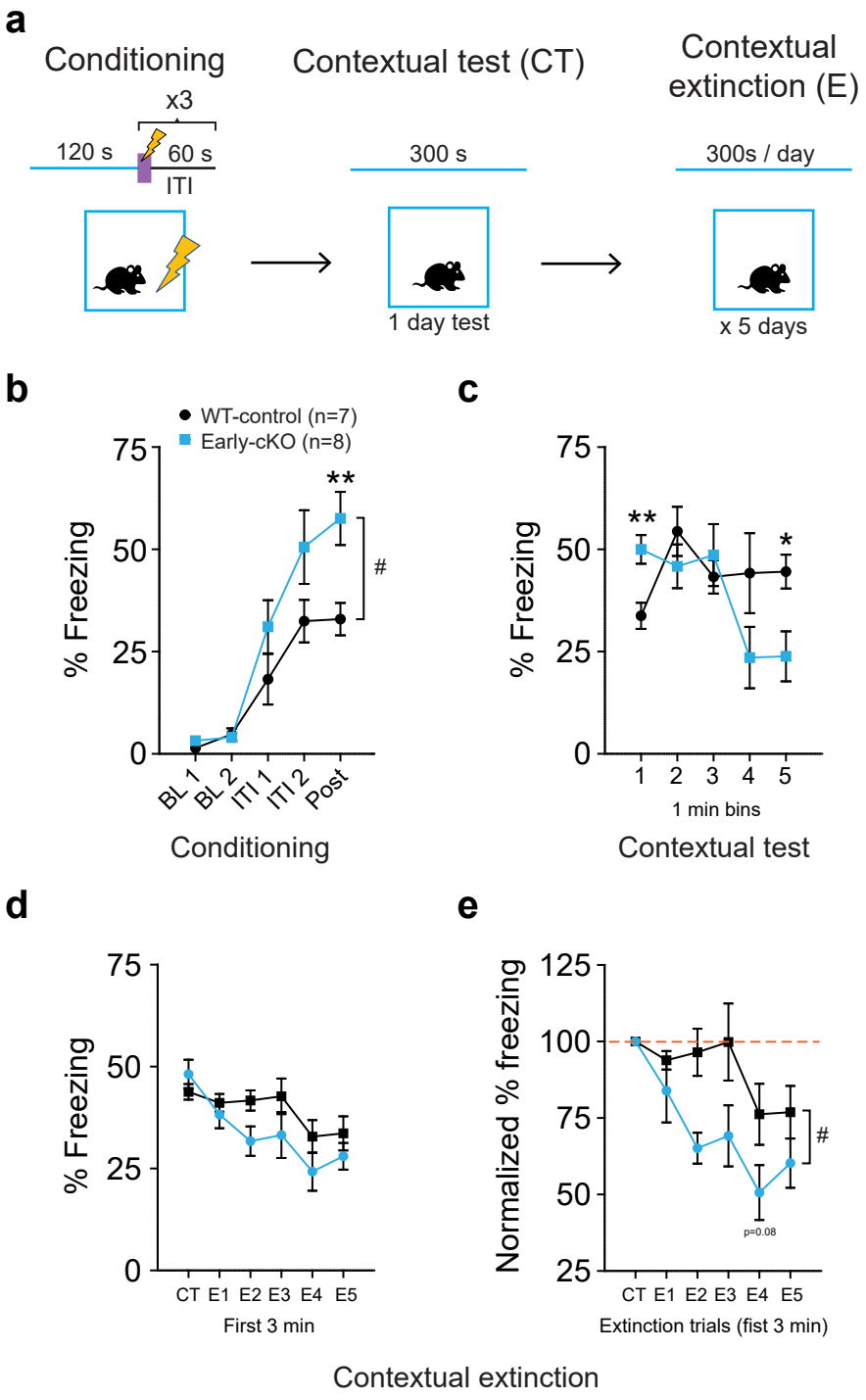

Figure 18. Early-cKO exhibit facilitation of contextual fear extinction.
a. Schematic representation of contextual fear extinction protocol. **b.** Early-cKO display enhanced learning of fear response after each CS-US presentation (Genotype $F_{(1,13)}$=5.46, $^{\#}p<0.05$; Time $F_{(4,52)}$=46.44; $^{***}p<0.001$; Interaction $F_{(4,52)}$=3.11; $^{*}p<0.05$). **c.** Enhanced recall in the first minute and fast short-term extinction of fear during 1 day context test (Genotype $F_{(1,13)}$=1.73, p=0.21, NS; Time $F_{(4,52)}$=2.93; $^{*}p<0.05$; Interaction $F_{(4,52)}$=3.78; $^{**}p<0.01$; post hoc Fisher LSD test; $^{***}p<0.0001$). **d.** Enhanced extinction of conditioned contextual fear in Early cKO (Genotype $F_{(1,13)}$=2.42, p=0.14; Time $F_{(5,65)}$=7.66; $^{***}p<0.001$; Interaction $F_{(5,65)}$=1.46; p=1.45,NS; post hoc Fisher LSD test; $^{*}p<0.05$). **e.** Normalized % freezing (first 3 min of test) show enhanced extinction of conditioned contextual fear in Early cKO (Genotype $F_{(1,13)}$=8.36, $^{\#}p<0.05$; Time $F_{(5,65)}$=6.86; $^{***}p<0.001$; Interaction $F_{(5,65)}$=1.49; p=0.21, NS). Significance was 2-way RM ANOVA, and post hoc Fisher LSD test, $^{**}p<0.01$, $^{*}p<0.05$. All error bars represent mean ± SEM. WT-control, n=7; Early-cKO, n=8. BL: Baseline, ITI: intertrial interval betlen USs, Post: post-conditioning.

Early-cKO mice exhibit altered fear responses during contextual recall when compared to WT-controls, being higher at the beginning of the recall and significantly diminished with time, indicating that Early-cKO exhibit a enhanced new inhibitory extinction learning.

I next investigated extinction of the conditioned fear by reintroducing the mice into the conditioning context for 5 minutes per day during 5 consecutive days. The first 3 minutes of recall were considered as "retrieval" for each day since no significant difference was observed in the averaged freezing percentage in this time during the test (Figure 18e). I found that Early-cKO exhibit a significantly faster extinction of contextual fear in the first 3 days of this protocol when compared to WT-control littermates (2-way RM ANOVA normalized % freezing: Genotype $F_{(1,13)}$=8.36, $^{\#}p<0.05$; Time $F_{(5,65)}$=6.87;$^{***}p<0.001$; Interaction $F_{(5,65)}$=1.49, NS). The enhanced extinction of learned contextual fear reaffirms previous observations in CTA extinction (Figure 16f), as well as in cued fear conditioning (Figure 17g).

These results can be interpreted in different ways; first, one could suggest that extinction learning is enhanced since fear responses are lower than WT-control (except extinction day 5). An alternative interpretation is that this apparent enhanced extinction is due to the slow establishment of the amnesia observed at 7 days in the previous experiments (Section 2.3.3.1). These results suggest that the early ablation of Arc/Arg3.1 affects neuronal circuits involved the in control, learning and expression of fear; and at the same time suggest that the presence of this protein after the second week of postnatal development is also necessary for the proper consolidation of fear-related memories.

2.3.4. Genetic ablation of Arc/Arg3.1 during early postnatal development impairs oscillatory network activity in the hippocampus and PFC

Formation of explicit memories and navigation are two higher cognitive functions which heavily rely on the hippocampus and its interactions with the cortex. Parallels between their underlying mechanisms raised the hypothesis that both draw on similar computations performed by hippocampal networks (Buzsaki & Moser 2013). Oscillations in the ϑ and γ frequency bands are considered essential for synchronizing cortico-hippocampal networks during navigation, spatial learning and memory retrieval (Lisman & Jensen 2013). SPW-Rs are considered to be important in memory consolidation for transferring labile information from the hippocampus to the neocortex (Ego-Stengel & Wilson 2010, Girardeau *et al* 2009). I next asked whether the strong deficits in fear and spatial long-term memory observed in the Early-cKO mice could arise from impairments

in any of the aforementioned network functions. To address this question, simultaneous depth recordings were performed from the PFC and Hpc of urethane-anaesthetized mice and measured LFP (Figure 19 and 63) (data adquiered and analyzed by Jasper Grendel).

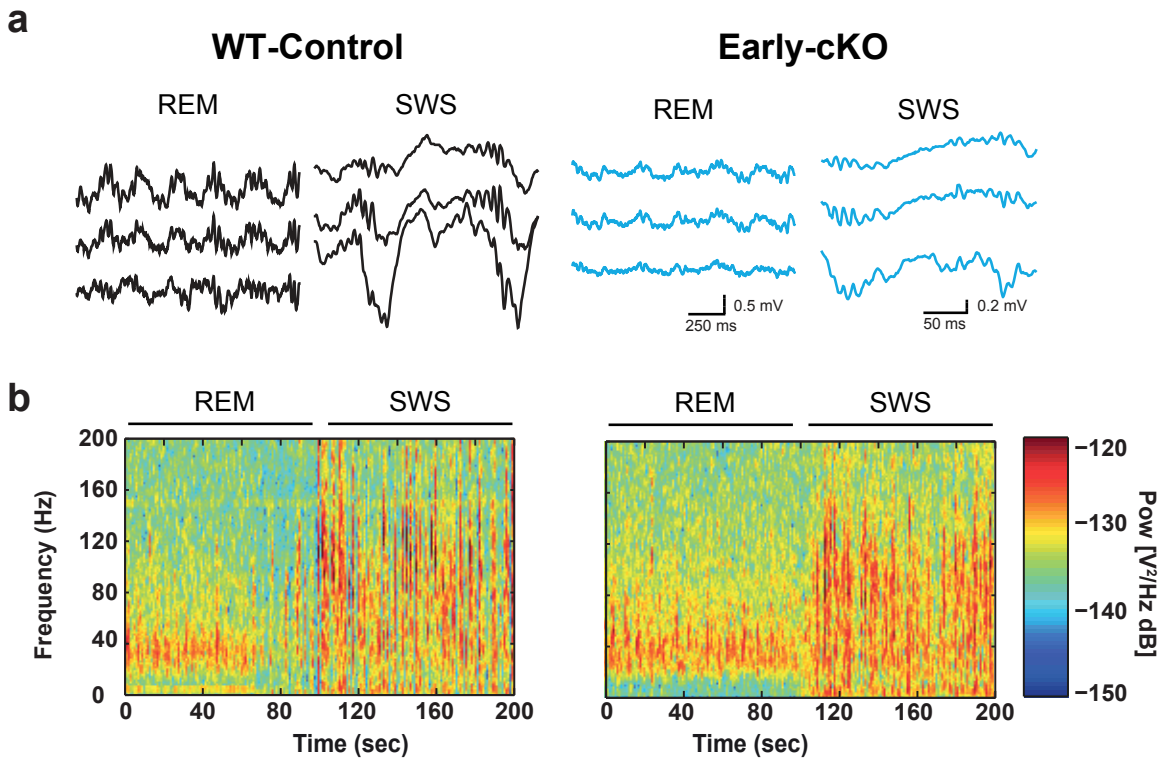

Figure 19. Spontaneous local field potentials (LFPs) recorded from the CA1 pyramidal layer
a. Exemplary raw traces from hippocampus CA1 striatum pyramidale (plus one channel 100 µm above or below) during paradoxical/REM-like sleep or SWS-like states. Genotype is color coded throughout the figure: black: WT-control, blue: Early-cKO. **b.** Time-frequency spectrograms of LFP-activity recorded from the CA1 pyramidal layer in urethane-anesthetized mice show spontaneous alternation of REM-like and non-REM-like sleep (SWS) network activity. The whitened, 200-s-long LFP spectrogram excerpts are approximately centered on transitions between a REM-like and a SWS-like state (courtesy of Jasper Grendel).

During REM-like sleep, WT mice exhibited clear ϑ band (4-6 Hz) accompanied by γ (20-50 Hz) oscillations in the CA1 pyramidal layer and in the PFC. Slow wave sleep epochs were characterized by slow oscillations (0.2-1.2 Hz) and large dips in the LFP in the stratum radiatum accompanied by high frequency (~130 Hz) ripples in CA1. Strikingly, Early-cKO mice show a prominent reduction in ϑ and γ power in the PFC and DG, but in CA1 only ϑ was significantly reduced while γ power exhibits a nonsignificant reduction in striatum pyramidale. Ripple occurrence in CA1 were WT-like but their amplitudes were significantly lower, and correlated with smaller sharp wave amplitudes in striatum radiatum (Figure 20).

The occurrence of SPWs in stratum radiatum of Early-cKO mice was increased and their amplitudes were similar to WT-controls. However, amplitudes of SPWs co-occurring with detected ripples (SPW-R) were significantly lower suggesting a failure of the CA1 network to generate ripple oscillations in response to CA3 input. The latter results could indicate an insufficiently syn-

chronized CA3 output caused by the removal of Arc/Arg.3.1 during the second postnatal week, explaining partially the failure in off-line long-term consolidation of explicit memories presented by the Early-cKO.

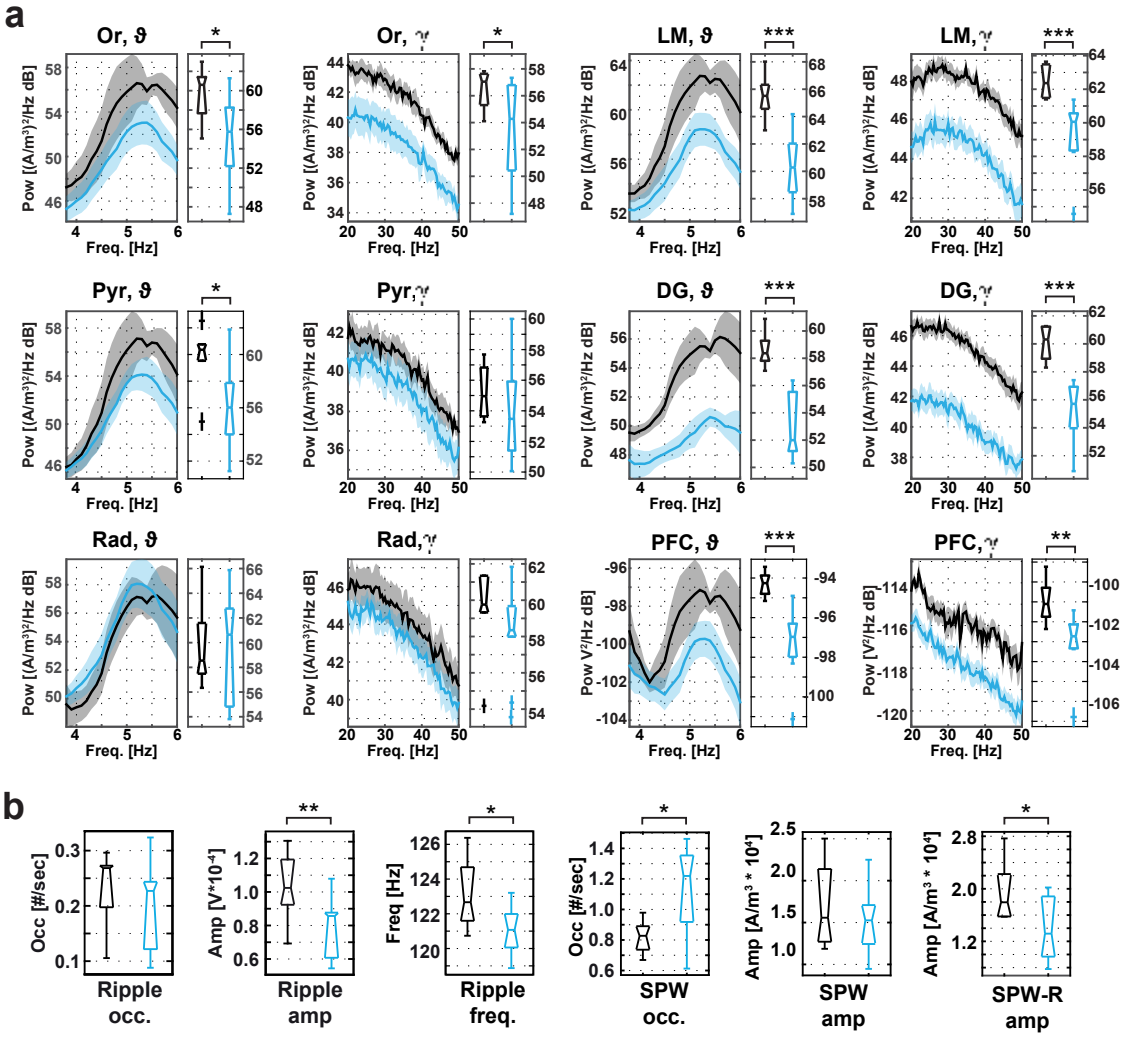

Figure 20. Arc/Arg3.1 during early postnatal development defines oscillatory network activity in the hippocampus and in the PFC

Power spectra from paradoxical REM sleep for both the theta (ϑ) and gamma (γ) band in hippocampus (calculated from the LFP after current-source-density [CSD] analysis) and PFC (from the LFP) showing mean ± SEM., together with their corresponding boxplots, showing median, 25th and 75th percentiles (hour glass markers) and outliers (crosses). **a.** All parameter except srt. rad ϑ, srt. rad and srt. pyr γ are reduced in Early cKO (Str. Or, ϑ WT-control: 60.6 dB, 57.7 dB – 61.4 dB; Early-cKO: 55.8 dB, 52.2 dB – 58.3 dB; *p<0.05. Str. Or. γ WT-control: 57.0 dB, 55.3 dB – 57.6 dB; Early-cKO: 54.3 dB, 50.4 dB – 56.8 dB; *p<0.05. Str. LM. ϑ WT-control: 65.6 dB, 64.6 dB – 66.3 dB; Early-cKO 60.3 dB, 58.5 dB – 62.0 dB; ***p<0.001. Str. LM. γ WT-control: 62.4 dB, 61.5 dB – 63.5 dB; Early-cKO 60.1 dB, 58.4 dB – 60.6 dB; ***p<0.001. Str. pyr. ϑ, WT-control: 60.4 dB, 59.5 to 60.8 dB, Early-cKO 56.0 dB, 54.0 to 59.9 dB, *p<0.05. Str. Pyr γ, WT-control 55.0 dB, 53.6 to 56.8 dB, Early-cKO 53.5 dB, 51.4 to 55.9 dB, NS. Str. DG. ϑ WT-control: 58.4 dB, 57.8 dB – 59.3 dB; Early-cKO 52.0 dB, 51.2 dB – 55.5 dB; ***p<0.001. Str. DG. γ WT-control: 60.3 dB, 58.9 dB – 61.2 dB; Early-cKO 55.7 dB, 54.0 dB - 56.9 dB; ***p<0.001. Str. Rad. ϑ WT-control: 58.6 dB, 57.5 dB – 61.6; Early-cKO 60.6 dB, 54.8 dB – 62.8 dB; NS. Str. Rad. γ WT-control: 59.8 dB, 59.3 dB – 61.3; Early-cKO 58.3 dB, 58.0 dB – 59.7 dB; NS. PFC ϑ, WT-control -94.3 dB, -94.8 to -93.9, Early-cKO, -97.0 dB, -98.0 to -96.3 dB; **p<0.001; PFC γ, WT-control -101.1 dB, -101.7 to -100.3 dB, Early-cKO -102.7 dB, -103.3 to -102.1 dB, **p<0.01). **b.** Ripples and SPWs were independently detected and measured from SWS states. Boxplots showing medians, 25th and 75th percentiles (hour glass markers) and outliers (crosses). Early-cKO mice exhibited normal occurrence of ripples (WT-control 0.27/s, n=7, Early-cKO 0.23/s, n=9, p=0.15) but a significant decrease in amplitude (WT-control 1.02 *10-4 V, n=7, Early-cKO 0.86 *10-4 V, n=9, **p<0.01) and in frequency (WT-control 122.7 Hz, n=7, Early-cKO 121.1 Hz, n=9, *p<0.05). Occurrence of SPWs was significantly increased (WT-control 0.83/s, n=6, Early-cKO 1.22/s, n=9, *p<0.05) but not their amplitude (WT-control 1.56*104 A/m3, n=6, Early-cKO 1.52 * 104 A/m3, n=9, p=0.25. Amplitudes of SPW-Rs was significantly reduced in the Early-cKO (WT-control 1.79*104 A/m3, n=6, Early-cKO 1.32 *104 A/m3, n=9, *p < 0.05). Data were courtesy of Jasper Grendel.

2.4. Early postnatal expression of Arc/Arg3.1 delimits a sensitive period for neural circuits underlying emotional processes

The Early-cKO mice partially recapitulate the amnesic phenotype previously described for the constitutive KO (Plath *et al* 2006), but additionally appeared to show a stronger aversive learning in CTA and FC, and a protracted fear memory (for at least a week) probably related to enhanced acquired aversive responses and facilitation in extinction of learned fear. These differences together with the initial observation of Arc/Arg3.1 mRNA expression in structures related to emotional processes and the severe impairment in ϑ and γ oscillations in the PFC, rise the hypothesis that Arc/Arg3.1 expression during the early postnatal development is not only necessary for learning and memory networks, but could participe in the functional development of circuits involved in the emotional processes and might define a sensitive period for these structures.

2.4.1. Arc/Arg3.1 ablation during early postnatal development induces heightened conditioned aversive responses in adult mice.

2.4.1.1. Disruption of Arc/Arg3.1 expression in the midst of postnatal development induces unique and enhanced fear responses during fear acquisition.

The traditional theoretical model for Pavlovian associative learning was described by Rescola and Wagner (Rescorla & Wagner 1972); in this model, associative learning is acquired through a dynamic and gradual process of repetitive experiences, and the relationship between learning strength and practice is not-linear, but rather asymptotic. To investigate the effect of ablating Arc/Arg3.1 during early postnatal development on conditioned fear responses and learning of fear, I employed a specialized fear conditioning protocol where a train of 5 CS-US pairs are delivered with a fixed inter-trial interval (ITI) (Figure 21a - Protocol 3 and Figure 61f), thus allowing the evaluation of learning curves and conditioned responses to each CS and ITI, as well as learning stability. I also included conventional KO mice to investigate whether the enhanced fear responses arise from a sensitive period delimited by Arc/Arg3.1 expression in the postnatal development.

I analyzed the fear-induced learning curves from several groups of WT-control (n=51), constitutive Arc/Arg3.1 KO (hereafter named KO, n=28) and Early-cKO (n=32) mice. Acquisition strength was assessed from the percent freezing during the ITI intervals (Figure 21b). I observed that all genotype groups acquired fear association in a similar asymptotic manner. Remarkably, constitutive KO exhibited enhanced learning of fear but reached an similar freezing to WT-controls in the last ITI and post-conditioning time (2 way-RM for ITI intervals WT-control vs KO: Genotype

$F_{(1,77)}$=9.85, $^{\#\#}$p<0.01; ITI $F_{(5,385)}$=214.04; ***p<0.0001; Interaction $F_{(5,385)}$=5.81; ***p<0.0001). As observed and expected from previous fear conditioning experiments, Early-cKO displayed significantly enhanced fear responses after each of the US-CS when compared to WT-control littermates (2 way-RM for ITI intervals WT-control vs Early-cKO: Genotype $F_{(1,81)}$=40.84, $^{\#\#\#}$p<0.001; ITI $F_{(5,405)}$=259.86; ***p<0.001; Interaction $F_{(5,405)}$=11.87; ***p<0.0001) and present a stronger enhancement in fear acquisition when compared to KO mice except in the 4th ITI (2 way-RM for ITI intervals KO vs Early-cKO: Genotype $F_{(1,58)}$=7.27, $^{\#\#}$p<0.01; ITI $F_{(5,290)}$=181.49; ***p<0.001; Interaction $F_{(5,290)}$=258.597; p=0.06, NS; post hoc Fisher's LSD multiple pair-wise comparisons: WT-control vs Early cKO; **p<0.01, ***p<0.001; KO vs Early-cKO, $^{++}$p<0.01, $^{+}$p<0.05).

I next evaluate the learning curve and fear responses during each tone presentation (second CS component). In contrast to the conditioning procedure previously used, the tone presented during this protocol had a higher intensity (98 dB) and lower frequency (2 kHz). I observed a similar scenario for KOs with enhanced fear responses during intermediate tones but normal baseline and stabilization at the last tone. Notably, the Early-cKO mice only show stronger responses in the first and second presentation of the tone and then approached to WT levels in the rest of the presentations (2 way-RM for tone presentation: Genotype $F_{(2,117)}$=2.78, NS; Tone $F_{(4,468)}$=86.41; ***p<0.0001; Interaction $F_{(10,504)}$=11.53; **p<0.01; post hoc Fisher's LSD multiple pair-wise comparisons: WT-control vs Early cKO; ***p<0.001; KO vs Early-cKO, $^{+}$p<0.05). Hence, it seems that Early-cKO mice display a susceptibility for this type of tone (not previously seen for tones with milder properties, *e.g.* Figure 17b) or it is also possible that the tone per se becomes an US, suggesting that Early-cKO possess an altered fear regulation system that leads to altered conditioned responses.

In addition, I tested if this protocol could induce long-lasting fear memories and whether Early-cKO mice protract the information for longer time due to their apparent enhanced fear learning. I performed contextual and cued test in two separated cohorts of mice. As observed with protocol 1 and 2, Early-cKO mice showed similar retrieval during 2 minutes of contextual and cued fear memories when tested 1 day after fear conditioning (%freezing during context: WT-control 28.2±4.63; Early-cKO 23.50±3.52, t_{26}=0.83, NS; %freezing in altered: WT-control 11.47±4.44; Early-cKO 6.44±1.58, t_{26}=1.19, NS; %freezing during cue: WT-control 51.71±5.52; Early-cKO 51.27 ± 4.75, t_{26}=0.06, NS). As previously observed, Early cKO exhibit a severe impairment in the retrieval of contextual memory within the first week (%freezing during context: WT-control 18.87±3.06; Early-cKO 0.68±0.38, t_{26}=6.11, ***p<0.0001), but implicit memory to the tone was still intact at 7 days when compared to WT-controls (%freezing in altered: WT-control 11.47±4.44; Early-cKO 6.44±1.58, t_{26}=0.95, NS; %freezing during cue: WT-control 43.16±5.13%; Early-cKO 42.16±5.36 %, t_{29}=0.89, NS).

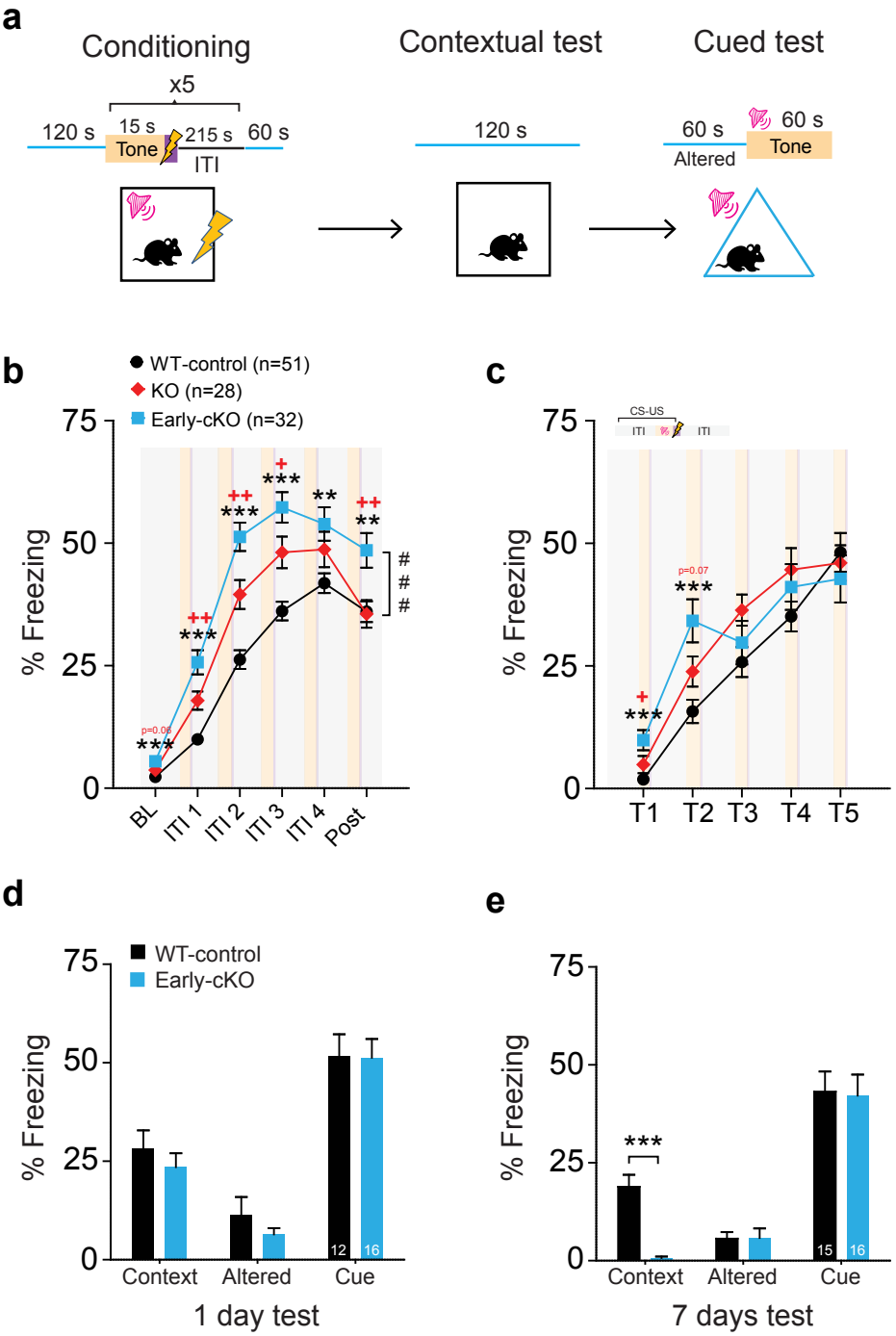

Figure 21. Early-cKO exhibit enhanced associative fear responses in FC learning
a. Schematic representation of delay fear conditioning protocol. **b.** Early-cKO exhibited enhanced learning of fear during ITI when compared to WT-control and KO (2 way-RM for ITI intervals: Genotype $F_{(2,108)}$=20.61, $^{###}$p<0.0001; Time $F_{(5,540)}$=323.9; ***p<0.0001; Interaction $F_{(10,504)}$=11.53; ***p<0.0001; post hoc Fisher's LSD multiple pair-wise comparisons: WT-control vs Early cKO; **p<0.01, ***p<0.001; KO vs Early-cKO, $^{++}$p<0.01, $^{+}$p<0.05) **c.** Early-cKO exhibited enhanced learning of fear during CS when compared to WT-control and KO (2 way-RM for tone presentation: Genotype $F_{(2,117)}$=2.78, NS; Tone $F_{(4,468)}$=86.41; ***p<0.0001; Interaction $F_{(10,504)}$=11.53; **p<0.01; post hoc Fisher's LSD: WT-control vs Early cKO; ***p<0.001; KO vs Early-cKO, $^{+}$p<0.05). **d.** Early-cKO displayed normal contextual and cued fear retrival at 1 day after conditioning (%freezing during context: WT-control 28.2±4.63; Early-cKO 23.50±3.52, t_{26}=0.83, NS; %freezing in altered: WT-control 11.47±4.44; Early-cKO 6.44±1.58, t_{26}=1.19, NS; %freezing during cue: WT-control 51.71±5.52; Early-cKO 51.27±4.75, t_{26}=0.06, NS **e.** Impared contextual but protracted cued fear memory at 7 days delay in Early-cKO (%freezing during context: WT-control 18.87±3.06; Early-cKO 0.68±0.38, t_{26}=6.11, ***p<0.0001; %freezing in altered: WT-control 11.47±4.44; Early-cKO 6.44±1.58, t_{26}=0.95, NS; %freezing during cue: WT-control 43.16±5.13; Early-cKO 42.16±5.36, t_{29}=0.89, NS). Significance was assessed with two-tailed unpaired t-test and 2-way RM ANOVA, and post hoc Fisher's LSD multiple pair-wise comparisons, **p<0.01, *p<0.05. BL: Baseline, ITI: intertrial interval betlen USs, Post: post-conditioning.

These results lead to hypothesize that although Early-cKO mice lack consolidation of contextual memory, it is possible that the circuits for fear control hold explicit fear responses for longer time depending of the strength or repetitions of the CS-US pairing, since cued memory was impaired in these animals in 7 days only when one CS-US pairing (with milder tone) was used (Figure 17j). It remains also unclear if the auditory system and sensibility to high intensity sounds in Early-cKO are identical to WT-controls, and future evaluation of startle reactivity should be conducted in these animals to rule out whether these different results between FC protocol arise from innate fear or hearing impairments.

2.4.1.2. Increased acquisition of CTA in Early-cKO compared to conventional Arc/Arg3.1 KO mice

After having found that Early-cKO possessed stronger learning of fear responses with 3 different FC protocols, I re-analyzed the CTA experiments and retested fear responses to the taste-LiCl pairing, by analyzing the fluid consumed before, during and a day after CTA in 17 WT-control, 8 KO and 11 Early-cKO mice that were exposed to the same procedure and tested for CTA memory. Although CTA is based in the same Pavlovian's principle as FC, it offers a different and more executive-related read out for aversive responses (liquid consumption, Figure 22a).

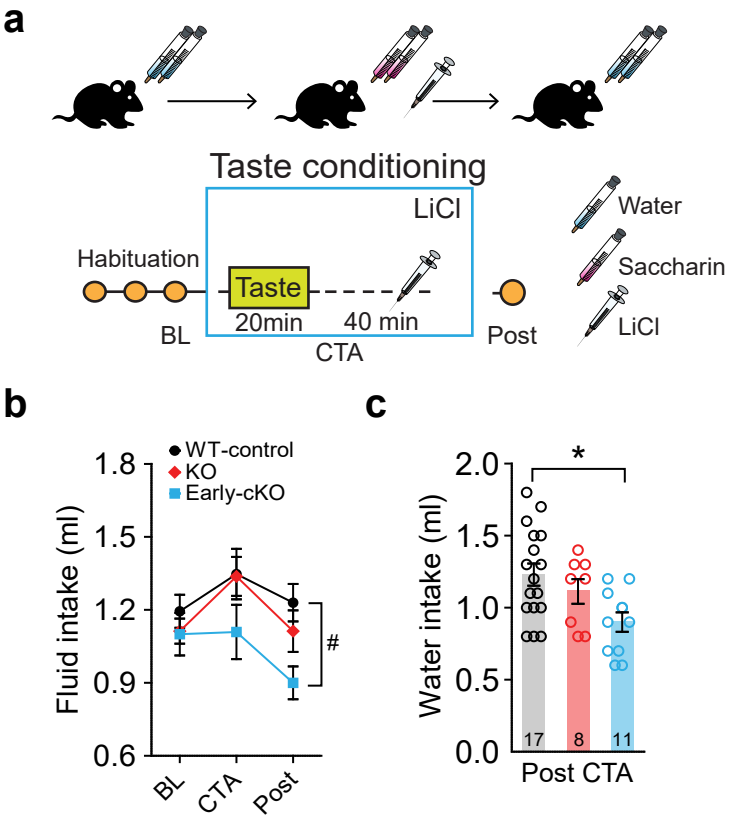

Figure 22. Early postnatal removal of Arc/Arg3.1 induces stronger aversive response after CTA
a. Schematic representation of CTA procedures.
b. Fluid intake before [BL], during [CTA] and post-conditioning [Post]: Genotype $F_{(2,33)}$=3.82, $^{\#}p<0.05$; conditioning $F_{(2,66)}$=3.72; $^{*}p<0.01$; Interaction $F_{(4,66)}$=0.76, NS.
c. Early-cKO showed enhaced aversive learning 1 day after CTA: WT-control; 1.23±0.08, KO; 1.11±0.09; Early-cKO 0.90±0.07 ml (1-way ANOVA: $F_{(2,35)}$=4.744, $^{*}p<0.05$, Tukey's multiple comparison test $^{*}p<0.05$).
WT-control, n=17; KO, n=8 and Early-cKO, n=11. All error bars represent mean ± SEM.

Confirming previous findings and despite liquid deprivation over 4 days, only Early-cKO developed a transient but significantly enhanced aversion for consuming water after CTA when compared with WT-controls against lack of significant changes during habituation, conditioning or testing phases (figure 16c and 22b-c) (2-way RM-ANOVA: Genotype $F_{(2,33)}$=3.82, $^{\#}p<0.05$; conditioning $F_{(2,66)}$=3.72; *p<0.01; Interaction $F_{(4,66)}$=0.76, NS). Notably, I found that conventional KO mice lacked this effect (Figure 22b-c) (1-way ANOVA: $F_{(2,35)}$=4.744, *p<0.05, Tukey's multiple comparison test *p<0.05), suggesting that removing Arc/Arg3.1 in the early postnatal development may disrupt a sensitive period in the normal development of emotional perception of conditioned stimuli that otherwise seem to develop normally if the gene is always absent in the KO.

2.4.2. Early postnatal removal of Arc/Arg3.1 produces a strong reduction in unconditioned avoidance behavior

2.4.2.1. Adult Early-cKO display normal locomotor and explorative behavior

The heightened conditioned responses found in Early-cKO mice during FC and CTA experiments rise the hypothesis that the early removal of Arc/Arg3.1 during early postnatal development might affect a sensitive period for the functional development of circuits related to emotional processing and interpretation of aversive stimuli, and therefore it might lead to changes in other type of emotional behaviors in the adult mice such as unconditioned avoidance or anxiety, which are not affected in the constitutive Arc/Arg3.1 KO mice (Plath *et al* 2006).

One of the first tests developed to assess emotionality in rats was the open field task (Hall, 1934), where the animal is subjected to an unknown empty environment and is not allowed to escape due to the presence of surrounding walls. Although open field is a less sensitive task for evaluating natural unconditioned avoidance, the time the animal spends in the illuminated center or the latency to entering to the central part is usually used as the starting point for further testing of anxiety-related behaviors (Crawley, 1999).

I previously tested open field activity of Early-cKO during NOR test, where the mice appeared normal in locomotor activity (section 2.3.1.1). I retested a cohort of mice in an open field arena for 10 min and analyzed their behavior across one minute bins to assess habituation and avoidance of illuminated spaces (figure 23a-b). As in the NOR experiment, I found no differences in the path length (Figure 23c) (WT-control: 49.51±3.16, n=14; Early-cKO: 44.34±3.38 m, n=16, t_{28}=1.106, p=0.27, NS) or time spent in the center (Figure 23d) (WT-control: 10.92±1.50; Early-cKO: 22.75±7.30 s; t_{28}=1.50; p=0.75, NS) during the entire 10 min of testing. I found nonetheless

a nonsignificant tendency in Early-cKO to habituate faster to the open field, reflected by shorter path lengths after the 6th min (figure 23 e-d) (2way RM-ANOVA for path lengths: Genotype $F_{(1,28)}$=1.22, NS; Time $F_{(9,252)}$=17.55; ***p<0.0001; Interaction $F_{(9,252)}$=0.46; NS) and spend longer time in the center during the last minutes of testing (2way RM-ANOVA : Genotype $F_{(1,28)}$=2.23, NS; Time $F_{(9,252)}$=2.30; *p<0.05; Interaction $F_{(9,252)}$=1.07; NS) (figure 23 h-j). This tendency was specifically observed in males (2way RM-ANOVA for path lengths: Genotype $F_{(1,17)}$=0.31, NS; Time $F_{(9,153)}$=7.94; ***p<0.0001; Interaction $F_{(9,153)}$=0.82; NS; time spent in center: Genotype $F_{(1,17)}$=2.04, NS; Time $F_{(9,153)}$=2.20; *p<0.05; Interaction $F_{(9,153)}$=0.79; NS).

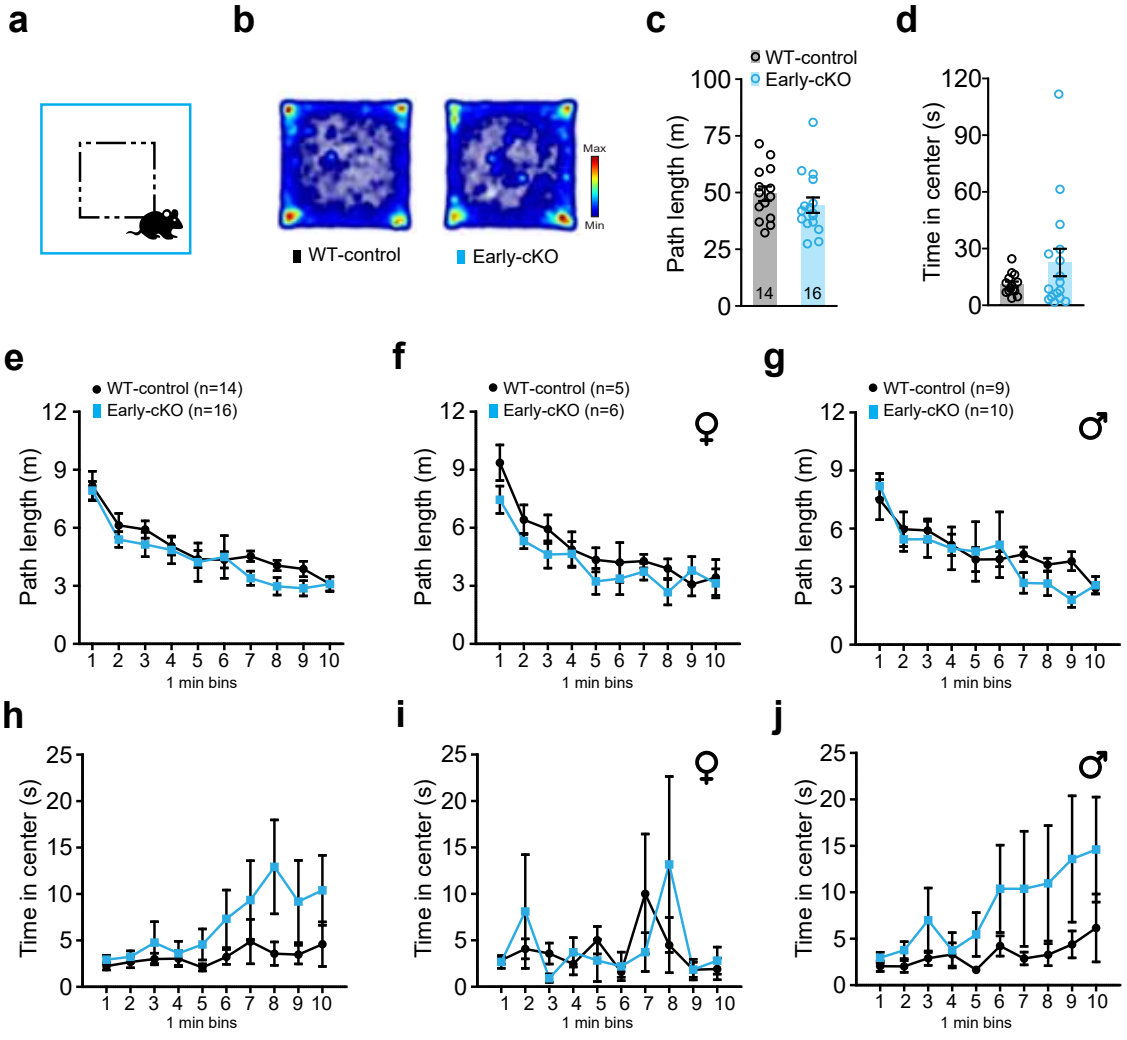

Figure 23. Adult Early-cKO display normal explorative behavior.
a. Schematic representation of open field test. **b.** Average density plots for open field during 10 min test. **c.** WT-control and Early-cKO exhibit similar path lengths (WT-control: 49.51±3.16, n=14; Early-cKO: 44.34±3.38m, n=16, t_{28}=1.106; NS) **d.** and time spent in the center (WT-control: 10.92±1.50 s; Early-cKO; 22.75±7.30 s; t_{28}=1.50; NS). **e.** Early-cKO tend to habituate faster and move less after minute 6 (Genotype $F_{(1,28)}$=1.22, NS; Time $F_{(9,252)}$=17.55; ***p<0.0001; Interaction $F_{(9,252)}$=0.46; NS). **f.** Path length in female WT-control (n=5) and Early-cKO (n=6) during 10 min bin analysis (Genotype $F_{(1,9)}$=8.01, NS; Time $F_{(9,81)}$=17.28; ***p<0.0001; Interaction $F_{(9,81)}$=0.90; NS). **g.** Path length in male WT-control (n=9) and Early-cKO (n=10) during 10 min bin analysis (Genotype $F_{(1,17)}$=0.31, NS; Time $F_{(9,153)}$=7.94; ***p<0.0001; Interaction $F_{(9,153)}$=0.82; NS). **h.** Early-cKO tend to stay longer in the center of the open field after the 5th min (Genotype $F_{(1,28)}$=2.23, NS; Time $F_{(9,252)}$=2.30; *p<0.05; Interaction $F_{(9,252)}$=1.07; NS). **i.** Time in the center in female WT-control (n=5) and Early-cKO (n=6) during 10 min bin analysis (Genotype $F_{(1,9)}$=0.03, NS; Time $F_{(9,81)}$=1.24; NS; Interaction $F_{(9,81)}$=0.82; NS). **j.** Time in the center in male WT-control (n=9) and Early-cKO (n=10) during 10 min bin analysis (Genotype $F_{(1,17)}$=2.04, NS; Time $F_{(9,153)}$=2.20; *p<0.05; Interaction $F_{(9,153)}$=0.79; NS).

These results suggest that Early-cKO mice possess similar explorative behavior for novel environments, without significant hyper or hypo activity during the testing time but show a non-significan tendency for faster habituation and decreased level of unconditioned avoidance for the center. It is then reasonable to propose that the unconditioned avoidance in Early-cKO may be different to their WT-control. To test this hypothesis, it is necessary to use specific ethological paradigms, where the normal exploratory drive and unconditioned avoidance behavior can be properly evaluated.

2.4.2.2. Early-cKO exerts strong anxiolytic-like behavior in the elevated plus-maze

To better address the unconditioned avoidance behavior of the Early-cKO mice, I subjected them to an elevated-plus maze (EPM). The EPM is a widely used ethological paradigm for studying anxiety-like behavior in rodents, and is based on the natural aversion of rodents to open and iluminated places. EPM addresses also elements of neophobia, exploration and aproach/avoidance conflicts. Generally, the behavior of mice in the EPM is characterized by natural avoidance to open arms and consistent preferece for closed arms, this behavior can be supressed by prototypical anxiolytic medications such as benzodiazepines and enhanced by anxiogenic agents like monoamine oxidase (MAO) inhibitors (Walf & Frye 2007). Thus, it has been proposed as a behavioral model to study anxiety-like behavior in rodents.

I subjected a cohort of 30 WT-control, 12 KO and 24 Early-cKO mice to EPM for 5 minutes and evaluated the time in each area (center, open and closed arms), and the number of entries to each zone (Figure 24a). Surprisingly, I found that only Early-cKO spent significantly longer times in the open arms (Figure 24b-c) (2-way ANOVA for % times in arms: Genotype $F_{(2,189)}$=0.03; NS, Arm $F_{(2,189)}$=182.4, ***p<0.001, Interaction $F_{(2,189)}$=14.99***p<0.001; Tukey HSD test: ***p<0.001, **p<0.01, *p<0.05) and made significantly fewer entries into the center and the closed arms (Figure 24d) (2-way ANOVA for number of entries: Genotype $F_{(2,189)}$=9.896; ***p<0.001, Arm $F_{(2,189)}$=83.78, ***p<0.001, Interaction $F_{(2,189)}$=2.35, NS; Tukey HSD test: ***p<0.001, **p<0.01, *p<0.05). Notably, the constitutive KO mice showed only a nonsignificant trend of spending longer times in the open arms, compared with WT-controls. KO mice also moved with significantly longer paths in the maze when compared to WT-control and Early-cKO (Figure 24e) (Kruskal-Wallis test, H=10.37, p<0.01; Dunn's multiple comparison test: **p<0.01, *p<0.05). This strong reduction of unconditioned threat response in the Early-cKO mice was found in both genders when compared to their respective WT-control littermates (Figure 24f-i), without significant effect for the interaction between gender and phenotype (3-way ANOVA: Genotype: $F_{(1,137)}$ = 0.001; NS, Gender: $F_{(1,137)}$=0.01, NS, Arm: $F_{(2,137)}$=136.93,***p<0.001; Genotype x Gender: $F_{(1,137)}$=0.0001,

NS; Genotype x Arm: $F_{(2,137)}$=22.17, ***p<0.001, Gender x Arm. $F_{(2,137)}$=2.96, NS; Genotype x Gender x Arm: $F_{(2,137)}$=0.88, NS).

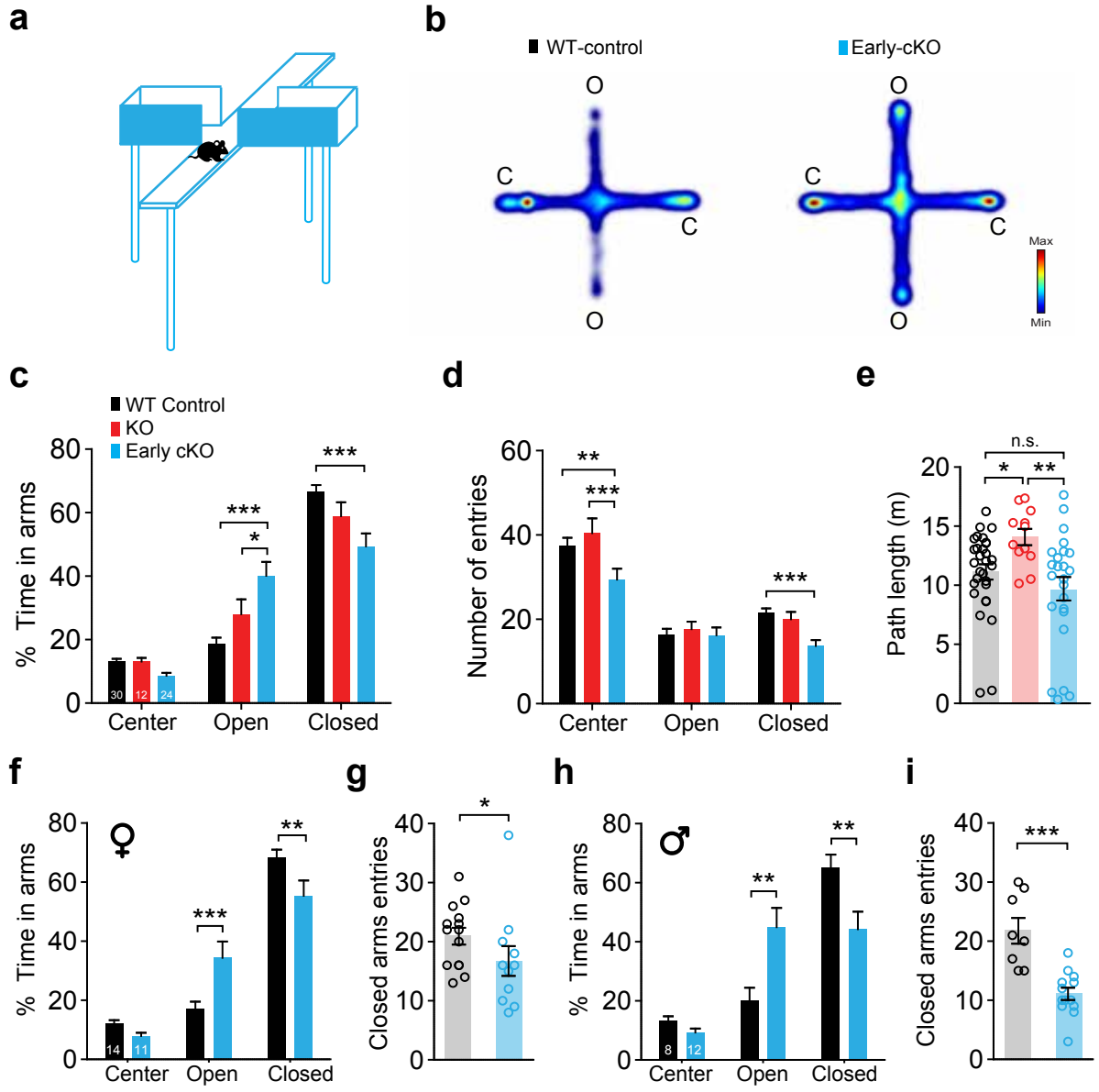

Figure 24. Early-cKO exert strong anxiolytic-like behavior in the elevated plus-maze
a. Schematic representation of EPM. **b.** Representative average density plots for EPM during 5 min test in a group of WT-control and Early-cKO. **c.** Early-cKO explore and stay longer in open arms (2-way ANOVA for % times in arms: Genotype $F_{(2,189)}$=0.03; NS, Arm $F_{(2,189)}$=182.4, ***p<0.001, Interaction $F_{(2,189)}$=14.99***p<0.001; Tukey HSD post hoc test: ***p<0.001, **p<0.01, *p<0.05) **d.** Early-cKO enter less frequently to the center and closed arms (2-way ANOVA for Number of entries: Genotype $F_{(2,189)}$=9.896; ***p<0.001, Arm $F_{(2,189)}$=83.78, ***p<0.001, Interaction $F_{(2,189)}$=2.35, NS; Tukey HSD test: ***p<0.001, **p<0.01, *p<0.05). **e.** Normal explorative behavior in Early-cKO but longer path in KO (Kruskal-Wallis test, H=10.37, p<0.01; Dunn's multiple comparison test: **p<0.01, *p<0.05). **f.** Anxiolytic behavior in Early-cKO females show higher exploration of the open arms (2-way ANOVA for % times in arms: Genotype $F_{(1,69)}$=0.001; NS, Arm $F_{(2,69)}$=137.2, ***p<0.001, Interaction $F_{(2,69)}$=11.76, ***p<0.001; Tukey HSD test: ***p<0.001, **p<0.01) and **g.** less entries to closed arms (WT-cKO: 20.93±1.42; Early-cKO: 16.73±2.52, Mann-Whitney U; 40.50; p<0.05). **h.** Anxiolytic behavior in Early-cKO males showed by higher exploration of the open arms (2-way ANOVA for % times in arms: Genotype $F_{(1,57)}$=4.93-5; NS, Arm $F_{(2,57)}$=36.55, ***p<0.001, Interaction $F_{(2,57)}$=10.37, ***p<0.001; Tukey HSD test: **p<0.01) and **i.** less entries to closed arms (WT-cKO: 20.93 ± 1.42; Early-cKO: 16.73 ± 2.52, Mann-Whitney U; 40.50; p<0.05).

These results indicate that the removal of Arc/Arg3.1 during early postnatal development interferes with a sensitive period for circuits involved not only in the control of conditioned aversive

responses, but at the same time produces a counterintuitive effect in networks related to the perception of potential threats (such as the open arms in the EPM).

2.4.2.3. Early-cKO exhibit reduced unconditioned avoidance in light-dark box

So far, I found that the genetic ablation of Arc/Arg3.1 during early postnatal ablation yields an ambivalent effect in avoidance responses: Early-cKO displayed stronger aversive responses after CTA (aversion to water consumption) and FC (enhanced fear acquisition) alongside exhibiting a stark reduction of unconditioned avoidance in the EPM. I next confirmed this finding by using yet another paradigm based on unconditioned avoidance, the light-dark box (LDB). The LDB assesses the conflict that exists between a natural exploratory drive and the stress induced by exposure to novel and brightly lit environments. The mice are exposed to a small arena divided in two compartments linked through a small opening; one comparment is a small covered and dark cage while the other is a brightly illuminated open arena (Figure 25a and Figure 56). Although the EPM and LDB are based on the same ethological principal, the latter presents a clear distinction of a potential threat (a highly illuminated open field) in contrast to the protective environment (dark enclosed area), hence offering a more aversive and stringent situation for the investigation of anxiety-related behaviors (Figure 25a).

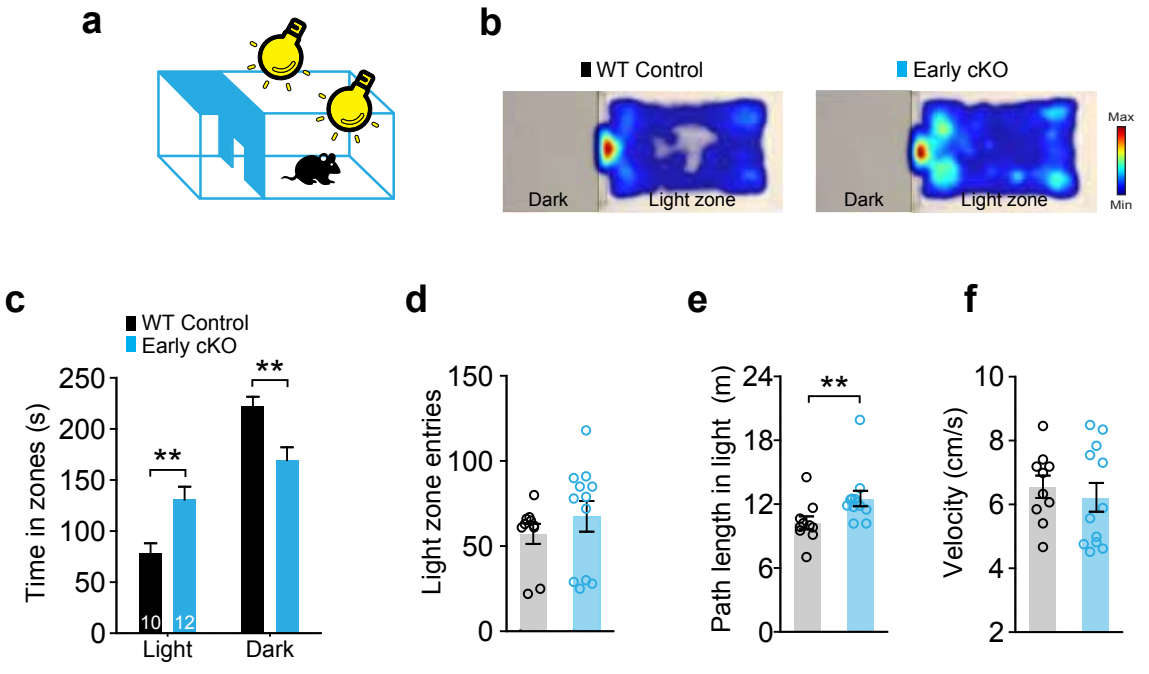

Figure 25. Early-cKO exhibit reduced unconditioned avoidance in light-dark box
a. Schematic representation of light-dark box test. **b.** Averaged density plots for in light-dark box during 5 min test in WT-control and Early-cKO. **c.** Early-cKO explore and stay more time in the light zone (2-way ANOVA for time in zones: Genotype $F_{(1,40)}=7.83^{-14}$; NS, Zone $F_{(1,40)}=60.77$, ***p<0.001, Interaction $F_{(1,40)}=20.12$; ***p<0.001; Tukey HSD post hoc test: **p<0.01) **d.** Early c-KO display a nonsignificant trend for entering more frequently to the light zone (WT-control 57.2 ± 5.88, Early-cKO 67.65 ± 9.02, Mann-Whitney U:35.5, NS). **e.** Early-cKO presented longer paths in light zone (WT-control 10.18±0.61m; Early-cKO 12.45±0.72 m; Mann-Whitney U:18, **p<0.01); **f.** but similar speed during exploration when compared to the WT-control littermates (WT-control 6.53±0.35; Early-cKO 6.20±0.45 cm/s; Mann-Whitney U:53, NS). Error bars represent mean ± SEM. WT-control, n=10; Early-cKO, n=12.

I tested a group of 10 WT-control and 12 Early-cKO mice in the LDB task for 5 minutes and analyzed the time in each compartment, entries to the light zone and distance moved in the lit zone. In agreement with the strong anxiolytic-like behavior presented in the EPM, Early-cKO spent significantly longer time in the light zone when compared with their WT-control littermates (Figure 25b-c) (2-way ANOVA for time in zones: Genotype $F_{(1,40)}$=7.83-14, NS, Zone $F_{(1,40)}$=60.77, ***p<0.001, Interaction $F_{(1,40)}$=20.12; ***p<0.001; Tukey HSD test: **p<0.01) and explored it actively with a longer paths (WT-control 10.18±0.61; Early-cKO 12.45±0.72 m; Mann-Whitney U:18, **p<0.01) but with similar speed (Figure 25f) (WT-control 6.53 ± 0.35m; Early-cKO 6.20 ± 0.45 cm/s; Mann-Whitney U:53, NS), confirming that their judgment in confronting situations with potential threats (such as the bright arena) is altered. Accordingly, Early-cKO displayed also a nonsignificant trend for entering more frequently into the light zone (Figure 25d) (WT-control 57.2±5.88, Early-cKO 67.65±9.02, Mann-Whitney U: 35.5, p=0.11, NS).

The light-dark box test confirmed the observation in the EPM, suggesting that the removal of Arc/Arg3.1 during early postnatal development leads to an altered behavioral responses to threats; because Early-cKO mice exhibit diminished innate anxiety-like behavior (response to potential threat) but enhanced responses to actual dangers, since in two different behavioral paradigms (CTA and FC) this genetic ablative strategy induces a paradoxically enhanced activation of defensive and aversive responses such as and enhance learning of fear and aversion to water consumption after CTA.

2.4.3. Genetic ablation of Arc/Arg3.1 during early postnatal development impairs structural and functional connectivity of circuits of emotional processing

During the perinatal and early postnatal period, the brain is particularly susceptible to adverse stimuli that are associated with an increased risk of stress and fear-related neuropsychiatric disorders during adulthood. Expression of Arc/Arg3.1 during development and its involvement in diverse forms of plasticity that are prominently induced during development (e.g. mGluR-LTD and homeostatic plasticity) (Gao *et al* 2010, Park *et al* 2008), suggest that postnatal ablation of Arc/Arg3.1 might impact synaptic refinement and connectivity between regions in the developing brain. In the next section, I describe how the disruption of the natural expression of Arc/Arg3.1 during development, leads to a dramatic change in functional brain connectivity and to abnormal emotional and social behavior in the adult animal.

2.4.3.1. Adult Early-cKO mice display abnormal structural morphology in the dorsal CA3 region of the hippocampus and in the lateral septum

The observations that complete loss of memory was common to the KO and Early-cKO mice while the emotional phenotype was uniquely expressed in the latter, strongly suggest that the circuits mediating these two behaviors, might have been differentially affected in these mice. I hypothesize that the disruption of Arc/Arg3.1 expression during the second postnatal week causes a dysfunctional development of local networks and might at the same time interfere with long-range connectivity.

To analyze morphological and functional connectivity changes in brains of adult mice, I performed magnetic resonance imagining (MRI) in 3 to 4 month-old WT (n=9), KO (n=8), WT-controls (n=11), and Early-cKO mice (n=11) under resting and light isoflurane anesthesia (Figure 64 and 65). After scanning, image acquisition and format conversion of each image file; the images were reoriented, segmented, smoothed and fitted to a brain surface model producing a clean intracranial volume for brain tissue volume analysis (white and gray matter volumes) (data analysis was porformed with the help of Jasper Grendel).

Using the aforementioned procedures, we found that only brains of Early-cKO mice displayed significantly reduced gray matter volume in the dorsal CA3 region of the hippocampus ($p<0.001$) and in the lateral septum ($p<0.001$) when compared to their WT-control littermates (Figure 26a).

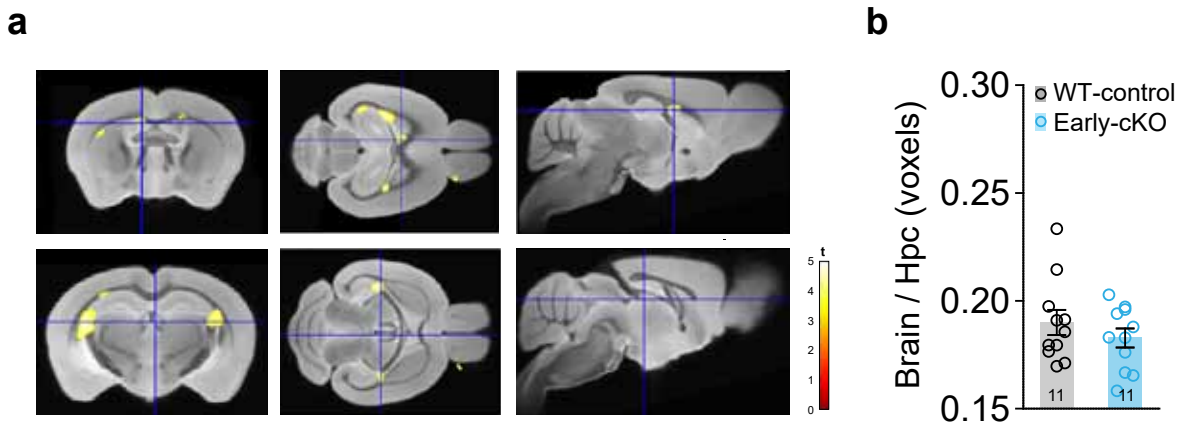

Figure 26. Adult Early-cKO exhibit morphological abnormalities of gray matter in the dCA3-fimbria-LS
a. Coronal, transversal and sagittal view of T1 lighed images highlighting CA3 and lateral septum gray matter abnormalities. Yellow areas represent decreased voxel content when comparared to WT-controls ($p<0.001$). **b.** WT-controls and Early-cKO exhibit similar hippocampal volumes (WT-control 0.19 ± 0.01, Early-cKO 0.18 ± 0.004, $t_{20}=0.99$, $p=0.33$, NS). Error bars represent mean ± SEM. WT-control n=11, Early-cKO n=11.

Because the differences in gray matter can result from changes in overall hippocampal volume,

we measured manually the volume of the dorsal hippocampus in the non-processed T2-weighted images and normalized it to the total brain volume. We found no significant differences in hippocampal volumes (Figure 26b) (WT-control 0.19 ± 0.01, Early-cKO 0.18 ± 0.004, t20=0.99, p=0.33, NS), suggesting a specific CA3 change in gray matter. Contrasting to these findings, the same analysis showed identical morphology for WT and constitutive KO mice.

These results indicate that Arc/Arg3.1 may not be necessary for the gross morphological development of the brain because KO mice displayed comparably normal brain anatomy, as determined from MRI analysis. However, the abnormalities in gray matter found in Early-cKO demonstrate that removal of the gene after an initial period of upregulation can generate structural changes.

2.4.3.2. Absence or removal of Arc/Arg3.1 during postnatal development results in impaired functional brain connectivity

In previous experiments using intracranial multielectrode recordings, it was identified that Early-cKO mice exhibited a severe impairment in prefrontal and hippocampal network oscillatory activity that could underlie the impairment in the consolidation of long-term memories. Additionally, alterations of prefrontal network activity have been linked with changes in emotional processing (Likhtik *et al* 2014), social behavior (Yizhar *et al* 2011) and anxiety-like phenotypes (Adhikari *et al* 2010). It is intriguing how disturbed local networks in the PFC or Hpc change long-range functional connectivity to other structures involved in emotional control such as amygdala, and their link with behavioral outcome in adult mice.

To evaluate long-range functional connectivity in mice lacking Arc/Arg3.1, I used resting state functional magnetic resonance imaging (rsfMRI). In humans and nonhumans primates rsfMRI allow mapping intrinsic network organization and connectivity in absence of explicit tasks, based mainly on coherent brain activities that are mostly detected from low frequency oscillations (less than 0.1Hz) of blood oxygenation level dependent (BOLD) perturbations of the magnetic resonance signal, and furthermore the identification of large-scale networks associated with specific brain functions (Gozzi & Schwarz 2016). It has been recently shown that rsfMRI measurements under light isoflurane anesthesia can be successfully and reliably performed in mice to investigate intrinsic connectivity at resting (Guilfoyle *et al* 2013), opening the possibility to translate investigation from mouse models to functional studies in humans.

I performed rsfMRI in WT (n=9), KO (n=8), WT-control (n=11) and Early-cKO (n=11) mice and assessed global functional connectivity by quantifying the correlation coefficient of BOLD signals

across selected brain regions (Volumes of interest [VOIs], Figure 65a). We selected as VOIs brain regions involved in mnemonic, synchronous activity and emotional processes: Anterior Cingulate Cortex (ACC), Amygdala (Amy), dorsal CA3 (dCA3), entire dorsal hippocampus (dHpc), dorsal Lateral Septum (dLS), Habenula, Infralimbic subregion of the medial Prefrontal Cortex (IL), primary motor cortex (M1), Medial Septal Nucleus (MB/DB), Pontine nucleus (Pontine), Prelimbic subregion of the medial Prefrontal Cortex (PrL), Septal hippocampal nucleus (SHV), ventral CA3 (vCA3) and the entire ventral hippocampus (vHpc). These VOIs were selected based on educated guess and a prior seed (VOI) to volume and cluster analysis, where VOIs were compared with the BOLD signal of the rest of the brain.

After having identified potential VOIs, a further VOI-VOI based analysis was conducted in WT-controls. A network of functionally connected regions were identified, these appear to have a hierarchical organization from subcortical regions such as reticular pontine nucleus, MS/DB, LS, habenula and cortical regions such as dHPC and PFC (vmPFC and ACC). The regions of this identified functional network are related with the generation of synchronic activity (Larson-Prior *et al* 2014) and orchestration of mnemonic and emotional processes (Williams & Gordon 2007) (Figure 27a und b).

Remarkably, both the constitutive absence and postnatal conditional ablation of Arc/Arg3.1 resulted in a different type of change in functional connectivity of adult brain networks. Firstly, KO mice exhibit a significantly higher functional connectivity between the MS/DB and IL (correlation coefficients: WT, -0.03; KO; 0.09, $p<0.001$ after false discovery rate -FDR- correction for multiple comparisons), and the vCA3 and habenula (correlation coefficients: WT, -0.07; KO, 0.04; $p<0.001$ after FDR-correction). Interestingly, these changes were not detected in the previously analyzed WT network and appeared to be a gain of altered connectivity.

In contrast to KO mice, Early-cKO mice exhibited a significant decreased functional connectivity between two components of the PFC, the IL and ACC (correlation coefficients: WT, 0.27; Early-cKO; -0.16, $p<0.001$ after FDR-correction), between the ACC and the dCA3 (correlation coefficients: WT, 0.08; Early-cKO, -0.06, $p<0.001$ after FDR-correction), and dHpc and Habenula (correlation coefficients: WT, 0.22; Early-cKO, 0.13; $p<0.001$ after FDR-correction). Different to what it was found for KO mice, these changes in connectivity are observed in preexistent functional connectivity previously detected in the WT network (Figure 27b-d). Decreased functional connectivity of the dCA3 with other areas was expected taking in account the significantly reduced gray manner found in this region (Section 2.4.3.1).

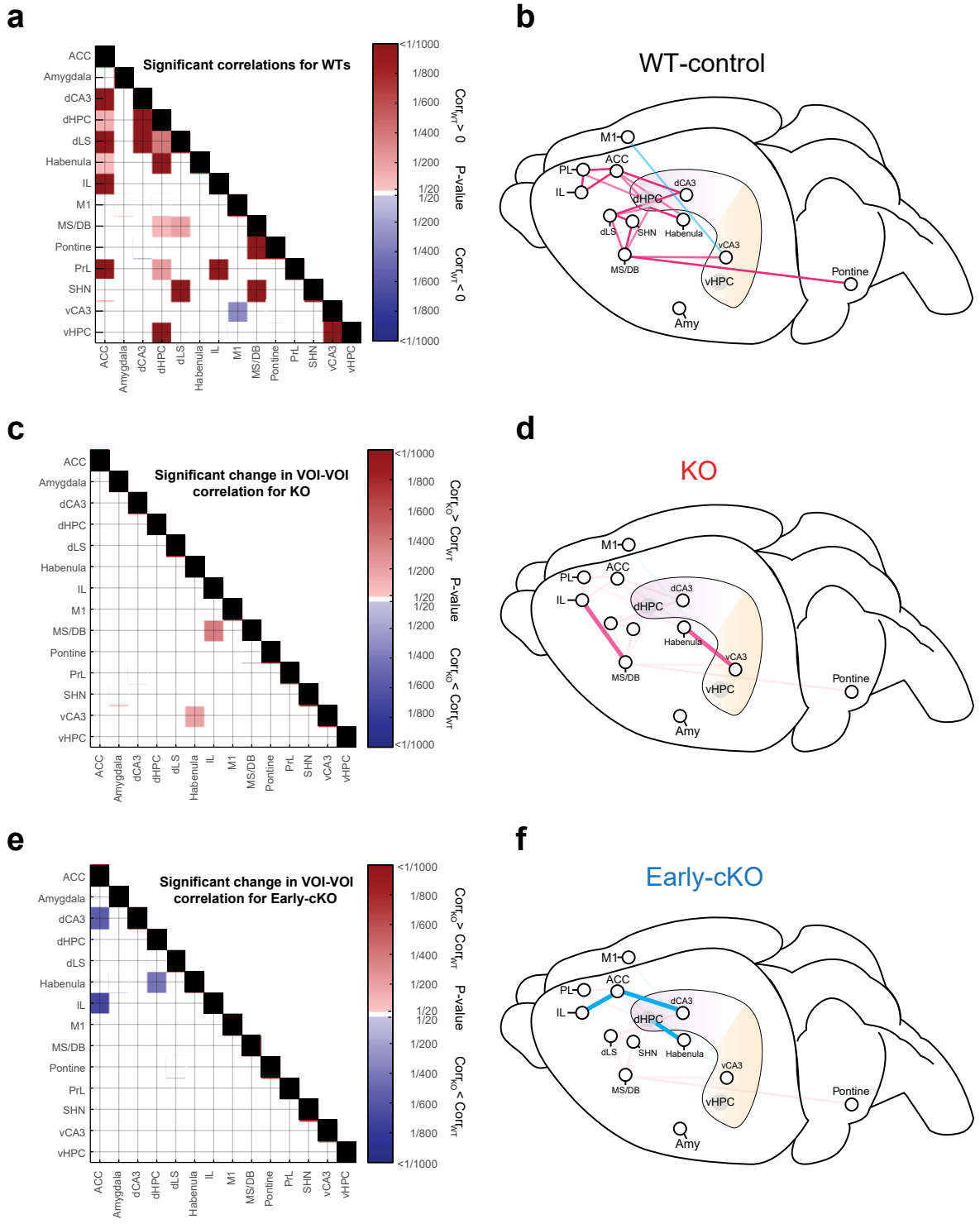

Figure 27. Absence or removal of Arc/Arg3.1 during postnatal development results in impaired functional connectivity of adult brains.
a. Significant BOLD signal correlations for WT/WT-control mice after rsfMRI analysis. **b.** Schematic and neuroanatomical representation of functional connectivity in WT mice. Red lines depict increased connectivity while blue color represents decreased functional connectivity. **c.** Significant changes in VOI-VOI correlations for KO mice when compared to their WT littermates. **d.** Schematic and neuroanatomical representation of impairment in functional connectivity in KO mice. **e.** Significant changes in VOI-VOI correlations for Early-cKO mice when compared to their WT-control littermates'. **f.** Schematic and neuroanatomical representation of impairment in functional connectivity in Early-cKO mice. Connectivity sketch was taken and modified from (Tovote *et al* 2015).

Structural and functional changes in the connectivity of dCA3 in Early-cKO mice suggest that Arc/Arg3.1 is essential for postnatal development of this structure and its later function in mnemonic processes in adult mice. Furthermore, rsfMRI analysis reveals that developmentally driven Arc/Arg3.1 expression during the early postnatal period in the prefrontal cortex is necessary for the establishment of its normal functional connectivity, and it is probable that the removal of Arc/Arg3.1 during the beginning of its natural upregulation imbalances the functional development of this structure.

2.4.4. Early postnatal removal of Arc/Arg3.1 affects social cognition.

Developmental alteration in the PFC microcircuitry has been suggested as a hallmark of neuropsychiatric disorders with shared social deficits such as schizophrenia and autism spectrum disorders (Bicks *et al* 2015, Selemon & Zecevic 2015). I next sought to investigate this PFC function when Arc/Arg3.1 was postnatally removed and determined if such observed functional impairments affect not only mnemonic and emotional processes but social cognition.

To evaluate whether changes in functional connectivity and reduced oscillatory activity in the PFC correlate with social cognition, I evaluated social behavior in a group of 8 WT-control and 11 Early-cKO adult mice performing the widely used three-chambered sociability test (Moy *et al* 2004a). In the three-chambered sociability test (Figure 28a), mice are habituated and tested individually in an arena divided into 3 chambers that are connected through small openings. During the sociability test, where one of the chambers contains a social stimulus (an unfamiliar mouse into a cup) and the other a novel object, WT mice will generally spend more time exploring both in the chamber and the cup of the unfamiliar mouse compared to those of the inanimate object. In the next session, which assesses reaction to social novelty, the object is replaced by a novel mouse. WT mice generally prefer to interact with the novel mouse over the previously familiarized one, as indicated by relatively higher exploration times of both the novel mouse's chamber and cup.

During the habituation phase, WT-control and Early-cKO mice exhibited comparable path lengths (Figure 28d) (WT-control, 40.48±2.43; Early-cKO, 44.65±2.33 m, t_{17}=1,216; p=0.24, NS) and velocities (Figure 28e) (WT-control, 13.79±0.80; Early-cKO, 15.95 ± 0.98 cm/s, t_{17}=1,64; p=0.12, NS), suggesting normal exploratory behavior. In the sociability test (Figure 28b), WT-controls and Early-cKO mice spent significantly longer times in the chamber containing the mouse (Time in chamber: WT-control; Object 202.8±8.91; Mouse 262.6±13.77 s, paired-t test, t_7=3.09, *p<0.05; Early-cKO; Object 205.0±8.91; Mouse 258.8±9.99 s, paired-t test, t_{10}=3.06, *p<0.05).

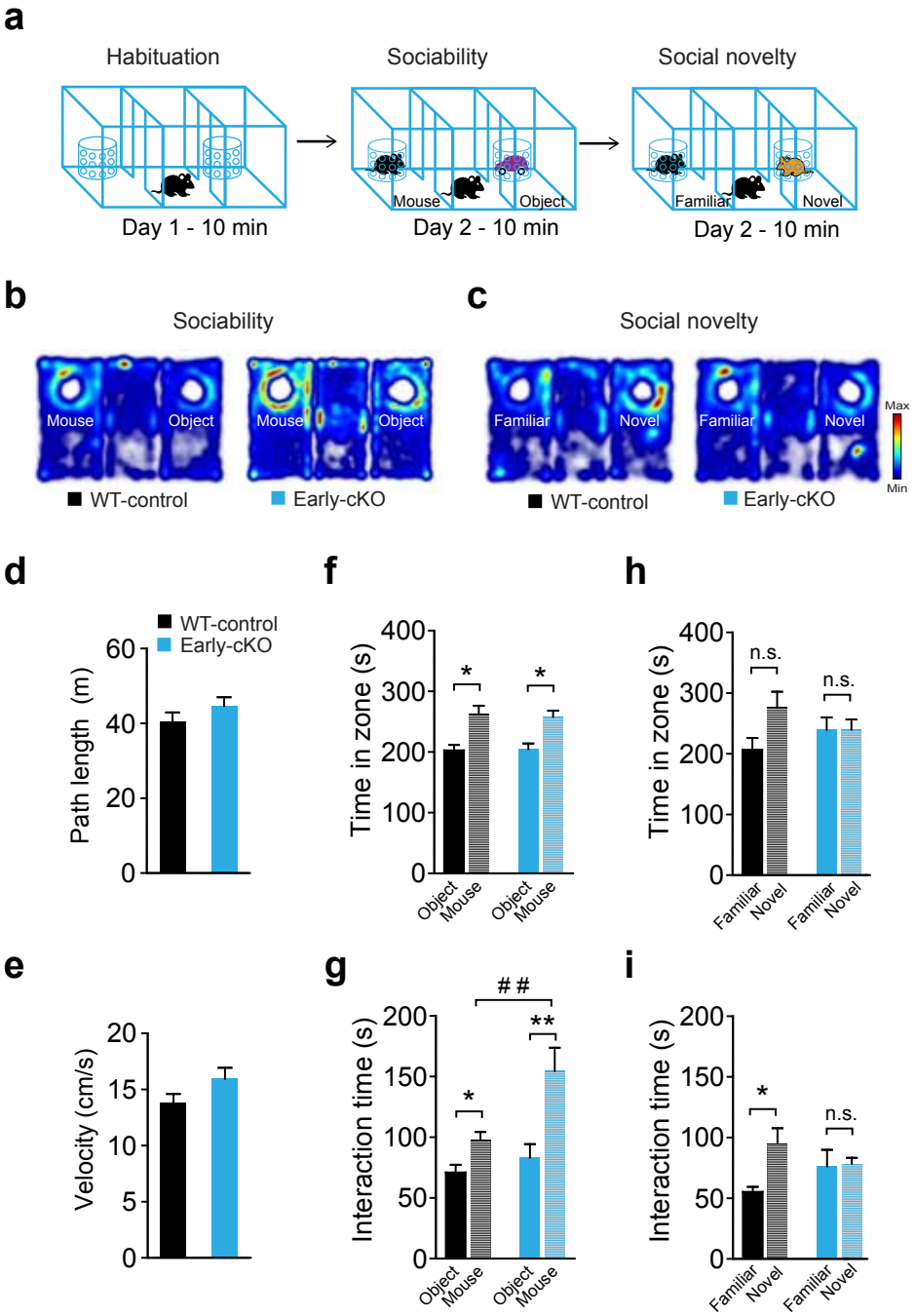

Figure 28. Early postnatal removal of Arc/Arg3.1 affects social cognition.
a. Schematic representation of three-chambered sociability and novelty test. **b.** Representative average density plots for the sociability test of mice exposed to the arena where the object was located in the left chamber (WT-control, n=4, Early-cKO, n=4). **c.** Representative average density plots for the social recognition test of mice exposed to the arena where the novel mouse was located in the left chamber (WT-control, n=4, Early-cKO, n=4). **d.** Early-cKO move similar distances to WT-controls in habituation phase (WT-control 40.48±2.43; Early-cKO 44.65 ± 2.33 m, t_{17}=1.216; NS) and **e.** exhibit comparable velocity (WT-control 13.79±0.80; Early-cKO 15.95±0.98 cm/s, t_{17}=1.64; NS). **f.** WT-controls and Early-cKO mice spent preferentially longer time in the chamber containing the mouse (Time in chamber: WT-control: Object 202.8±8.91; Mouse 262.6±13.77 s, paired-t test, t_7=3.09, *p<0.05; Early-cKO: Object 205.0±8.91; Mouse 258.8±9.99 s, paired-t test, t_{10}=3.06, *p<0.05). **g.** Early-cKO have a significantly longer social interaction when comparared to WT-control (2-way ANOVA interaction time: Genotype $F_{(1,34)}$=6.441, *p<0.05; Cup $F_{(1,34)}$=12.78, **p<0.01, Interaction $F_{(1,34)}$=2.69, NS; Post-hoc Tukey test: Genotype within mouse; ##p<0.01). Interaction time: WT-control; Object 70.99±6.31; Mouse 97.45±6.92 s, paired-t test, t_7=2.41, *p<0.05; Early-cKO; Object 83.28±11.00 ; Mouse 154.5±19.21 s, paired-t test, t_{10}=3.72, **p<0.01. **h.** Early c-KO have no bias for chambers with familiar or novel social stimuli (Time in chamber: WT-control, Familiar 206.6±19.47; Novel 276.5±25.77 s, paired-t test, t_7=1.62, NS; Early-cKO; Familiar 239.5±20.46; Novel 239.7±16.92 s, paired-t test, t_{10}=0.01, NS). **i.** Early-cKO exhibit impaired preference for social novelty (Interaction time: WT-control, Familiar 55.24±4.11; Novel 95.13±12.57 s, paired-t test, t_7=2.52, *p<0.05; Early-cKO; Familiar 76.17±13.74; Novel 78.58±4.74 s, paired-t test, t_{10}=0.17, NS). Error bars represent mean ± SEM. WT-control, n=8; Early-cKO, n=11.

Remarkably, Early-cKO mice not only exhibited a significantly longer interaction with the cup containing the social stimulus as WT-control (Figure 28g) (Interaction time: WT-control; Object 70.99±6.31; Mouse 97.45±6.92 s, paired-t test, t_7=2.41, *p<0.05; Early-cKO; Object 83.28± 11.00; Mouse 154.5±19.21 s, paired-t test, t_{10}=3.72, **p<0.01) but this interaction was significantly higher when compared to WT-controls (2-way ANOVA interaction time: Genotype $F_{(1,34)}$=6.441, *p<0.05; Cup $F_{(1,34)}$=12.78, **p<0.01, Interaction $F_{(1,34)}$=2.69, NS; Post-hoc Tukey test: Genotype within mouse; $^{\#\#}$p<0.01). These results could suggest two possibilities: (i) the strong anxiolytic-like behavior of Early-cKO mice is extended to the social domain, presenting disminished social anxiety for novel social interactions or (ii) these animals display a stronger curiosity and motivation for social stimuli.

I next tested social novelty preference over 10 minutes short after the sociability test (10 min ITI) by replacing the object by a novel mouse (Figure 28c). Here, only WT-control were able to recognize the novel mouse and spent longer time interacting around the cup containing the novel social stimulus (Figure 28h-i) (Time in chamber: Familiar 206.6±19.47; Novel 276.5± 25.77 s, paired-t test, t_7=1.62, p=0.15 NS; Interaction time: Familiar 55.24±4.11; Novel 95.13±12.57 s, paired-t test, t_7=2.52, *p<0.05), whereas Early-cKO spent similar time in both chambers and around the cups containing either the familiar or novel mouse (Figure 28h-i) (Time in chamber: Familiar 239.5±20.46; Novel 239.7±16.92 s, paired-t test, t_{10}=0.01, p=0.99, NS; Interaction time: Familiar 76.17±13.74; Novel 78.58±4.74 s, paired-t test, t_{10}=0.17, p=0.89, NS).

The three-chamber sociability test confirms the anxiolytic-like phenotype of Early-cKO mice in the social domain and suggests that early postnatal ablation of Arc/Arg3.1 might alter social recognition in the adult mice. Different to humans, rodents have as main source of social information the olfactory or pheromone signals; impairments in social recognition can reflect a deficit in the normal olfactory function or neuroendocrinological regulation (Winslow & Insel 2004) that remain to be tested in the Arc/Arg3.1 KO and Early-cKO mice.

3. Discussion

The main goal of the first part of this dissertation was to investigate Arc/Arg3.1 expression during early postnatal development and the impact of its genetic removal on behavior, network properties and functional brain connectivity of the adult brain. I first examined and quantified through *in situ* hybridization the expression of this gene in the first postnatal month, and confirmed that the third week exhibited a sharp increase of Arc/Arg3.1 mRNA in the majority of examined structures; I hypothesized that this developmental upregulation in gene expression is essential for shaping memory and emotional functions.

I adopted three strategies to investigate this hypothesis: (i) behavioral assessment of adult conditional KO mice (early postnatal cKO), (ii) local field potential (LFP) recordings and, (iii) resting state functional magnetic resonance imaging (rsfMRI). I will discuss this part by critically reviewing the results and trying to interpret them within a framework of current knowledge and theories about the cellular and molecular functions of Arc/Arg3.1. The function of Arc/Arg3.1 in the development of corticolimbic circuits necessary for memory and emotions has not been investigated to date and the results presented in this dissertation point to its role in the ontogenesis of brain network functions that support cognitive processes in the adult brain.

3.1. Arc/Arg3.1 mRNA is upregulated in the first postnatal month reflecting experience-dependent synaptic development dynamics

The dynamics of Arc/Arg3.1 expression during the first postnatal month in the majority of examined structures mirrors closely the normal development of synapse number; which starts low at birth, increases sharply during the third week and stabilizes after the fourth postnatal week in the cortex and hippocampus (Lohmann & Kessels 2014). In areas where synaptic numbers peak earlier, Arc/Arg3.1 mRNA peaks earlier in parallel, for example, the mammillary bodies and the olfactory bulb (Matsutani & Yamamoto 2004). Similarly, in regions that undergo delayed synaptic development such as the visual (Tagawa *et al* 2005) and PFC cortices, the Arc/Arg3.1 mRNA expression is longer as well (Huttenlocher & Dabholkar 1997).

Notably, the expression of Arc/Arg3.1 mRNA appears to be partially driven by sensory experiences, because it is detected earliest at P7 in the olfactory bulb where newborn olfactory neurons detect maternal odors and other olfactory environmental cues that guide suckling behavior (Logan *et al* 2012) and later in the rest of the brain after P14, when young mice open their eyes

and the onset of hearing and active exploration start. The abrupt synaptogenesis triggered by sensory experiences is remarkably accompanied by the onset of Arc/Arg3.1 expression in sensory cortices (somatosensory and visual cortex) and structures related to multimodal integration such as the Claustrum (Cl) (Kim *et al* 2016). As described for sensory cortices, the expression of the Arc/Arg3.1 gene seems to correlate with the normal synaptic development and synaptic density previously described in the literature (Steward & Falk 1991).

With regard to hippocampal development, it is very interesting that Arc/Arg3.1 mRNA expression is detected at first in CA3 (P7) and only after P14 in other subfields such as CA1 where plasticity can be fully maintained only after this time (Liao & Malinow 1996). This suggests a sequential development where CA3 might drive CA1 functional development. During the third postnatal week, other essential molecular events for synaptic plasticity development occur, such as the upregulation of CaMKII proteins (Yasuda *et al* 2003) and the switch of GluN2B to GluN2A (Rodenas-Ruano *et al* 2012), as well as the experience-dependent increase in GluA1-containing synaptic AMPARs (Jitsuki *et al* 2011). It is possible that the recently described interactions of Arc/Arg3.1 (GAG domain N-lobe) with NMDAR subunits (GluN2B for GluN2A), CaMKII-β (Okuno *et al* 2012) and TARPγ2 (Stargazin) (Zhang *et al* 2015) are necessary for synaptic events during early postnatal development that control synaptic strength through AMPA content and elimination of nonfunctional synapses, as it has been shown in cerebellar development *in vitro* (Mikuni *et al* 2013).

Arc/Arg3.1 is in a position to influence postnatal synaptic development of functional networks permanently, altering their functionality and output in the adult behavior. Moreover, the sharp upregulation of Arc/Arg3.1 during the third postnatal week in regions related to sensory, mnemonic and emotional processing suggests that this time window is a sensitive period for synaptic development and could eventually influence the cognitive and emotional behavior in the adult mouse. I hypothesized that developmentally expressed Arc/Arg3.1 participates in the synaptic stabilization of networks for mnemonic and emotional processes, and its removal during this developmental period may affect normal network function and connectivity, as well as emotional and cognitive performance of the adult stage.

3.2. Arc/Arg3.1 gene is effectively knocked out by the implementation of the Cre-*LoxP* system and CaMKIIα promoter

To investigate the aforementionated hypothesis, I employed an Arc/Arg3.1 floxed mouse line

(Arc/Arg3.1$^{f/f}$) together with Cre-mediated recombination to achieve spatio-temporal removal of Arc/Arg3.1. Despite a normal appearance of Arc/Arg3.1$^{f/f}$ mice, it has been reported that insertion of short DNA sequences for targeting genomic loci can accidentally show off-target effects in gene expression or even alter the expression of unrelated genes. Occasionally, distant regulatory elements could be located in introns of unrelated genes on the same chromosome, and disrupted by the insertion of short inserted sequences (Meier *et al* 2010). Moreover, noncoding sequences such as promoters and introns frequently contain important elements that not only regulate the transcription of the gene but also its translational control through NMD, as in the case of Arc/Arg3.1.

I tested these possible off-target effects of the inserted *LoxP* sites by examining the expression of Arc/Arg3.1 mRNA and protein after maximal neuronal activity (kainate-induced seizures) and evaluating the behavior of Arc/Arg3.1$^{f/f}$ mice in comparison with WT littermates. These two genotypes appeared to be biochemical and behaviorally identical indicating that the Arc/Arg3.1$^{f/f}$ mouse line can allow the genetical removal of this gene in a time and site specific matter without off-target effects when the Cre recombinase system is implemented. Furthermore, this mouse line grants the possibility to investigate if the postnatal upregulation of Arc/Arg3.1 participates in the functional development of the brain and have an impact in the adult behavior.

To evaluate the latter possibility, I manipulated the expression of Arc/Arg3.1 in the early postnatal development by generated a conditional KO through the breeding of Arc/Arg3.1$^{f/f}$ mouse with a CamKIIα-iCre transgenic mice. In these mice, a perinatal inactivation of the floxed sequence was expected via the expression of iCre in principal neurons of the CNS (Casanova *et al* 2001). I corroborated the iCre activity by using the ROSA LacZ indicator mouse line and detected mild LacZ staining from P0, but very similar to what was described for the developmental expression of CaMKII peptides, I observed a total absence of Arc/Arg3.1 mRNA only after the second postnatal week (between P7-P14) (see Figure 10).

It is possible that in this transgenic line, iCre is only mildly expressed perinatally and reached the required levels for effective recombination only in the second postnatal week. Alternatively, epigenetic factors (*e.g.* DNA methylation, tight chromatin packaging) that shield the Arc/Arg3.1 locus and prevent its expression might also protect it from recombination until the natural expression is activated in the second postnatal week, and thereby the gene becomes accessible to Cre-mediated recombination.

This approach proved highly efficiency for genetic removal of Arc/Arg3.1 in the CNS after the

first postnatal week with no residual expression during adulthood (Figure 11). Previous reports have shown that Arc/Arg3.1 mRNA in adult rats and mice is exclusively expressed in CaMKIIα positive neurons (Tagawa *et al* 2005, Vazdarjanova *et al* 2006); the use of CamKIIα-iCre transgenic mice for genetic removal of the gene confirms these findings and gives the opportunity to study the complete lack Arc/Arg3.1 after the second postnatal week, and indirectly investigate if the expression of Arc/Arg3.1 during embryologic development could explain the behavioral and electrophysiological phenotypes previously seen in the constitutive KO mice.

3.3. Early postnatal deletion of Arc/Arg3.1 causes profound deficits in consolidation of long-term memories and impairs the oscillatory activity of cortico-hippocampal networks

After having validated the genetic approach for postnatal inactivation of Arc/Arg3.1 during its early developmental upregulation, I investigated the impact of this ablation in mnemonic processes in adult mice by performing a battery of widely used memory assays for rodents: novel object recognition (NOR), Morris water maze (MWM), contextual and cued fear conditioning and conditioning taste aversion (CTA). In regard to memory consolidation, I found that Arc/Arg3.1 ablation during the second postnatal week produced a similar phenotype and recapitulated what it was previously described for the constitutive absence of the gene (KO mice), because although Early-cKO mice exhibit an equivalent or stronger learning as their WT-control littermates, they were unable to consolidate any information into long-term memories. Some subtle differences were found in these mnemonic phenotypes when I compared my results to those reported in the literature.

The Early-cKO mice improved during the acquisition of the MWM and although their performance some days was significantly lower and did not completely overlap with their WT-control littermates, they reached an asymptotic learning curve indicating only a discreet deficit during the beginning of spatial acquisition (Figure 13). These results indicate a better spatial learning than previously reported for the KO (Plath *et al* 2006) or KO-GFP KI mice (Peebles *et al* 2010). These differences might have two different explanations: (i) They arose from differences in MWM configuration and protocol used in my experiments which were not identical to those in the literature; or (ii) the circuits for spatial processing could have started developing before (e.g. medial entorhinal cortex and CA3 subfield of the hippocampus, Figure 5) the conditional ablation of Arc/Arg3.1 took place, and therefore I could observe a relatively better performance in this type of learning when compared to WT controls. Thus, it is possible that circuits for spatial processing use Arc/Arg3.1-mediated plasticity events to wire and tune the navigational system before this postnatal

period.

Alternatively, and in contrast to the MWM protocol used in the previous reports, my procedure consisted in more days of training blocks, which could have led to overtraining and recruitment of nonspatial or extrahippocampal strategies. In order to investigate if the deficit in learning of spatial strategies previously described for KO mice is due to an earlier developmental impairment than those in Early-cKO, a new MWM training in my experimental conditions must be performed in a cohort of KO mice for making a direct comparison. Nonetheless and supporting the idea that Early-cKO presented a better learning of spatial information than KO mice, Early-cKO appeared to hold for a longer time some features of the spatial information and presented a significant preference for the target quadrant (not significantly different to WT-controls) during the first probe trial (24 hrs test). This retrieved spatial information was, however, less accurate and completely abolished after 7 days when a second probe trial was performed (Figure 14). These results contrasted with earlier impairments in the retention of spatial reference memory described for KO mice by previous reports. It is then very likely that Early-cKO mice have a more developed system to process and learn spatial information than KO mice.

During fear conditioning experiments, I found that the postnatal ablation of Arc/Arg3.1 produced a heightened learning of fear compared to WT-controls and KO mice, contextual memory is extended for a week and depending on the strength and intensity of the used CS (tone), the cue memory is protracted for 7 days or longer (Figure 21), but the long-term memory eventually subsided. As previously described by Plath *et al* (Plath *et al* 2006) and Yamada *et al* (Yamada *et al* 2011) in two different lines of KO mice, the constitutive lack of this gene leads to a loss of contextual and fear memory in 24 hours after conditioning without differences during acquisition or short-term memory. This protraction of fear memory presented by the Early-cKO is probably explained by their enhanced learning of conditioned stimuli as well as an altered emotional processing. The mechanisms underlying the exacerbated fear acquisition will be discussed later.

The profound impairment in consolidation of long-term memories in the Early-cKO mice could be explaining by the proposed role of Arc/Arg3.1 in synaptic plasticity during cellular consolidation (LTP, LTD and homeostatic scaling), as previously shown by other publications (Gao *et al* 2010, Park *et al* 2008, Plath *et al* 2006, Shepherd *et al* 2006). We additionally found that Arc/Arg3.1 expression during the early postnatal development is necessary for the proper emergence of oscillatory activity of cortico - hippocampal networks (PFC and the hippocampus, section 2.3.4). The expression of Arc/Arg3.1 during the second week of development appears necessary for development of ripples and to shape ϑ and γ oscillatory activity in mnemonic-related structures.

These could be then used in the third and fourth- postnatal week for spatial learning and contextual algorithms for efficient and stable consolidation of information. I hypothesized that Arc/Arg3.1 does so by shaping connectivity within and between cortico-hippocampal networks, possibly by linking activity in these networks to synaptic and neural plasticity. In line with this hypothesis, NMDA receptors- and BDNF signaling pathways that regulate Arc/Arg3.1 expression are also known to affect network function and behavior during sensitive periods of cortex and hippocampus development (Monteggia *et al* 2004).

Intriguingly, these findings parallel the ontogeny of network activity in the hippocampus. Studies in rodents have reported a period of intense modulations extending between P7 and P30, starting with a sharp increase in γ oscillations around P7, followed by an increase in ϑ power at P8-9 and the sudden emergence of ripples at P10-P12. The Early-cKO mice still show Arc/Arg3.1 expression in the first postnatal week. This expression supports the initial increase of hippocampal γ oscillations (stratum pyramidale) and the emergence of ripples but is not sufficient for the maturation of networks as Arc/Arg3.1 is removed in these animals during the second week before P14. The delayed expression of Arc/Arg3.1 in the PFC reflects the late development of this brain region (Brockmann *et al* 2011, van Eden *et al* 1991) and explains why PFC γ oscillations are strongly impaired in the Early-cKO.

3.4. Early-cKO mice exhibit intensified extinction

In the MWM and the CTA experiments, mice were subjected to two subsequent training paradigms; in the MWM a reference-based navigation to a hidden platform was followed by directional navigation to a flagged platform, and in the CTA mice learned first an association between two stimuli (sucrose and malaise) followed by a dissociation of these stimuli (extinction). The Early-cKO mice exhibited faster learning of the cued spatial task and complete extinction of the CTA memory when compared to WT-controls (Figure 15 a-d and 16 f). I interpreted these results as the consequence of the lack of consolidation which allows the Early-cKO mice to better learn a novel task (cued MWM) or show an enhanced extinction.

Additionally, I also found that during my first fear conditioning experiment, the Early-cKO mice presented faster extinction of auditory fear conditioning during the second minute of testing when compared to their WT-controls (Figure 17g); suggesting that the findings in cued MWM and CTA could have been the result not only from the amnesic phenotype but alternatively of an enhanced extinction learning. To test this possibility, I took advantage of the protraction (7 days) in fear

memory presented by Early-cKO mice and designed a protocol to investigate the extinction of contextual fear. Notably, I found that Early-cKO mice exhibited significantly faster short-term extinction to the context in the last 4th and 5th minute of retrieval. Similarly, to CTA experiments, an enhanced extinction of contextual fear was observed in the next 3 days of the extinction protocol (Figure 18e). It is tempting to affirm that fear learning (including fear extinction) is enhanced or that the interpretation of threats in Early-cKO mice is altered, not only because the acquisition of conditioned stimuli is enhanced but also because extinction is facilitated, this misinterpretation may be extended to other types of aversive stimuli such as in CTA.

Extinction learning is a type of inhibitory learning that involved three key regions: the amygdala, the infralimbic region (IL) of the mPFC and the Hpc (ozeske *et al* 2015). During postnatal development, a sensitive period (between P10 and P16) for erasure of fear memories by extinction has been described, after this period extinction is ineffective and fear recovers spontaneously by renewal, this phenomenon correlates with the immaturity of perineural nets in the BLA (Gogolla *et al* 2009) and the lack of myelin-associated inhibitors in the BLA and IL cortex (Bhagat *et al* 2015). It is possible that Arc/Arg3.1 mediates (in the BLA or IL) developmental synaptic plasticity that shapes the connectivity during this sensitive period and its removal before the closing of this window may lead to an infantile behavior where fear memories can be easily extinguished.

Understanding the development of neural circuits of fear extinction and the underlying cellular and molecular mechanisms is important for improving current treatments of acquired- and trait fear-related disorders such as post-traumatic stress disorders and generalized-anxiety. Further investigation is needed to evaluate the specific role of Arc/Arg3.1-mediated plasticity in the developmental maturation of the BLA and the IL cortex and its relation to sensitive periods for fear memory erasure.

3.5. Conditional genetic ablation of Arc/Arg3.1 during early postnatal development leads to imbalanced functional connectivity within the corticolimbic circutry

3.5.1. Early genetic inactivation of Arc/Arg3.1 facilitates the acquisition and expression of conditioned aversive stimuli

CTA and FC experiments demonstrated the necessity of Arc/Arg3.1 expression after the second postnatal week for the consolidation of implicit and explicit memories. In addition, they revealed that Early-cKO mice exhibited an enhanced acquisition of aversion and heightened fear learning

to the CS-US presentations. Both phenomena were always stronger in Early-cKO mice than in constitutive KO, suggesting that interfering with Arc/Arg3.1 expression during the second postnatal week results in a different phenotype for fear control than a constitutive lack of the gene. Since the second postnatal week is a critical time in the development of emotional and fear control circuitry, it is attractive to hypothesize that Arc/Arg3.1 might participate in tuning connectivity within this circuitry.

The ability to learn and store fear memories is vital for survival. The control of fear responses and learning of conditioned fear rely on neural circuits that are shaped during development, likely through experience. Aversive learning of odor-footshocks associations appears at P10 and coincides with the development of learning-induced synaptic plasticity in the amygdala (Thompson *et al* 2008). I demonstrated that at the same time Arc/Arg3.1 is naturally upregulated (second postnatal week) in areas related to fear and emotional processes, and is in the position to affect synaptic plasticity induced by novel olfactory experiences. The removal of the gene at this time leads to stronger responses to conditioned fear and to amnesia of fear experience in adult mice, resembling the immature behavior exhibited by rodent during the second postnatal week (Callaghan & Richardson 2012, Moriceau & Sullivan 2006). This could be interpreted as if a period of synaptic plasticity had been opened but never closed due to the lack of Arc/Arg3.1-mediated plasticity, leading to an immature behavior in the adult mouse.

CTA, similar to FC is a form of Pavlovian conditioning that is partially mediated by structures in the gustatory pathway such as the nucleus of the solitary tract (NST), the parabrachial nucleus (PbN), parvocellular thalamic and ventral posteromedial nucleus (VPMpc), the gustatory cortex (GC) in the agranular insular cortex (IC), and limbic structures such as amygdala and lateral hypothalamus (Welzl *et al* 2001). Subdivisions of the PFC have been implicated in the modulation of conditioned responses and CTA extinction (Gonzalez *et al* 2015, Uematsu *et al* 2015). Early-cKO mice present a strong impairment of CTA consolidation and a generalization of taste aversion that extends to liquid consumption after CTA (second day post-CTA). These findings raise the possibility that components of the neural circuit that underly aversion acquisition have not developed properly due to the temporal disruption of Arc/Arg3.1.

CTA is a form of associative learning that emerges early in development, few studies reports that aversive associations with taste or odor can be induced even at the late embryogenic stages (E18) (Gruest *et al* 2004a) and in the early postnatal ages (P3). This form of learning depends on protein synthesis for its consolidation and reconsolidation (Gruest *et al* 2004b); suggesting that different to explicit memories, the circuits supporting CTA memory mature pre or perinatally with

the exception of regulatory regions (such as the amygdala) and ACC; these regions are involved in the perception of aversive stimuli and develop later (after P10) (Raineki *et al* 2009).

If the circuits that consolidate CTA memory are already mature before the genetic ablation of Arc/Arg3.1 takes place in the Early-cKO mice, the expression of Arc/Arg3.1 would be necessary at any moment (independent of the developmental process) for the molecular events that consolidate this form of memory, and only modulatory regions that participate in the perception and acquisition of aversive and unpleasant stimuli (such as Amy and ACC) are affected by this developmental intervention in a sensitive period of their development.

3.5.2. Deletion of Arc/Arg3.1 during early postnatal development produces anxiolytic-like behavior

After having discovered that Early-cKO mice displayed heightened acquisition and expression of conditioned aversive responses and facilitated fear extinction, I sought to determine their innate level of anxiety by testing their behavior in ethological paradigms such as open field, elevated-plus maze, and light-dark box. These tasks assess the natural exploratory drive, risk assessment and innate unconditioned avoidance that rodents display to open and illuminated environments. I found that although Early-cKO exhibited normal exploratory behavior in the open field with a mild tendency in males to habituate faster and explore longer time the center, these animals displayed a strong anxiolytic-like behavior represented by a reduced unconditioned avoidance of open arms in the EPM and longer exploration of the light zone of the LDB. As the anxiolytic behavior was singularly observed in the Early-cKO mice but not in the constitutive KO, I speculate that it reflects a developmental effect of Arc/Arg3.1 removal during the second postnatal week because constitutive KO mice were not different to their WT-control mice.

Anxiety-related behavior in developing rodents is often investigated via ultrasonic vocalizations (USVs) examination. USVs are produced by pups when they are separated from their mothers, siblings or when deprived of food or heat. The production of USVs is minimal in the newborn, peaks at P6-8 and progressively decreases to low levels at P18 (Allin & Banks 1972). Ethological paradigms for testing innate anxiety-like behavior such as EPM or LDB can only be performed in young mice after the full exploratory behavior is established, thus earliest measurements are reported in adolescent rodents and show contradictory results (Lynn & Brown 2010, Macrì *et al* 2002). Innate and unconditioned fear can be evaluated during development by the investigation of unconditioned freezing to predator or startle responses to bright light. Although these responses are not considered strictly as anxiety-like behaviors, they could give an indication of how fear and

anxiety circuitry develop. Freezing to predator odors emerges around P10 and coincides with the development of sensory input to the amygdala and increase in corticosterone levels (Moriceau *et al* 2004). In contrast, acoustic startle responses emerge later at P18 (Weber & Richardson 2001), indicating that Arc/Arg3.1 ablation in Early-cKO occurred in a period where circuits for innate avoidance and fear are developing and the expression of Arc/Arg3.1 may be necessary for the synaptic refinement of these circuits.

My results show a seemingly paradoxical effect of Arc/Arg3.1 ablation in the early postnatal period on systems that control and modulate avoidance responses and fear. On one hand, unconditioned avoidance appears significantly reduced but on the other hand, the acquisition and immediate expression of conditioned aversive and acquired fear responses seem to be heightened, supporting the hypothesis that anxiety and fear may be mediated by different circuits that display independent development. These paradoxical behavioral outcomes may be, in part, the result of changes in functional connectivity within the PFC, the dHpc and habenula that are discussed later.

Additionally, one could hypothesize that the enhanced fear learning may be explained by the enhanced short-term plasticity (LTP) that was previously reported by Plath *et al* (Plath *et al* 2006) in constitutive Arc/Arg3.1 KO mice. Regulation of AMPARs endocytosis by Arc/Arg3.1 is believed to be the mechanism by which Arc/Arg3.1 contribute to the consolidation of synaptic plasticity. In the absence of Arc/Arg3.1, the turnover of AMPARs in the synapses slows down and recently stimulated synapses would display higher content of synaptic AMPARs that might explain the enhanced induction and short-term LTP. The lack of AMPARs trafficking mechanisms from and to synaptic compartments could explain the impairment of long-term consolidation of this type of plasticity.

Similar synaptic impairments might be present in neurons of the amygdala and could also affect acquired fear responses. However, enhanced acquisition of fear or aversive responses was not observed previously in the constitutive KO mouse lines (Plath *et al* 2006, Yamada *et al* 2011) and in my experiments with KO mice, these phenotypes were milder than in the Early-cKO mice (Figure 21 and 22). To test these hypothesis electrophysiological measurements of synaptic plasticity should be made directly in the Amygdala and PFC of Early-cKO mice.

3.5.3. Early postnatal ablation of Arc/Arg3.1 alters the functional connectivity of the PFC, hippocampus and habenula

I confirmed the importance of Arc/Arg3.1 for the consolidation of memories; in addition, I discov-

ered that Arc/Arg3.1 expression during early postnatal development supports normal maturation of oscillatory network activity in the PFC and Hpc. However, removal of the gene in the midst of postnatal development procreated intensified fear learning and anxiolytic behavior that were not otherwise prominent in the conventional KO. These findings led me to hypothesize that early expression and function of Arc/Arg3.1 open developmental plasticity processes that could not be properly closed due to the premature removal of Arc/Arg3.1. Producing an imbalance in the functional organization of the circuits involved in innate avoidance and fear learning.

To test this hypothesis, I performed MRI imaging experiments and identified changes in brain structures and functional connectivity of corticolimbic regions previously linked with memory, fear and anxiety (Figure 27). Surprisingly, only the Early-cKO displayed a significant change in gray matter volume in the dCA3 subfield of the Hpc and in the dorsal LS (dLS). Given that the overall volume of the cortex and hippocampus did not differ between WT-controls and Early-cKO (Figure 26b), these findings might indicate a specific reduction in the volume of dCA3, or the overlaying alveus, possibly due to reduced dendritic or synaptic volume in these regions.

This could be explained by a model in which Arc/Arg3.1 mediates, sequentially, opposing forms of structural plasticity, such as synaptic sprouting and pruning. Specific regions which express Arc/Arg3.1 prior to the Cre-recombination (*e.g.* CA3 and LS) could thus experience one modification (pruning) but not the subsequent sprouting. An alternative model might be that local plasticity within the CA3 and LS occurs in the presence of initially expressed Arc/Arg3.1, yet the plasticity driven by inputs from later-developing regions fails. This would lead to a misbalance in microstructural development that affect the local connectivity of specific brain circuits involved in memory consolidation (dCA3) and emotions regulation (LS). A more detailed histological analysis should be performed to resolve this model and identify specific structural alterations.

The dCA3 receives strong inputs from the entorhinal cortex and DG and is highly connected with CA1 and the contralateral CA3 regions through recurrent axons, as well as with the dLS (Witter 2007). It is proposed that CA3 encode spatial representation and episodic memories (Nakashiba *et al* 2008) by the generation of sharp-waves (Nakashiba *et al* 2009) and coherent population activity in the ϑ and γ frequency bands with other cortical and hippocampal regions. The LS receives strong glutamatergic input from CA3 regions and is predominantly composed of GABAergic projection neurons interconnected with various hypothalamic nuclei and midbrain regions such as the PAG. The LS receives also inputs from the amygdala, bed nucleus of the stria terminalis, PFC and entorhinal cortex. These anatomic connections indicate that LS may be an important modulator of emotional and mnemonic processes. Accordingly, the circuitry from the

LS to hypothalamic nuclei have been directly linked with maintained anxiety mediated by stress (Anthony *et al* 2014) and it is proposed that θ oscillations in the hippocampus are modulated by the LS activity (Chee *et al* 2015).

Structural changes of dCA3 and LS could indirectly explain alterations in memory consolidation and anxiolytic-like behavior of the Early-cKO, as well as the reduced θ frequency band and impairment in SPW-Rs properties. Intriguingly, these morphological alterations are not observed in the constitutive KO mice, suggesting the existence of a sensitive period for developmental Arc/Arg3.1 expression in these structures. Within the hippocampus, CA3 is the subfield showing the earliest upregulation of the Arc/Arg3.1 gene (P7) and it is plausible that a transient heightened plasticity induced by Arc/Arg3.1 before its ablation (in the second postnatal week) causes a developmental imbalance, locally and to its anatomical target regions (CA1, CA3 and LS). This imbalance does not occur in brains that constitutively lack Arc/Arg3.1.

Additionally, fMRI analysis revealed that the constitutive or developmental deletion of Arc/Arg3.1 produce different changes in functional connectivity at the resting state (rsfMRI). Increased resting state connectivity between IL and medial septum and between the habenula and vCA3 was observed in the constitutive KO, whereas reduced functional connectivity between the ACC, IL, dHpc and habenula was specifically found in the early ablation of Arc/Arg3.1.

So far, little is known about the functional connectivity between the habenula and other brain regions and its importance to different behaviors. The habenula is a diencephalic structure located in the dorsomedial portion of the thalamus and is an important anatomic link between the forebrain and hindbrain. The lateral habenula appears to encode reward prediction error signals, negative responses to pain stimuli (Bianco & Wilson 2009) and may play a role in maintaining hippocampal θ oscillations during REM sleep and spatial learning (Goutagny *et al* 2013), while the medial habenula seems to modulate anxiety-like behaviors and fear response (Yamaguchi *et al* 2013). Some of the behavioral phenotypes that I found in the Early-cKO could have its neurobiological subtract in an altered maturation of the habenula and its functional connectivity. The development of the habenula might need Arc/Arg3.1-mediated plasticity and the maturation of this structure in the absence of Arc/Arg3.1 should be studied in the future.

Additionally, components of the PFC have been constantly linked with diverse cognitive functions such as risk assessment and decision-making, adaptation to stress, anxiety control (Shiba *et al* 2016), consolidation of remote fear memories, extinction of fear (Izquierdo *et al* 2016) and social cognition (Bicks *et al* 2015); part of these functions appeared to be altered to some degree in the

Early-cKO mice. Moreover, an imbalanced connectivity in the PFC has been constantly proposed as one of the main physiopathological hallmarks of neurodevelopmental disorders such as autism spectrum disorders (ASD), attention deficit hyperactivity disorders (ADHD)(Schubert *et al* 2015) and schizophrenia (Selemon & Zecevic 2015).

3.5.4. Early postnatal deletion of Arc/Arg3.1 affects social cognition in the adult brain

Social cognition in rodents involves a group of complex processes that are required to identify and interpret social signals for guiding the behavior in groups. Increased neuronal activity in several brain regions has been detected and positively correlated with social behaviors such as components of the PFC (IL, PrL and Orbital cortex) (Kim *et al* 2015). Special interest has been given to the study of the excitatory/inhibitory balance in local PFC networks due to the fact that developmental neuropsychiatric disorders characterized by disturbances in social behavior usually show diminished γ synchrony in these circuits (Gonzalez-Burgos *et al* 2015) and acute manipulation of the excitability in these regions impairs normal sociability in mice (Yizhar *et al* 2011).

Early-cKO displayed a strong functional phenotype in the PFC, the LFP measurements demonstrated a profound impairment in both γ and θ synchronicity, and rsfMRI suggested that the local networks displayed disturbances in mid-range functional connectivity between specific subregions of the PFC (IL and ACC) and long-range connectivity with the dHPC (specifically dCA3). This developmental imbalance in local- and long-range connectivity specifically with the hippocampus and habenula may explain the specific social behavioral phenotype, where social anxiety is decreased but social recognition seems to be abrogated.

Social cognition emerges and develops postnatally as the result of close interactions with parental care and peers. Social stimuli in neonates and young infants originate mainly from tactile and olfactory stimulation of the dam (mother and littermates). Early studies showed that brief daily social separation (3-15 min) and handling of pups in the first postnatal week produce dramatic changes in social anxiety and resilience to stress in the adulthood (Levine *et al* 1957), suggesting that the first postnatal week constitutes a critical period in the development of social and emotional behavior, and stress systems (hypothalamic–pituitary–adrenal axis - HPA).

Early-cKO mice present normal Arc/Arg3.1 expression in the first postnatal week when it could be gradually upregulated by tactile and olfactory stimuli from the dam, thus the neurodevelopmental mechanisms for social and stress resiliency may be initiated by experience-dependent synaptic events associated with Arc/Arg3.1 expression, but the genetic removal in the second

week might interrupt this process and its final tuning, especially in regions where the synaptic development is prolonged until adolescence (such as in the PFC), resulting in a functional synaptic imbalance and an infantile social behavior with lower levels of social anxiety. Furthermore, it remains to be investigated if this diminished social anxiety in Early-cKO mice is the result of developmental changes in stress responses or stress resilience. The activation and function of the HPA should be evaluation in the future by corticosterone measurements in blood after different environmental stress stimuli (e.g. exposure to novel environments or conspecifics) or application of anxiogenic drugs (e.g. caffeine).

Social recognition is based on the natural preference towards a longer olfactory investigation of novel conspecifics; it is then intriguing if the lack of social recognition presented by Early-cKO occurs as the result of changes in olfactory recognition. The increased sociability presented by Early-cKO mice in comparison with their WT-controls indicate that these animals respond to olfactory cues but the lack of short-term social recognition may indicate that discrimination of different olfactory stimuli could be impaired and before affirming that Early-cKO mice display a social recognition deficit this possibility should be investigated by an olfactory discrimination test. Odors regulate the expression of Arc/Arg3.1 mRNA in olfactory bulb ensembles in adulthood (Guthrie *et al* 2000) and early postnatal development (Figure 5b), as well as after mating behavior in rats (Matsuoka *et al* 2002), suggesting that Arc/Arg3.1 may play a role in the acquisition and consolidation of odor-related information.

Alternatively, if olfactory recognition in Early-cKO mice is unaltered, a loss of social recognition memory could account for these findings. Social recognition in rodents has been shown to be mediated by semiochemicals (pheromones, allomones and kairomes) that transmit social signals between subjects and bind to specific receptors in the olfactory epithelium and vomeronasal organ, this information conveys later onto the olfactory bulb that projects to the medial nucleus of the Amygdala (MeA). In turn, the MeA transfers the information to the LS that orchestrates communication and consolidation of the information with the Hpc and hypothalamic areas. Other subcortical and cortical areas such as the bed nucleus of stria terminalis, entorhinal cortex, and the PFC have been linked to social recognition memory (Maroun & Wagner 2016). Changes in gray matter in the LS and dCA3, and functional changes in connectivity with the PFC were found in Early-cKO mice, suggesting that if an actual social recognition deficit is displayed by these animals, Arc/Arg3.1 expression during postnatal development might be essential for the proper development of these hubs in the social recognition circuitry. Future investigation of these anatomical regions should be conducted to investigate the contribution of Arc/Arg3.1 in synaptic plasticity and molecular changes that tune the development of circuits that underlie different

aspect of social cognition.

3.6. Conclusions and outlook

One distinctive aspect of this thesis is the use of diverse and interdisciplinary methods, including biochemical assessment, genetic mouse models, behavioral examination, electrophysiology (LFP) and brain imaging (MRI). These methods allowed me to unveil novel functions of Arc/Arg3.1 at a specific time of life and linked them with sensitive periods of postnatal development. I presented novel evidence about the natural expression of Arc/Arg3.1 during early postnatal development and its contribution to the proper functional oscillatory activity and connectivity of corticolimbic networks involved in the consolidation of long-term memories and the control of emotional processes such as anxiety-like behaviors, acquired aversion and social cognition.

The discovery that Early-cKO mice displayed a profound impairment in the consolidation of long-term memories that recapitulates the mnemonic phenotype previously described for the constitutive KO, allows me to hypothesize that memory systems might develop later than the second postnatal or that removal of Arc/Arg3.1 at any age is detrimental for memory. The function of Arc/Arg3.1 in the fully developed adult networks during consolidation of memory has been studied by knock-down of its mRNA (Table 1), and in the second part of this dissertation, I demonstrate that Arc/Arg3.1 expression in the adult brain is required for the consolidation of implicit fear memory (Part II). These findings strengthen the premise that Arc/Arg3.1 is always necessary for the consolidation of long-term memory, possibly via the recruitment of cell ensembles that through Arc/Arg3.1-mediated plasticity store novel information.

The second highlight of this thesis is the discovery of Arc/Arg3.1 as a molecule necessary during postnatal development for the proper tuning of oscillatory activity and long-range functional connectivity of corticolimbic regions that control emotional processes. The differential phenotype presented by the Early-cKO mice (only mildly showed by KO mice) of enhanced learning of aversive responses and reduced unconditioned avoidance lead me to hypothesize that the postnatal expression of Arc/Arg3.1 influences a sensitive period for the emergence of these behaviors. In a hypothetical model (Figure 29), I propose that the genetic removal of Arc/Arg3.1 during the second postnatal week (after its developmental expression has already begun) produces an imbalance in the functional or structural maturation of synaptic connections that were first initiated by an early expression of the gene. These processes would remain open and would not close properly in the absence of the gene, producing reduced functional connectivity of brain regions

that had started their synaptic refinement. These developmental synaptic changes are probably never initiated in the constitutive KO or are compensated by other molecular and network mechanisms. Functional maturation of synapses and spine elimination are developmental processes essential for the refinement of network oscillatory activity and functional connectivity in different brain regions. An in-depth study of molecular changes during the postnatal brain and plasticity development in the absence of Arc/Arg3.1 is necessary to probe this hypothesis in the future.

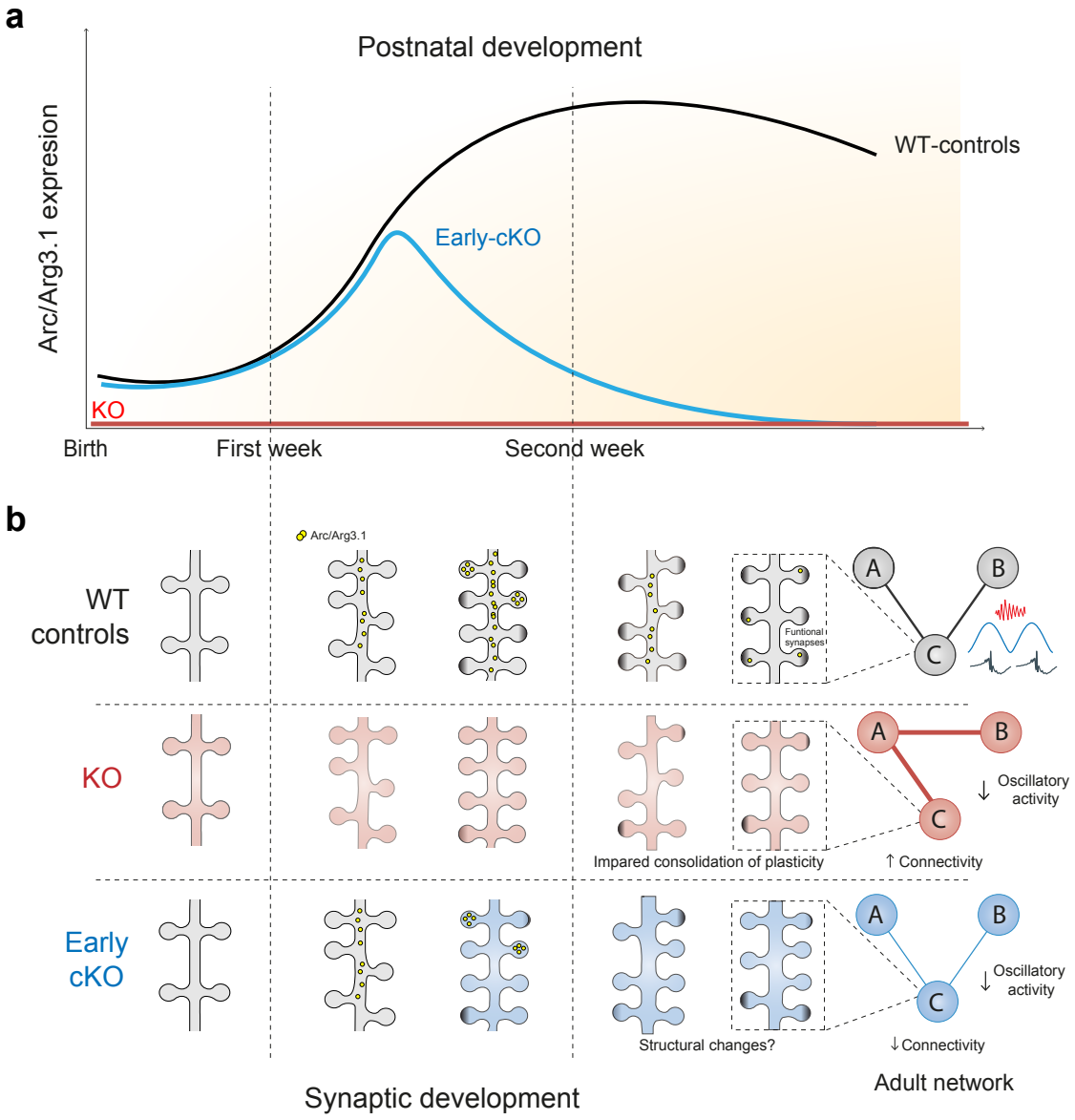

Figure 29. Expression and effects of genetic removal of Arc/Arg3.1 during postnatal development
a. In the first two postnatal weeks, diverse molecular events surge gradually for building neuronal networks and prepare the brain to deal with novel information. Arc/Arg3.1 expression starts postnatally during the second week and may participate in the tagging and selection of functional synapses (Okuno *et al* 2012) and synaptic elimination (Mikuni *et al* 2013). **b.** Adult networks with regular oscillatory activity mature via local synaptic refinements by selection of functional synapses via expansion and pruning of excessive dendritic spines (upper row). Some of these processes might not initiate or be compensated in the complete absence of Arc/Arg3.1 (middle row). The genetic removal of Arc/Arg3.1 during the second postnatal week might lead to an imbalance in the local synaptic development refinement that in turn results in lower function connectivity and impaired oscillatory behavior of the adult brain, and changes in emotional processes and social cognition. Modified from (Bourgeron 2015).

The findings of the first part of my thesis are the entry point to study how Arc/Arg3.1 participates and becomes an important player in sensitive periods of the postnatal development, and possibly in neurodevelopmental disorders, such as schizophrenia (Fromer *et al*., 2014), fragile X syndrome (Niere *et al*., 2012), autism spectrum and intellecual disability (Greer *et al*., 2010). Disorders that share mnemonic, emotional and social deficits and in which Arc/Arg3.1 has been constantly implicated

Part II:
Role of Arc/Arg3.1 in circuits for fear and anxiety in the adult brain

4. Introduction

The genetical removal of Arc/Arg3.1 during the second postnatal week revealed a dramatic and profound behavioral phenotype in the adult Early-cKO mice that includes impairments in the consolidation of long-term memories, increased learning of aversive response to conditioned stimuli, diminished unconditioned avoidance and deficits in social cognition. In addition, oscillatory activity in the PFC and Hpc, as well as functional connectivity within and between these structures was highly altered. Overall, removal of Arc/Arg3.1 during postnatal development reaffirmed its importance for mnemonic capacity, learning and memory, but also revealed a new role in the control of fear and anxiety.

Because Arc/Arg3.1 is not only expressed during development but also in response to experience and plasticity-producing activity in the adult brain (Bramham *et al* 2010, Vousden *et al* 2015), I hypothesized that Arc/Arg3.1 participates in the regulation of acquired behavior such as fear, emotional control and unconditioned avoidance in the adult brain. In the second part of this dissertation, I sought to dissect the role of Arc/Arg3.1 in fear and anxiety circuits of the adult brain. To do so, I took advantage of the well-characterized Arc/Arg$^{f/f}$ mouse line and additionally, I established recombinant adeno-associated viral vectors (rAVV) to deliver Cre recombinase to specifically target brain regions that have been linked with fear and anxiety. I used fear conditioning and elevated-plus maze, as main behavioral paradigms due to their reproducibility, consistency of results and close link to fear and anxiety.

4.1. Anxiety and fear-related disorders

As introduced in the first part of this dissertation, fear is defined as a normal emotional state that is caused by the exposure to a real threat or stimuli previously associated with danger, while anxiety is defined as the feeling of uneasiness, unprovoked worries, and apprehension over potential threats or expected negative events. Bouts of sporadic anxiety are normally experienced by healthy people in specific situations of uncertainty or stress, but if this feeling persists and is presented in a disruptive or disproportionate manner interfering with the normal social functioning, it is considered a psychiatric disorder (APA 2013). Anxiety disorders are among the most prevalent and incapacitating psychiatric disorders worldwide and are characterized by excessive fear and avoidance, often in response to specific situations and the in absence of real threats. Hence, special attention has been given to investigate the neural circuits and molecular events that contribute to the normal fear and avoidance that are thought to be the root of these complex

disorders.

In the fifth edition of the Diagnostic and Statistical Manual for Mental Disorders 5th edition (DSM-V) (APA 2013), anxiety and fear-related disorders are grouped into three main categories: obsessive-compulsive and related disorders, trauma and stressors-related disorders, and anxiety disorders. In the anxiety disorders group, the following categories are recognized: separation anxiety disorder, selective mutism, specific phobias, social anxiety disorder, panic disorder, agoraphobia, generalized anxiety disorder, substance/medication-induced anxiety disorders and anxiety disorders due to another medical condition. Two additional categories that do not fit the preceding ones are also defined: other specific anxiety disorder and selective mutism expressed in childhood. If the criteria from DSM-V is used, anxiety and fear-related disorders have an estimated lifetime prevalence of 14 to 33.7% in adults, posing an enormous problem for health care systems with a substantial economic and personal burden (Bandelow & Michaelis 2015). Moreover, anxiety disorders are associated with problems in workplace performance (Waghorn *et al* 2005), increased risk of cardiovascular morbidity and mortality, and elevated rates of substance abuse (Scott 2014).

The treatment of the anxiety disorders is difficult due to limited therapeutics and pharmacological strategies. The pharmacological treatments are based on the use of serotonin/ norepinephrine reuptake inhibitor (SSRIs), tricyclic antidepressants, monoamine oxidase inhibitors (MAOIs), and lastly and only as second-line or adjunctive use the benzodiazepines, the latter due to tolerability effects and abuse issues (Murrough *et al* 2015). Since the arsenal of treatment remains limited, there is an imperative need for the development of novel and more effective strategies. Understanding the normal function of neuronal circuits that mediate fear and avoidance is consequently an imperative for improving the effectiveness of future treatments of such a prevalent health problem.

The study of new treatment strategies in clinical trials carries enormous costs and ethical consideration (DiMasi *et al* 2003); as a result of these limitations, research funding and health regulatory agencies demand that novel strategies of treatment are probed to have a specific biological target that is relevant to the specific disorder or disease ,and a predictable safety profile for the future use in human populations. Preclinical studies for the validation of animal models are therefore essential for the study of neurobiological subtracts of human anxiety and fear-related disorders and evaluation of novel compounds or therapeutically interventions (Cryan & Holmes 2005).

4.2. Neuronal circuit for fear and anxiety

The understanding of neuronal circuits that mediate anxiety and fear originates largely from studies that used lesions and inactivation of specific brain regions in animal models. Currently, the development of tracers, immediate early genes detection, genetic manipulations and imaging techniques (live microscopy and fMRI) have brought deeper knowledge about anatomical and functional connectivity, and the molecular and cellular underpinning. Using these experimental approaches, key neuroanatomic loci that control fear and anxiety have been identified such as the amygdala (Amy), the bed nucleus of the stria terminalis (BNST), ventral hippocampus (vHpc) and components of the Prefrontal cortex (PFC) (Tovote *et al* 2015). Although certain overlap has been shown, differences between the circuits for fear and anxiety have also been recently addressed by these newer approaches.

4.2.1. Neuronal circuits for fear

In their seminal investigation, Klüver and Bucy described that the bilateral temporal lobectomy in monkey produced a syndrome characterized by the lack of anger and fear, visual agnosia, hyperorality, hypersexuality and loss of social interactions (Bucy & Kluver 1955). These experiments led to the hypothesis that the temporal lobe is essential in the processing of emotions. Most of what is known about learned fear arise from literature about Pavlovian fear conditioning (FC). FC is a powerful behavioral tool for studyng circuits involved in associative memory and the mechanisms for fear generation and control. Using FC three main hubs for fear generation, expression and acquisition have been identified: Amygdaloid complex (Amy), Hippocampus (Hpc) and prefrontal cortex (PFC).

Amygdaloid complex: Among the structures located in the temporal lobe, special attention has been given to the Amygdaloid complex, because a bilateral lesion in this temporal structure produces a strong deficit in the acquisition and expression of conditioned fear stimuli and certain forms of unconditioned fear (Janak & Tye 2015). The amygdaloid complex is a group of more than 10 nuclei. Those involved in fear can be divided into two main sub-areas: the basolateral amygdala (BLA) and the central amygdala (CeA). The BLA has a cortical origin containing 80% of spiny glutamatergic projecting neurons and 20% GABAergic interneurons (McDonald 1982) and can be divided at the same time in lateral (LA), basal (BA) and basomedial amygdala (BMA) nuclei. The CeA has a striatal origin and can be divided in lateral (CeL) and medial (CeM), both containing mainly GABAergic spiny neurons that project to areas in autonomic centers that are involved in fear expression such as ventral Periaqueductal Gray matter (vPAG) and mesencephalic and

pontine reticular nuclei (Swanson & Petrovich 1998).

The role of the BLA subdivisions in the acquisition and expression of auditory fear conditioning has been well studied during the last two decades and its broadly accepted that the integrity of these structures mediates the acquisition, consolidation and expression of normal auditory conditioned fear (Moscarello & LeDoux 2014). Auditory information about the CS from the auditory cortex and multiple sensory modalities from multimodal areas of the thalamus and nociceptive information about the US coming from the PAG and spinomesencephalic tract converge into the LA. Several reports suggest that synaptic plasticity in the LA is necessary for the consolidation of CS-US associations (cued fear memory) (Nabavi *et al* 2014, Pape & Pare 2010) in a limited set of neurons that will represent a fear memory trace ensemble (Kim *et al* 2014). Additionally, the role of the CeA has been dissected; Ciocchi *et al*. described that CeL is required for the acquisition while CeM activity is necessary for the expression of conditioned auditory fear responses (Ciocchi *et al* 2010).

Hippocampus: The hippocampus is a limbic structure located in the medial portion of the temporal lobe and is described as an essential element for consolidation of episodic memories. The Hpc forms connections with structures involved in emotional processing such as PFC, Amygdala, septal nuclei, hypothalamus, raphe nuclei and locus coeruleus (Bannerman *et al* 2004). Lesions or manipulations of the vHpc produces conflicting results because pre and post-training lesions reduces cued fear expression while temporally-restricted inactivation reduces fear expression only when performed prior to training (Maren & Holt 2004, Sierra-Mercado *et al* 2011).

Prefrontal cortex: The amygdala and Hpc are connected and modulated at the same time with and by cortical areas. Special effort has been made to investigate cortical regions that contribute to the emotional control and support remote memory storage of fear experiences; the best candidate appears to be the prefrontal cortex because lesions or pharmacological manipulations in its subdivisions produce changes in emotional behaviors such as anxiety and fear (Heidbreder & Groenewegen 2003). In rodents, the medial prefrontal cortex (mPFC) is anatomically divided in a descending manner from the most dorsal region in medial precentral cortex (PrCm), the anterior cingulate cortex (ACC, dorsal and ventral part), the prelimbic cortex (PrL) and the infralimbic cortex (IL) (Van Eden & Uylings 1985). Most of the literature in rodents groups in agreement the PrL and IL cortex and names them in a single term: ventromedial prefrontal cortex (vmPFC); while rostral ACC is taken as a single anatomical division:

- *vmPFC*: The vmPFC receives massive input from the BLA that terminates mainly in ventral

ACC, PrL and IL cortices, and the vmPFC projects in turn back to the BLA and the CeA (McDonald 1998). The vmPFC also receives direct inputs from the vHpc and projects back indirectly to the Hpc via the nucleus reunions (NR), mediodorsal nucleus of the thalamus, entorhinal cortex and amygdala (Vertes 2006). Preconditioning lesions that include the dorsal PL and ACC enhanced cued and contextual fear conditioning expression (Morgan & LeDoux 1995), whereas preconditioning manipulations of the ventral PL and IL blocked conditioned fear expression (Frysztak & Neafsey 1991).

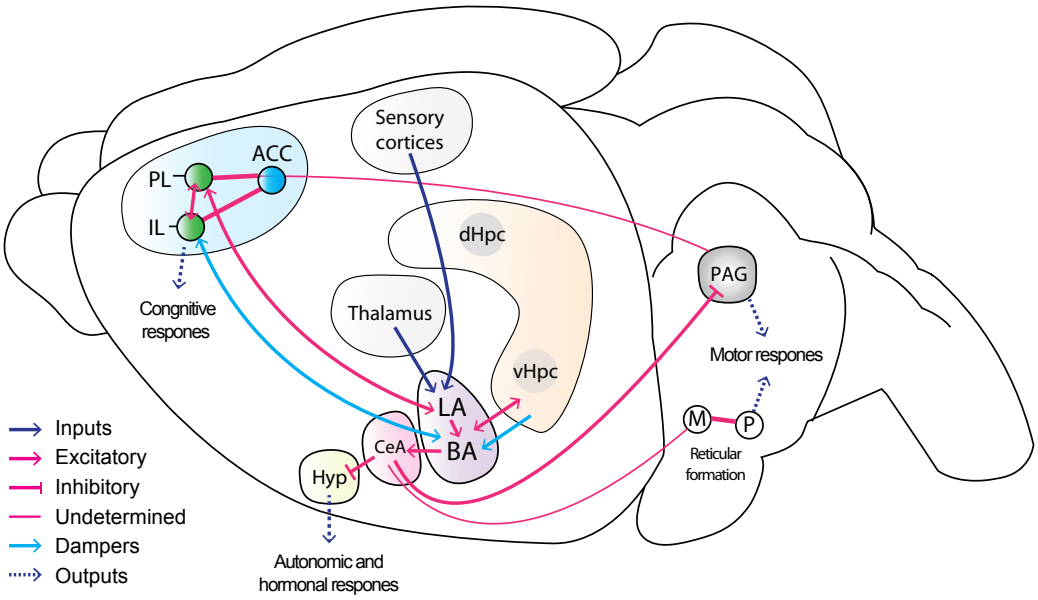

Figure 30. Neuronal circuits for fear
Fear states are mediated by a network of cortical and subcortical components. ACC, anterior cingulate cortex; PrL, prelimbic cortex; IL, infralimbic cortex; dHpc, dorsal hippocampus; vHpc, ventral hippocampus; PAG, periaqueductal gray matter; LA, lateral amygdala; BA, basal amygdala; CeA, central nucleus of the Amygdala; M, mesencephalic; P, pontine reticular formation; Hyp, hypothalamus. Connectivity sketch was taken and modified from (Tovote *et al* 2015).

- *rACC*: In humans and non-humans primates the cingulate cortex is located in the medial wall of each hemisphere adjacent to the corpus callosum; in rodents, the anterior cingulate cortex (ACC) is only located in the PFC and corresponds to the most dorsal part (Seamans et al 2008). The ACC has been linked with emotional processing, expression of negative emotions, nociceptive and unpleasantness perception (Stevens et al 2011); and to storage of remote fear memories (Frankland & Bontempi 2005, Goshen et al 2011, Teixeira et al 2006), its dysfunctional activation has been implicated in the neuropsycophatology of a variety of neuropsychiatric and neurological disorders such as Posttraumatic Stress disorder (PSTD), chronic pain (Zhuo 2016), anxiety (Mochcovitch et al 2014), depression (Dutta et al 2014), and schizophrenia (Bersani et al 2014). The ACC projects to the amygdala, vmPFC and subcortical structures such as hypothalamus and PAG, suggesting a critical role in emotional control (Heidbreder & Groenewegen 2003). Circuits

in the ACC have been directly linked with the generation of fear and aversive responses, because direct electric stimulation to this region produced fear-like freezing and auditory fear memory (Tang et al 2005); moreover pre-training lesions that are limited to the rostral ACC produce deficits in the acquisition of auditory fear conditioning (Bissiere et al 2008).

These three hubs for conditioned fear show reciprocal interactions. BLA and the mPFC are entrained in ϑ oscillations only when fear is discriminated from safe stimuli (Likhtik *et al* 2014), a mechanism by which BLA activity is hypothesized to gate fear responses in the mPFC (Sotres-Bayon *et al* 2012). Similarly, entrainment in ϑ rhythm during fear expression has been shown between LA and the Hpc, probably as part of the complementary process with regard to spatial and contextual information managed by this latter structure (Seidenbecher *et al* 2003).

4.2.2. Circuit for anxiety-like behavior

Although the neuronal circuits for anxiety overlap with those used by the brain for mediating fear responses, recent studies have revealed novel aspects of specific circuits mediating and controlling anxiety-like behaviors in rodents. Special attention has been given to the cortico- hippocampal-amygdala, bed nucleus of the stria terminalis (BNST) and septo-hipocampal microcircuits.

Cortico-hippocampal-amygdala circuits: The BLA can bidirectionally control anxiety-like behavior: activation of the BLA projection neurons that are connected with the vHpc enhance anxiety-like behavior (Felix-Ortiz *et al* 2013), whereas activation of excitatory BLA axonal projections that terminate in the CeL produces anxiolytic-like behavior (Tye *et al* 2011). Additionally, synchronization in ϑ rhythm between the vHpc and the mPFC during anxiety-like behaviors has been shown (Adhikari *et al* 2010), particularly with mPFC neurons that encode for anxiogenic features of the context (Adhikari *et al* 2011) leading to the hypothesis that cortico-hipocampal circuits are essential for controlling context-related information in unconditioned avoidance during anxiety-like behavior.

Extended amygdala circuit: A major target of projections from BLA and CeA is the BNST. BLA inputs to the anterodorsal BNST (adBNST) and promotes anxiolytic-like behavior via connections to the ventral tegmental area (VTA), lateral hypothalamus and parabrachial nucleus (PB). In contrast to the adBNST, the adjacent subdivision, the ventral BNST (vBNST) elicits avoidance by activating excitatory inputs to the VTA (Kim *et al* 2013); suggesting opposite effects of BNST-VTA circuits in the generation of anxiety-like behaviors.

Septo-hippocampal circuit: it has been hypothesized that septal-hippocampal circuits mediate stress-induced anxiety states, they are supposed to detect uncertainty, and promote attention and arousal by modulation of hippocampal and prefrontal ϑ oscillations (Chee *et al* 2015). Recently Anthony *et al*. described that the lateral septum (LS), a structure with which CA3 is strongly interconnected, suppresses fear and anxiety through its output to the hypothalamus (Anthony *et al* 2014).

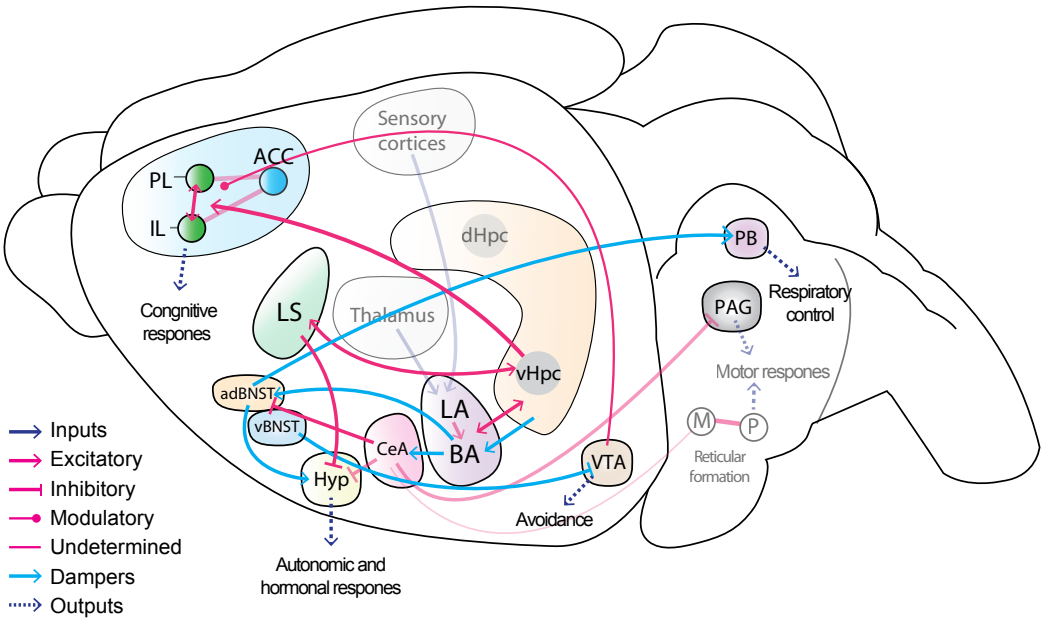

Figure 31. The anxiety network
Anxiety states are mediated by a network of interconecred cortical and subcortical structures. ACC, anterior cingulate cortex; PrL, prelimbic cortex; IL, infralimbic cortex; dHpc, dorsal hippocampus; vHpc, ventral hippocampus; PAG, periaqueductal gray matter; LA, lateral amygdala; BA, dasal amydala; CeA, central nucleus of the amygdala; M, mesencephalic; P, pontine reticular formation; Hyp, hypothalamus; PB, parabraquial nucleus; adBNST, anterodorsal bed nucleus of the stria terminalis; vBNST, ventral bed nucleus of the stria terminalis; VTA, ventral tegmental area. Connectivity sketch was taken and modified from (Tovote *et al* 2015).

4.2.3. Arc/Arg3.1 in fear and anxiety-like behavior

Arc/Arg3.1 expression has been extensively linked to the consolidation of different types of fear-motivated memory and investigated by the use ODNs and constitutive KO mouse lines, and it is accepted that Arc/Arg3.1 expression is required for the consolidation of long-term fear memories (Table 2). Regarding auditory fear conditioning, Ploski *et al* showed that blocking Arc/Arg3.1 mRNA via ODNs infusions in the LA; the consolidation but not the acquisition of fear is impaired (Ploski *et al* 2008). Furthermore, Gouty-Colomer *et al* have recently shown that Arc/Arg3.1 is expressed in ensembles of principal neurons in the LA after auditory fear conditioning; these Arc/Arg3.1-positive ensembles are more likely to encode memory traces because these neurons presented enhanced intrinsic excitability and synaptic potentiation by thalamic inputs

that were specifically recruited during associative learning in auditory FC (Gouty-Colomer *et al* 2016). Intriguingly, it remains to be investigated if synaptic plasticity in the LA is impaired in the Arc/Arg3.1 KO mice.

Arc/Arg3.1 KO mice presented a normal acquisition of fear and unaltered expression of unconditioned avoidance in elevated O-maze and Light-dark box (Plath *et al* 2006), and the studies where Arc/Arg3.1 mRNA is knocked down did not report changes in anxiety-related behaviors. Nonetheless, my findings in fear and anxiety in the Early-cKO mice presented in the first part of this thesis, and several reports showing that Arc/Arg3.1 is upregulated after chronic application of antidepressants (first line of treatment in anxiety and fear-related disorders) (Beveridge *et al* 2004, Pei *et al* 2004a, Pei *et al* 2004b) suggest that Arc/Arg3.1 expression in certain areas of the proposed circuit for fear and anxiety might participate in the control, generation or modulation of these behaviors.

4.3. Manipulation of fear and anxiety circuits

The study of cerebral circuits has been classically conducted by the use of lesions, drugs and tracer injections for interfering with the function of a specific brain region or to reveal axonal trajectories. With the development and advances in molecular virology, the use of viral vectors for introducing transgenes and fluorescent markers in the brain parenchyma has allowed the understanding of specific molecules and functions of circuits involved in specific behaviors (Nassi *et al* 2015). In general, viral vectors have proven to be the best and more efficient way for gene delivery *in vivo*, when compared to synthetic nanoparticles or liposome vectors, and particularly they are widely studied and continuously improved for research and therapeutically usage. Different types of viruses have been investigated for gene delivery in the nervous system, such as retroviruses, lentiviruses, adenoviruses, herpes simplex and adeno-asociated virus -AAV-based- viral vectors. Among these vectors, lentivirus and rAAV vectors are preferred for *in vivo* applications in the CNS due to their minimal host immune response, easy production and implementation in regular laboratory conditions (Choudhury *et al* 2016).

After having validated our Arc/Arg$^{f/f}$ mouse (Section 2.2), I standardized a series of rAAV vectors that expressed the Cre recombinase gene as a molecular tool for manipulating the expression of this important gene and dissect its function in specific components of the fear and anxiety circuitry.

4.3.1. rAAV viral vectors for gene manipulations in brain circuits

I chose rAAV vectors to deliver the genes of interest for its better spread through the brain extracellular space (Cetin *et al* 2006), as result of the differences in diameter of the viral particles: in comparison the lentivirus vectors, which have a diameter of approximately 100 nm, rAAV have a diameter of 20-30 nm, allowing better diffusion in the adult extracellular space that possesses a width of approximately 40-60nm (Thorne & Nicholson 2006).

Wild-type AAVs are single-stranded DNA, non-enveloped parvoviruses with icosahedral capsid that requires a co-infection with adenoviruses or herpes simplex viruses for replication and production of viable viral particles. AAVs package a genome of approximately 4.7 kb flanked by approximately 145 bp inverted terminal repeats (ITRs) on the 5' and 3' ends, and consists of two open reading frames (ORFs). Each ORFs encode four replication proteins (Rep) and three capsid proteins (Cap/VP), and an assembly activating protein (AAP) (Figure 32a). The three structural capsid proteins assembly at VP1:VP2:VP3 ratio of 1:1:10 into a 60-subunit icosahedral capsid with the help of the AAP (Figure 32b).

AAV vectors are an ideal delivery system for the CNS due to the following aspects: transference of genes in postmitotic cells like adult neurons (Hellstrom *et al* 2009); neurotropism when applied directly to the brain tissue (Davidson *et al* 2000); after infection, the genome remains as a single episome with low rate of integration into the host cell genome (McCarty *et al* 2004); minimal immune reaction or cytotoxicity (Han *et al* 2010); production with high titers (Grieger *et al* 2006) and purity in conventional laboratory facilities (Zolotukhin 1999); and stable transgene expression in brain tissue (in the human brain up to 10 years) (Leone *et al* 2012).

The wild-type genome of AAVs contains all necessary cis-acting elements for the replication and packaging between the ITRs; thus, all viral coding sequences can be removed and adapted for gene delivery by inserting exogenous DNA between flanking ITRs (Figure 32c) (Hirata & Russell 2000). Replication and assembly for rAAV virions are achieved by supplying the AAV Rep and Cap proteins in trans along with the necessary adenoviral helper functions (Figure 32c). In standard laboratory settings, the most commonly used protocol for manufacturing rAAV is the transfection of plasmid DNA into eukaryotic cells such as Human Embryonic Kidney 293 cells (HEK293). HEK293 cells constitutively express E1a/b (Adenoviral proteins) required for AAV replications. These cells are then triple transfected with equimolar amounts of the vector construct plasmid (prAAV-promoter-transgene) and helper plasmids that provide the AAV Rep and Cap functions as well as the Ad5 genes (VA RNAs, E2A and E40EF6) (Figure 32c) (Grimm 1998). Af-

ter transfection, expression of virions peaks between 48-72 hours and the cells can be harvested and media collected for further purification (Figure 51a-d). High purity rAAV particles are injected in the brain parenchyma of anesthetized mice using stereotaxic surgery and microsyringes with a fine needle (Figure 33a and section 8.6).

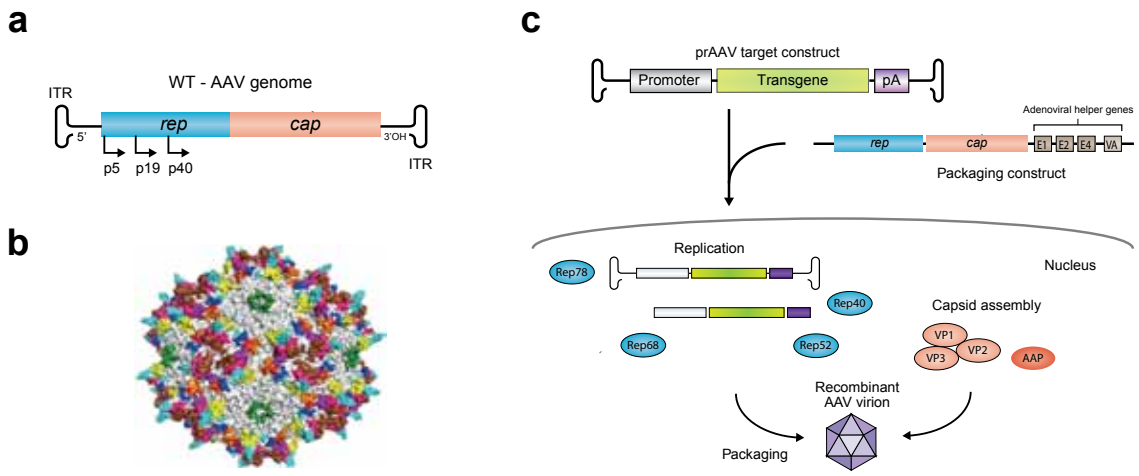

Figure 32. AAV structure and biology
a. Schematic representation of the 4.7-kb single-stranded DNA genome of AAV. **b.** Crystal structure of the AAV capsid with hypervariable regions of VP3 [Taken from (Xie *et al* 2002)]. **c.** rAAV vectors are generated by insertion of a transgene of interest betwen ITRs and replacement of rep and cap ORFs, those are provided on packaging construct together with adenoviral helper genes necessary for replication [Modified from (Kotterman & Schaffer 2014)].

4.4. Hypothesis and aims of the second part

In the first part of this dissertation, I described that the expression of Arc/Arg3.1 in the early postnatal development contributes to the establishment of normal oscillatory activity and long-range functional connectivity of structures involved in memory and emotional processing such as the Hpc and the PFC. In the second part of this dissertation, I hypothesize that Arc/Arg3.1 expression in the adult brain is necessary for mediating aspects of fear and anxiety-related behavior in specific brain regions that are part of the proposed circuitry. Therefore, a conditional deletion of the Arc/Arg3.1 loci in specific regions of the fear and anxiety circuit would lead to impairments in the generation, expression and control of these behaviors when compared to WT-control animals. An alternative hypothesis is that Arc/Arg3.1 is only required during the postnatal development to establish circuits for memory and emotional process before adulthood and genetic removal of the gene in specific regions of the circuit would have no effect on fear or anxiety-related behavior in the adult mouse.

4.4.1. Specific goals

- To validate and standardize rAVV-carrying Cre recombinase gene for conditional ablation of Arc/Arg3.1 in specific brain regions involved in fear and anxiety-like behaviors.

- To investigate the behavioral impact of conditional deletion of Arc/Arg3.1 in specific brain regions involved in fear and anxiety-related behaviors in the adult brain.

5. Results

5.1. Validation of adeno-associated viral vectors for conditional gene ablation in specific brain circuits.

To achieve a site-specific ablation of Arc/Arg3.1 without side effects, I produced a series of control and Cre-carrying rAAV viral vectors and tested them *in vitro* and *in vivo* using different titers. It was previously suggested and further confirmed by our Early-cKO approach that Arc/Arg3.1 is exclusively expressed in positive neurons for CaMKIIα (Vazdarjanova *et al* 2006), therefore, CaMKIIα (Mayford *et al* 1996) or Synapsin 1 (Syn) (Schoch 1996) promoters were selected for driving the expression of fluorescent proteins (eGFP or Venus) or the Cre recombinase solely in neurons.

5.1.1. Cre carrying-rAAV viral vector driven by CaMKIIα promoter

To establish efficient principal neuron-specific expression of the mouse brain *in vivo*, I tested and constructed rAAV-viral vectors that expressed enhanced Green Fluorescent Protein (eGFP), Cre recombinase or ligand-dependent chimeric Cre recombinase ($CreER^{T2}$) transgenes under the CaMKIIα promoter.

5.1.1.1. Delivery and expression of rAAV-CaMKIIα–eGFP in the mouse hippocampus

I first produced and injected a control rAAV viral vector expressing eGFP under the CaMKIIα promoter of 1.3 kb (Figure 33a) (Dittgen *et al* 2004), in order to establish the procedures for rAAV stereotaxic injections in the mouse brain and characterize transgene expression driven by CaMKIIα promoter.

Based on current literature and multiple trials, I used a viral titer of approximate $5x10^8$ viral genome copies per microliter (vg/µl) as an optimal titer to target the entire volume of the mouse hippocampus when 1-3 µl were injected in the dHpc and vHpc (Figure 33b-d). The 1.3 kb fragment of the CaMKIIα promoter drives the expression of the eGPF transgene mainly in the granular cell layer of the DG and str. pyramidale of CA1 as observed in clarified samples after 15 days of transduction *in vivo* (Figure 33e). These results suggest expression exclusively in pyramidal cells. By performing these pilot experiments, I achieved the successful transduction of more than 80% of the pyramidal neurons in the entire hippocampus.

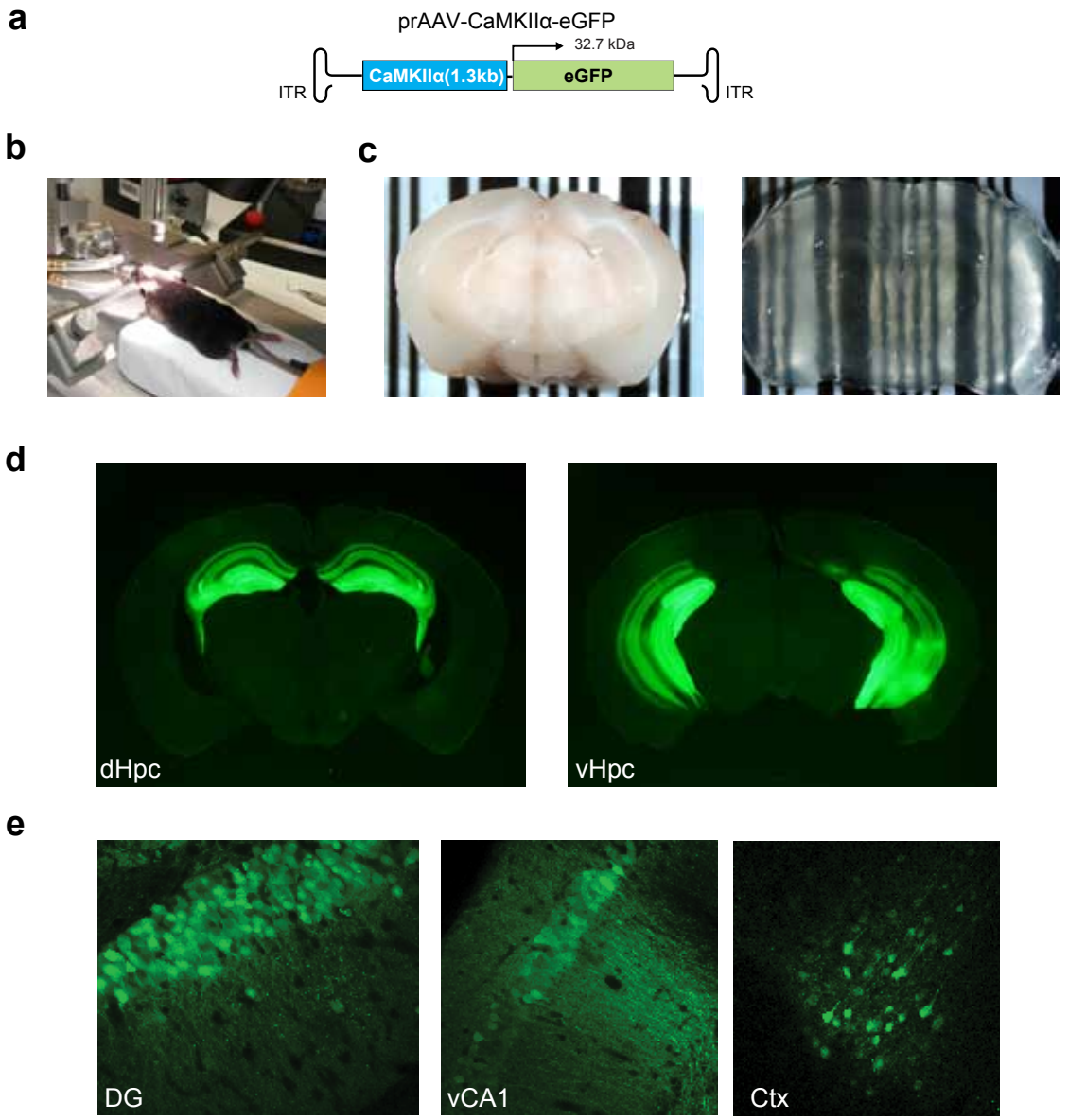

Figure 33. Viral eGFP expression in the pyramidal neurons of the mouse hippocampus
a. Schematic representation of prAAV-CaMKIIα-eGFP construct (Dittgen *et al* 2004). **b.** Stereotactic delivery and viral-mediated expression of transgenes in the mouse hippocampus. **c.** Clarification of mouse thing coronal brain slices (1mm) after bilateral injection of rAAV-CaMKIIα-eGFP vector. **c.** Representative images of coronal slices expressing eGFP 15 days after bilateral injection of rAAV-CaMKIIα-eGFP vector in the hippocampus. **e.** eGFP expression was observed in pyramidal neurons of the Dentate Gyrus (DG), vCA1 and the cortex (leaky transduction) when stack images were taken by confocal microscopy in clarified brain slices.

5.1.1.2. Validation of Cre-mediated Arc/Arg3.1 ablation in the hippocampus of adult mice by rAAV-CaMKIIα-Cre vectors

I produced rAAV vectors carrying Cre recombinase under the control of CaMKIIα promoter (prAAV-CaMKIIα-Cre) and infected cultures of primary cortical neurons with 1 µl of virus for each coverslip using a titer of $2x10^8$ vg/µl (Figure 34a). I confirmed by immunocytochemistry that Cre recombinase was effectively transduced by rAAV vectors with high expression and efficiency

after 7 days of infection (Figure 34b). Subsequently, I used high-performance liquid chromatography (HPLC) - purified rAAV-CaMKIIα-Cre vectors for unilateral stereotaxic delivery in the the dHpc of WT mice. Seven days after viral transduction, the brains were examined by immunostaining against Cre-recombinase and CaMKIIα, confirming that the 1.3 kb fragment of the CaMKIIα promoter is able to drive rAAV-mediated Cre expression in mature principal neurons of the adult mice hippocampus (Figure 34c).

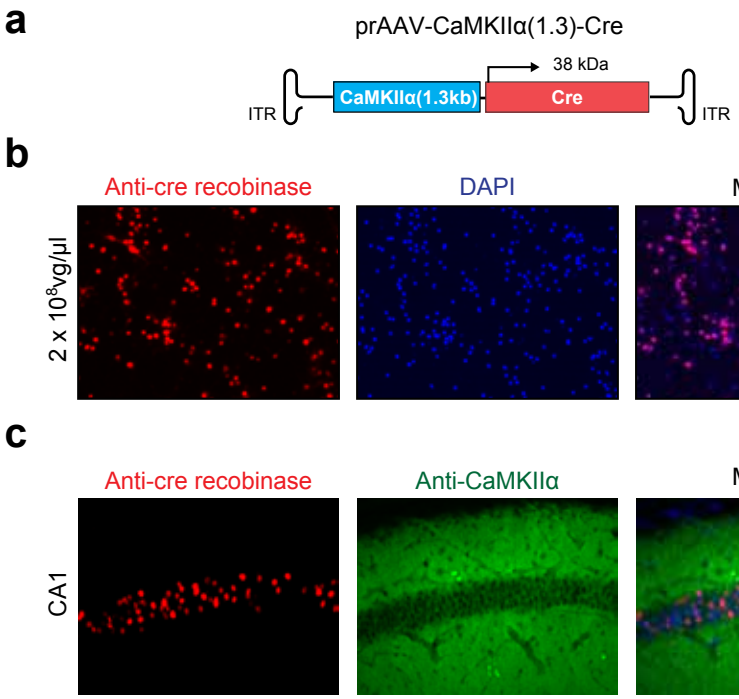

Figure 34. rAAV-mediated Cre expression in the principal neurons
a. Schematic representation of target plasmid for production of rAAV-CaMKIIα-Cre viral vector.
b. Primary cortical neurons infected with 1 µl of rAAV-CaMKIIα-Cre vector with a titer of $2x10^8$ vgc/µl during 7 days. Cre recombinase expression present with high efficiency.
c. Cre recombinase is expressed in CaMKIIα positive neurons in the str. pyramidale of the CA1 region.

I used two different titters of rAAV-CaMKIIα-Cre viral vectors for injecting Arc/Arg3.1$^{f/f}$ mice unilaterally in the dHpc (Figure 35a). The animals were euthanized 30 days later, their brains extracted and immunostained using specific antibodies against Cre recombinase, Arc/Arg3.1, cleaved caspase-3 (cell death marker) and iba-1 (microglia activation marker). I determined that Arc/Arg3.1 was successfully ablated in the dHpc by 1.4 µl of rAAV-CaMKIIα-Cre with a titer of $5x10^8$ vg/µl. This amount and concentration of the vector produced minimal microglia activation (local innate immune response) and no detectable cell death. Furthermore, I observed a reduction of more that 80% of the Arc/Arg3.1 protein and the ablation was always correlated with the Cre expression, showing that rAAV-CaMKIIα-Cre viral vector is suitable for specific ablation of Arc/Arg3.1 in principal neurons of the hippocampus.

I next characterized the timeline of Arc/Arg3.1 ablation with rAAV-CaMKIIα-Cre by examining three different time points after unilateral hippocampal injection: 3, 5 and 7 days (Figure 35b). To maximize Arc/Arg3.1 expression, convulsive seizures were induced by intraperitoneal injection

of kainate. After 60-90 min of seizure onset, animals were euthanized and their brains dissected and immunostained against Cre, Arc/Arg3.1, Iba-1 and Cleaved-caspase 3. I observed that although the Cre expression was evident as early as 3 days, only after 7 days a complete ablation was achieved without toxicity. I concluded that the use of rAAV-CaMKIIα-Cre viral vectors allows a fast genetic ablation of the gene of interest in a temporal, region and cellular specific manner.

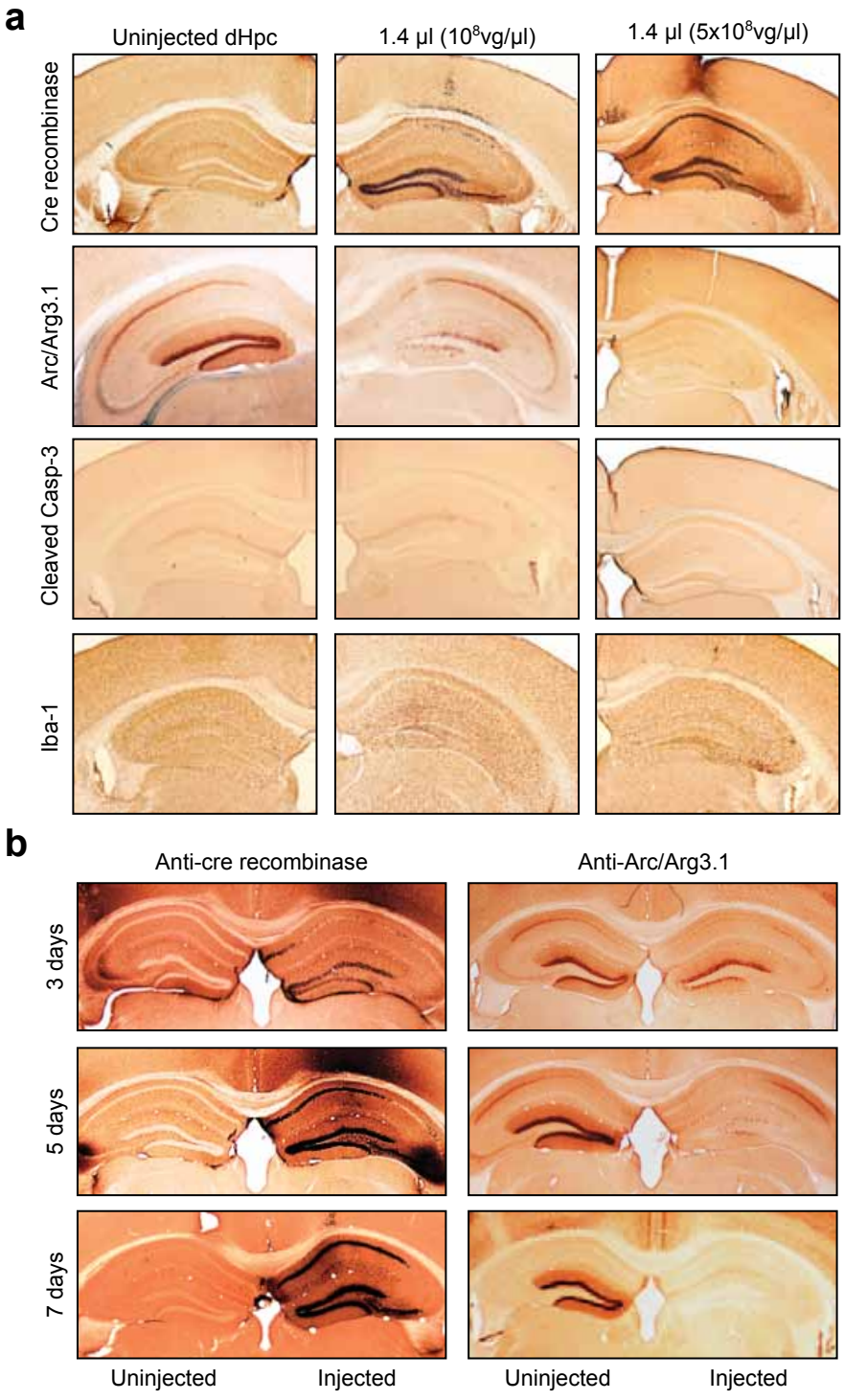

Figure 35. Cre-mediated Arc/Arg3.1 ablation in the dorsal hippocampus of adult mice
a. Arc/Arg3.1$^{f/f}$ mice were injected unilaterally in the dorsal hippocampus with 1.4 µl of rAAV-CaMKIIα-Cre vector using two different titers (10^8 and $5x10^8$ vg/µl). Brains were examined by immunostaining 30 days after injection. Efficient ablation without signs of cell death (cleaved caspase-3) or innate immune activation (Iba-1) was found.
b. Arc/Arg3.1$^{f/f}$ mice were injected unilaterally in the dHpc with 1.4 µl of rAAV-CaMKIIα-Cre with a titer $5x10^8$ vg/µl and ablation was tested by Arc/Arg3.1 immunostaining at different time points: 3, 5 and 7 days. In each point, convulsive seizures were induced by intraperitoneal injection of kainate to induce Arc/Arg3.1 expression at maximum.

5.1.1.3. rAAV viral vectors carrying an inducible ligand-dependent chimeric Cre recombinase

To study memory processes across time, the precise temporal manipulation of genes would be an ideal approach to determine their role in different stages of the cognitive process. Next, I sought to clone and validate a rAAV vector carrying a ligand-dependent chimeric Cre recombinase (so called CreER^{T2} recombinase) which can be tightly controlled in time. The CreER consist of the Cre protein fused to mutated hormone-binding domains of the human estrogen receptor, which does not bind to endogenous steroid hormones but is sensitive to nanomolar concentrations of 4-hydroxy-tamoxifen (4-OHT), a synthetic estrogen receptor ligand (Feil 1996). This transgenic approach allows, in principle, a tight pharmacological control of Cre activity since the protein remains sequestered in the cytoplasm by chaperone proteins when the inducer in not present. Upon 4-OHT application, CreER^{T2} is translocated to the nucleus where it mediates recombination of *LoxP*-flanked genes (Figure 36a). The temporal control of the Cre activity circumvents Cre genotoxicity that arises from the accumulation of high enzyme levels in the nucleus (Forni *et al* 2006). Additionally, it has been shown that systemic applications of 4-OHT in adult mice does not interfere with standard behavioral testing (Vogt *et al* 2008), thus making the inducible CreER^{T2} system a valuable tool to study memory in adult mice.

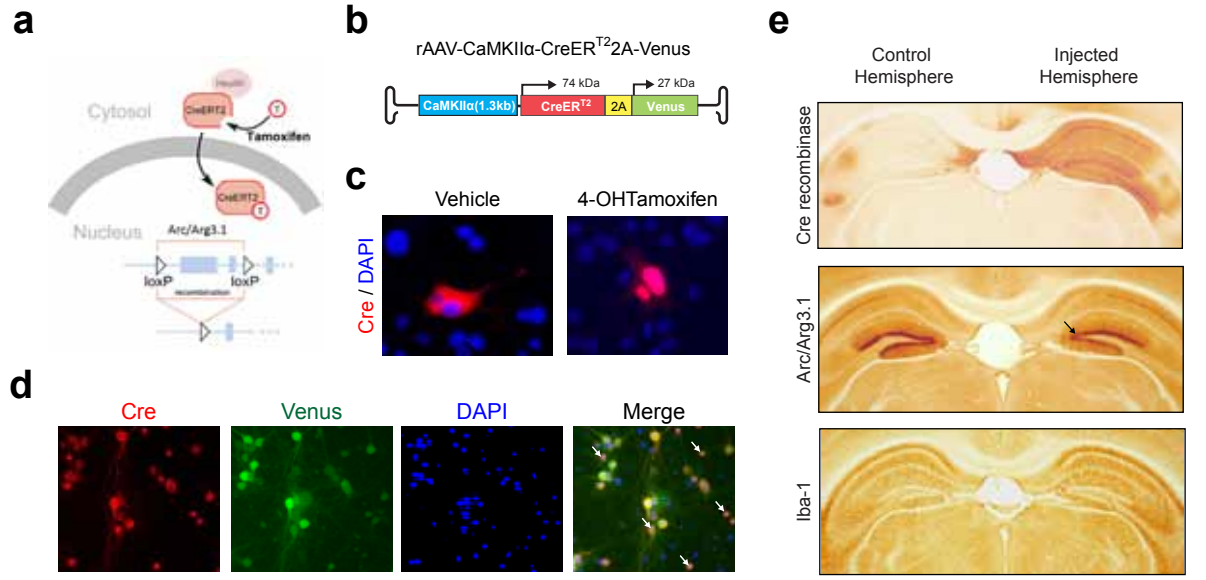

Figure 36. Inducible ligand-dependent Cre recombinase (CreER^{T2}) and viral CreER^{T2} expression in the pyramidal neurons and in the mouse hippocampus
a. Schematic representation of inducible CreER^{T2} recombination by 4-OH application [taken and modified from (Rodriguez Parkitna and Engblom 2012)]. **b.** Schematic representation of prAAV with CreER^{T2}2A-Venus constructs. **c.** Expression of CreER^{T2} in N2A cells and nucleus translocation upon 4-OHT application. **d.** Nuclear activity of the CreER^{T2} transgene in the absence of tamoxifen. Cultured cortical neurons infected with rAAV-CaMKIIα-CreER^{T2}-2AP-Venus expressed Cre in somata and nuclei (white arrows) in absence of any tamoxifen. **e.** Immunostaining with DAB and specific antibodies against Cre, Arc/Arg3.1 and Iba-1 in Arc/Arg3.1$^{f/f}$ mice 6 weeks after injections show widespread expression of Cre in the injected hippocampus but a modest reduction of Arc/Arg3.1 expression (black arrow). The absence of long- term toxicity and innate immune response is shown by the normal cellular morphology and the lack of microglia activation (Iba-1).

After cloning and production of a plasmid that expressed the CreER^{T2} transgene under the CaMKIIα promoter (Figure 36b) (prAAV-CaMKIIα-CreER^{T2}-2AP-Venus), its efficiency and 4-OHT sensitivity were tested in N2A cells and in primary cortical neurons. In the absence of 4-OHT, Cre recombinase was mainly located in the cytosol, as expected (Figure 36c). However, when cultures of primary cortical neurons were transduced with rAAV-CreER^{T2}-2AP-Venus, a fraction of the recombinase was also constitutively present in the nucleus in the absence of the inducer (Figure 36d). I utilized this leak-activity to inject mice with the rAAV-CreER^{T2}-2AP-Venus and obtained Arc/Arg3.1 knock-down for prolonged periods of time (6 weeks), thereby avoiding genotoxicity caused by high constitutive Cre recombinase activity (Figure 36e).

5.1.2. Cre carrying-rAAV viral vector driven by Synapsin I promoter

It has been previously shown that in addition to CaMKIIα promoter-based vectors, the use of Synapsin I promoter is suitable for efficient expression of proteins in mature neurons (Kugler *et al* 2003). I tested a second viral vector expressing a codon-improved version of the Cre recombinase (iCre) (Shimshek *et al* 2002) driven by a short fragment of the human Synapsin I (hSyn) promoter: rAAV-hSyp-iCre2AP-Venus (Figure 37a) (Tang *et al* 2009).

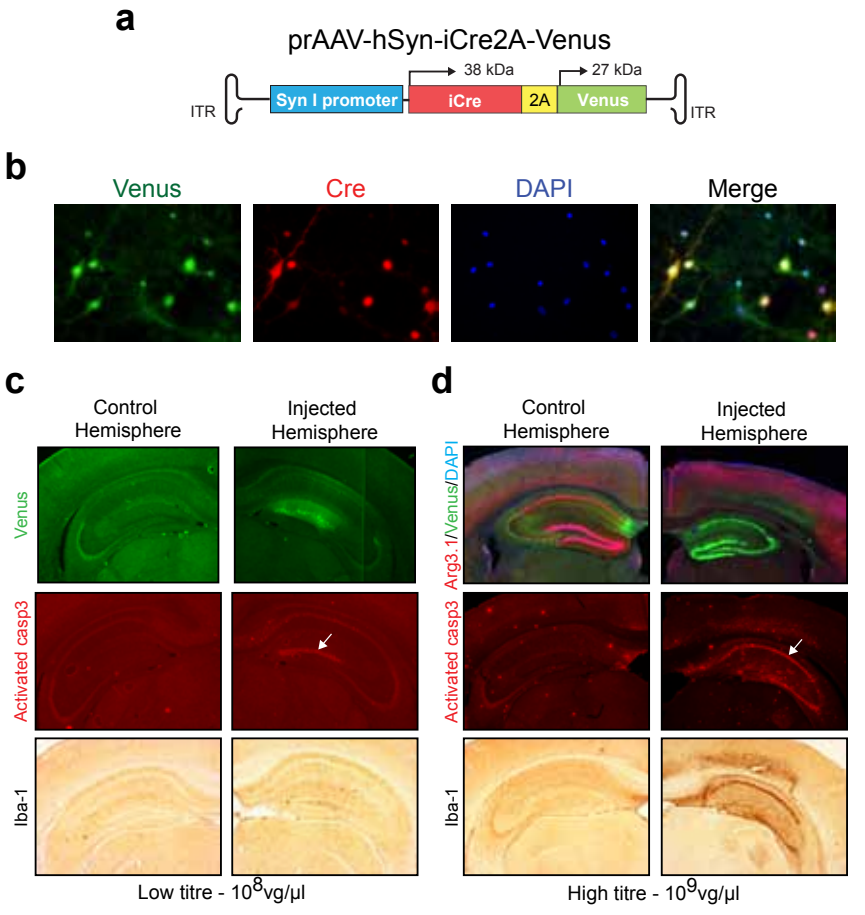

Figure 37. Codon-improved Cre recombinase expression driven by Synapsin promoter induces severe neurodegeneration
a. Schematic representation of prAAV-iCre2AP-Venus (Tang *et al* 2009).
b. Cultured cortical neurons infected with rAAV-Syn-iCre2AP-Venus co-express iCre in nuclei and Venus in the entire cell.
c. Immunostaining with specific antibodies against cleaved-caspase-3 and Iba-1 in mice 4 weeks after injections with low viral titer shows invariable activation of cell death cascade (activated capase 3) in transduced cells.
d. The use of high viral titer shows widespread expression of Venus in the dHpc but severe activated casp-3, neurodegeneration and microglial activation.

Similar to what was observed for the 1.3-kb CaMKIIα promoter-based vectors, I observed high expression of iCre and Venus in primary cultures of cortical neurons *in vitro* and in the mouse hippocampus *in vivo* (Figure 37b-d). Surprisingly and independent of volume or viral titer, I detected activation of cell death related-signaling when antibodies against activated caspase 3 were used (Figure 37c, white arrows). In accord with the caspase-3 activation, I found a strong neurodegeneration and severe activation of microglia (iba-1 immunostaining) that was accentuated at a higher viral titer (Figure 37d).

I hypothesized that the enhanced codon-improved expression of iCre might produce genotoxicity due to high expression and accumulation of the recombinase in the nucleus. Therefore, the iCre sequence was replaced by the prokaryotic sequence of Cre recombinase (Figure 38a). Next, I produced and purified through HPLC a batch of rAAV-hSyn-Cre2AP-Venus vectors, and tested them *in vivo* by injecting mice bilaterally in the dHpc with different viral titers. Four weeks after injections, brains were immunostained against Cre, Iba-1 and cleaved caspase 3. I found that the expression of prokaryotic Cre under the transcriptional control of the hSyp promoter leads to an invariable expression of toxic Cre levels that activates cell death cascades and eventual severe neurodegeneration, and robust microglial activation independent of the used viral titer (Figure 38b-d). Hence, I concluded that the short human synapsin 1 promoter is unsuitable for driving safe Cre expression in the brain for the long duration of the behavior experiments.

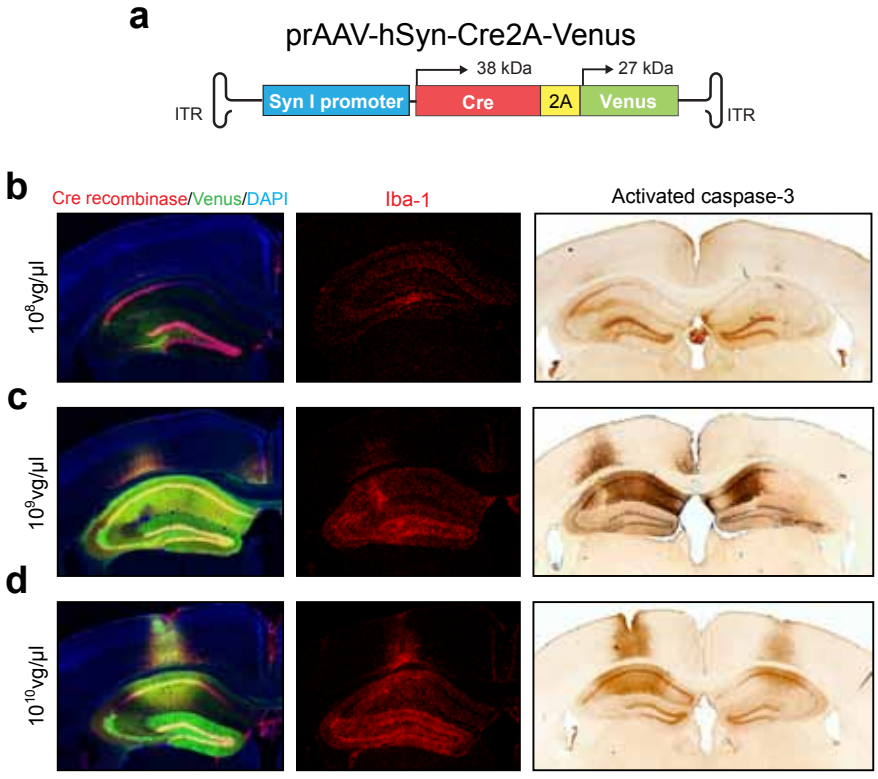

Figure 38. Prokaryotic Cre recombinase expression driven by Synapsin promoter induces severe activation of cell death signaling and inflammatory reaction
a. Schematic representation of the target plasmid prAAV-hSyn-Cre2AP-Venus.Mice were injected with 1.4 µl of rAAV-hSyn-Cre2AP-Venus viral vector in the dorsal hippocampus using different titters: **b.** 10^8 vg/µl **c.** 10^9 vg/µl and **d.** 10^{10}vg/µl; immunostaining with specific antibodies against Iba-1 and cleaved caspase-3 show that the expression of prokaryotic Cre under the transcription control of the synapsin I promoter leads to an invariable expression of toxic levels that produces severe microglial activation and cell death cascades independent of the viral titer.

In summary, I established all necessary procedures to utilize rAAV-vectors *in vivo* in order to manipulate brain circuits in the adult mouse. Moreover, I produced and characterized rAAV-vectors for transducing genes specifically in principal neurons and determined that 1.3-kb CaMKIIα promoter-based vectors are fast-expressing and fulfill safety criteria for driving Cre recombinase expression and thereby region and temporal recombination in the mouse brain.

5.2. Manipulation of fear and anxiety circuits in adult brain by conditional ablation of Arc/Arg3.1

After having developed and characterized a functional and nontoxic Cre-bearing rAAV-vector tool for *in vivo* procedures, I next aimed to assess the role of Arc/Arg3.1 in specific aspects of fear and anxiety-related circuits via genetic inactivation and behavioral testing. Together with the Cre-carrying rAAV vectors, I used the conditional ablation of Arc/Arg3.1, fear conditioning and elevated-plus maze as molecular and behavioral approaches, respectively, to study Arc/Arg3.1 function in fear and anxiety circuits.

5.2.1. Conditional ablation of Arc/Arg3.1 in amygdala has no effect on anxiety-like behavior but produces a strong impairment in auditory fear consolidation

I investigated the role of Arc/Arg3.1 in the amygdala in anxiety and fear by delivering rAAV-CaMKIIα-Cre viral vectors bilaterally in this structure and testing the mice after conditional ablation in the open field, elevated-plus maze and cued fear conditioning. Two cohorts of a total of 19 WTs (WT-controls) and 24 Arc/Arg3.1$^{f/f}$ (Amy-cKO) mice were bilaterally injected in the amygdala (Figure 39a), and after 7 days of infection (expected time for conditional ablation) behavioral testing was performed. After behavioral evaluation, all mice were euthanized and histological examination of the brain tissue was done using Nissl staining and immunohistochemical stain against Cre recombinase and Iba-1. Only animals with a bilateral expression of the cre recombinase and mild inflammatory response at the injection site were considered for the final analyses (Figure 39b).

I first investigated exploratory and unconditioned avoidance behavior in Amy-cKO mice by performing open field (Figure 39c) and elevated-plus maze test (Figure 39g). I found that WT-control and Amy-cKO behaved similarly in the open field; all mice walked comparably long paths (WT-control, 24.79±1.69 m; n=16; Amy-cKO, 25.83±1.89 m; n=11; t_{25}=0.41, p=0.69, NS) at similar velocities (WT-control, 8.28±0.56 cm/s; Amy-cKO, 8.63±0.63 m; t_{25}=0.41, p=0.69, NS) and

spent similar time in the center of the arena (WT-control, 21.40±5.13%; Amy-cKO, 25.57±6.24%; t_{25}=0.52, p=0.61, NS). Unconditioned avoidance behavior in the elevated-plus maze was also similar between WT-control and Amy-cKO mice; no differences between genotypes were evident in path length (WT-control, 9.85±0.68 m; Amy-cKO, 10.08±0.65 m; t_{23}=0.41, p=0.82, NS), frequency in the closed arms (WT-control, 17.47±1.93 m; n=15; Amy-cKO, 16.20±1.79 m; n=10; t_{23}=0.46, p=0.65, NS) or percentage of time spent in open arms (2-way ANOVA: Arm $F_{(2,69)}$=75.92, ***p<0.001, Genotype $F_{(2,69)}$=0.0006; p=0.98, NS; Interaction $F_{(2,69)}$=1.67, p=0.20, NS). These results suggest that ablation of Arc/Arg3.1 in the amygdala does not alter normal exploratory or anxiety-related behavior in adult mice.

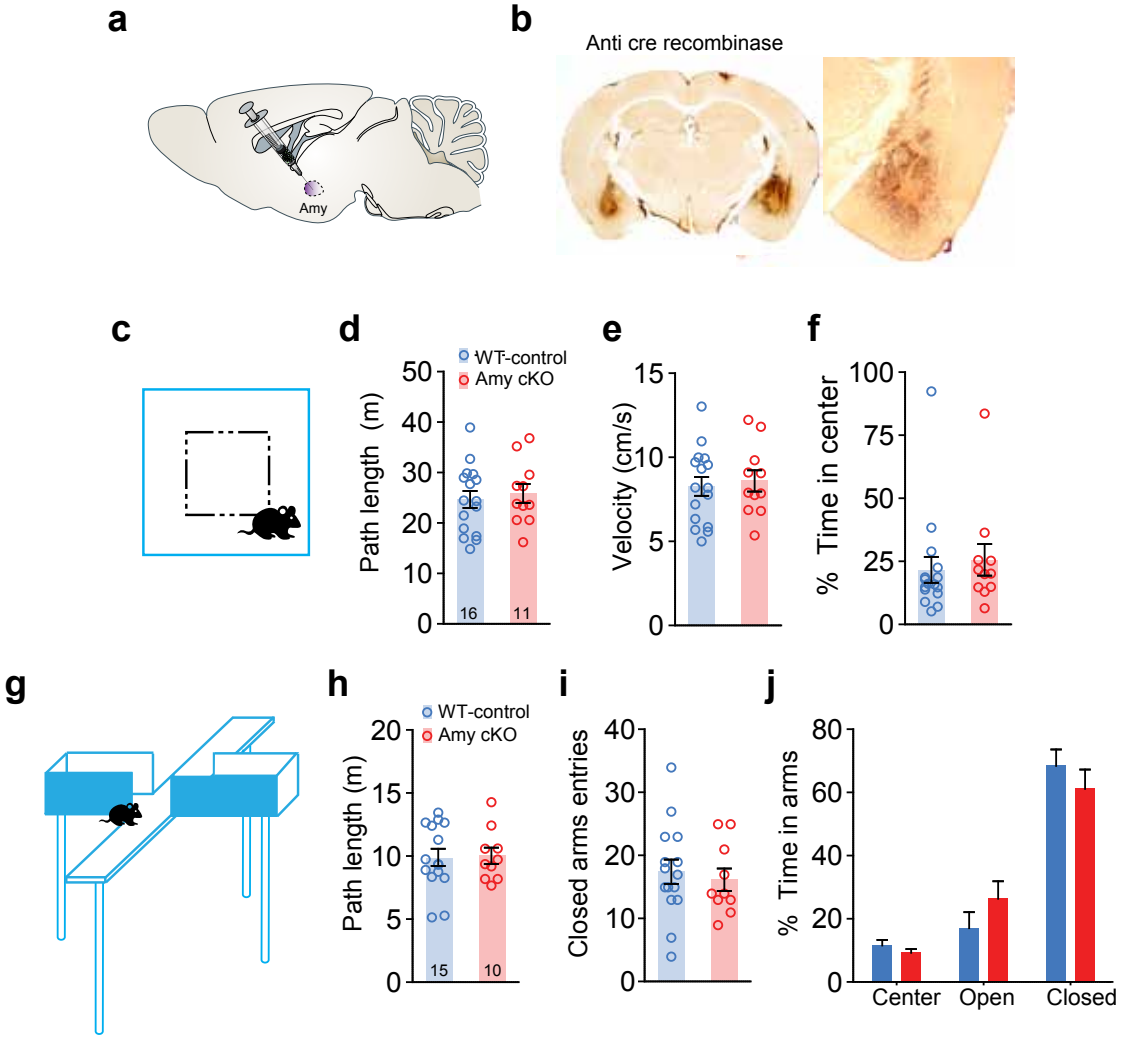

Figure 39. Conditional ablation of Arc/Arg3.1 in amygdala does not affect exploratory behavior and unconditioned avoidance
a. Schematic anatomical representation of injection in amygdala **b.** Exemplar of Cre recombines transduction in amygdaloid complex detected by immunostaining after rAAV-CaMKIIα-Cre viral vector injection. **c.** WT-control and Amy-cKO behaved similarly in the open field presenting comparable **d.** path lengths (WT-control, 24.79±1.69; Amy-cKO, 25.83±1.89 m; t_{25}=0.41, NS), **e.** velocities (WT-control, 8.28±0.56; Amy-cKO, 8.63±0.63 cm/s; t_{25}=0.41, NS) and **f.** percentage of time spent in the center of the arena (WT-control, 21.40±5.13; Amy-cKO, 25.57±6.24%; t_{25}=0.52, NS). Error bars represent mean ± SEM. WT-control, n=16; Amy-cKO, n=11. **g.** Comparable unconditioned avoidance in the elevated-plus maze between WT-control and Amy-cKO mice, **h.** Similar path length (WT-control, 9.85±0.68m; Amy-cKO, 10.08±0.65 m; t_{23}=0.41, NS). **i.** frequency in the closed arms (WT-control, 17.47±1.93; Amy-cKO, 16.20±1.79 m; t_{23}=0.46, NS) or **j.** percentage of time spent in each arm (2-way ANOVA: Arm $F_{(2,69)}$=75.92, ***p<0.001, Genotype $F_{(2,69)}$=0.0006; NS; Interaction $F_{(2,69)}$=1.67, NS). Error bars represent mean ± SEM. WT-control, n=15; Amy-cKO, n=10.

I next subjected rAAV-injected mice to fear conditioning using protocol 1 (Figure 40b and Figure 61d) and tested fear response to the tone in a novel context 24 h after conditioning. I observed that although Amy-cKO mice had a nonsignificant lower baseline (BL) freezing before conditioning, both WT-control and Amy-cKO were successfully conditioned and reached comparable levels of freezing after a single paired CS-US presentation (Post) (Figure 40c) (2-way ANOVA: Genotype $F_{(1,26)}$=0.56; p=0.46, NS; Time $F_{(1,26)}$=54.28, ***p<0.001; Interaction $F_{(1,26)}$=0.58; p=0.45, NS), suggesting that the expression of Arc/Arg3.1 in the amygdala might not be necessary for the acquisition of conditioned fear.

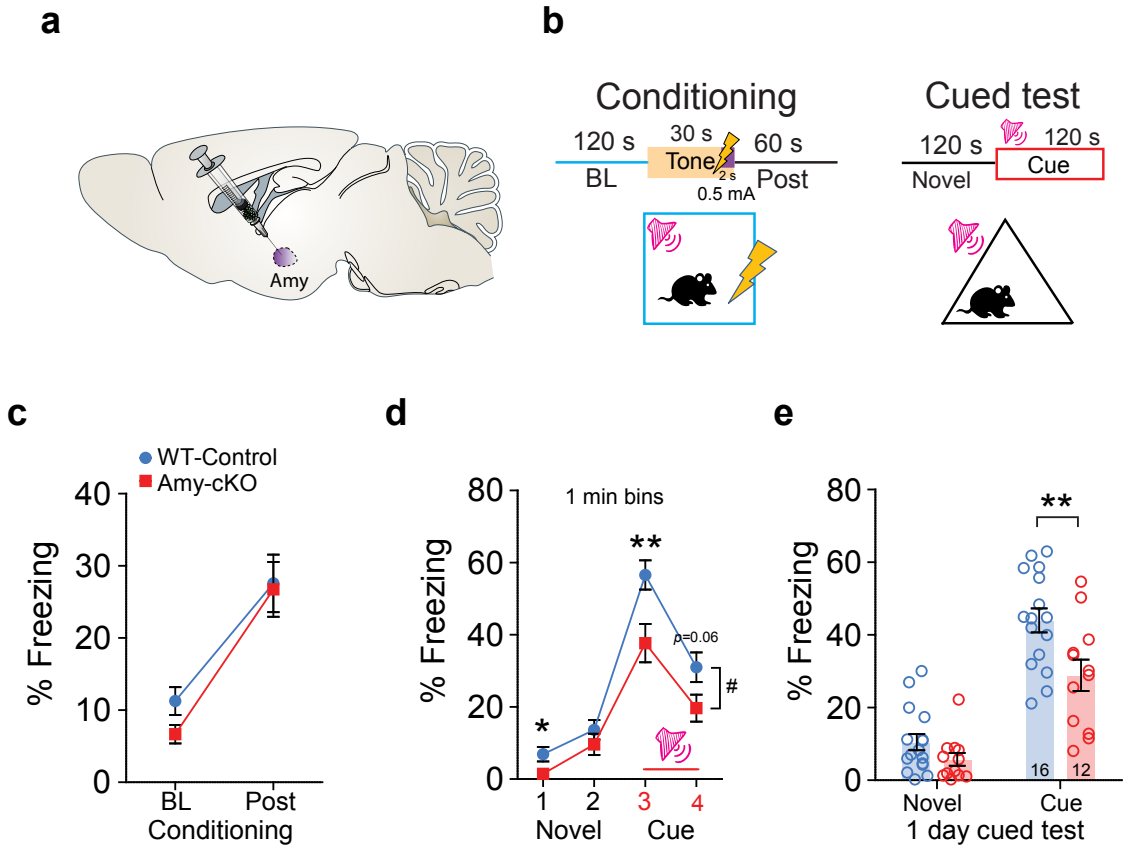

Figure 40. Conditional ablation of Arc/Arg3.1 in amygdala disrupts consolidation of auditory fear conditioning
a. Anatomical representation of injection in the amygdaloid complex. **b.** Schematic representation of FC protocol. **c.** WT-control and Amy-cKO acquired comparable levels of fear after conditioning (2-way RM-ANOVA: Genotype $F_{(1,26)}$=0.56; NS; Time $F_{(1,26)}$=54.29, ***p<0.001; Interaction $F_{(1,26)}$=0.58; NS) **d.** Amy-cKO mice exhibited impaired conditioned implicit fear retrieval (2-way RM-ANOVA for 1 min bin in cued test: Genotype $F_{(1,26)}$=6.86, #p<0.05; Bin $F_{(3,78)}$=104.58, ***p<0.001; Interaction $F_{(3,78)}$=3.36; *p<0.05; LSD post hoc test: *p<0.05, **p<0.01) **e.** Genetic ablation of Arc/Arg3.1 in amygdala significantly reduces fear in cued test 1 day after conditioning (WT-control, 43.78±3.31 %; Amy-cKO, 28.66±4.31 %; t_{26}=2.83,**p<0.01), with no differences in freezing during exposure to novel context (WT-control, 10.26±2.22 %; Amy-cKO, 5.52±1.77 %; Mann-Whitney U = 63, NS). Error bars represent mean ± SEM. WT-control, n=16; Amy-cKO, n=12.

One day after acquisition of fear, the mice were placed in a novel context for 2 min after which the conditioning tone was played for additional 2 min. The memory of the tone was gauged from their freezing response during the tone (Figure 40b). Notably, Amy-cKO mice displayed significantly reduced levels of freezing in the first minutes when introduced into the altered context suggesting a

diminished fear in novel contexts, as well as a highly significant reduction in freezing levels during the tone presentation (Figure 40d-e) (2-way RM-ANOVA for 1 min bin in cued test: Genotype $F_{(1,26)}$=6.86, #p<0.05; Bin $F_{(3,78)}$=104.6, ***p<0.001; Interaction $F_{(3,78)}$=3.36; *p<0.05; LSD post hoc test: *p<0.05, **p<0.01). Together these results suggest that the adult expression of Arc/Arg3.1 in the amygdala is essential for the consolidation of auditory Pavlovian fear memory.

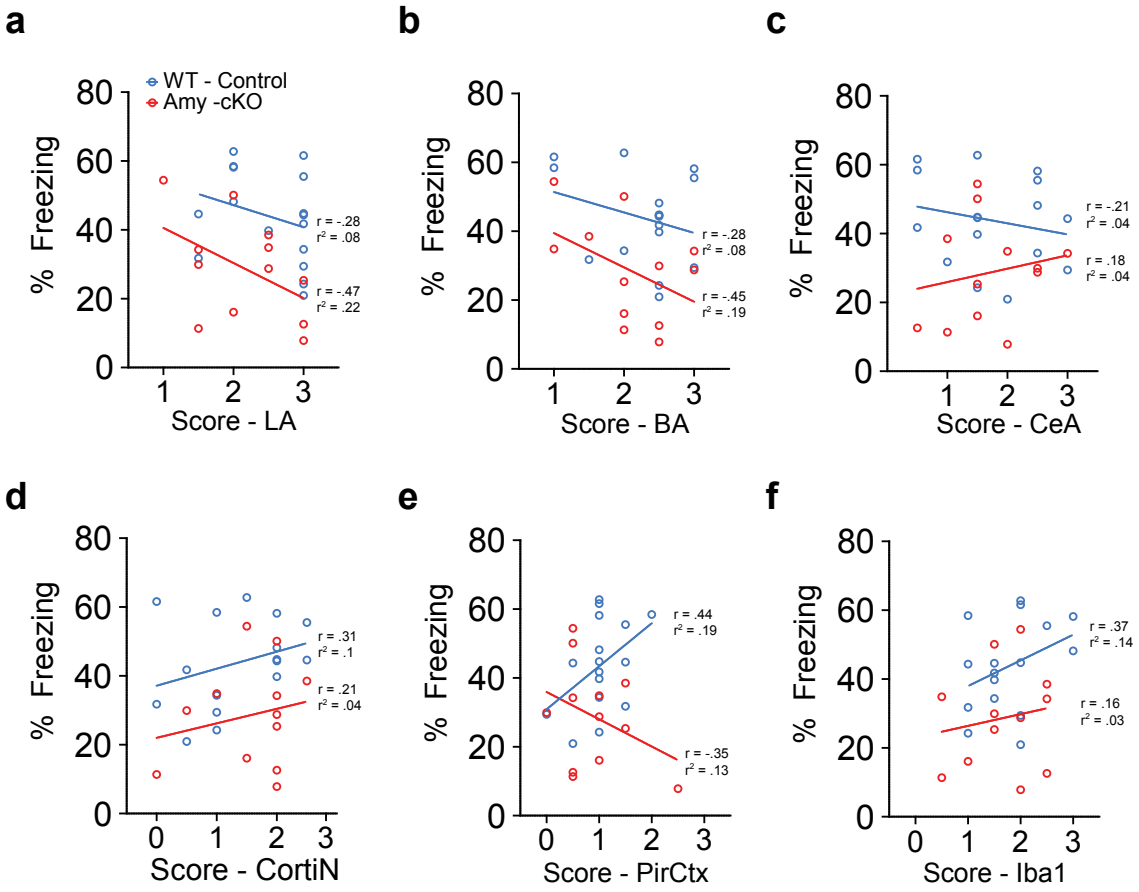

Figure 41. Disruption of implicit fear retrieval correlates with Arc/Arg3.1 ablation in BLA
Correlation and linear regression analysis between freezing during cued-test and Cre immunoreactivity in **a.** lateral amygdala (LA; WT-control, Pearson r=-0.29, r^2=0.08, NS; Amy-cKO Pearson r=-0.47, r^2=0.22, NS). **b.** basal amygdala (BA; WT-control, Pearson r=-0.28, r^2=0.08, NS; Amy-cKO Pearson r=-0.45, r2=0.19, NS). **c.** central amydala (CeA; WT-control, Pearson r=-0.21, r^2=0.04, NS; Amy-cKO Pearson r=0.18, r^2=0.04, NS). **d.** cortical nuclei (CortiN; WT-control, Pearson r=0.31, r^2=0.1, NS; Amy-cKO Pearson r=0.21, r2=0.04, NS). **e.** piriform cortex (PirCtx; WT-control, Pearson r=0.44, r^2=0.19, NS; Amy-cKO Pearson r=-0.35, r^2=0.13, NS). **f.** Iba-1 immunoreactivity (WT-control, Pearson r=0.37, r^2=0.14, NS; Amy-cKO Pearson r=0.16, r^2=0.03, NS). Scoring system: 1 (mild), when less than 35% of the structure shold cre or iba-1 immunoreactivity; 2 (moderate), betlen 35 and 70% of the structure presented increased cre or iba-1 stained; Strong (3) more than 70% of the structure was positive for Cre or inflammatory reaction. Each dot represents mean of freezing for each mouse during cue test. Slope represents linear regression approximation. WT-control, n=16; Early-cKO, n=12.

I next sought to examine the anatomical subdivision of the amygdaloid complex where the ablation of Arc/Arg3.1 took place by correlating Cre expression with freezing levels during implicit memory retrieval. I scored Arc/Arg3.1 ablation indirectly from the positive immunoreactivity to Cre recombinase and classified each structure into three categories: mild (1), when less than 35% of the structure showed immunoreactivity; moderate (2), between 35 and 70% of the struc-

ture showed positive stain; and more than 70% was scored as strong ablation or inflammatory reaction (3). Although none of the analyzed correlations were statistically significant, I found a negative medium correlation between Cre immunoreactivity and freezing levels for three structures: lateral amygdala (LA) (Figure 41a) (Person r = -0.47, r^2=0.22, NS), basal amygdala (BA) (Figure 41b) (Person r = -0.45, r^2=0.19, NS) and piriform cortex (PirCxt) (Figure 41f) (LA) (Person r = -0.35, r^2=0.13, NS). Moreover, I correlated the inflammatory response (Iba1 immunoreactivity) with freezing levels and found that only WT-controls displayed a nonsignificant medium positive correlation between this two variable (Figure 41g) (Iba1) (Person r = 0.37, r^2=0.14, NS). This analysis suggests that the deficit in cued fear memory is caused by the lack of Arc/Arg3.1 in cells of BLA and piriform cortex.

5.2.2. Deletion of Arc/Arg3.1 in the hippocampus facilitates fear acquisition and recall of remote cued fear memory

I next investigated the impact of ablating Arc/Arg3.1 in the hippocampus of adult mice (Figure 42a) on anxiety and fear (Figure 42b). I injected Cre carrying-rAAV vectors in the dorsal and ventral hippocampus of 17 WT (WT-controls) and 19 Arc/Arg3.1$^{f/f}$ mice (Hpc-cKO), and 7 days later mice were subjected to open field, elevated-plus maze and fear conditioning testing. On these injected animals, I investigated the exploratory behavior of 12 WT-control and 13 Hpc-cKO mice by performing open field test for 5 min (Figure 42c-f). I observed that both genotypes moved comparable distance (path lengths, WT-control, 25.89±1.8 m; Hpc-cKO, 22.74±1.31 m; t_{23}=1.39, p=0.18, NS) at similar velocities (WT-control, 8.82±0.63 cm/s; Hpc-cKO, 7.80±0.44 cm/s; t_{23}=1.36, p=0.18, NS), suggesting that their locomotor activity was intact. However, Hip-cKO mice displayed a significant reduction of the time spent (WT-control, 7.47±1.07 %; Hpc-cKO, 4.56±0.59 %; t_{23}=2.44, *p<0.05) and entry-frequency (WT-control, 16.5±1.82; Hpc-cKO, 11.23±0.98; t_{23}=2.60, *p<0.05) in the center of the field. These results suggest that genetic removal of Arc/Arg3.1 in the hippocampus might induce anxiogenic-like behavior without affecting locomotor activity. To test this hypothesis, it is necessary to use specific ethological paradigms, where the normal exploratory drive and unconditioned avoidance behavior is properly evaluated.

I decided to perform in addition elevated plus-maze test as an additional assay to examine anxiety-related behavior. In contrast to the obtained results in OF, I could not confirme any anxiety-like phenotype (Figure 42g-j), since both genotypes showed comparable time spent in the open arms of the maze (2way-ANOVA: Genotype, $F_{(1,69)}$ = 0.03, p=0.83, NS; Arm $F_{(2,69)}$ = 227.7, ***p<0.001; Interaction, $F_{(1,69)}$ = 0.19, p=0.87, NS), path lengths (WT-control, 10.5±0.74 m; Hpc-cKO, 11.74±.82 m; U = 50.50, p=0.14, NS) or entries to the closed arms (WT-control, 15.75±2.01; Hpc-cKO,

18.15±1.48 %; t_{23} = 0.96, p=0.34, NS). These results suggest that the genetic removal of Arc/Arg3.1 in the hippocampus does not significantly affect unconditionated avoidance in the EPM.

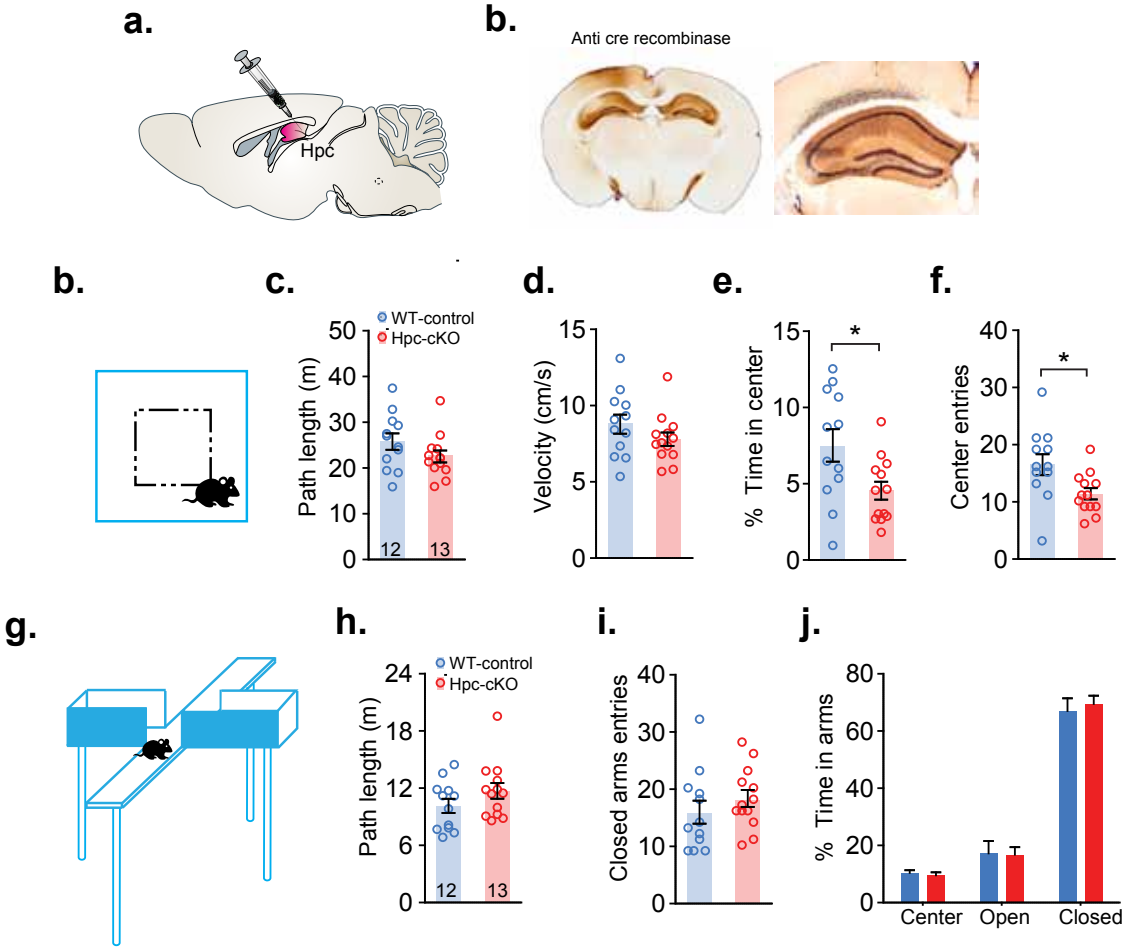

Figure 42. Genetic removal of Arc/Arg3.1 in hippocampus produces a mild anxiogenic -like behavior in the OF
a. Anatomical representation of hippocampal injection. **b.** Immunoreactivity of Cre recombinase after rAAV-CaMKIIα-Cre injection in hippocampus. Hpc-cKO mice exhibit normal locomotor activity in the open field gauged by their **c.** path length (WT-control, 25.89±1.8; Hpc-cKO, 22.74±1.31 m; t_{23} = 1.39, NS) **d.** Velocity (WT-control, 8.82±0.63; Hpc-cKO, 7.80±0.44 cm/s; t_{23}=1.36, NS) but appear to have an anxiety-like genotype shown by their **e.** decreased % time in center (WT-control, 7.47±1.07; Hpc-cKO, 4.56±0.59 %; t_{23}=2.44, *p<0.05) and **f.** entries to the center (WT-control, 16.5±1.82; Hpc-cKO, 11.23±0.98; t_{23}=2.6, *p<0.05). **g.** This effect is not confirmed by the elevated-plus maze, since no significant differences were found in: **h.** path lengths (WT-control, 10.5±0.74; Hpc-cKO, 11.74 ±0.82 m; U = 50.50, NS). **i.** time spent in arms (2way-ANOVA: Genotype, $F_{(1,69)}$=0.03, NS; Arm $F_{(2,69)}$=227.7, ***p<0.001; Interaction, $F_{(1,69)}$=0.19. or **j.** entries to closed arms (WT-control, 15.75±2.01; Hpc-cKO, 18.15±1.48 %; t_{23} = 0.96, NS). Error bars represent mean ± SEM. WT-control, n=12; Hpc-cKO, n=13.

I next investigated fear by using auditory fear conditioning (Figure 43b) and performed cued tests at 3 time points: 3 days (6 WT-control, 6 Hpc-cKO), 7days (10 WT-control, 14 Hpc-cKO) and 2 weeks (8 WT-control, 12 Hpc-cKO). The tests at 3 and 7 days time points were performed on independent groups that were retested at 2 weeks for assessing generalization of the auditory fear memory. In contrast to Arc/Arg3.1 ablation in the amygdaloid complex, removal of Arc/Arg3.1 from the hippocampus significantly facilitated the acquisition of fear, as Hpc-cKO mice exhibited significantly higher levels of freezing after CS-US presentation (Post) (Figure 43c) (2-

way RM-ANOVA: Genotype $F_{(1,34)}$=4.08; p=0.05, NS; Time $F_{(1,34)}$=70.06, ***p<0.001; Interaction $F_{(1,34)}$=3.28; p=0.08, NS; LSD post hoc test: *p<0.05). Suggesting that Arc/Arg3.1 expression in the hippocampus contributes to control of acquired fear.

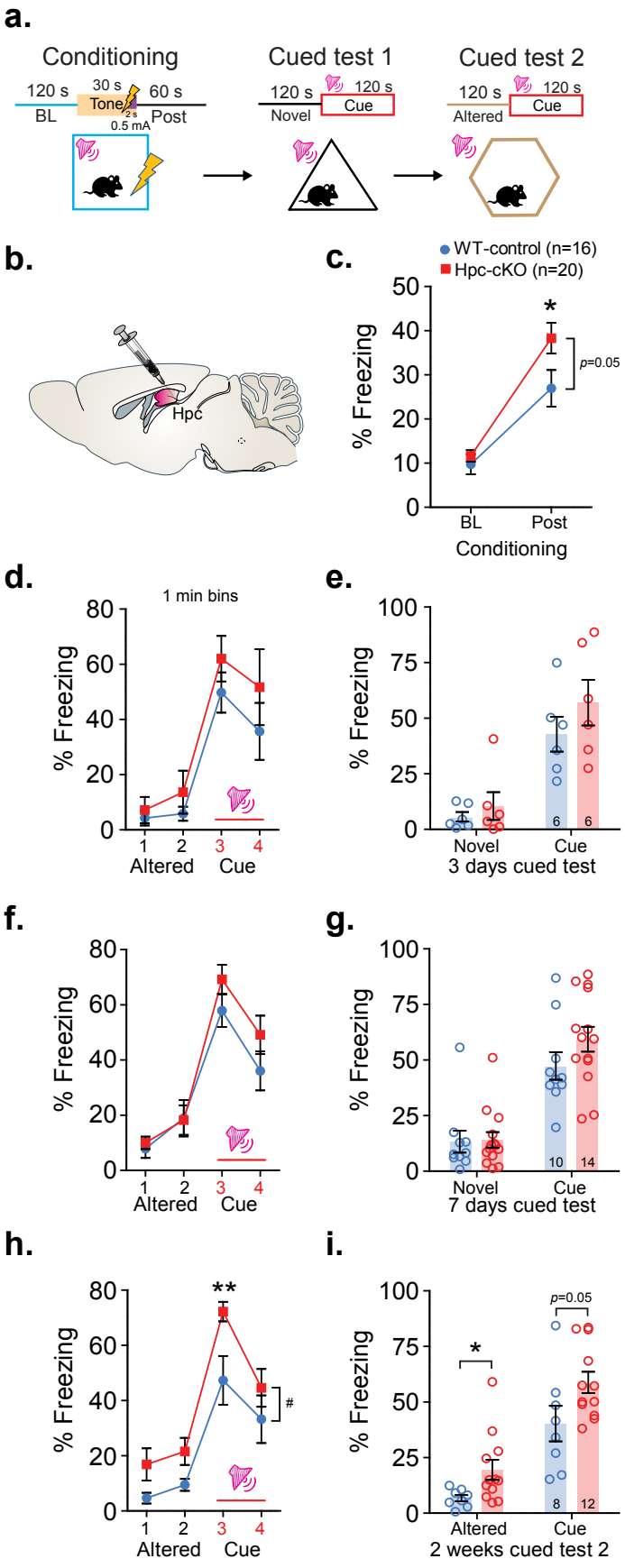

Figure 43. Conditional hippocampal deletion of Arc/Arg3.1 facilitates fear acquisition and retrieval of remote auditory fear memory

a. Schematic representation of fear conditioning and test protocols.

b. Anatomical representation of hippocampal injection.

c. Hippocampal removal of Arc/Arg3.1 significantly facilitates the acquisition of fear. Hip-cKO mice presented significantly higher level of immobility after CS-US presentation (Post) (2-way RM-ANOVA: Genotype $F_{(1,34)}$=4.08; p=0.05, NS; Time $F_{(1,34)}$=70.06, ***p<0.001; Interaction $F_{(1,34)}$=3.28, p=0.08, NS; LSD post hoc test: *p<0.05).

d. Cued fear retrieval 3 day after conditioning appears normal in Hpc-cKO mice evaluated by the freezing behavior in each minute bin (2-way RM-ANOVA: Genotype $F_{(1,10)}$=1.17; NS; Time $F_{(3,30)}$=39.43, ***p<0.001; Interaction $F_{(3,30)}$=0.51; NS); or

e. Total time of retrieval in novel context (WT-control, 5.04±2.14 %; Hip-cKO, 10.40±6.24 %; Mann-Whitney U = 17.50, p=1, NS) or cued test (WT-control, 42.71±7.84 %; Hip-cKO, 56.86 ± 10.25 %; Mann-Whitney U=10, p=0.24, NS)

f. WT-cKO and Hpc-cKO cued retrieval 7 days after conditioning in each minute bin (2-way RM-ANOVA Genotype $F_{(1,22)}$=1.11; NS; Time $F_{(3,66)}$=70.59, ***p<0.001; Interaction $F_{(3,66)}$=1.34; NS). or

g. Total time of retrieval: novel context (WT-control, 13.39 ± 4.94 %; Hip-cKO, 14.11 ± 3.48 %; Mann-Whitney U=62, p=0.66, NS) and cued test (WT-control, 40.26±7.99 %; Hpc-cKO, 58.41 ± 4.78 %, t_{22}=1.45, p=0.16, NS)

h. When retested 2 weeks after conditioning in an altered context, a significantly higher freezing was observed during the first minute of tone (2-way RM-ANOVA 1 min bin: Genotype $F_{(1,18)}$=6.19; #p<0.05; Time $F_{(3,54)}$=45.49, ***p<0.001; Interaction $F_{(3,54)}$=0.94; NS; LSD post hoc **p<0.01) and

i. Generalization to the altered context (WT-control, 7.03 ± 1.41 %; Hip-cKO, 19.20 ± 4.54 %; Mann-Whitney U=19, *p<0.05) and cue (WT-control, 40.26 ± 7.99 %; Hip-cKO, 58.41 ± 4.78 %; Mann-Whitney U=19, p=0.049).

Error bars represent mean ± SEM.

Despite of enhanced fear learninig, I observed comparable cued fear recall at 3 days after conditionated acquisition (Figure 43d-e)(2-way RM-ANOVA 1 min bin: Genotype $F_{(1,10)}$=1.17; NS; Time $F_{(3,30)}$=39.43, ***p<0.001; Interaction $F_{(3,30)}$=0.51; NS) and 7 days later (Figure 43f-g)(2-way RM-ANOVA 1 min bin: Genotype $F_{(1,22)}$=1.11; NS; Time $F_{(3,66)}$=70.59, ***p<0.001; Interaction $F_{(3,66)}$=1.34; NS).

When I retested the mice 2 weeks after conditioning using the same tone but an altered context (Figure 43a [cued test 2], h-i), an enhanced auditory implicit memory recall was observed especially in the first minute of cue retrieval (Figure 43h)(2-way RM-ANOVA 1 min bin: Genotype $F_{(1,18)}$=6.19; #p<0.05; Time $F_{(3,54)}$=45.49, ***p<0.001; Interaction $F_{(3,54)}$=0.94; NS; LSD post hoc **p<0.01), as well as a significant generalization to the altered context (Figure 43i) (WT-control, 7.03±1.41%; Hip-cKO, 19.20±4.54%; Mann-Whitney U=19, *p<0.05). These observations indicate that Arc/Arg3.1 expression in the hippocampus might not be necessary for the storage of aversive implicit experiences (such as the CS-US paring), but could facilitate its acquisition and expression especially when the memory is retrieved at remote time points, probably due to a loss of detailed information about the conditioned context.

5.2.3. Genetic removal of Arc/Arg3.1 in the ventromedial PFC has no effect on anxiety-like behavior or auditory fear conditioning

Because Arc/Arg3.1 expression is essential for the consolidation of fear in the amygdala and plays a role in the development of functional connectivity of some areas in the PFC, I hypothesized that expression of Arc/Arg3.1 in the PFC might play a role in emotional control and fear regulation in the adult brain. I sought to test this hypothesis by stereotaxic delivery of rAVV-Cre vectors in the PrL and IL areas (hereafter refereed as mPFC) (Figure 44a) and investigated the effect of Arc/Arg3.1 ablation on behavior by performing EPM and FC. Only animals with widespread expression of the Cre recombinase in these regions were taken in consideration for the final analyses (Figure 44b).

I tested 7 WT-control and 5 mPFC-cKO mice in the EPM (Figure 44c) and observed no effect of Arc/Arg3.1 ablation on unconditioned avoidance behavior. Mice in both groups covered similar distances in the maze (WT-control, 10.66±0.77; mPFC-cKO, 12.43±1.09 m; Mann-Whitney U=10.00, NS), spent comparable time in the arms (Figure 44e) (2way-ANOVA: Genotype, $F_{(1,10)}$=0.008, p=0.92, NS; Arm $F_{(2,20)}$=47.9, ***p<0.001; Interaction, $F_{(1,20)}$=0.83, p=0.44, NS) and entered with a nonsignificant higher frequency into the closed arms (WT-control, 16.00±2.65; mPFC-cKO, 23.20±2.15; Mann-Whitney U=10.00, p=0.12, NS). These findings indicate that Arc/

Arg3.1 deletion in the PrL and IL cortices may not affect anxiety-like behavior in adult mice.

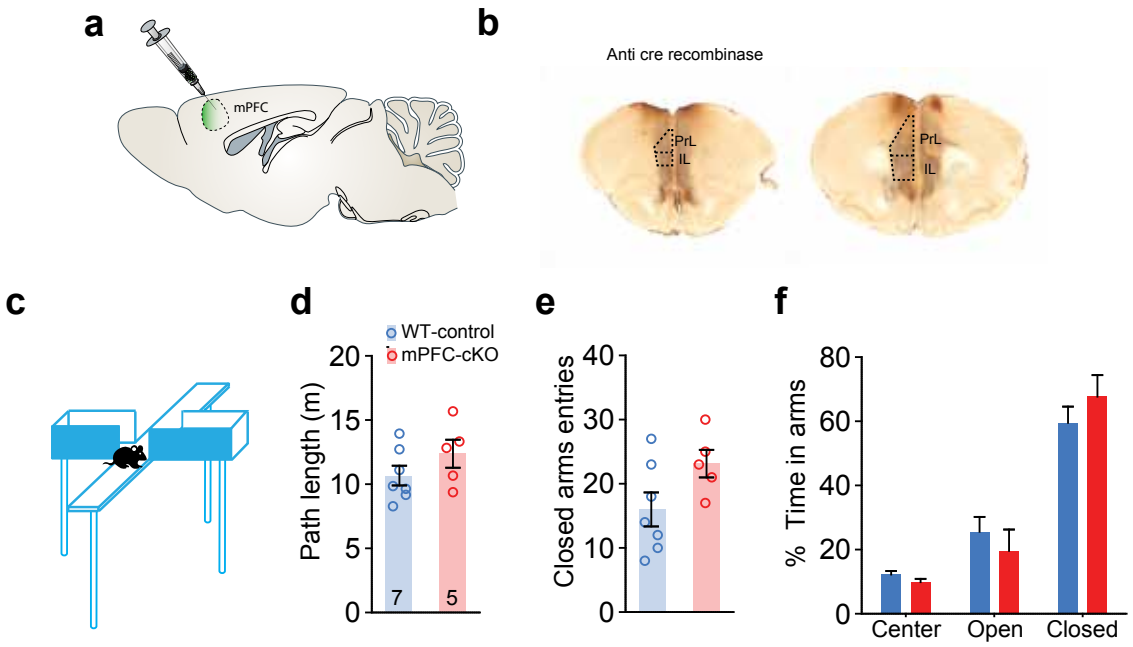

Figure 44. Conditional ablation of Arc/Arg3.1 in the prelimbic and infralimbic areas of the PFC has no effect on anxiety-like behavior
a. Anatomical representation of vmPFC injection. **b.** Immunoreactivity of Cre recombinase after rAAV-CaMKIIα-Cre injection prelimbic (PrL) and infralimbic (IL) areas of the mPFC. **c.** In the EPM mPFC-cKO mice exhibit normal locomotor activity gauged by their **d.** path length (WT-control, 10.66±0.77 m; mPFC-cKO, 12.43±1.09 m; Mann-Whitney U=10.00, NS) **e.** Both genotypes display similar frequency to closed arms (WT-control, 16.00±2.65; mPFC-cKO, 23.20±2.15 %; Mann-Whitney U = 10.00, NS) and **j.** time in each arm (2way-ANOVA: Genotype, $F_{(1,10)}$=0.008, NS; Arm $F_{(2,20)}$=47.9, ***p<0.001; Interaction, $F_{(1,20)}$=0.83, NS). Error bars represent mean ± SEM. WT-control, n=7; mPFC-cKO, n=5.

I next tested auditory fear acquisition and retention in a group of 12 WT-control and 14 mPFC-cKO mice, and observed that the conditional deletion of Arc/Arg3.1 in PrL and IL cortices did not affect the acquisition of fear because in the conditioning phase, both groups displayed comparable freezin after CS-US pairing (Figure 45c) (2-way RM-ANOVA: Genotype $F_{(1,24)}$=0.14; NS; Time $F_{(1,24)}$=25.22, ***p<0.001; Interaction $F_{(1,24)}$=0.0003; NS). Furthermore, I observed no statistical differences in expression of auditory fear on the 1 day cued test (Figure 45d-e) (2-way RM-ANOVA 1 min bin: Genotype $F_{(1,24)}$=2.27; NS; Time $F_{(3,72)}$=65.11, ***p<0.001; Interaction $F_{(3,72)}$=0.51; NS; time novel context: WT-control, 5.32±1.55 %; mPFC-cKO, 11.56±2.91 %; Mann-Whitney U=51.00, NS; Cue: WT-control, 36.99±5.49 %; mPFC-cKO, 45.14±5.17 %; t_{24} = 1.08, NS) or 2 weeks retest in an altered environment (Figure 45 f-g) (2-way RM-ANOVA 1 min bin: Genotype $F_{(1,24)}$=2.64; NS; Time $F_{(3,72)}$=28.76, ***p<0.001; Interaction $F_{(3,72)}$=0.75; NS; Altered context: WT-control, 12.87±3.72 %; mPFC-cKO, 21.32±4.22 %; t_{24}=1.48, NS; Cue: WT-control, 29.42±5.70 %; mPFC-cKO, 40.73±6.60 %; t_{24}=1.27, NS). These results suggest that Arc/Arg3.1 expression in the mPFC may not play a role in anxiety-like behavior, fear adquisition or expression in the adult brain.

.

Figure 45. Genetic removal of Arc/Arg3.1 in the vmPFC (PrL and IL cortices) has no effect on acquisition or retrieval of fear

a. Schematic representation of fear conditioning and test protocols.

b. Anatomical representation of PrL and IL cortices injection.

c. Ablation of Arc/Arg3.1 in PrL and IL coritices has no effect in acquisition of fear. (2-way RM-ANOVA: Genotype $F_{(1,24)}$=0.14; NS; Time $F_{(1,24)}$=25.22, ***p<0.001; Interaction $F_{(1,24)}$=0.0003; NS).

d. Cued fear retrieval 1 day after conditioning appears normal in mPFC-cKO mice evaluated by the freezing behavior in each minute bin (2-way RM-ANOVA 1 min bin: Genotype $F_{(1,24)}$=2.27; NS; Time $F_{(3,72)}$=65.11, ***p<0.001; Interaction $F_{(3,72)}$=0.51; NS); or

e. Total time of retrieval in novel context (WT-control, 5.32±1.55 %; mPFC-cKO, 11.56±2.91 %; Mann-Whitney U =51.00, NS) or cued test (WT-control, 36.99 ± 5.49 %; mPFC-cKO, 45.14 ± 5.17 %; t_{24} = 1.08, NS)

f. When retested 2 weeks after conditioning in an altered context, cued fear retrieval appears normal in mPFC-cKO mice evaluated by the freezing behavior in each minute bin (2-way RM-ANOVA 1 min bin: Genotype $F_{(1,24)}$=2.64; NS; Time $F_{(3,72)}$=28.76, ***p<0.001; Interaction $F_{(3,72)}$=0.75; NS) or

g. Total time of retrieval in altered context (WT-control, 12.87±3.72 %; mPFC-cKO, 21.32±4.22 %; t_{24}=1.48, NS) or during cue test (WT-control, 29.42 ±5.70 %; mPFC-cKO, 40.73±6.60 %; t_{24}=1.27, NS).

Error bars represent mean ± SEM.
WT-control, n=12; mPFC-cKO, n=14.

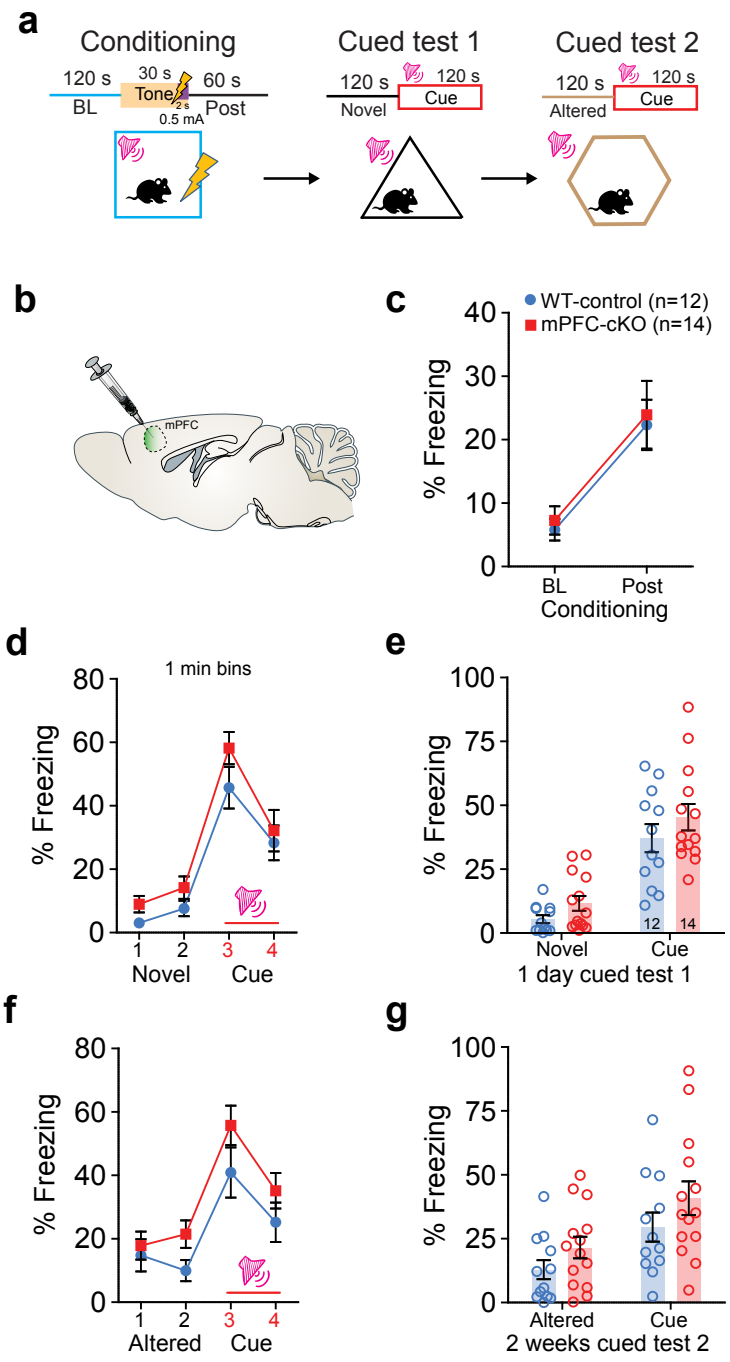

5.2.4. Selective deletion of Arc/Arg3.1 in the ACC reduces unconditioned avoidance and facilitates acquisition and retrieval of auditory fear conditioning

Since Arc/Arg3.1 expression during early postnatal development significantly influences the functional connectivity of the ACC, I hypothesized that Arc/Arg3.1 have a predominant role in this brain region. To address this hypothesis, I stereotaxically deliveried rAVV-Cre vectors to the ACC of 11 wild types (WT-control) and 10 Arc/Arg3.1$^{f/f}$ adult mice (ACC-cKO) (Figure 46a-b), and assessed unconditioned avoidance and conditioned auditory fear acquisition and expression.

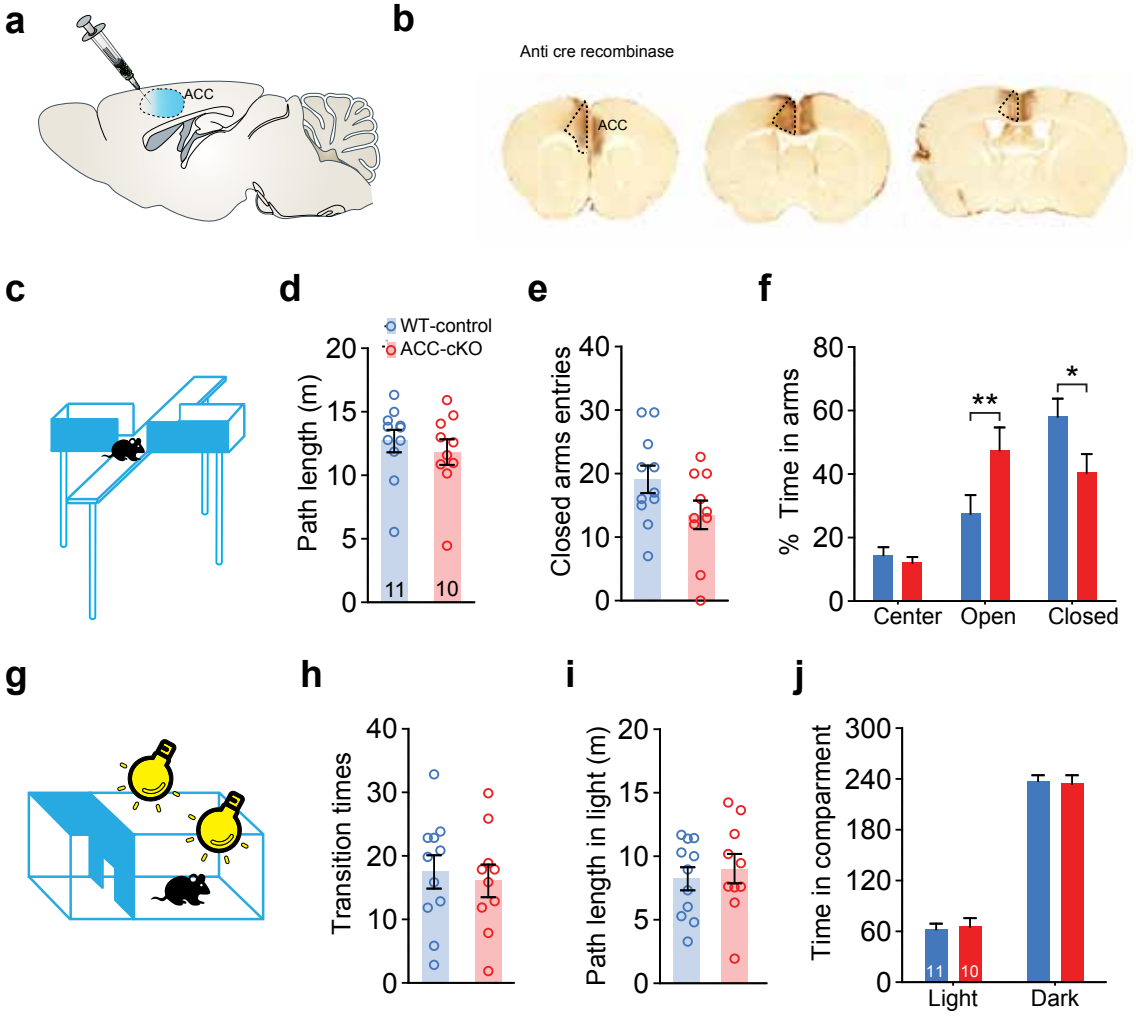

Figure 46. Selective deletion of Arc/Arg3.1 in the ACC produces mild anxiolytic-like behavior
a. Anatomical representation of ACC injection. **b.** Immunoreactivity of cre recombinase after rAAV-CaMKIIα-Cre injection in ACC. **c.** In the EPM ACC-cKO mice exhibit normal locomotor activity gauged by their **d.** path length (WT-control, 12.73±0.89; ACC-cKO, 11.81±1.01 %; Mann-Whitney U=43.00, NS) **f.** but reduced unconditioned avoidance presenting lesser entries to closed arms (WT-control, 19.09±2.17; ACC-cKO, 13.50±2.30; t_{19}=1.79, p=0.09) and **e.** increased time in open the arms (2way-ANOVA: Genotype, $F_{(1,57)}$=4.16^{-9}, NS; Arm $F_{(2,57)}$=25.04, ***p<0.001; Interaction, $F_{(2,57)}$=6.65, **p<0.01, LSD post hoc test **p<0.01, *p<0.05) **g.** This anxiolytic-like phenotype was not confirmed by the light-dark box test. **h.** WT-control and ACC-cKO mice exhibit similar time in both compartments (2way-ANOVA: Genotype, $F_{(1,38)}$=7.86^{-14}, NS; compartment $F_{(1,38)}$=418.3, ***p<0.001; Interaction, $F_{(1,38)}$=0.15, NS). **i.** Comparable transitions between compartments (WT-control, 17.64±2.62; ACC-cKO, 16.20±2.58; t_{19} = 0.40, NS) and **j.** path length in the light zone (WT-control, 8.30±0.91; ACC-cKO, 8.96±1.16; t_{19} = 0.45, NS). Error bars represent mean ± SEM. WT-control, n=11; ACC-cKO, n=10.

When injected mice were tested in the EPM (Figure 46c), I observed that both genotypes showed normal locomotion judged from the similar distances they moved in the maze (Path length in m: WT-control, 12.73±0.89; ACC-cKO, 11.81±1.01 %; Mann-Whitney U=43.00, p=0.42, NS). Notably, ACC-cKO mice displayed a statistically significant tendency to explore the open arms longer and avoided the closed arms (2way-ANOVA: Genotype, $F_{(1,57)}$ = 4.16^{-9}, NS; Arm $F_{(2,57)}$=25.04, ***p<0.001; Interaction, $F_{(2,57)}$=6.65, **p<0.01, LSD post hoc test **p<0.01, *p<0.05). This anxiolytic effect induced by the selective deletion of Arc/Arg3.1 in the ACC was not evident when the same animals were tested 24 h later in the light-dark box test, both treated groups displayed

the same time in both compartments (2way-ANOVA: Genotype, $F_{(1,38)}=7.86^{-14}$, NS; compartment $F_{(1,38)}=418.3$, ***p<0.001; Interaction, $F_{(1,38)}=0.15$, NS) and comparable frequency in the light zone (WT-control, 17.64±2.62; ACC-cKO, 16.20±2.58; $t_{19}=0.40$, NS).

These findings suggest that similar to what was observed in our Early-cKO mice; Arc/Arg3.1 expression in the ACC is partially responsible for the control of unconditioned avoidance and perception of potential threats in the adult brain. It is reasonable to hypothesize that the acute genetic deletion of Arc/Arg3.1 in the ACC altered the functional connectivity with anatomical hubs that control or generate avoidance responses and fear.

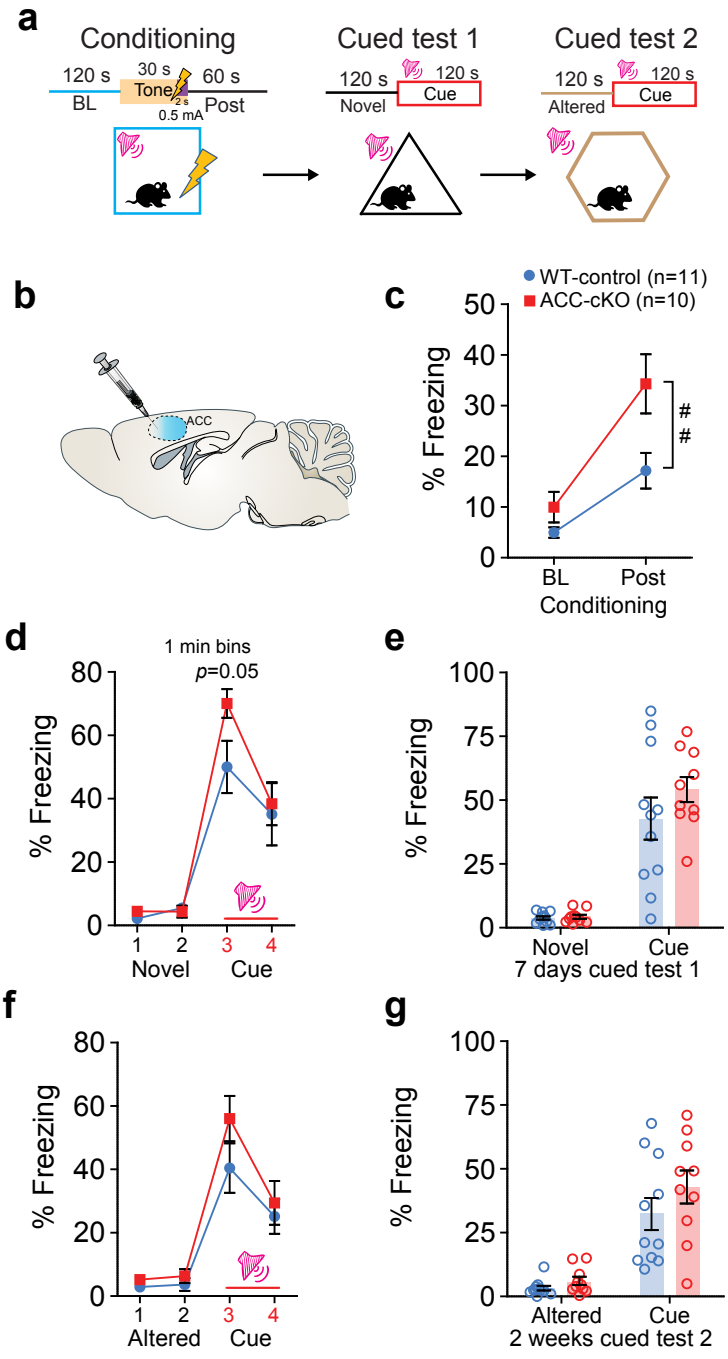

Figure 47. Conditional deletion of Arc/Arg3.1 in the ACC facilities acquisition and retrieval of auditory fear conditioning

a. Schematic representation of fear Conditioning and test protocols.

b. Anatomical representation of ACC injection.

c. Removal of Arc/Arg3.1 in ACC facilitates acquisition of fear. (2-way RM-ANOVA: Genotype $F_{(1,19)}=9.59$; $^{\#\#}p<0.01$; Time $F_{(1,41)}=25.19$, ***p<0.001; Interaction $F_{(1,41)}=3.05$; p=0.09, NS).

d. ACC-cKO mice display a tendency of higher freezing at 7 days cued fear retrieval in the first cue minute bin (2-way RM-ANOVA 1 min bin: Genotype $F_{(1,19)}=1.44$; NS; Time $F_{(3,57)}=62.29$, ***p<0.001; Interaction $F_{(3,57)}=1.87$; NS)

e. Comparable immobility in total time of retrieval in novel context (WT-control, 3.82±0.65 %; ACC-cKO, 4.39±0.80 %; t_{19} = 0.56, NS) or cue (WT-control, 42.54±8.27%; ACC-cKO, 54.22±4.89%; $t_{29}=1.18$, NS) when compared to WT-controls.

f. When retested 2 weeks after conditioning in an altered context, cued fear retrieval appears normal in ACC-cKO mice evaluated by the freezing behavior in each minute bin (2-way RM-ANOVA 1 min bin: Genotype $F_{(1,19)}=1.62$; NS; Time $F_{(3,57)}=49.68$, ***p<0.001; Interaction $F_{(3,57)}=1.12$; NS) or

g. Total time of retrieval in altered context (WT-control, 3.27±0.91%; ACC-cKO, 5.75±1.62%; Mann-Whitney U=37.50, NS) or during cued test (WT-control, 32.77±6.29%; ACC-cKO, 42.70±6.48%; $t_{19}=1.10$, NS).

Error bars represent mean ± SEM.
WT-control, n=11; ACC-cKO, n=10.

I next tested the role of Arc/Arg3.1 in fear by assessing auditory fear acquisition and recall in mice with specific ablation of the gene in the ACC (Figure 47a-b). Notably, I observed that similar to what was observed in Early-cKO and Hpc-cKO mice, ACC-cKO mice displayed significantly higher levels of freezing after one paired CS-US presentation (2-way RM-ANOVA: Genotype $F_{(1,19)}$=9.59; $^{\#\#}p<0.01$; Time $F_{(1,41)}$=25.19, $^{***}p<0.001$; Interaction $F_{(1,41)}$=3.05). This strong fear response is maintained for 7 days specially in the first minute during cue test (2-way RM-ANOVA 1 min bin: Genotype $F_{(1,19)}$=1.44; NS; Time $F_{(3,57)}$=62.29, $^{***}p<0.001$; Interaction $F_{(3,57)}$=1.87; NS; LSD post hoc test p=0.05), but is not observed 2 weeks post conditioning during a cue retest in an altered context (2-way RM-ANOVA 1 min bin: Genotype $F_{(1,19)}$=1.62; NS; Time $F_{(3,57)}$=49.68, $^{***}p<0.001$; Interaction $F_{(3,57)}$=1.21; NS). These results suggest that Arc/Arg3.1 expression in the ACC may be necessary for controlling normal avoidance and learning of fear responses, and the specific Arc/Arg3.1 KO from the structure may disengage this area from the circuit.

6. Discussion

The main goal of the second part of this dissertation was to investigate the role of Arc/Arg3.1 in specific brain regions that are proposed to mediate fear and anxiety-like behaviors in adulthood. In the first part of the thesis, I found that the ablation of Arc/Arg3.1 gives rise to effects that are specific to the early postnatal development in a sensitive period. Nevertheless, the Arc/Arg3.1 gene is upregulated after novel experiences in the adult animal and is proposed to be the signature of cells that are recruited to engrams that encode and consolidate relevant information (Denny *et al* 2014). I hypothesized that Arc/Arg3.1 participates in the regulation of acquired fear by modifying local circuits in different brain regions and may mediate normal emotional processing such as learned fear and unconditioned avoidance in the adult brain.

To investigate this hypothesis, I first focused on the standardization of a rAVV-based Cre recombinase tool that allows the conditional ablation of this gene in specific regions of the adult brain. Following this, I employed this tool together with the Arc/Arg3.1$^{f/f}$ mouse line, fear conditioning and unconditioned avoidance tasks to investigate the effect of Arc/Arg3.1 deletion in specific hubs of the proposed circuits. I found that while Arc/Arg3.1 is essential for the consolidation of implicit fear memory in the amygdaloid complex, in the ACC and Hpc its absence leads to an enhanced fear acquisition and mild effect in the expression of auditory fear conditioning. In anxiety, Arc/Arg3.1 seems to play a discreet role in the adult brain, because its specific ablation in the ACC exerted a mild anxiolytic effect.

I will review and discuss the obtained results and correlate them with the current literature in the field of fear and anxiety, taking in consideration the proposed role of Arc/Arg3.1 in cellular and molecular functions.

6.1. rAVV viral vectors and cre-*LoxP* system are effective tools for conditional gene deletion in specific circuits of the adult brain

rAVV viral vectors have been proved to be an excellent tool for delivering and transducing transgenes with high efficiency and low toxicity in the CNS. I cloned and investigated different prAAV constructs carrying Cre recombinases under the control of two neuronal specific promoters (CaMKIIα and hSyn1) to locally ablate the Arc/Arg3.1 gene in neurons of fear and anxiety-related circuits in the brain of Arc/Arg3.1$^{f/f}$ mice. I chose this approach based on the notion that other molecular approaches to downregulate mRNA expression and translation only provide transient

and incomplete reduction of the gene expression and may produce toxicity, and neuroinflamation that interfere with the behavioral readout.

RNA interference against Arc/Arg3.1 mRNA (e.*g.* shRNAs) delivered in viral vectors has shown to be neurotoxic and hinder auditory fear conditioning (de Solis *et al* 2015) without specific effect from the gene knock-down. Acute off-target effect of antisense oligonucleotides (ODN) have not yet been fully investigated and its stability *in vivo* is only achieved if administrated *in situ* repeatedly through a cannula, which is usually implanted in the specific brain region or cerebral ventricles (Whitesell *et al* 1993). In addition to the loss of cerebral tissue result from the cannulation procedure, the use of ODNs has a partial-efficacy in reducing Arc/Arg3.1 expression (<50%) (Guzowski *et al* 2000b) when compared with an estimated removal of the gene of more than 70% when the Cre carrying - rAAV vectors are used (section 5.1.1.). Moreover, ODNs might not remove preexistent Arg/Arg3.1 protein from protected compartments such as the post-synaptic density (PSD) and their effect on behavior might arise only from the hybridization and arrest of newly transcribed or pre-existing mRNA that is presumably subjected to local translation in dendrites. For the aforementioned reasons, the Cre-*LoxP* system combined with the validated rAAV- viral vectors offer a safer and more effective approach to specifically remove Arc/Arg3.1 from specific regions of the proposed circuits.

To validate this conditional genetic approach, I employed Cre recombinase and driven by two neuronal specific promoters: hSyn1 and CaMKIIα. Conspicuously, I found that both codon-improved and prokaryotic Cre recombinases driven by the hSyn1 promoter lead to an invariable activation of pro-apoptotic cascades (activated caspase-3 immunoreactivity) that with time and accumulation of the Cre transgene induced neurodegeneration and severe inflammatory activation (figures 37 and 38). Cre toxicity is big pitfall of the Cre-*LoxP* system and depends on the concentration and time of Cre expression. It has been proposed that Cre toxicity is the result of the promiscuity of the endonuclease activity at recognizing cryptic *LoxP* sites (Thyagarajan *et al* 2000) if expressed at high levels or for prolonged periods of time, producing DNA damage by double-strand breaks and nicks (Loonstra *et al* 2001).

With my validation experiments, I found that the Cre toxicity is avoided for up to 30 days when the expression of the Cre transgene was driven by the CaMKIIα promoter (Figure 35), and this safety profile was maintained for longer periods of time if a ligand-dependent chimeric Cre recombinase ($CreER^{T2}$) was expressed instead. It is plausible that the hSyn1 promoter has a stronger and broader activity than the CaMKIIα promoter, leading to higher and toxic levels of the transgene even when low titters of the vector are used. Choosing the rAAV-CaMKIIα-Cre and defining the

conditions for its safe usage, allowed me to proceed with investigating the role of Arc/Arg3.1 in fear and anxiety circuits in the adult brain.

6.2. Adult expression of Arc/Arg3.1 in the basolateral amygdala is essential for the consolidation but not the acquisition of auditory Pavlovian fear conditioning

One of the most studied structures in relation to emotional control, fear and anxiety is the amygdaloid complex. The role of the amygdala in generation, control and expression of implicit fear memories has been extensively investigated by lesions, electrical stimulation and more recently optogenetic manipulations (Janak & Tye 2015). I stereotaxically delivered rAAV-Cre vector to the amygdaloid complex of a cohort of mice, and tested fear and anxiety-related behavior after ablation of Arc/Arg3.1 gene. I observed that this intervention produced no effect on exploratory behavior or unconditioned avoidance, suggesting that Arc/Arg3.1 in this structure may essential for anxiety-like behavior, similar to what has been described in some studies where lesions in the amygdala were performed (Decker *et al* 1995, Treit & Menard 1997). The genetic removal of Arc/Arg3.1 in the amygdaloid complex yielded no effect on fear acquisition but induced a highly significant influence on the consolidation of implicit fear memory (Figure 40). Furthermore, I found that this effect seemed to positively correlate with the extent of Arc/Arg3.1 ablation in the BLA and piriform cortex (Figure 41).

Because Arc/Arg3.1 has been directly linked to consolidation of synaptic plasticity, other groups tried to investigate Arc/Arg3.1 expression as a molecular indicator of cellular plasticity during auditory fear conditioning. They showed that only neurons expressing Arc/Arg3.1, which are specifically recruited by fear conditioning in the lateral amygdala, displayed an enhanced intrinsic excitability and higher probability to mediate synaptic potentiation with thalamic inputs (Gouty-Colomer *et al* 2016). Moreover, the infusion of ODNs that specifically hybridize with Arc/Arg3.1 mRNA in the LA blocks the consolidation but not the acquisition of cued fear conditioning (Maddox & Schafe 2011, Ploski *et al* 2008). Nontheless, the efficiency of the ODNs against Arc/Arg3.1 is limited to applications between 3 to 6 hours before fear acquisition or retrieval. Consolidation can be also prevented by application of ODNs 12 hours after acquisition by inhibiting a second wave of Arc/Arg3.1 expression (12 hours after acquisition) (Nakayama *et al* 2016, Nakayama *et al* 2015). Thus, experiments using ODNs suggest that the upregulation of Arc/Arg3.1 is a transient phenomenon that can be compensated by other molecular or systemic mechanisms.

My experiments using the Cre-*LoxP* system in the BLA showed a stark impairment in the consoli-

dation of auditory fear conditioning confirming the indirect observations from ODNs application and IEGs analysis, underscoring the importance of the amygdala as a structure for storing auditory implicit memories and highlighting the expression of Arc/Arg3.1 as an essential molecular requirement for the consolidation of this type of memory. Likewise, these results confirmed that Arc/Arg3.1 is essential for the consolidation of implicit memory in the BLA in the adulthood and may indicate that the amnesic phenotypes found in the Early-cKO line is not only an effect of a developmental failure but reflects a constitutive requirement for Arc/Arg3.1 as consolidation molecule throughout the life span. Further examination of electrophysiological properties and plasticity in the BLA-ablated neurons is needed to confirm whether Arc/Arg3.1-mediated synaptic plasticity is the celullar mechanism used for the consolidation of implicit memory in this structure.

6.3. The expression of Arc/Arg3.1 in the adult hippocampus facilitates the acquisition of conditioned fear and contributes to the control of generalized fear

The dHpc has been strongly linked with the rapid consolidation of contextual and spatial information; in contrast the vHpc has been associated with emotional control, anxiety-related behaviors and expression of fear (Bannerman *et al* 2004). Here, I found that genetic deletion of Arc/Arg3.1 in the hippocampus induced changes in the open field that might indicate a mild anxiogenic-like behavior (longer time in center) without affecting locomotor activity. However, a more suitable paradigm for investigating anxiety-like behavior such as EPM did not confirm any difference in unconditioned avoidance, indicating that it is unlikely that removal of Arc/Arg3.1 in the hippocampus produces changes in anxiety-like behavior (Figure 42).

Seminal experiments by aspiration lesions of the entire hippocampus in rats showed that this structure was involved in locomotor activity as these lesions induced hyperactivity in the open field test (Hannigan *et al* 1984). Moreover, lesions or pharmacological inactivation of the vHpc induces anxiolytic-like behavior in ethological paradigms such as EPM (Kjelstrup *et al* 2002), probably as a secundary effect of the hyperactivity. In contrast to these studies, my results showed a mild opposite tendency toward anxiongenic-like behavior in the OF without apparent changes in locomotor activity, but this effect was not confirmed in a more stringent behavioral test for unconditioned avoidance like the EPM. Both OF and EPM are based on the innate avoidance displayed by rodents to explore open and illuminated spaces. OF is considered a less sensitive paradigm to investigate anxiety-like behaviors, because the potential threat (center) is defined by illumination conditions that are always very variable among the literature. Nonetheless, it is possible that Arc/Arg3.1 expression in the ventral hippocampus contributes partially to the integration of safety sig-

nals from amygdala inputs and the contextual processing of environments with discreet potential threats (center of the open field). It is also plausible that interfering with Arc/Arg3.1 in the vHpc produces changes in functional connectivity and synchronicity with the PFC, which is a proposed mechanism for controlling contextual based avoidance (Padilla-Coreano *et al* 2016).

I also found that the broad ablation of Arc/Arg3.1 in the hippocampus produces an enhancement in fear acquisition and a generalization of fear responses when the cued memory was retested with 2-week delay in a different environment. These findings may have two possible explanations: (i) the genetic removal of Arc/Arg3.1 was extended to the vHpc which has been implicated in fear acquisition and expression. The absence of the gene in the ventral portion might lead to an imbalance and altered acquisition of the safety/fear signals from the amygdala (Barkus *et al* 2010). (ii) the dorsal hippocampus has been shown to be necesary for the long-term storage of detailed contextual information (Wiltgen *et al* 2010), hence it is possible that detailed information about the context (where the conditioning took place) was not consolidated and a stronger implicit memory and generalization to an altered context reflets an impairment in retrival of detailed contextual information. These findings linked Arc/Arg3.1 expression in the adult hippocampus with the generalization of fear by the loss of contextual details and highlight its role in the stability and control of fear circuits.

Consolidation of detailed contextual information and pattern separation are mnemonic processes that have been attributed to combinatory ensembles of cells in the DG. It is believed that these cells storage the details of the information via synaptic plasticity (McHugh *et al* 2007). In agreetment, ensambles of Arc/Arg3.1-positive neurons mediating contextual acquisition have been found in the DG (Denny *et al* 2014) and the LTP induced in granule cells via entorhinal cortex stimulation appears to be dependent of Arc/Arg3.1 (Plath *et al* 2006). These reports support the possibility that generalization of cued memory and enhanced freezing in al altered context when Arc/Arg3.1 is removed from the DG is due to an imparaiment in patter separation and consolidation of detail information. It remains to be investigated whether the adult conditional ablation of Arc/Arg3.1 recapitulates deficits in LTP in the DG observed in the constitutive KO mice (Plath *et al* 2006).

6.4. Absence of Arc/Arg3.1 in the vmPFC has no effect on fear or anxiety circuits

The amygdala is strongly connected and modulated at the same time by the subregions of the PFC (PrL, IL and ACC cortices). These regions have been extensively studied in fear and anxiety-

related behaviors, and are proposed to exert top down modulation on the amygdala and hindbrain nuclei that contribute to the expression of fear and unconditioned avoidance (Adhikari *et al* 2015). For investigating Arc/Arg3.1 in the PFC and its role in fear and anxiety related-behaviors, I stereotaxically delivered rAAV-Cre vectors to the the vmPFC (PrL and IL) and ACC in 2 cohorts of animals, respectively, and tested their behavior in EPM and auditory fear conditioning.

Surprisingly and in contrast to what was expected from inactivation (Lacroix *et al* 2000), optogenetic manipulations (Courtin *et al* 2014) or studies using ODNs (McReynolds *et al* 2014) , our findings suggest that Arc/Arg3.1 in the adult and fully developed vmPFC does not play a role either in anxiety-related behaviors or in implicit fear acquisition or retrieval. It remains still unsolved if other types of fear learning and memory that have been linked with the PrL or IL cortices function may require Arc/Arg3.1 expression such as extinction of fear (Sierra-Mercado *et al* 2011, Sotres-Bayon & Quirk 2010) or trace fear conditioning (Blum *et al* 2006, Gilmartin & Helmstetter 2010, Kwapis *et al* 2014).

6.5. Arc/Arg3.1 expression in the adult ACC contributes to anxiety-like behavior and to fear acquisition

When the animals Arc/Arg.31-ablated in the ACC were tested in EPM, I observed a significant anxiolytic-like behavior that was not confirmed by the LDB. The EPM and LDB are ethological paradigms to investigate unconditioned avoidance in rodents, and both paradigms share the similar principle: the animals should choose between protected and enclosed compartments and illuminated open zones. These two paradigms differ in the shape and intensity of light used for the open spaces, the small and brightly illuminated open field in the LDB represent a more aversive and dangerous threatening environment for the mice when compared to the illuminated open arms in the EPM.

Arc/Arg3.1 in the ACC might participate in the detection threshold of discreet potential threats. In rodents, pharmacological inactivation of the ACC produced anxiolytic and depressive-like behaviors (Kim *et al* 2011). ACC has projection to BLA, Hyp and PAG by which it can influence the avoidance behavior (Etkin *et al* 2011) and this connectivity may be partially altered when Arc/Arg3.1 is genetically removed leading to a mild anxiolytic phenotype.

In addition, I found an enhanced fear acquisition and cued fear expression in the auditory fear conditioning after removal of Arc/Arg3.1 in the ACC. Numerous studies in humans have implicated

the ACC in anxiety and fear-related disorders (Damsa *et al* 2009)., deficit in acquisition of auditory fear conditioning (Bissiere *et al* 2008) and impairments in the retrieval of remote contextual spatial fear memory (Frankland & Bontempi 2005, Teixeira *et al* 2006). The adult ablation of Arc/Arg3.1 in the ACC reflected some of the effects observed in the Early-cKO mice, suggesting that Arc/Arg3.1 may elicit some functional changes in this structure that are beyond a sensitive period of postnatal development. My results suggest that the expression of Arc/Arg3.1 in the ACC might participate in maintaining the normal balance between anxiety-like behavior and aversive learning also in the adult life.

The ACC shows different forms of synaptic plasticity that are proposed to mediate storage of remote unpleasant and fear-related memories, and regulate sensory and emotional responses (Koga *et al* 2015). The necessity of Arc/Arg3.1 for these forms of synaptic plasticity remains to be investigated, and it is also intriguing if the enhanced acquisition of fear responses of ACC-cKO and Early-cKO mice is due to changes in the perception of unpleasant sensory stimuli and perception of pain, functions tightly linked with the normal activity in the ACC (Zhuo 2016).

6.6. Conclusions and outlook

In the second part of this dissertation, I investigateg how expression of Arc/Arg3.1 in the adult brain affects fear and anxiety-like behavior by modifying local and inter-areal connectivity within the presumed circuitry of these behavior. I combined the stereotaxic delivery of Cre-carryng rAVV viral vectors in the Arc/Arg3.1$^{f/f}$ mouse line and behavioral assessment as main methodological approaches.

I confirmed that Arc/Arg3.1 in adulthood is essential for the consolidation of implicit fear memory in the microcircuits of the amygdaloid complex without affecting acquisition of fear or anxiety-like behavior, suggesting that Arc/Arg3.1-mediated plasticity in this region might be a cellular mechanism for the consolidation of this type of associative memory. Furthermore, these findings confirmed that Arc/Arg3.1 plays a role in memory consolidation beyond the postnatal development. Arc/Arg3.1 may have a similar function in other microcircuits that mediate the consolidation of other types of memory, *e.g.* consolidation of detailed contextual information in the DG.

I observed that the genetic removal of Arc/Arg3.1 in the adult Hpcand ACC enhanced the acquisition of fear and resulted only in mild change in anxiety-like behaviors, contrasting with the Early-cKO mice that showed a strong phenotype in these emotional behaviors. These conflicting

results point at two main possibilities: (i) Arc/Arg3.1 expression during early postnatal development delimits a critical period for the establishment of circuits that mediate fear acquisition and unconditioned avoidance because the specific ablation during this period but not before (KO mice) of after (adult ablation) produces a strong change in this type of behavior; or (ii) Arc/Arg3.1 expression during early postnatal development only participates in a sensitive period for emotional development that takes place after birth, and these specific phenotypes might appear in adulthood if the entire network is targeted and not only single components. Future studies using inducible Cre transgenic lines for genetic removal of Arc/Arg3.1 and rescue strategies in the entire adult brain are necessary to investigate this possibility.

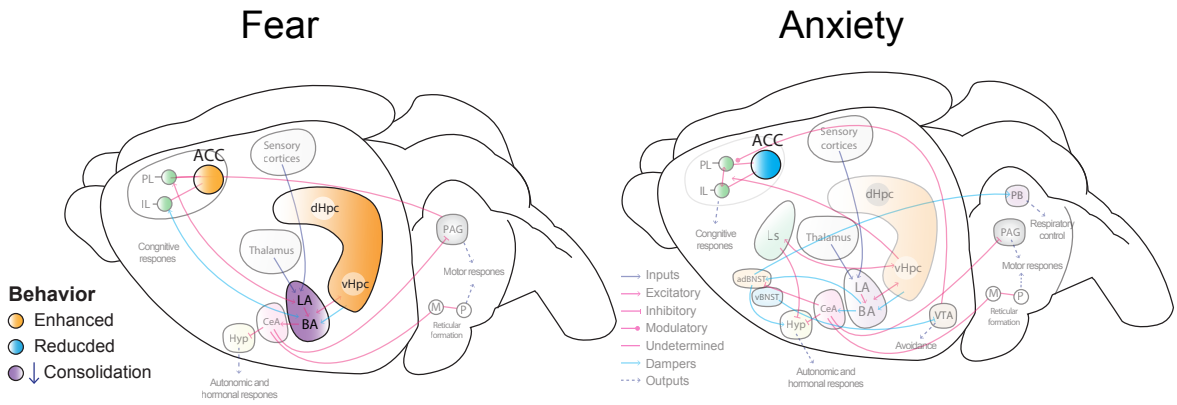

Figure 48. Genetic removal of Arc/Arg3.1 in specific components of circuits for fear and anxiety.
Arc/Arg3.1 is essential for the consolidation of implicit fear memory in the Amygdaloid complex, in the ACC and Hpc its absence leads to an enhanced fear acquisition and mild effect in the expression of auditory fear conditioning. In anxiety, Arc/Arg3.1 seems to play a discreet role in the adult brain, because its specific ablation in the ACC exerted a mild anxiolytic effect only in the EPM.

Taken together, the findings described in this thesis confirmed the importance of Arc/Arg3.1 in the consolidation of memory thoughtout the lifespan and provided novel information about its role during the ponstnatal development and emotional control, sheding light on the normal function of Arc/Arg3.1 in the corticolimbic circuity and givingn new insights for future investigation of Arc/Arg3.1-mediated plasticity in the anxiety and fear-related disorders where this protein could become a potential modulatory target.

7. Materials

7.1. Chemicals, solutions, buffers and media

7.1.1. Solutions and buffers for molecular biology

Table 4. Chemically competent E.coli strains

Strain	Use
Top 10	Amplification of prAVV helper plasmids
Xl-1	Amplification of plasmid DNA
Stbl3	Amplification of prAVV target plasmids containing Inverted Terminal Repeat (ITR) sequences
SURE	Amplification and cloning of rAVV target plasmids containing Inverted Terminal Repeat (ITR) sequences

Table 5. Lysogeny broth (LB) agar plates

Reagent	Final concentration
LB-Medium (Luria/Mille; Carl Roth)	25 %
Agar, Kobe I (Carl Roth)	15 %
Ampicillin	100 µg/ml

Table 6. 2x YT medium pH 7.0 (Carl Roth)

Reagent	Final concentration
Tryptone 3.5%	16 g/l
Yeast extract 2%	10 g/l
NaCl 0.5%	5 g/l
Ampicillin	100 µg/ml

Table 7. Super Optimal Broth (SOC) medium

Reagent	Final concentration
Tryptone	2 %(w/v)
Yeast extract	0.5 %(w/v)
NaCl	10 mM
KCl	2.5 mM
$MgCl_2$	10 mM
$MgSO_4 \cdot 7H_2O$	100 mM
Glucose	20 mM

The solution was first prepared containing the first four reagents, sterilized at 121 °C, and then added sterile $MgCl_2$, MgSO4·7H2O and glucose. The pH was adjusted to 7.

Table 8. Sucrose-Triton-EDTA-Tris (STET) solution

Reagent	Final concentration
Sucrose	8 %(w/v)
Triton X-100	0.1 %(v/v)
EDTA pH 8	50 mM
Tris/HCl pH 8	50 mM

Table 9. CTAB (Cetyltrimethyl ammonium bromide) stock

Reagent	Final concentration
CTAB	5 %
NaCl	0.5 M

Table 10. DNA loading buffer 10x

Reagent	Final concentration
TrisHCl pH 7.6	10 mM
Glycin	50 %
EDTA pH 8	60 mM
Bromophenol blue	0.25 %

Table 11. This acetate – EDTA (TAE) buffer 50x

Reagent	Final concentration
Tris acetate	2 M
EDTA	0.05 M

Table 12. Enzymes used for cloning and digestions

Reagent	Concentration		Incub. Temp.	Specificity 5' – 3'	Company
Bgl I	10	U/µl	37°C	GCCNNNN^NGGC	MBI Fermentas
EcoRI	10	U/µl	37°C	G^AATTC	MBI Fermentas
KpnI	10	U/µl	37°C	GGTAC^C	MBI Fermentas
NcoI	10	U/µl	37°C	C^CATGG	New England Biolabs
SmaI	20	U/µl	25°C	CCC^GGG	Roche
XhoI	10	U/µl	37°C	C^TCGAG	Roche
SacI	10	U/µl	37°C	AGT^ACT	MBI Fermentas

Table 13. Used kits

Kit	Company	Product number
Nucleo Bond Xtra Midi EF	Macherey-Nagel	740410
PCR Clean-up und gel extraction kit	Macherey-Nagel	740609
Mini Quick Spin DNA columns	Roche	11814419001
Pierce™ BCA Protein Assay	ThermoFisher scientific	23225
Vectastain ABC Kit	Vector Labs	PK-4000
SureClean kit	Bioline	BIO-37048

Riboprobe® *in vitro* Transcription combination System (SP6/T7)	Promega	P1450
Illustra ProbeQuant G-50 Micro Columns	GE Healthcare	28-9034-08

7.1.2. Solutions and buffers for biochemistry

Table 14. Phosphate buffered saline (PBS) 10x

Reagent	Final concentration
NaCl	1.37 M
KCl	27 mM
Na_2HPO_4(*$2H_2O$)	81 mM
KH_2PO_4	14.7 mM

*No pH adjustment necessary

Table 15. Tail lysis buffer

Reagent	Final concentration
Tris pH 8.5	100 mM
EDTA pH 8	5 mM
SDS	0.2 %
NaCl	200 mM

Table 16. Tris – EDTA (TE) buffer

Reagent	Final concentration
Tris HCl pH 7.6	10 mM
EDTA pH 8	1 mM

Table 17. Triton-X lysis buffer

Reagent	Final concentration
PBS	1 x
EDTA	5 mM
EGTA	5 mM
NaF	50 mM
Na_3VO_4	1 mM
Triton-X100	1 % (v/v)
PMSF	1 mM
Aprotinin	4 µg/mL
Leupeptin	1 µg/mL

Table 18. SDS – page separating gel

Reagent	Final concentration
Acrylamid:Bisacrylamid (29:1; 30%w/v)	10 %

Tris-HCl pH 8.8	380 mM
SDS	0.1 %(w/v)
Ammonium Persulfate (APS)	0.05 %(w/v)
Tetramethylethylenediamine (TEMED)	0.05 %(w/v)

Table 19. SDS – PAGE staking gel

Reagent	Final concentration
Acrylamid:Bisacrylamid (29:1; 30%w/v)	4 %
Tris-HCl pH 6.8	125 mM
SDS	0.1 %(w/v)
APS	0.05 %(w/v)
TEMED	0.05 %(w/v)

Table 20. Protein sample buffer 5x

Reagent	Final concentration
Tris-HCl pH 6.8	250 mM
SDS	10 %(w/v)
Glycin	50 %(w/v)
Dithiothreitol (DTT)	500 mM
Bromophenol blue	0.01 ml

Table 21. Running buffer for SDS-PAGE 10x

Reagent	Final concentration
Tris-Base	250 mM
Glycin	1.92 M
SDS	1 %

Table 22. Blotting buffer

Reagent	Final concentration
Tris-Base	25 mM
Glycin	192 mM
Methanol	10 %

7.1.3. Solutions and media for cell cultures

Table 23. Basis medium

Reagent	Final concentration
FBS (PAA, Cat.# A15-104)	10 %
Pen/Strep (PAA, Cat.# P11-010)	1 %
HEPES (PAA, Cat.# S11-001)	10 mM

Table 24. Complete DMEM growth medium

Reagent	Final concentration
FBS (PAA, Cat.# A15-104)	10 %
Pen/Strep (PAA, Cat.# P11-010)	1 %
DMEM (PAA, Cat.# E15-843)	1 x

Table 25. HEPES medium

Reagent	Final concentration
FBS (PAA, Cat.# A15-104)	10 %
Pen/Strep (PAA, Cat.# P11-010)	1 %
HEPES (PAA, Cat.# S11-001)	10 mM
DMEM (PAA, Cat.# E15-843)	1 x

Table 26. PBS-MKN buffer

Reagent	Final concentration
PBS (PAA, Cat.# H15-001)	1 X
KCl	2.5 mM
$MgCl_2$	1 mM
NaCl	300 mM

Table 27. HANKS medium

Reagent	Final concentration
HANKS' balanced salt 10x (Sigma H2387-10X1L)	1 x
$NaHCO_3$	0.035 %(w/v)
HEPES	2 % (w/v)

Table 28. HANKS medium plus FCS

Reagent	Final concentration
HANKS medium	80 %(v/v)
FCS	20 %(v/v)

Table 29. Neuronal growth medium

Reagent	Final concentration
Lonza PNBM (Clonetics cc-3256)	250 ml
NDF-1 (Clonetic cc-4459HH)	4 ml
L-Glutamine (Clonetic cc-4460HH)	2 ml
GA-1000 Gentamicine sulfate (Clonetic cc-4460HH)	200 µl

7.1.4. Solutions and buffers for histology

Table 30. Paraformaldehyde 4%

Reagent	Final concentration
PBS	1 x
Paraformaldehyde (Carl Roth)	4 %

This solution was prepared at 60°C, its pH adjusted to 7.4 with NaOH supplements and filtered through 0.45 µm pore filter

Table 31. Blocking solution

Reagent	Final concentration
PBS	1 x
Horse Serum	10 %
Boverin Serum Albumin (BSA)	0.2 %
Triton 10%	0.3 %

Table 32. Carrier solution

Reagent	Final concentration
PBS	1 x
Horse Serum	1 %
Bovine Serum Albumin (BSA)	0.2 %
Triton 10%	0.3 %

Table 33. Cresyl violet solution

Reagent	Final concentration
Cresyl Violet (Sigma C-1791)	1 %(w/v)
Glacial acetic acid	1 %(v/v)

Table 34. Hydrogel monomer solution

Reagent	Final concentration
Acrylamide (v/v) (Bio-Rad)	4 %
Bisacrylamide (v/v) (Bio-Rad)	0.05 %
Photoinitiator VA0044 (Wako)	0.25 %(v/v)
10x PBS	1 x
PFA	4 %
Saponin (optional)	0.05 %

Hydrogel monomer solution was always prepared on ice and store at -20°C.

Table 35. Clearing solution (pH 8.5)

Reagent	Final concentration
Boric acid (Sigma)	200 mM
Sodium dodecyl sulfate	4 %

Table 36. Detergent rinse for ß-Gal-staining solution

Reagent	Final concentration
Na_2HPO_4-NaH_2PO_4 (pH7.3)	100 mM
MgCl2	2 mM
NP-40	0.02 %(v/v)
Sodium deoxycholate	0.01 %(w/v)

Table 37. ß-Gal-staining solution

Reagent	Final concentration
Detergent rinse for solution	1 x
$K_3[Fe(CN)_6]$	5 mM
$K_4[Fe(CN)_6]\cdot 3H_2O$	5 mM
X-Gal	1 mg/ml

Table 38. Saline sodium citrate buffer - 20x SSC in DEPC (pH 7)

Reagent	Final concentration
Detergent rinse for solution	1 x
$K_3[Fe(CN)_6]$	5 mM
Prepared in 0.1% diethylpyrocarbonate (DEPC)	

Table 39. Denhardt's Solution 50 x

Reagent	Final concentration
BSA (w/v)	1 %
Ficoll	1 %
Polyvinylpyrrolidone	1 %
DEPC water	Until 10 ml vol

Table 40. Hybridization solution

Reagent	Final concentration
SSC	4 x
Formamide	50 %
Denhardt's Solution	1 x
Dextran Sulfate (w/v)	10 %
Salmon sperm ssDNA	0.5 mg/ml
Yeast t-RNA	0.25 mg/ml

Table 41. RNAse buffer

Reagent	Final concentration
NaCl	125 mM
This-HCl	2.5 mM
RNAse A (AppliChem)	5 mg

7.1.5. Pharmacological compounds used *in vivo* and *in vitro*

Table 42. Pharmacological substances

Drug	Use	Dose	Route	Company
Ampiciline	Antibiotic for cell cultures	100 µg/ml	Added to media	Sigma
Gentamicine	Antibiotic for cell cultures	1 µg/ml	Added to media	Sigma
OH-Tamoxifen	CreERT^2 modulation in cells	0.25 µM	Added to media	Sigma
OH-Tamoxifen	CreERT^2 modulation in mice	50 mg/kg	Intraperitoneal	Sigma
Kainic acid	Seizures inducer	14.8 mg/kg	Intraperitoneal	Abcam
Carprofen	Analgesia	5 mg/kg	Subcutaneous	IDT Biologika GmbH
Isoflurane	Anesthesia	1-5 % 0.5l/min of O2	Inhalation	Abbott
Urethane	Terminal anesthesia	1.5 g/kg	Intraperitoneal	Sigma
Urethane	Anesthesia for electro-physiology	0.8 g/kg	Intraperitoneal	Sigma

7.1.6. Primers and DNA probes for *in situ* hybridization

Table 43. Primers used for genotyping

Name	Sequence	For/Rev	Genotype
TDA	AAGGGCTACTGGTGGCATGTGTGCA	For	Arc/Arg3.1$^{-/-}$, Arc/Arg3.1$^{f/f}$
TDB	CACTGCAGGGAGGGGAAACAAGCA	Rev	Arc/Arg3.1$^{-/-}$, Arc/Arg3.1$^{f/f}$
TDC	TCACCTTCAGCTCTCCGGCTGAGCT	Rev	Arc/Arg3.1$^{-/-}$, Arc/Arg3.1$^{f/f}$
FP E196	ATGCGCTGGGCTCTATGGCTTCTG	For	CaMKII-iCre
RP E198	TGCACACCTCCCTCTGCATGCACG	Rev	CaMKII-iCre

Table 44. Primers used for titering, sequencing and cloning rAAV vector plasmids

Name	Sequence	For/ Rev	Virus / Use
p-syn-forw	GCCGGCCCAGCCGGACCG-CACCACGC	For	prAAV-Syn-iCre2A-Venus/ Sequencing
p-WE-rever	CTGACAACGGGCCA-CAACTCCTCATAAAGAGACAG-CAA	Rev	prAAV-Syn-iCre2A-Venus/ Sequencing
iner-syn -Forw	CTCTGACAGATGCCAGGACA	For	prAAV-Syn-iCre2A-Venus/ Sequencing
iner-we-Rever	GGATCTTGAAGTTGGCCTTG	Rev	prAAV-Syn-iCre2A-Venus/ Sequencing
Cre SeqPrimer	CGTAACCTGGATAGTGAAA-CAGG	Fov	pAAV-CaMKIIα-Cre/ Sequencing
Cre-Rever	TTTCGTTCTGCCAATATGGA	Rev	prAAV-CaMKIIα-Cre/ Sequencing
Cre-Forw	CTGATTTCGACCAGGTTCGT	For	prAAV-CaMKIIα-Cre/ Sequencing

CreER^{T2}-Primer1-F	CATTTGGGCCAGCTAAACAT	For	pAAV-CaMKIIα-CreER^{T2}2A-Venus / Sequencing
CreER^{T2}-Primer1-R	ACGAACCTGGTCGAAATCAG	Rev	prAAV-CaMKIIα-CreER^{T2}2A-Venus / Sequencing
CreER^{T2}-Primer2-F	CGCTCATGATCAAACGCTCT	For	prAAV-CaMKIIα-CreER^{T2}2A-Venus / Sequencing
CreER^{T2}-Primer2-R	AGTAAGCCCATCATCGAAGC	Rev	prAAV-CaMKIIα-CreER^{T2}2A-Venus / Sequencing
CreER^{T2}-Primer3-F	AGCACCCTGAAGTCTCTGGA	For	prAAV-CaMKIIα-CreER^{T2}2A-Venus / Sequencing
CreER^{T2}-Primer3-R	GATGTGGGAGAGGATGAGGA	Rev	prAAV-CaMKIIα-CreER^{T2}2A-Venus / Sequencing
Kpn-CreER^{T2}	CCGTGGTACCACCATGTC-CAATTTACTG	For	pAAV-CaMKIIα-CreER^{T2}2A-Venus / Cloning
CreER^{T2}-Eco-oS	CAATGAATTCAGCTGTG-GCAGGGAAACCC	Rev	prAAV-CaMKIIα-CreER^{T2}2A-Venus / Cloning
Eco-2AP-Venus	CCGTGAATTCGAGGGCAGAG-GAAGTCTTC	For	pAAV-CaMKIIα-CreER^{T2}2A-Venus / Cloning
2AP-Venus-Eco	CAATGAATTCTTACTTGTA-CAGCTCGTCC	Rev	prAAV-CaMKIIα-CreER^{T2}2A-Venus / Cloning
EcoRI-Cre	CAGCGAATTCCACCAT-GCCCAAGAAGAAG	For	prAAV-CaMKIIα-Cre2A-Venus / Cloning
Cre-XhoI	GCCCTCGAGATCGCCATC TTC-CAGCAGGC	Rev	prAAV-CaMKIIα-Cre2A-Venus / Cloning
WE for	CTATGTTGCTCCTTTTACGCTATG	For	Titration rAAVs
WE rev	TCATAAAGAGACAGCAACCAG-GAT	Rev	Titration rAAVs

Table 45. *In situ* hybridization probe sequence

Name	Target	5'-start	3'-end	Length (NT)
pGEM Arg3.1-3'UTR	3'UTR	N 2342 CCCAGCCGA..	N 2923 ... TGGCCTTTG	582

7.2. Antibodies

Table 46. List of primary antibodies

Antigen	WB	IHC	Species	Code	Company
Arc/Arg3.1	1:30000	1:1000	Rabbit	156-003	Synaptic systems
Arc/Arg3.1	1:500000	1:150	Mouse	C7 SC-17839	Santa Cruz
GAPDH	1:00000		Mouse	MAB 374	Millipore
Arc/Arg3.1		1:1500	Rabbit	Lot 800/5904	AG Kuhl
Cre recombinase		1:2000 ICC1:1000	Mouse	MAB 3120	Millipore
Cleaved caspase-3		1:1500	Rabbit	9661	Cell Signaling
CaMKIIα		1:200	Rabbit	Ab52476	Abcam
GFP		1:2000	Chicken	Ab13970	Abcam
Iba-1		1:1000	Rabbit	19-19741	Wako

Table 47. List of secondary antibodies

Antigen	Conjugate	Host	WB	IHC/ICC	Code	Company
Chicken-IgG	Alexa 555	Goat		1:10000	A21437	Invitrogen
Guinea Pig-IgG	Alexa 488	Goat		1:10000	A11073	Invitrogen
Mouse-IgG	Biotin	Horse		1:10000	BA-2000	Vector
Mouse-IgG	HRP	Goat	1:10000		PI-2000	Vector
Mouse-IgG	Alexa 488	Goat		1:10000	A11001	Invitrogen
Mouse-IgG	Alexa 555	Goat		1:10000	A21422	Invitrogen
Rabbit-IgG	Biotin	Goat		1:10000	BA-1000	Vector
Rabbit-IgG	HRP	Goat	1:10000		PI-1000	Vector
Rabbit-IgG	Alexa 488	Goat		1:10000	A11039	Invitrogen
Rabbit-IgG	Alexa 555	Goat		1:10000	A21437	Invitrogen
Rabbit-IgG	Alexa 633	Goat		1:10000	A21103	Invitrogen

Anibodies were purchased from the following companies (in alphabetical order): Abcam (Abcam plc, Cambridge, UK); Cell Signalling Technology (Cell Signaling Technology Danvers, USA); Enzo (Enzo Life Sciences, NY, USA); Millipore (distributed by Merck Chemicals, Schwalbach, Germany); Invitrogen (distributed by Thermo Fisher Scientific, Waltham, USA); Santa Cruz (Santa Cruz Biotechnology, Heidelberg, Germany); SySy (Synapic Systems, Göttingen, Germany), Vector laboratories (California, USA); Wako (Wako Pure Chemical Industries, VA, USA).

7.3. Technical equipment

7.3.1. Equipment for DNA handling

Measurement of DNA concentration: NanoDrop2000 Spectrophotometer (Thermo Scientific Waltham, USA)
Agarose-electrophoresis chambers: PerfectBlue chamber (PeqLab, Erlangen, Germany)
PCR Thermocycler: T-Professional Trio Thermocycler (Biometra, Göttingen, Germany)
Quantitative PCR: Applied Biosystems 7900HT Fast Real-Time PCR System (Thermo Scientific, Waltham, USA)
DNA and stained protein detection: Bio-Rad UV-transilluminator Molecular Imager Gel Doc System (Biorad, Hercules, California).

7.3.2. Equipment for protein analysis

Measurement of protein concentration: SLT Rainbow Scanner (SLT Labinstruments, Salzburg,

Austria).

SDS-PAGE chamber: Minigel-Twin chamber (Biometra, Göttingen, Germany).

Western-Blotting: Trans-cell tank blot chamber (Biorad, Hercules, CA, USA).

Inmunodetection by chemioluminoscence: ImageQuant LAS4000mini detector (GE Healthcare, Little Chalfont, United Kingdom).

7.3.3. Equipment for mouse behavioral analysis, surgeries and histology

Fear conditioning system: Multi Conditioning System (TSE, Bad Homburg, Germany).

Stereotactic frame: Stereotaxic Alignment System (David Kopf instruments, Tujunga, California).

Programmable syringe pump: InjectoMate - Microinjection System (Neurostar, Tübingen, Germany).

Precision syringes for brain injections: Neurosyringe (Hamilton Bonaduz, Switzerland).

Anesthesia equipment: Harvard apparatus (Holliston, MA, USA).

Vibratome for free floating sections: VT 1200 S microtome + VibroCheck (Leica, Itzlar, Germany).

Cryostat for frozen sections: Cryostat HYRAX C60 (Carl Zeiss, Oberkochen, Germany).

7.4. Microscopes

Epifluorescence microcopy: Carl Zeiss LSM 700 Imager.M2.

Diode 488/555/639.

Software: ZEN 2012 Blue edition (Carl Zeiss, Oberkochen, Germany).

Bright field microscopy: Carl Zeiss Stemi 2000C Stereomicroscope.

Software: ZEN 2012 Blue edition (Carl Zeiss, Oberkochen, Germany).

Bright field microscopy: Olympus Bx51. Bright field. (Tokyo, Japan).

Software: Neurolucida (mbf bioscience, Williston, VT, USA).

Confocal Microscope: Olympus Fluoview 1000

Laserlinien: AR (458nm, 476nm, 488nm, 514nm); GreNE (543nm); HeNe (633nm).

Filter: AOTF (Acousto-Optical-Tunable-Filter).

Software: Olympus Fluoview.

7.5. Software

Image processing and analysis: Image J (Fiji – NIH, Bethesda, Maryland, USA); Quantity One 4.6.9 (Biorad, Hercules, CA, USA), Adobe Photoshop CS5 12.0.4, Adobe Illustrator CS5 15.0.2 (Adobe, San José, CA, USA).

DNA sequences analysis: Serial cloner 2.6.1 freeware.

Quantitative PRC results were proceed and analyzed with Applied Biosystems 7900HT Sequence Detection Systems software v2.3 (Foster City, CA, USA).

Behavioral acquisition and tracking system: EthoVision XT 6.1 (Noldus, Wageningen, The Netherlands), TSE Fear Conditioning System Software (TSE Systems, Bad Homburg, Germany).

Data analysis, statistics and figures generation: Prism 5.02 (La Jolla, CA, USA), SPSS Statistics 19 (IBM, New York, USA), SigmaPlot 12.5 (Systat Software, San José, CA, USA), MATHLAB R2015a (Mathworks, Natick, MA, USA), Adobe Illustrator 15.0.2 and Photoshop 12.0.4 (Adobe, San José, CA, USA).

Data, text and references processing: Microsoft Office Plus 2010 (Microsoft, Redmond, USA), EndNote X7.1 (Thomson Routers, New York, NY, USA), Adobe InDisign CS5 7.0.4 (Adobe, San José, CA, USA).

The database software TBase (4Dv14.3 Germany) was used for mice colony management.

8. Methods

8.1. Experimental animals

The care, handling and experimental procedures in the preparation of this thesis were performed in accordance with the German legislation (§ 8 des Tierschutzgesetzes vom 18. Mai 2006 BGBl. IS. 1207,1313), and approved by the local authorities of the city of Hamburg under the license name "Identifizierung und Charakterisierung plastizitätsspezifischer Gene im Säugetiergehirn" (supervised by PD Dr. Guido Hermey or Dr. Ora Ohana).

Mice from the strain C57Bl/6J aged 3-6 months were used for all the experiments and reproduced, and kept in groups in the ZMNH-vivarium and experimental rooms with an inverted 12:12 light/dark cycle (8:00-20:00 dark period) under standard and controlled conditions of housing (23±1°C, 40-50% humidity, food and water *ad libitum*). One week prior to behavioral (expect for social interaction/recognition tests), electrophysiological or imaging experiments the animals were housed in individual cages, and manually handled by the experimenters at least 3 times before any test to acclimate to experimental environments and experimenters.

8.1.1. Generation of the floxed Arc/Arg3.1 and conventional KO mouse lines

One of the main tools for the development of the present thesis is the conditional *LoxP*-flanked Arc/Arg3.1 line (Arc/Arg3.1$^{f/f}$). This line was previously generated by Dr. Björn Dammermann (Dammermann 1999), Dr. Anika Bick-Sander (Bick-Sander 2002) and Eric Therstappen under the supervision of Prof. Dr. Dietmar Kuhl and Dr. Michael Bösl in the ZMNH-facility for transgenic animals.

Briefly, genomic fragments of the Arc/Arg3.1 locus were isolated from λ phage genomic library prepared from 129/Sv(ev) embryonic stem (ES) cells. The targeting construct was cloned by introducing a *LoxP* site at position -1720, and a neomycin resistance cassette flanked by two *LoxP* sites was inserted at position +2690 into the second intron (Figure 49). The targeting vector was linearized at a unique NotI site and electroporated into R1 ES cells; positive clones were identified by Southern blot analysis and targeted ES cell clones were transiently transfected with Cre recombinase plasmid. Three types of recombinations were possible (Figure 49 b-c); clones with type I and II recombination were identified by southern blotting and injected separately into C57Bl/6J blastocysts to generate a conditional Arc/Arg3.1$^{f/f}$ (Dammermann 1999) or KO mouse line (Plath *et al* 2006), respectively. Male chimeras were backcrossed into C57Bl/6J, and two

congenic lines were founded by backcrossing the first generation of transgenic Arc/Arg3.1$^{f/f}$ and Arc/Arg3.1$^{-/-}$ into C57Bl/6J for more than ten generations as recommended by the Bandury conference for genetic background in mice (Banbury 1997).

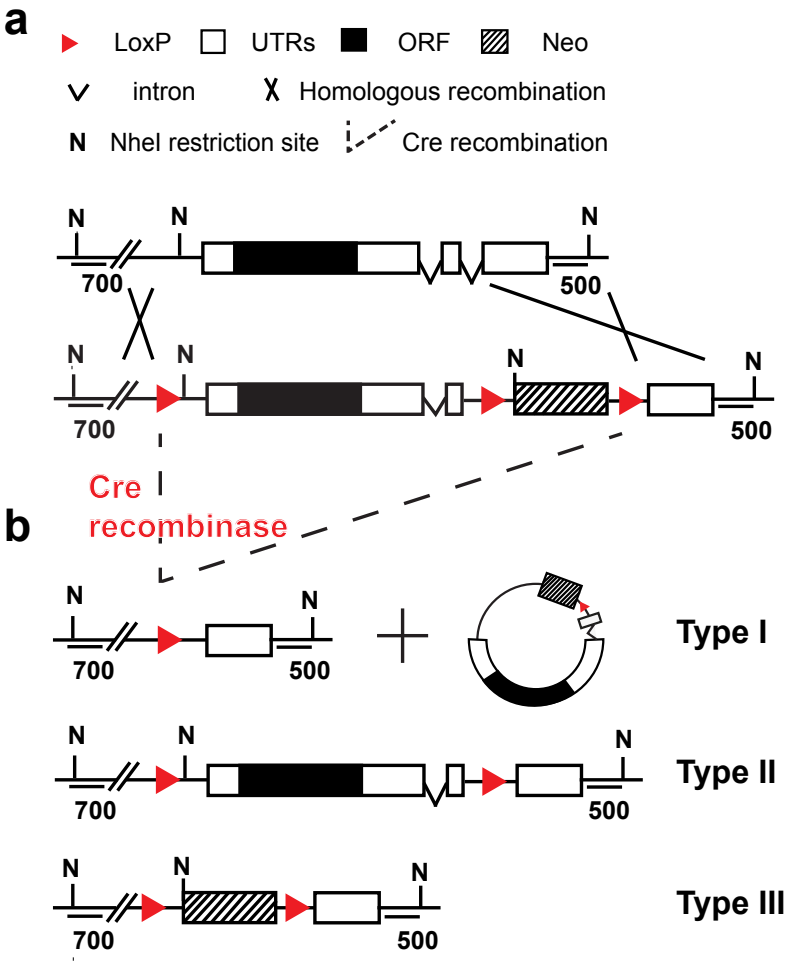

Figure 49. Gene targeting approach, and generation of conditional and knockout Arg/Arg3.1 locus
a. Homologous recombination of target vector carrying conditional *LoxP*-flanked Arc/Arg3.1 allele. **b.** Cre mediated recombination of flanked Arg/Arg3.1 locus. [Modified from (Dammermann 1999)]

Arc/Arg3.1$^{f/f}$ and Arc/Arg3.1$^{-/-}$ mutant mice can be reproduced and maintained when breeding according to Mendelian laws; both lines of mice appeared normal and reached the same age and body weight as their wild-type littermates.

The two *LoxP* sequences in Arc/Arg3.1$^{f/f}$ mice can be recognized by Cre, a 38 kDa recombinase from bacteriophage P1 that mediates excision of the flanked DNA sequence (Exon I and II) leaving only one *LoxP* site in the genome, and thereby inactivating the Arc/Arg3.1 locus (Gama Sosa *et al* 2010) (Figure 50 b). In the Arc/Arg3.1$^{f/f}$ mice, a variety of molecular biological approaches allows control of Cre expression. First, crossing Arc/Arg3.1$^{f/f}$ mice to a mouse line which expresses Cre under a specific promoter, allows for both a cell-type and developmentally dependent

ablation of Arc/Arg3.1. Secondly, delivery of the Cre transgene to the brain parenchyma through the use of viral vectors additionally allows for targeting specific anatomical regions of interest. This flexibility makes the Arc/Arg3.1$^{f/f}$ line a valuable tool for studying Arc/Arg3.1 function *in vivo*.

8.1.2. Arc/Arg3.1 early conditional knockout mice (Early cKO)

Ablation of Arc/Arg3.1 during postnatal development was achieved by crossing Arc/Arg3.1$^{f/f}$ mice with mice from a BAC-transgenic mouse line designated as Arc/Arg3.1+/+,iCre+, expressing a codon-improved Cre recombinase under the control of the full CaMKIIα promoter [Tg(CaMKIIα-cre)1Gsc] (Casanova *et al* 2001). The calcium/calmodulin-dependent protein kinase II α (CaMKIIα) is one of the subunits of the CaMKII holoenzyme and is expressed in all principal neurons (projecting neurons) of the nervous system, and is essential for their normal synaptic function (Lisman *et al* 2012). During the rodent development similar to Arc/Arg3.1 mRNA levels, CaMKII peptides can be detected in low concentrations starting at P5 and display a dramatic increased during the second and third postnatal week (Kelly & Vernon 1985). For those aforementioned reasons the use of the Tg[CaMKIIα-cre]1Gsc line appeared to be appropriate for conditionally ablating Arc/Arg3.1 during its normal upregulation during postnatal development.

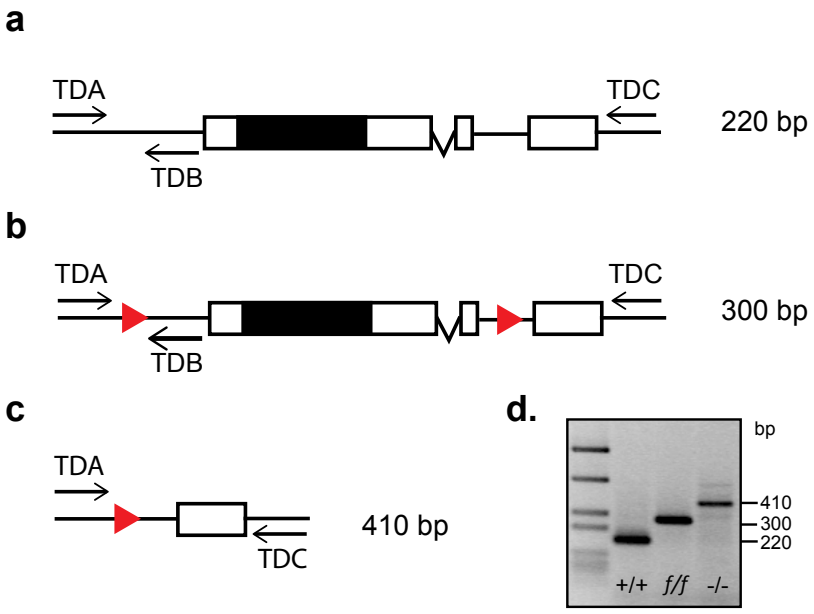

Figure 50. Schematic representation of Arc/Arg3.1 locus and genotyping strategy in used lines
a. Arc/Arg3.1$^{+/+}$(WT) **b.** Arc/Arg3.1$^{f/f}$ (LoxP flanked) and **c.** Arc/Arg3.1$^{-/-}$ (KO) loci. **d.** Representative agarose gel for genotyping PCR. Arrows depict the priming sites used to detect wild type, transgenic or KO mice in genomic DNA. [Modified from (Plath 2004)].

In generation F2, Arc/Arg3.1$^{f/+,\ iCre+}$ mice were crossed with Arc/Arg3.1$^{f/+}$, obtaining Arc/Arg3.1$^{-/-,\ iCre+}$ (heterozygous cKO mice for Cre loci), Arc/Arg3.1$^{f/+,\ iCre+}$, Arc/Arg3.1$^{f/f}$, Arc/Arg3.1$^{+/+}$ and

Arc/Arg3.1$^{+/+, iCre}$. Arc/Arg3.1$^{+/+, iCre}$ (WT-control) and Arc/Arg3.1$^{-/-, iCre}$ (Early-cKO) genotypes from generation F3 were used for all experiments. Mice were genotyped at the time of birth and re-genotyped after the end of the experimental procedures using primers listed in Table 43 and conventional Polymerase Chain Reaction (PCR) protocol (Table 48) for Arc/Arg3.1 locus (figure 50). Briefly, tail biopsies were stored at -20°C in 96 well PCR-microplates or 1.5 ml conical tubes until PCR assays. Tails were lysed by adding 50 or 100 µl of tail lysis buffer (Table 15) and 50 or 90 µg proteinase K to each well or tube respectively, incubated 3 hrs at 55°C by shaking (up to 350 rpm) or at 37°C overnight. Proteinase K was inactivated by heat at 95°C for 15 min and 150 to 800 µl of TE buffer (Table 16) was added to each well or tube respectively. 2 µl of tail lysate was used for PCR reactions.

8.1.3. ROSA26 Cre-reporter mouse line

I tested in parallel temporal and spatial pattern of the iCre activity by crossing our Arc/Arg3.1$^{f/f}$ and Arc/Arg3.1$^{-/-,iCre+}$ with an additional indicator knock-in mouse line (Gt[ROSA]26Sor^{tm1Sor}) that expresses β-galactosidase enzyme (lacZ gene) under the Rosa26 promoter upon deletion of a floxed neo expression cassette (stop sequence) (Soriano, 1999).

8.2. Molecular biology

8.2.1. Polymerase chain reaction (PCR)

A basic PCR protocol (Table 48) was used for amplifying DNA with different purposes: genotyping, re-genotyping and plasmid insertion amplification.

Table 48. Basic PCR protocol

Step	Thermoprofile	Temperature	Time (min:sec)	Cycles
1	Initial denaturation	50 °C	03:00	1x
2	Denaturation	95 °C	00:30	20-40 X
3	Primer annealing	50-70 °C	00:30	
4	Amplification	72 °C	00:30	
5	Final extension	72 °C	04:00	1x
6	Resting temperature	4°C	-	1x

The annealing temperature for each primer depends on the CG content and primer length; melting temperatures were calculated for each pair using online tools such as ThermoFisher Tm Calculator and annealing temperatures were set 2°C below the lowest melting temperature. The amplifi-

cation time was calculated for the length of each primer knowing that the amplification speed of all used polymerases is at least 1000 bp/min. Each PCR reaction was prepared according to the Table 49, as follows:

Table 49. Basic PCR reaction mix

Reagent	Volume
Forward primer (10µM)	1µl
Reverse primer (10µM)	1µl
dNTPs (10-25mM each)	1µl
10x reaction buffer (with MgCl2)	5µl
Polymerase	x µl
DNA (genomic, plasmid, viral)	x µl
H_2O	Up to 50µl

Standard amounts of plasmid DNA (0.5µl) and genomic DNA (1-2 µl) were used. DreamTag polymerase (5U/µl – ThermoFisher scientific, Waltham, USA) was used for analytic DNA, and Pwo DNA polymerase (1µl – Rapidozym) was used to amplify plasmid DNA. PCR products were separated by electrophoresis at 10V/cm in 1xTAE (table 11) agarose gels (0.5 to 2%) and visualized in a UV-transilluminator chamber (Bio-Rad, Hercules USA) after incubation in ethidium bromide solutions.

8.2.2. Quantitative PCR

Quantitative PCR was used for titrating recombinant Adeno-Associated Viral vectors (rAAVs) and performed using Applied Biosystems 7900HT Fast Real-Time PCR System. PCRs were performed in 20 µl volume using FastStart Universal SYBR Green Master (Roche, Mannheim, Germany) supplemented with 150 nM of each primer enlisted in table 44 (WE for and WE rev primers), and 2 µl of plasmid DNA diluted in series (template DNA) or viral DNA. Each sample was run in 3 replicas. The PCR profile contained an initial denaturation step of 50°C for 2 min, followed by 40 cycles of 95°C denaturation for 15s, and annealing and extension of 60°C for 1 min and 15s respectively.

As positive controls and for calculating a standard curve, a minimum of four serial dilutions of recombinant Adeno-Associated Viral vectors plasmid (prAVV) corresponding to the specific virus were prepared (containing 10^2, 10^3, 10^4 and 10^5 plasmid copies per µl) to titer. The number of copies of each plasmid was calculated using the equation for DNA mass:

$$\boldsymbol{m}_{plasmid} = \boldsymbol{n} \times \frac{1\ mole}{6.023^{23}} \times \frac{660g}{mole}$$

$$\boldsymbol{m}_{plasmid} = \boldsymbol{n} \times 1.096^{-21}\ {}^{g}/_{bp}$$

$$\boldsymbol{m}_{copies} = \frac{g\ of\ plamsid}{\boldsymbol{m}_{plasmid}}$$

Where

$\boldsymbol{m}_{plasmid} = DNA\ mass$

$\boldsymbol{n} = DNA\ size\ in\ bp\ (base\ pairs)$

$\boldsymbol{m}_{copies} = Plasmid\ copies$

Standard curves were generated by plotting the threshold cycle values (Ct) against the log plasmid concentration. The R-squared value of this curve was required to be higher than 0.9. Ct values of viral DNA were then calculated from the linear regression equation. Data was acquired and analyzed with Applied Biosystems 7900HT Sequence Detection Systems software v2.3 (Figure 51b-c).

8.2.3. Transformation of competent bacteria with DNA

DNA can be introduced into cells by transformation in order to store or replicate plasmids. Depending on the purpose, different strains of competent bacteria were used (Table 4). Briefly, 50 µl of specific bacteria strain were thawed on ice and gently mixed with at least 10 ng of desired plasmid DNA. After 30 min of incubation on ice, the bacteria were heat-shocked at 37°C for 3 min and then recovered by adding 250 µl of preheated SOC media (Table 7) and 30 min of incubation at 37°C with gentle shaking (250rpm). The mixture was plated on LB-agar plates (Table 5) containing the appropriate antibiotic for storing or ligation confirmation, or inoculated in 500 ml of 2x YT medium (table 6) for amplification at 37°C overnight.

8.2.4. Plasmid DNA purification

8.2.4.1. Small-scale preparation of plasmid DNA (Mini-preparation)

Single bacterial colonies from LB plates were selected using pipette tips. Each of them was inoculated to 2ml of 2x YT medium containing the appropriate antibiotic and incubated at 37°C overnight. Approximately 1.5 ml of the grown bacteria were centrifuged at 4000 rpm for 5 min, the sediment was mixed by shaking (250rpm) with 200 µl STET solution (Table 8) and 15 µl lysozyme (10mg/ml in 10mM TrisCl pH 8 - Sigma, St. Louis, USA) for 5 min, heated at 95°C for 2 min and centrifuged at 13000 rpm for 5 min. The pellet was removed with a sterile toothpick and 10 µl of CTAB solution (table 9) was added to the supernatant, mixed gently and centrifuged

at 13000 rpm for 5 min. The supernatant was discarded and the sediment dissolved with 300 µl of 1.2 M NaCl and 750 µl of 100% ethanol. The plasmid DNA was precipitated at 13000 rpm for 15 min and the resulting pellet washed with 100% ethanol. The pellet was dried by vacuum and dissolved in 30 µl H_2O.

8.2.4.2. Preparation of plasmid DNA by alkaline lysis with SDS (Midi-preparation)

Macherey – Nagel endotoxin free (EF) kits (Table 13, MN, Düren, Germany) for large-scale plasmid DNA purification were used. All buffers were provided by the manufacturer. Bacteria were grown in 500 ml of 2x YT medium containing the appropriated antibiotic at 37°C overnight and pelleted by centrifugation at 5000 rpm at 4°C for 15 min. 16 ml of buffer RES-EF was added to bacteria cell pellet and lysed by sodium hydroxide/SDC treatment with 16 ml of buffer LYS-EF, after inverting the tubes 3 times 16 ml of NEU-EF buffer was added; their content was poured into NucleoBond Xtra Midi EF filter columns, which were previously neutralized with 15 ml of EQU-EF buffer. The filter columns were then washed 3 times using 5 ml of FIL-EF buffer, 35 ml of ENDO-EF buffer and 15 ml of WASH-EF buffer, respectively. The DNA was eluted from the column to 15 mL conical tube by adding 5 ml of ELU-EF buffer, and next precipitated with 3.5 ml isopropanol by centrifugation at 5000 rpm for 60 min; the pellet was dried and transferred to 1.5 mL conical tubes in 400 µl of TE-EF buffer. 40 µl of 3M of Sodium acetate pH 5.2 (CH_3COONa – EF) and 800 µl of 100% ethanol-EF were added and the mixture was centrifuged at 13000 rpm for 15 min. The supernatant was carefully discarded and the pellet was washed with 400 µl of 70% ethanol-EF. The DNA was air dried and dissolved in H2O – EF. DNA concentration was measured using the NanoDrop2000 Spectrophotometer (ThermoFisher scientific, Waltham, USA).

8.2.5. Digestion, extraction and ligation

The digestion of plasmid DNA and PCR products was performed using conditions and buffers recommended by the manufacturer of the respective endonuclease enzyme (Table 12, MBI Fermentas, New England Biolabs, and Roche). If possible, 1µl of DNA was digested by 1U of the enzyme in a reaction volume of 20 µl with the indicated buffer, and incubated for 20 min for FastDigestTM-enzymes and for 2 hours for regular enzymes at the recommended temperatures (Table 12).

The digested DNA was analyzed by electrophoresis on agarose gels (0.5-2% w/v) and the DNA fragment of interest excised out by using a clean blade, and collected in a 2ml conical tube. The DNA was extracted from the agarose using NucleoSpin Gel and PCR Clean-up kit (Table 13, MN,

Düren, Germany) according to manufacturer instructions. 200 µl of Buffer NTI was used to melt each 100 mg of the gel by incubating the mixture gel/buffer at 50°C for 10 min, vortexing it briefly every 2-3 min until it was completely dissolved. The dissolution was poured onto a NucleoSpin column placed in a 2 ml collection tube, centrifuged for 60 s at 11000 rpm. The flow-through was discarded and the column place back to the collection tube. The column was washed with 700 µl of buffer NT3 by centrifugation at 11000 rpm for 1 min. The DNA was eluted from the column in a 1.5 ml conical tube by adding 15 – 30 µl of buffer NE and centrifugation at 11000 rpm for 60 s.

For ligation, a minimum of 20 ng of vector DNA was incubated with 150-600 ng of insert DNA, 1U of T4 DNA ligase (ThermoFisher scientific, Waltham, USA), 2 µl of ligation buffer and H2O in a final volume of 20 µl at room temperature for 2 h or at 4°C overnight.

8.2.6. Cloning of the Cre recombinase gene into rAVV plasmids

8.2.6.1. Cloning of the Cre gene under the control of CaMKIIα promoter

To achieve Arc/Arg3.1 ablation exclusively in principal neurons, prAAV-CaMKIIα–eGFP [gift from Pavel Osten (Dittgen *et al* 2004), Addgene plasmid # 27227] was modified by Steffen Schuster (former diploma student in the IMCC, ZMNH) and eGFP was replaced by the Cre recombinase (Schuster 2009). Briefly, the Cre recombinase was excised from pPGKcrebpA vector (Gu 2013) using XhoI and ligated into the XhoI-linearized pEGFP-C1 vector (Clontech laboratories, Saint-Germain-en-Laye, France). pEGFP-C1 was excised by SacI to remove the redundant sequence of Cre, the products of this restriction reaction were separated by electrophoresis. The DNA fragment containing Cre transgene was purified from the gel and re-ligated into the pEGFP-C1 vector. Cre was excised from this vector by BgI I and EcoRI double restriction enzyme reaction, separated by electrophoresis and purified from the agarose gel. eGFP was excised from the vector prAAV-CaMKIIα–eGFP by BgII and EcoRI, and the prAAV-CaMKIIα product ligated with Cre. The plasmid was sequenced after cloning and its expression was tested in N2A cells before viral production.

8.2.6.2. Cloning of the Cre gene under Synapsin 1 promoter

A plasmid carrying the codon-improved Cre recombinase (iCre) (Shimshek *et al* 2002) under the control of the the human synapsin I promoter (prAAV-hSyp1-iCre2AP-Venus) was a gift from Prof. Dr. Rolf Sprengel (Max Planck Institute for Medical Research, Heidelberg) (Tang *et al* 2009). Prokaryotic Cre gene was obtained by PCR amplification from the prAAV-CaMKIIα-Cre vector using

primers EcoRI-Cre (Forward): CAG CGA ATT CCA CCA TGC CCA AGA AGA AG, Cre-XhoI (Reverse): GCC CTC GAG ATC GCC ATC TTC CAG CAG GC], and the product was inserted by 5'-EcoRI and 3'-XhoI restriction and ligation into prAAV-Syp1-iCre2AP-Venus in the place of iCre.

8.2.6.3. Cloning of an inducible ligand-dependent chimeric Cre recombinase

With the assistance of Dr. Daniel Mensching, I cloned and characterized a novel prAAV vector (rAAV-CaMKIIα-CreER^{T2}2AP-Venus) where a fragment of the CaMKIIα (1.3 kb) promoter drives the co-expression of equimolar quantities of CreER^{T2} and Venus fluorescent protein by implementing 2A peptide sequence in the same ORF (de Felipe *et al* 2006) (Figure 33b). Briefly, the CreERT^2 transgene was amplified from pCAG-CreER^{T2} vector [gift from Connie Cepko (Matsuda & Cepko 2007), Addgene plasmid #14797] by PCR using the primers Kpn-CreER^{T2} (Forward): CCG TGG TAC CAC CAT GTC CAA TTT ACT G, CreER^{T2}-Eco-oS (Reverse): CAA TGA ATT CAG CTG TGG CAG GGA AAC CC and the product was inserted by 5'-KpnI and 3'-EcoRI restriction and ligation into pAAV-CaMKIIα(1.3)-EGFP [gift from Pavel Osten , (Dittgen *et al* 2004) Addgene plasmid # 27227)] in the place of EGFP. 2A peptide-Venus was amplified from prAAV-Syn-iCre2A-Venus vector (Tang *et al* 2009) using the primers: Eco-2AP-Venus (Forward) CCG TGA ATT CGA GGG CAG AGG AAG TCT TC and 2AP-Venus-Eco (Reverse) CAA TGA ATT CTT ACT TGT ACA GCT CGT CC; and inserted by 5'-blunt and 3'-EcoRI restriction and ligation into pAAV-CaMKIIα(1.3)-CreER^{T2}. The plasmid was sequenced after cloning.

8.2.7. DNA sequencing

To verify if sequences of the amplified DNA and cloned plasmids were correct, DNA was analyzed by Sanger sequencing (Sanger 1981). This procedure was performed in the Bioanalytics service group by PD Dr. Sabine Hoffmeister-Ullerich at the ZMNH-UKE. Sequence verification and alignments was accomplished using the freeware software Serial cloner 2.6.1.

8.3. Biochemistry

8.3.1. SDS-PAGE (Sodium dodecyl sulfate polyacrylamide gel electrophoresis)

Proteins of viral products or brain lysates were analyzed according to their molecular light by one-dimensional electrophoretic separation in sodium dodecyl sulfate-polyacrylamide gels (SDS-

PAGE) using vertical two-step gel system (Minigel-Twin Biometra GmbH, Göttingen, Germany). 10% separating SDS-PAGEs (Table 18) were first prepared and polymerized during 30 min. Subsequently, a stacking gel (Table 19) was poured onto the gel system and a plastic comb inserted until polymerization gel was complete. The gels were loaded with denaturalized protein samples in protein sample buffer (Table 20) and run in running buffer (Table 21) at 80 V until the sample front passed the stacking gel, after which the voltage was increased to 150V, and the proteins separated for approximately 1.5 h.

8.3.2. SYPRO ruby luminescent gel staining

After SDS-PAGE, proteins from brain lysates were analyzed by immunoblotting (8.3.3). In case of viral proteins analysis after rAAV purification, SYPRO ruby luminescent gel staining (Lonza, Rockland, USA) was used according to manufacturer instructions. Briefly, gels were fixed by incubation in 100 ml solution of 50% methanol / 7% acetic acid for 60 min at room temperature. After fixation and brief wash with H_2O, the gel was stained with 25 ml of SYPRO ruby for 1 hour at room temperature and constant shaking, then washed with 100 ml of 10% methanol / 7% acetic acid during 30 min at room temperature and photographed in a UV-transilluminator chamber (Bio-Rad, Hercules, USA) (Figure 51d).

8.3.3. Western blotting

Brain tissues were homogenized with Triton-X lysis buffer (Table 17). Protein concentrations were assessed using Pierce™ BCA Protein Assay Kit following manufacturer's instructions (ThermoFisher scientific, Waltham, USA). Equal amounts of protein were separated on 10% SDS-PAGE and transferred to Polyvinylidene fluoride (PVDF) membranes (Merck Millipore, Darmstadt, Germany) for 2 h at 4°C with 110V using Mini-PROTEAN TransBlot system (Bio-Rad, Hercules, USA) and blotting buffer (Table 22).

Membranes were blocked with 5% non-fat milk in PBS with 0.01% Tween-20 for 1 h at room temperature and incubated overnight with a polyclonal anti-Arc/Arg3.1 antibody (1:300000, Synaptic Systems, Göttingen, Germany), or monoclonal anti-GAPDH antibody (1:500000, Merck Millipore, Darmstadt, Germany) at 4°C. After secondary antibody incubation (Table 47), bands were visualized using Super Signal chemiluminescence reagent (ThermoFisher scientific, Waltham, USA) and the signals were detected by ImageQuant LAS 4000 (Fujifilm, GE Healthcare Europe, Freiburg, Germany). Densitometry analysis was done with ImageJ – NIH freeware (Washington DC, USA).

8.4. Cell cultures and rAAV vectors production

8.4.1. AAV-293 cell cultures

AAV-293 cell line (Stratagene, Agilent Technologies, Santa Clara, CA, USA) was used to produce rAAV viral vectors. AAV-293 cells are derived from HEK293 cell line and produces the adenovirus E1 gene *in trans* (Graham *et al* 1977), allowing the packaging of rAAV viral particles upon co-transfection of three plasmids: an iInverted terminal repeats (ITR) transgene cassette plasmid (target plasmid), prAAV helper plasmid (pDP1) and E1-deleted prHelper plasmid (pDG) (Grieger *et al* 2006). The cells were cultured in a gas incubator under 5% CO_2 and 95% humidity at 37°C, and always manipulated under a laminar flow hood under sterile and EF conditions. For the establishment of AAV-293 cell cultures, 10 ml of complete DMEM growth medium (Table 24, PAA, Pasching, Austria) was added to the thald cell suspension in a 15 ml conical tube and centrifuged at 200 g0 for 3 min at room temperature. The pellet was re-suspended in 5 ml of fresh medium and transferred to a 75 cm^2 culture flask containing 10 ml of fresh medium. Cell growth and confluency were monitored daily. Once the confluency reached 50%, the growth medium was removed and the cells were washed with 10 ml of PBS. Subsequently, 5 ml of pre-warmed trypsin-EDTA solution (PAA, Pasching, Austria) was added for 3 min to release adherent cells and inactivated by adding 5 ml of growth medium. 2 ml of the cell suspension were transferred to 175 cm^2 tissue culture flasks containing 28 ml of pre-warmed fresh growth medium. The fresh suspension was transferred to cell culture incubator and monitored daily to maintain a confluency of 50%.

8.4.2. rAAV vectors production

AAV-293 cells were transferred from 5 culture flasks of 175 cm^2 into 20 cell culture dishes of 14.5 cm diameter, as described later. The cultures were co-transfected with three different plasmids (prAAV target plasmid, pDP1 and pDG) using polyethylenimine (PEI 1mg/ml, Polyscience, Warrington, USA) and OptiMen I (Thermo-Invitrogen, Waltham, USA). A plasmid mixture containing 500 µg of plasmid with a ratio of 1:2.5 (pAAV:pDP-pDG), 30 ml of Optimen and 2.4 ml of polyethylenimine (PEI) was prepared and incubated for 15 min at room temperature. 1.6 ml of the mixture was added to each dish of cells and incubated in the cell culture incubator for 6 h, 30 ml of fresh medium was added to each dish afterward.

The cells were harvested 48 to 72 h after transfection depending on cell viability and morphology. The medium was removed and collected for further purification, and 2.5 ml of PBS was added to

each dish. The cell suspension from 10 dishes was removed using a cell scraper and pulled in a 50 ml conic tube. The cells were precipitated by 5 min centrifugation at 650 g_0, the supernatant was discarded and the pellet re-suspended in 7.5 ml of 50 mM Tris / 150 mM NaCl Buffer (pH=8). 61.2 µl benzonase (Novagen, Merck Millipore, Darmstadt, Germany) and 382 µl of 10 % Sodium-Deoxycholate were added to the cell suspension and incubated for 30 min at 37°C in a water bath. 390 mg of NaCl was added and dissolved at 56°C for 30 min. The cell suspension was then frozen at -80°C overnight, and stored until purification.

8.4.3. rAAV isolation and concentration of viral particles

The cell suspension was thaw in a water bath at 37°C and centrifuged at 6800 g_0 and 4°C for 30 min. The supernatant was filtered using 0.8 µm filter units (Merck Millipore, Darmstadt, Germany). The filtered supernatant was then purified by iodixanol gradients or affinity chromatography with AVB Sepharose High Performance (GE Healthcare Bio-Sciences AB, Brussels, Belgium) (Figure 51).

8.4.3.1. Iodixanol gradient purification of rAAV

Discontinuous iodixanol (OptiPrep™ Density Gradient Medium, Sigma-Aldrich, St-Lois, USA) gradients were manually prepared using a 10 ml syringe with a 20-gauge needle. 3 ml of 54% iodixanol, 3 ml of 40% iodixanol, 4 ml of 25% iodixanol and 7 ml of 15 % iodixanol 1M NaCl were dripped into a Beckman Quick-Seal 16x76 mm ultracentrifuge tubes (Beckman Coulter, Miami, FL, USA). 7 ml of filtered supernatant of the cell suspension was carefully served into iodixanol gradient and ultracentrifuged at 60000 rpm for 2 h at 12°C. After ultracentrifugation 4 ml of the 40% phase were removed using a 5 ml syringe with a 20-gauge needle and mixed with 15 ml PBS-MKN buffer (table 26). The mixture was filtered using 4 centrifugation cycles of 5000 g_0 at 4°C during 5 min in wet Amicon Ultra 15 ml centrifugal filter (Merck Millipore, Darmstadt, Germany) for concentrating the virus in a final volume of 150 µl of PBS-MKN. The final product was finally filtered through a 0.22 µm Millex-GV filter (Merck Millipore, Darmstadt, Germany) using a 3 ml syringe. The virus was aliquoted and used only for *in vitro* experiments.

8.4.3.2. Affinity chromatography purification of rAAV

For all experiments *in vivo*, rAAV vectors Were produced by the aforementioned procedures in sections 8.4.1 and 8.4.2, and the media and cell suspension purified using affinity chromatography with AVB Sepharose High Performance (Hellstrom *et al* 2009) (GE Healthcare Bio-Sciences

AB, Brussels, Belgium) in the vector facility at UKE - HEXT Core facilities by Dr. Ingke Braren. After column purification, the virus in the eluate was precipitated with 10% PEG-8000 (Polyethylenglycol-8000) and 1 M NaCl, by incubation for 3 h at 4°C and two centrifugation cycles at 5000 g_0 for 2 min at 4°C, and re-suspended and stored in PBS – EF at 4°C. After purification, titration of genome copies is achieved by quantative PCR (Section 8.2.2; Figure 51 b-c) and high purity is confirmed by identification of capside proteins (VP1, VP2 and VP3) in an SDS-gel stained with SYPRO ruby luminescent stain (section 8.3.2; Figure 51d)

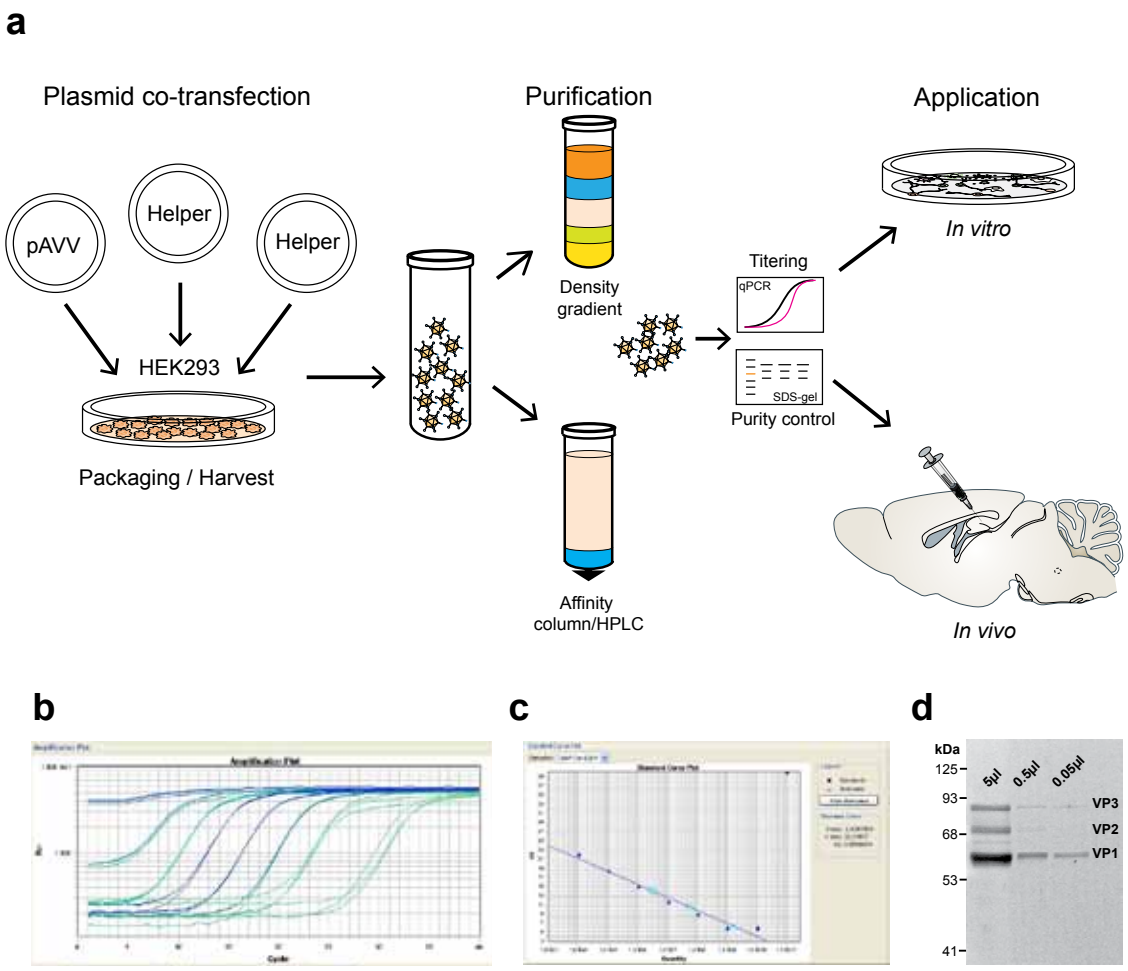

Figure 51. rAAV viral vectors production, titration and quality control.
a. Schematic representation of rAVV production and applications. **b.** Examples of quantitative pPCR amplification plots by rAAV titration. **c.** rpAAV standard curve for determination of viral genome copies. **d.** SDS-gel stained with SYPRO ruby luminescent stain showing high purity denaturalized rAAV particles in three different concentrations.

8.4.4. Neuro-2a cell cultures

Neuro-2a (N2A) cell line was derived from a spontaneous neuroblastoma tumor of an albino murine strain and established as a cell line by R.J. Klebe and F.H. Ruddle in 1969 (Olmsted *et al* 1970). This cell line was passaged and handle as described for AAV-293 cells but always in small

culture flasks (25cm^2).

8.4.5. Transfection of N2A cell cultures

N2A cells were used to test prAAV constructs and transfected with Lipofectamin 2000 (Thermo-Fisher scientific, Waltham, USA). Cells were seeded 24 h before transfection in multi-well plates (150000 cells/well) containing small glass coverslips (12 mm diameter). 250 µl of pre-warmed OptiMEM (Thermo-Invitrogen, Waltham, USA) was mixed with 4 µl of plasmid DNA, separately 10 µl of Lipofectamin 2000 was slowly pipetted into 250 µl OptiMEM and incubated for 5 min at room temperature. The latter was added and mixed slowly into the DNA mix and incubated for 20 min at room temperature. 100 µl of transfection mixture was slowly dripped onto each well, and the transfection efficiency and cell viability checked 24 h later.

8.4.6. Cortical primary neuron cultures

Primary cortical or hippocampal neurons were cultivated from wild-type C57Bl/67 mice. Pregnant mice were euthanized under isoflurane anesthesia and decapitated at 16-17.5 days after breeding with wild-type males; embryos were removed from the uterus horns and sacrificed by decapitation. Brains were removed and hippocampi or cortices were micro- dissected under microscopy visualization on ice and HANKS' medium supplemented with 20% FCS (Table 28), and collected into conical tubes containing the same solution. The collected tissue was washed twice with HANKS' medium with sedimentation by gravity flow, 2 ml of digestion buffer with 2 mg of papain and 1 mg of DNAase (3KU in 0.15M NaCl) was added and incubated for 30 min at 37°C and 5% CO^2. After incubation, the digested tissue was washed twice with HANKS' medium and resuspended in 2ml of dissociation buffer with DNAse. By using a Pasteur pipette the cells were dissociated by pipetting 20 to 40 times, after which the suspension was centrifuged at 100 g_0 for 10 min. The pellet was re-suspended in neuronal growth medium (Table 29) and the cells seeded on poly-L-lysine coated glass coverslips with a density of 120000 cells/cm^2 on 6 cm plastic dishes. The cultures were grown until days *in vitro* (DIV) 15 for rAAV vectors infection.

8.4.7. Immunocytochemistry

After having obtained transfected or infected cells, the glass coverslips were transferred to 24 well plates, washed twice with 1xPBS and fixed with 4% paraformaldehyde (PFA - Table 30) for 15 min. The PFA was removed and the cells washed twice with 1x PBS and permeabilized by incubation with PBS / 0.05% saponin (PBS-S) for 30 min at 4°C. Each cover slip was placed

"cell side down" on a previously served drop of 50 µl of primary antibody (in PBS-S) on Parafilm (Bemis NA, Neenah, USA) and incubated in a humidified chamber for 2 h at 4°C. The coverslips were transferred back to the multi-well plate and washed with PBS-S three times. Each coverslip was incubated with a secondary antibody using the same procedure as with the primary antibody, and incubated for 1 hour at room temperature. After secondary antibody incubation, the cells were washed three times with PBS-S and twice with H_2O. Each coverslip was mounted cell side down on a drop of mounting medium (80% Immu-Mount mixed with 20% ProlongGold antifade with 4′,6-Diamidin-2-phenylindol (DAPI), ThermoFisher scientific, Waltham, USA) served in glass microscope slides. The slides were stored in the dark at 4°C until microscopic examination.

8.5. Histology of brain tissue

8.5.1. Intracardiac perfusion and fixation of mouse brains

Mice were anesthetized with a single intraperitoneal injection of Urethane (Sigma, St. Louis, USA) at dose of 1.5g/Kg body light (b.w.) using a 27-gauge needle and a 1 ml syringe. Anesthetic depth was always confirmed by observing the lack of pad withdraw reflex after interdigital stimulation. The mouse was fixed in supine position to an operation table and a horizontal laparotomy was performed at the inferior level of the diaphragm using blunt scissors. For exposing the pleural cavity the diaphragm was incised followed by lateral thoracotomies along both lateral sides of the thoracic cage, with the frontal part of the rib cage lifted and folded over the head and the posteroinferior tip of the sternum fixed to the table with a needle, the heart and major vessels were then exposed. A 15-gauge blunt perfusion needle was passed through the apex of the left ventricle and advanced until the aortic arch; the needle was fixed using a hemostat clamp and was plugged to pre-ensembled peristaltic pump (Perimax, Spectec, Erding, Germany) with a pre-filled tube with cold 1xPBS. The right atrium was opened by a small incision and perfused at 70 rpm first with 20 ml of 1xPBS for clearing the blood and subsequently, once the liver was observed to have turned pale with a ~25 ml 4% PFA solution. Then, the mouse was decapitated and the brain dissected out using student vannas spring scissors, standard forceps and spatula (Fine Science Tools, Heidelberg, Germany). The brains were collected in snap-cap glass bottles (Carl Roth, Kalksruhe, Germany) containing 5 ml of 4% PFA.

8.5.2. Nissl staining

Coronal brain slices, 40 µm thick, were made using a vibratome (VT1000S, Leica, Itzlar, Ger-

many). The slices were mounted on glass microscope slides (Thermo scientific, Waltham, USA) and dried overnight. The tissue was first de-fatted overnight with mixture 1:1 mixture 100% of ethanol/chloroform. On the next day, the tissue was rehydrated by soaking the slides in 100% ethanol follow by 95% (v/v) ethanol solution, and then incubated in 0.1% (w/v) cresyl violet solution (Table 33) for 5 minutes, rinsed with distilled H2O and incubated in 95% (v/v) ethanol solution for maximum 30 min, checking the staining intensity every 5 min. After having obtained the desired stain intensity, the slides were dehydrated by incubation twice in 100% ethanol and twice in xylene. The slices were dried and covered with microscopy mounting medium (Entellan – Merck Millipore, Darmstadt, Germany).

8.5.3. Immunostaining of free floating sections

Coronal brain slices (40 µm) were transferred to multiwell plates and incubated with 0.3% (v/v) H_2O_2 solution for 30 min (in case of 3,3'-Diaminobenzidine – DAB – staining), subsequently washed three times with 1xPBS and then incubated at room temperature in the blocking solution (Table 31) for 1 h and overnight at 4°C with primary antibody (Table 46) prepared in carrier solution (Table 32). Next day, the slices were washed three times with 1xPBS and incubated with secondary antibodies (table 46) for 2 h at room temperature. After secondary antibody incubation, the slices were washed three times with 1xPBS and mounted with mounting medium (80% Immu-Mount mixed with 20% ProlongGold antifade with DAPI, ThermoFisher scientific, Waltham, USA). In case of DAB staining, after having washed the secondary antibody, immunoreactivities were detected using a Vectastain ABC Kit (Vector Labs, Burlingame, USA). Slices were then incubated in an AB solution and the signals visualized by application of DAB as a chromogenic (Sigma-Aldrich, Sigma, St. Louis, USA) and prepared in the buffer provided by the manufacturer. The DAB reaction was stopped by three consecutive washes of 1xPBS. The slices were dried and covered with microscopy mounting medium (Entellan – Merck Millipore, Darmstadt, Germany).

8.5.4. CLARITY of thick brain slices

CLARITY procedure was adapted and modified after Chung *et al* (Chung *et al* 2013). Intracardiac perfusion of the mouse brain was performed with 20 ml cold 1xPBS and 20 ml freshly thawed hydrogel monomer solution (Table 34) with a slow speed (10ml/min) as described previously in section 8.5.1. After dissecting the brain out of the skull, it was transferred to a 50 ml plastic tube containing 20 ml of hydrogel monomer solution on ice and incubated for 2 to 3 days at 4°C. Subsequently, with two adjacent 17-gauge needles inserted through the lid, the tube was degassed by applying N_2 from a plastic tubing system to one of these needles, allowing the air in the tube

to exit through the other. After 30 min of de-gassing, the nitrogen flow was discontinued, both needle holes were rapidly covered with modeling clay and the lid was tightly covered with Parafilm (Bemis NA, Neenah, USA). The tube was incubated for approximately 3 h at 37°C until the solution was polymerized. The embedded sample was extracted manually from the gel and incubated twice in clearing solution (Table 35) for 24 h at 37° by rotation. After 48 h of dialyzing out residues of the hydrogel monomer solution, the brain was sliced in 3 mm slices. The slices were passively clarified by incubation with clearing solution by rotation during a week at 37° and replacing the solution every 3 days. After having obtained expected clarification, the tissue was incubated 3 days in Focus Clear (CelExplorer Labs, Burlington, USA) until complete transparency was achieved. The thick section was then transferred to a glass slide and surrounded by a putty ring, embedded in Focus Clear (CelExplorer Labs, Burlington, USA) and covered with a glass coverslip. The section was kept at room temperature and protected from light until confocal imaging.

8.5.5. ß-galactosidase staining

To examine Cre-mediated recombination in the brain, Tg(CaMKIIα-Cre)1Gsc mice were crossed with ROSA26-lacZ reporter mice (Soriano 1999) and Arc/Arg3.1$^{f/f}$ mice. Brains obtained from their offspring were processed for X-gal staining. Briefly, brains were rapidly removed and quick-frozen on a metallic surface surrounded by liquid nitrogen and kept at -80°C until further processing. Sagittal brain sections (14 µm) were prepared using cryostat (cryostat HYRAX C60 - Carl Zeiss, Oberkochen, Germay) and mounted on glass slides (Superfrost plus, Thermo-Scientific, Waltham, USA). Slides were air dried and stored at -80°C until use. Sections were fixed with 0.2% glutaraldehyde, washed twice with detergent rinse solution (Table 36) for 10 min, and stained by incubation in X-gal staining solution (Table 36 and 37) at 37°C for 19 h protected from light. Next day, the sections were fixed with 4% PFA for 10 min and washed 5 min in distillated H_2O. The section were subsequently dehydrated by incubation of 3 min each in ascending concentration of ethanol (60, 80, and 96%), air-dried and covered with coverslip and Entellan (Merck Millipore, Darmstadt, Germany).

8.5.6. Radioactive *in situ* hybridization

A fragment corresponding to nucleotides 2342-2923 of the Arc/Arg3.1 3'untranslated region (UTR) sequence (Table 45) was used as a probe and specificity of signals was verified by comparing the antisense probe with the sense control. The cDNA sequence was previously inserted into the pGEM-T-Easy® vector (Promega, Madison, USA), linearized using NcoI (New England Biolabs, Frankfurt am Main, Germany) and purified with the SureClean kit (Bioline, Luckenwalde,

Germany) following manufacturer's guidelines.

Radiolabeling of RNA probes was achieved by *in vitro* transcription of 1 µl of linearized plasmid using Riboprobe® *in vitro* Transcription Combination System (Promega, Madison, USA) according to the instruction of the manufacturer. Briefly, 2 µl of 10x transcription buffer, 2 µl of 100 mM DTT, 1 µl of 10 mM ATP, 1 µl of 10 mM CTP, 1 µl of 10 mM GTP (Promega, Madison, USA), 1 µl of RNasin® Ribonuclease Inhibitors (Promega, Madison, USA), 1 µl of T7 (Promega, Madison, USA) or SP6 polymerase (Roche, Basel, Switzerland), and 8 µl of 80 µCi [α35S]-UTP (Hartmann Analytic, Braunschlig, Germany) were incubated for 2 hours at 37°C. After transcription, the product reaction was incubated in 1 µl of DNAse (Promega, Madison, USA) for 20 min at 37°C to remove DNA template. Transcribed probes were then purified using Illustra ProbeQuant G-50 Micro Columns (GE Healthcare), and the probe was diluted in 10 µl 1M DTT, added to 100 µl of hybridization mixture, to a final concentration of 8000 cpm/µl (measured with a scintillation counter).

Sagittal or coronal brain cryosections (14µm) mounted on glass slides (Superfrost plus, Thermo, Waltham, USA) were fixed in 4% PFA for 15 min at RT, washed three times with 1xPBS/1%DEPC, and equilibrated with 0.1 M Triethanolamine (pH 8) for 3 min following acetylation by 10 min incubation of 0.1 M Triethanolamine (pH 8) with recently added 350µl acetic anhydride at RT. The sections were dehydrated by incubation of 3 min each in ascending concentrations of ethanol (30, 50, 80, 95 and 100%) and air-dried. 110 µl of hybridization mixture with the labeled probe were poured on each slide, then covered and fixed with glass coverslips and DPX mounting medium (Sigma, St. Louis, USA), respectively. Sections were incubated for 30 min at RT and 55°C overnight afterward.

On the next day, sections were allowed to cool to RT for 10 min, after which the DPX was removed and the slides were washed with 4x SSC (Table 38) for 20 min at RT, coverslips were removed and washed twice for 10 min in 4x SSC, followed by incubation in RNAse buffer (RNAse A) at 37°C for 30 min. Later, a high stringency wash was performed for 15 minutes in 2x SSC, 15 minutes in 1x SSC, 15 minutes in 0.5x SSC, 30 minutes in 0.1x SSC at 55 °C and 10 min in 0.1x SSC at room temperature. Sections were dehydrated for 5 min in 50% and 95% ethanol. After being dried at room temperature, slides were exposed to autoradiography films for 44 days (Ektascan B/RA Films, Kodak, Rochester, USA) and developed using standard techniques. For quantification of Arc/Arg3.1 mRNA, an additional series of hybridized slides together with an autoradiographic 14C microscale (GE Healthcare, Europe, Freiburg, Germany) were exposed to Storage Phosphor Screen BAS-IP films during 5 days (BAS-IP MS 2025, Fujifilm, Tokyo, Ja-

pan) and scanned with Multi-purpose Image Scanner FLA-900 (Fujifilm, Tokyo, Japan). 16-bit digitalized images were subjected to densitometry analysis of regions of interest (ROI) using ImageJ - NIH freeware (Bethesda, Maryland, USA). Measured mean gray levels were converted into approximated nanocuries per gram (nCi/g) of tissue (Miller 1991). Measure values from ROIs of an adult constitutive Arc/Arg3.1 KO was taken as background signal. The average signal from 2 to 3 consecutive brain sections obtained in multiple *in situ* hybridization experiments (n=3) were pooled together for final descriptive statistics. For the presented figure (Figure 5), images of a representative experiment exposed to IP films were normalized to the same color calibration scale (using PhotoShop, Adobe, San José, USA) and compared to the same experiment exposed to standard autoradiography film for presentation of comparative data.

8.6. Stereotaxic viral vector delivery in the brain

8.6.1. Mouse anesthesia and analgesia

Mice were anesthetized by using a complete anesthesia system for small animals based on Fluovac delivery and scavenging (Harvard apparatus, Holliston, USA). 4 to 5% of isoflurane (Abbot, Illinois, USA) in 100% oxygen flowing at 0.5l/min in an induction chamber was used for inducing anesthesia. After fixation in the stereotaxic frame, the isoflurane level was adjusted to 1.5-2% for maintaining anesthetic depth during the entire surgery. After surgery Carprofen (IDT Biologika, Dessau-Roßlau, Germany) prepared in 0.9% sterile saline solution (Braun, Melsugen, Germany) was injected subcutaneously at a dose of 5mg/kg bodylight for analgesia.

8.6.2. Surgical procedures and stereotaxic viral vector delivery

Mice were head fixed under isoflurane anesthesia to a rodent stereotaxic frame (David Kopf Instruments, Tujunga, USA) (Figure 52). Body temperature during the surgery was constantly monitored and controlled by a feedback temperature controller system (DC Temperature controller, FHC, Bowdoin, ME, USA) consisting of a rectal thermometer that regulated power to a heating pad located under the body of the mouse. The skull was shaved and disinfected with Betaisodona (Mundipharma, Limburg, Germany) and 70% ethanol. A midline incision was made with a scalpel, and the sutures, bregma and lambda reference points were visualized by wiping the skull surface with a cotton swab dipped in 30% H_2O_2. The target for injections was measured on the skull surface in the **x** and **y** coordinates from bregma under microscopic observation. Small craniotomies were drilled according to the anatomical coordinates, avoiding cortical lesions (Table 50).

Table 50. Stereotaxic coordinates for targeting specific brain areas

Target Area	y	x	z		Injected volume	
			Step 1	Step 2		
Dorsal Hippocampus (dHpc)	-2.00	±1.65	-1.8	-1.4	0.8 µl	0.4 µl
Ventral Hippocampus (vHpc)	-3.20	±3.20	-3.2	-2.2	0.4 µl	0.4 µl
Medial prefrontal cortex (mPFC)	+1.60	±0.35	-1.8	-1.4	0.4 µl	0.4 µl
Antior cingulate cortex (ACC)	+1.00	±0.35	-1.6	-1.3	0.5 µl	0.5 µl
Restrosplenia cortex (RSP)	-1.80	±0.40	-0.7	-0.5	0.4 µl	0.4 µl
Amygdaloid complex	-1.33	±3.25	-4.40		0.7 µl	
Cornu Ammonis region 3 (CA3)	-2.00	±2.30	-2.30		1 µl	

A Hamilton syringe (Neuros Syringes, Bonaduz, Switzerland) with a 33-gauge needle controlled by an injection robot (Neurostar, Tubingen, Germany) was preloaded with the required volume of virus and lowered into the previously drilled craniotomies, to the required depth (Table 50). The injection speed was set at 0.15 µl/min. After the injection the needle was left stationary for 5-10 min allowing the volume to spread in the tissue. The skin edges of the surgical wound were approximated and glued with tissue adhesive (VetbondTM, 3M, St. Paul, USA), and Carprofen/ saline administered subcutaneously for analgesia. Mice were placed on heating mats until completely recovery from anesthesia. Soft food was administered during the recovery days.

Figure 52. Stereotaxic setup for rAAV vectors delivery
a. Computer for controlling injection robot, **b.** Stereotactic meter connected to the stereotactic frame, c. Binocular microscope, **d.** Stereotactic frame. **e.** Temperature controller system, **f.** Drill and surgical tools.

After experimental procedures with the injected animals, brains were dissected and the injection site, viral spread, and inflammatory reaction were always determined by histological procedures using fluorescent markers or immunostaining with specific antibodies.

8.7. Behavioral investigation

8.7.1. Open field

Rodents have a natural aversion for open spaces, when exposed to unfamiliar empty arena; their normal behavior is to explore the arena avoiding the center and gradually decrease the exploratory activity (habituation). The open field test was performed in a cubic box (50 × 50 × 50 cm^3) made with white forex plates under dim illumination by indirect diffused room light (4 X 40W bulbs) (Figure 53). To evaluate the exploratory behavior, mice were placed carefully in the center of the arena, and videos were recorded for 5 -10 min using a camera installed at the ceiling above the arena, analyzed by using a tracking program (Ethovision XT 6.1, Noldus Information Technology, Wageningen, Netherlands). Path length, velocity and time spent in center (25x25 cm^2) were calculated. The arena was thoroughly cleaned with 70% ethanol between each subject.

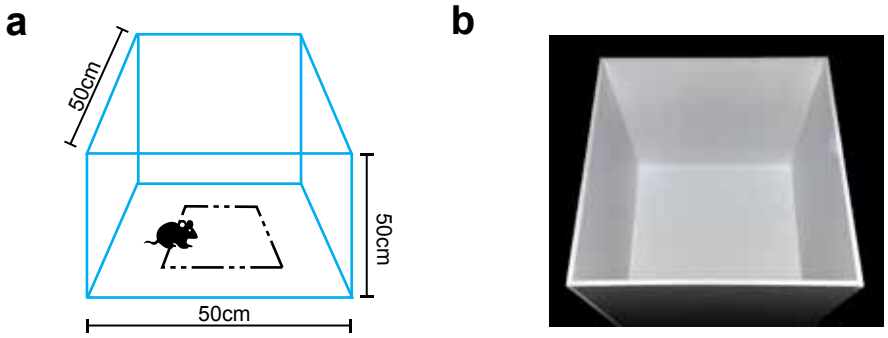

Figure 53. Open field test
a. Schematic representation and dimension of the open field, dash line represents the center defined in the tracking software. **b.** Representative photograph of the open field arena.

8.7.2. Elevated O-maze and elevated plus-maze

The elevated O-maze and plus-maze are tests based on the natural tendency of rodents to avoid potentially threatening environments such as open and high spaces. The concept of these paradigms as models for investigation anxiety-like behaviors in rodents was validated pharmacologically in rats (Pellow *et al* 1985) and mice (Lister 1987). Normally, the rodent prefers the protected zones by side walls and slowly and carefully explores the open zones by dipping the head and exploring the cliff and finally exploring the open arm with the whole body. These tests have the advantage of using the normal exploratory drive without the need of applying additional aversive stimuli.

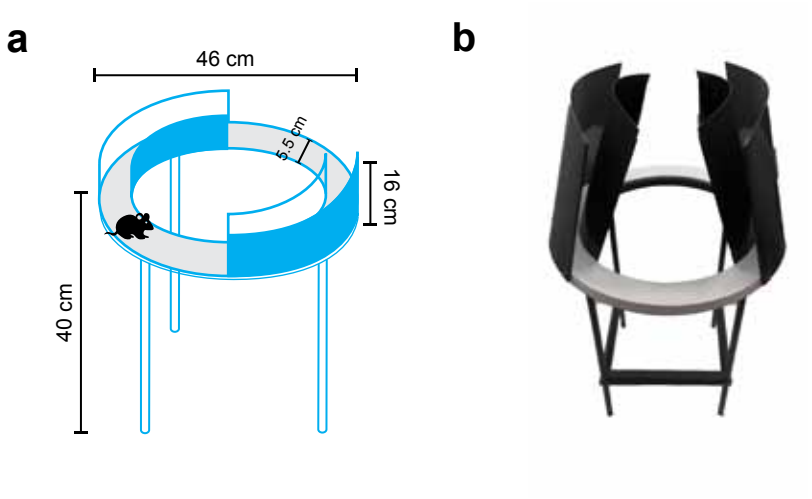

Figure 54. Eleveted O-maze test
a. Schematic representation and dimension of the Eleveted O-maze. **b.** Representative photograph.

The elevated O-maze was constructed with a grey plastic material and had an annular runway (diameter 46 cm, width 5.5 cm) elevated 40 cm from the ground. Two opposing 90° sectors of the runway were closed by an inner and outer inclined wall made of grey polyvinyl chloride (height 16 cm). The two remaining sectors were unprotected (Figure 54). The maze was 40 cm higher above the floor and exposed to diffuse room light (4 X 40W bulbs). Each mouse was placed into the wall closed sector and allowed to explore the maze for 10 min. Time spent in the open sectors and head dips into the open sectors were analyzed by Ethovision XT video-tracking program (Noldus Information Technology) and manually counted, respectively. 70% ethanol was used to clean the maze betlen subjects.

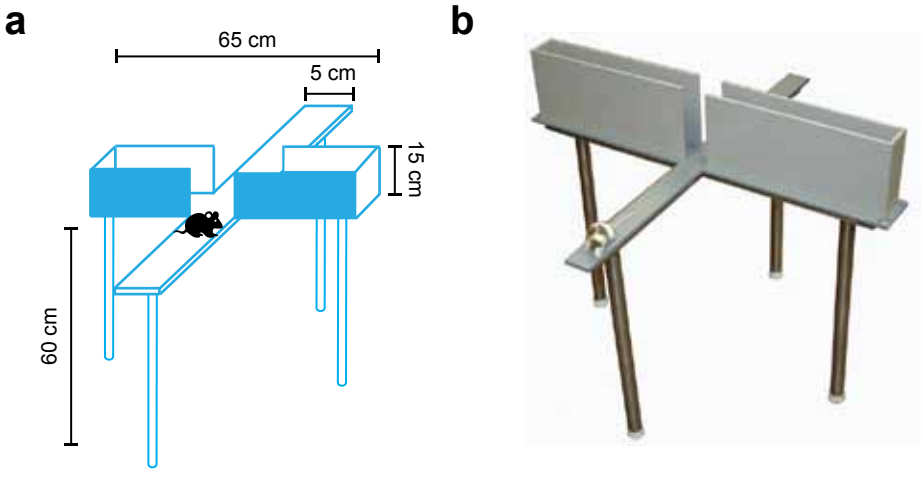

Figure 55. Eleveted plus-maze test
a. Schematic representation and dimension of the Eleveted plus-maze. **b.** Representative photograph (taken and modified from www.stoeltingco.com/anymaze/mazes/anxiety-depression/elevated-plus-maze.html).

The elevated plus-maze is based on the same principle as the EOM, made of white forex plates and consisted a central area (5x5 cm) and four arms (30x5 cm), of which two are open and two

are bordered by 15 cm high walls, and elevated 60 cm high above the floor level (Figure 55). The animal was placed in the center of the maze and its behavior record during 5 min. Time spent in the open, closed and central sectors and number of entries in each arm were recorded and counted by Ethovision XT video-tracking program (Noldus Information Technology, Wageningen, Netherlands). 70% ethanol was used to clean maze betlen subjects. This test was preferred to the O-maze due to the extensive literature available with its use.

8.7.3. The light-dark box test

The light-dark box is a complementary test to investigate unconditioned avoidance in experimental animals, and is based on the natural preference of rodents for dark and enclosed environments over brightly lit open spaces. It was introduced by Crawley and Goodwing in 1980 as a model to study anxiolytic-like behaviors (Crawley & Goodwin 1980). The light-dark box arena consisted of an open top white box (20x45x20 cm) made from forex plates. Within this box, placed against the short side, one third of the total surface was enclosed by a dark box (20x15x20 cm) made from grey polyvinyl chloride plastic, with a 7.5x7.5 cm opening in the wall facing the open area of the larger box (Figure 56). The lit chamber was directly illuminated by two 100W desk lamps located on each side avoiding any shadow effect. Total time in and number of entries into the lit compartment were analyzed and counted respectively by Ethovision XT video-tracking program (Noldus Information Technology, Wageningen, Netherlands). 70% ethanol was used to clean the maze between subjects.

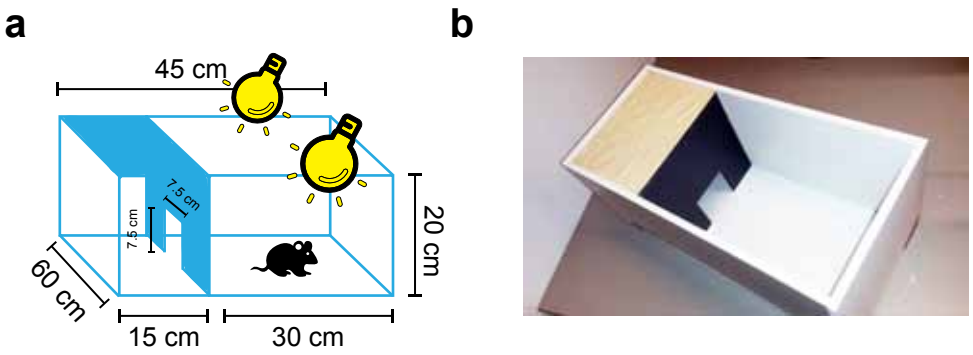

Figure 56. Light-dark box test
a. Schematic representation and dimension of the Light-dark box. **b.** Representative photograph

8.7.4. Novel object recognition test

Non-spatial, non-conditioned and non-stress related explicit memory can be tested in rodents by using the novel object recognition task (NOR). NOR can be performed without using reward or

punishment, and allows investigation of long-term explicit memory through the natural exploratory drive and curiosity for novel objects. This test was first described in rats by Ennaceur and Delaciour on 1988 (Ennaceur & Delacour 1988). In this behavioral paradigm, mice were trained and tested in the open field arena (section 8.7.1). During the habituation phase, mice were introduced in the open field arena for 10 min for 2 consecutive days. On the following day, mice explored two identical objects in the same arena for 10 min. Objects were positioned equidistantly from the wall of the arena. Memory retention was then tested 24 h later by placing the mice back into the arena with an identical copy of the familiar object and a novel object (Figure 57). To avoid possible object and place preference, training and novel object varied, and the location of the novel object was counterbalanced between the left and the right for different animals. The objects and area were carefully cleaned with 70% ethanol to eliminate olfactory cues. Experiments were done under indirect diffused room light (4 X 40W bulbs). Discrimination index was calculated as time spent exploring novel object / (time spent exploring familiar object + time spent exploring novel object).

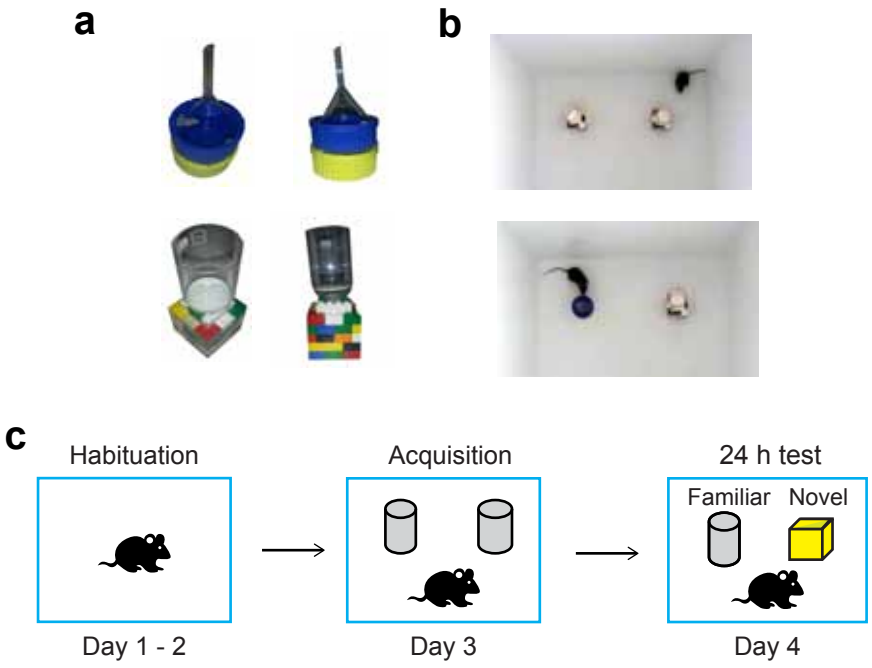

Figure 57. Novel object recognition test
a. Pairs of objects used in NOR. **b.** Representative photograph of acquisition and test phases. **c.** Schematic representation of NOR test protocol.

8.7.5. Morris water maze

Spatial learning and memory were evaluated with the Morris water maze test (MWM) (Morris 1984). The MWM is one of the most frequently used tools in behavioral neuroscience and consisted of a circular pool filled with opaque water with a hidden platform in a fix position. Rodents

learn to localize the escape platform during subsequently repeated trials by using distant visual cues around the pool. Our MWM setup comprised of a circular pool (1.5 m in diameter) filled with an opaque mixture of water (21±2°C) and white non-toxic water-soluble paint. A submerged circular platform (14 cm in diameter) was positioned 1.0 cm below the water surface. Four reference cues with geometrical patterns in white and black (Figure 58 a) were attached to the edges of the tank in an asymmetric manner (Figure 58 b and c). Other cues within the room were blocked from view by white plastic curtains.

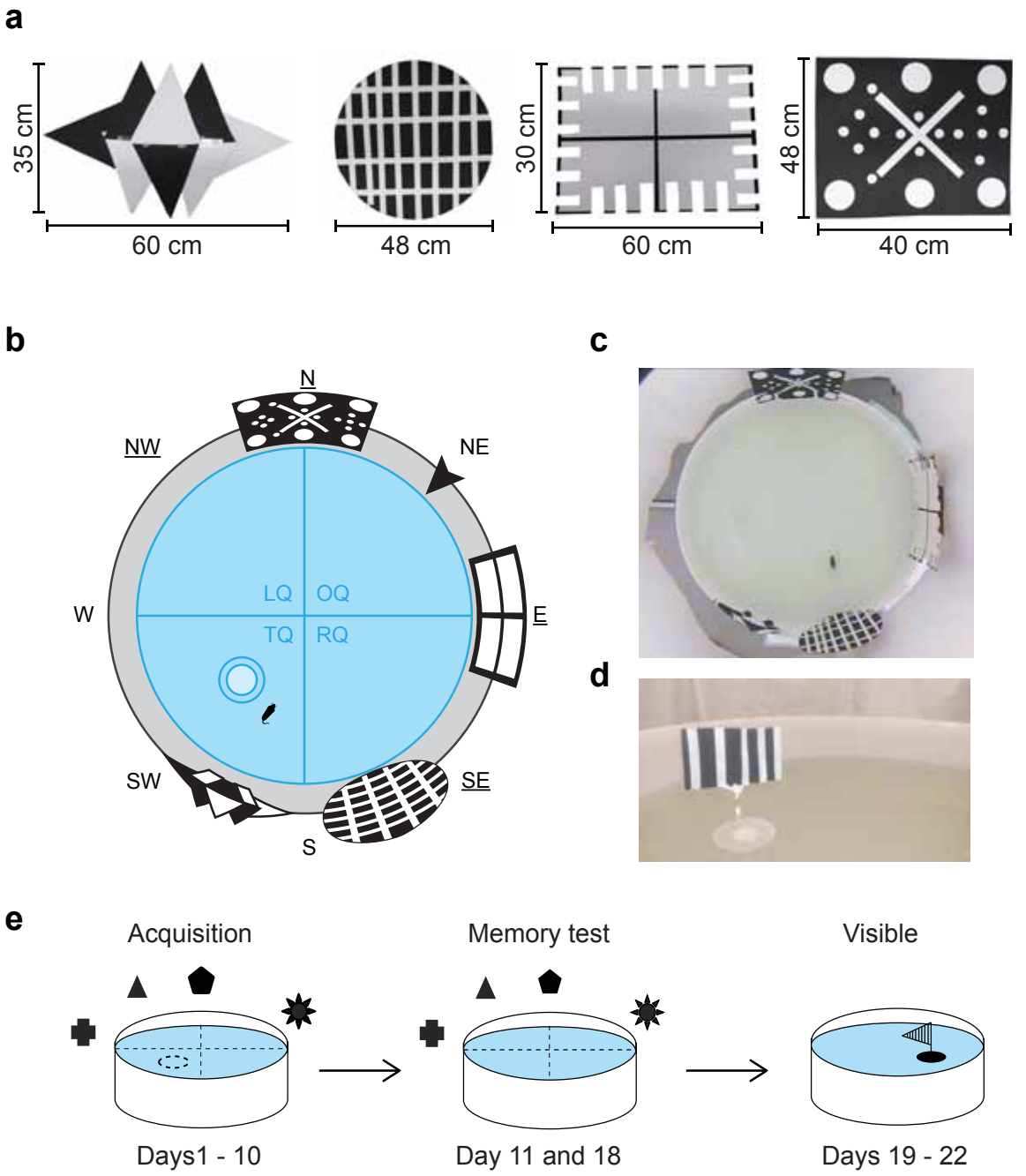

Figure 58. Morris water maze setup and procedure
a. Referential cues around the pool. **b.** Schematic representation of the water maze setup. North (N), South (S), Ist (W), East (E), Northeast (NE), NorthIst (NW), SouthIst (SW), Southeast (SE), Target quadrant (T), Opposite quadrant (O), Right quadrant (R), Left quadrant (L) **c.** Representative photograph of the water maze setup in the acquisition phase **d.** Flag used to signal the escape platform in the visible platform test. **e.** Schematic representation of the water maze training and testing procedure. (Figure 58b courtesy of Dr. Lars Binkle).

The maze was indirectly illuminated by diffused light (4 X 40W bulbs). During the acquisition phase, mice were allowed to find the hidden platform. Four starting positions were designated and mice were released from a semi-randomly assigned starting position each day (Vorhees & Williams 2006). If mice failed to find the platform within 60 s, they were manually guided towards it. All mice were allowed to stay on the platform for another 60 s in the first trial, 30 s for the second trial, and 15 s for the rest of trials in the following days. Four acquisition trials were performed each day during 10 consecutive days. A learning curve was generated based on the time that mice spent in finding the submerged platform (escape latency to the platform) and the total distance moved during exploring (path length).

To assess long-term spatial reference memory, mice were subjected to a single probe trial (60 s) 1 day or 7 days after training, during which the platform was removed from the maze and mice were released from the starting position in the opposite quadrant (Figure 58b arrow in NE position). An annulus zone, defined as a circular area 28 cm in diameter (twice the size of the platform) was defined in each quadrant. Number of crossings of and time in each annulus zone, and time in each quadrant were analyzed for the first 30s of each probe trial because there is evidence that quadrant preference decreases after that time by extinction (Vorhees & Williams 2006).

A visible platform test (Figure 58d-e) was performed during three days at the end of the whole experiment as a control procedure to test visual or motor impairments. During this phase, the platform was still submerged but cued with a black and white striped flag placed on its surface (Figure 58d). To ensure that the animal was using the cue placed on the platform, the location of the platform and the starting points were changed to semi-randomized positions during each trial (60 s). Videos for each trial were recorded and tracked by Ethovision XT video-tracking program (Noldus Information Technology, Wageningen, Netherlands).

8.7.6. Conditioned taste aversion

A paradigm to reliably test implicit memory in rodents is the conditioned taste aversion (CTA). CTA is a form of classical conditioning with a sickness-inducing substance as the unconditioned stimulus (US) and a taste stimulus (saccharin or sucrose) as the conditioned stimulus (CS). In this model, a sweet taste is paired with a malaise-inducing drug. If the conditioning and thus the associative memory is successfully acquired and maintained; mice will avoid the sweet taste when they are presented with a paired choice test (saccharin/water). CTA was adapted from Rosenblum *et al* (Rosenblum *et al* 1993). Ad libitum access to water was discontinued for 3 days, during which water was provided once per day for 20 min from two pipettes placed in the metal-

lic lid of their home cage, each containing 10 ml of water. On the fourth day (conditioning), mice were allowed to drink 0.5% sodium saccharin (Sigma, St. Louis, USA) solution from two similar pipettes for 20 min, and 40 min later were injected with 0.14 M lithium chloride (LiCl, Sigma-Aldrich, St. Louis, USA); in a dose of 2% body light (b.w.) intraperitoneally. On the fifth day, mice were given access to the water for 20 min.

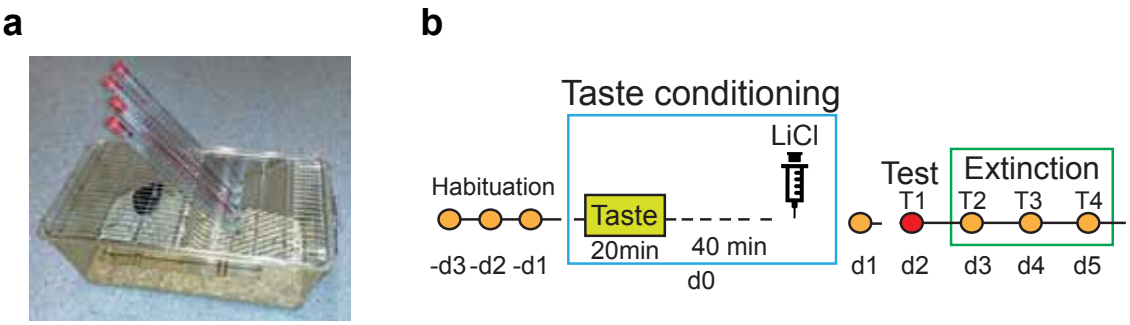

Figure 59. Conditioned taste aversion memory and extinction paradigm
a. Representative photograph of pipette arrangement for CTA procedures. b. Schematic representation of CTA protocol.

On the testing day (second day after the conditioning), mice were allowed to drink from 4 pipettes, two of which contained 10 ml of the conditioned taste solution (saccharin) and two with 10 ml water (Figure 59a). The order of the pipettes was always counterbalanced and the volume of fluid consumed from each pipette was registered. An aversion index was calculated as the volume of water consumed divided by the total consumed fluid (ml water/ml water + ml saccharin). To assess CTA extinction, the mice were continuously tested as described for 4 more days (Figure 59b). To avoid conflict by circadian effects, water or saccharin was given at the same time every day during the entire procedure and a strict control of weight and general health conditions were monitor during the entire procedure.

8.7.7. Flinch-jump procedure

Deficits in conditioning procedures could arise from differences in sensitivity to nociceptive stimuli. The nociception to foot shocks can be evaluated by the flinch-jump technique of Evans (Evans 1961). The flinch-jump threshold was tested in the TSE Multi-Conditioning System (TSE Systems, Bad Homburg, Germany). Mice were placed into a transparent arena with a metallic grid as floor and allowed to explore for 30 seconds. Then, with 30 s intervals, 0.5 s long foot shocks, were delivered with intensities increasing in a stepwise manner from 0.1 mA to 1.0 mA, step size 0.05 (figure 56 a). Behavioral responses (no response, flinch or jump) were noted and manually scored for each shock by two evaluators blinded to the genotypes. The lowest shock intensity eliciting flinch and/or jump was taken as a threshold value (Figure 60 b-c).

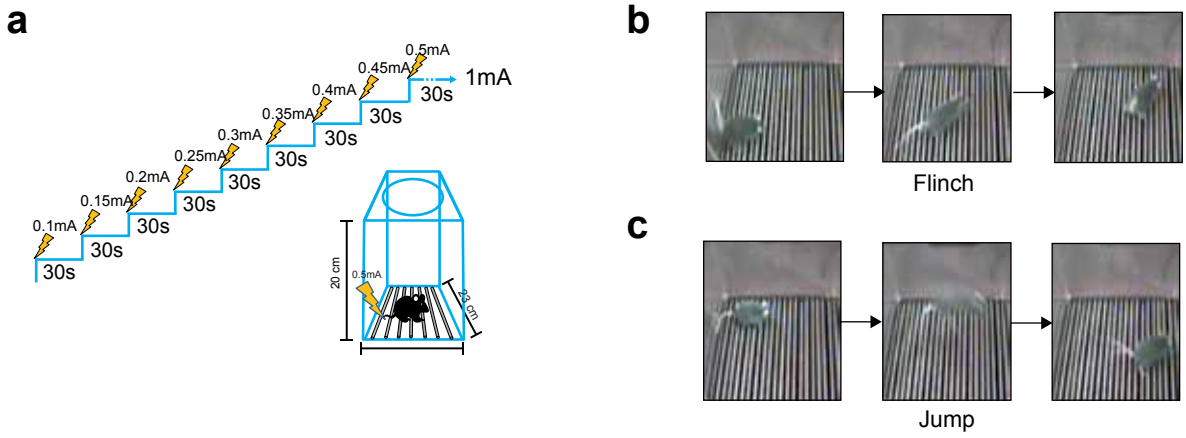

Figure 60. Jump-Flinch procedure to test nociceptive threshold
a. Schematic representation of the applied stimuli. **b.** Representative sequence in a flinch response. **c.** Representative sequence in a jump response.

8.7.8. Fear conditioning and extinction

Pavlovian fear condition is a broadly used method to investigate fear, aversive learning and memory. In this laboratory paradigm, a non-aversive and innocuous stimulus such as a tone or environmental cues –CS- is paired with an aversive stimulus, usually a foot shock –US-. The aversive stimulus induces fear responses (e.g. increased heart and respiratory rate, urination, defecation, freezing, among others defensive behaviors) and the previously neutral stimulus acquires aversive properties through associative learning. Thereafter when presented alone, the CS will evoke defensive behaviors, humoral and sympathetic responses (Orsini & Maren 2012). Contextual and cued fear conditioning was performed using TSE Multi-Conditioning System (Figure 61a-c) (TSE Systems, Bad Homburg, Germany) and immobility was used as readout of the level of experienced fear (% Freezing). After having acclimatized to being handled for 3 consecutive days, mice were placed into the conditioning chamber and three different protocols were used for inducing fear memory:

Protocol 1 (1xCS-US, Figure 61d): The conditioning context consisted of the following: (1) a transparent rectangular prismatic floorless arena made of acrylic (20x23x35 cm) with a removable lid, (2) a metallic grid floor for footshock delivery, (3) bright white light (>50 Lux), (4) constant background noise emitted from an internal fan (28 dB) and (5) 70% ethanol was used as cleaning solution and olfactory cue. The mice were allowed to explore the arena for 2 min. A tone of 75 dB and 10000 Hz was then played for 30 s. During the last two seconds, a footshock of 0.5 mA was delivered. The animals remained in the chamber for 1 min and were returned to their home cage. Contextual fear memory was tested at different time points placing the mice back in the

original conditioning context for 3 min. Cued fear memory was tested an hour later in an altered context consisting of (1) an opaque rectangular prismatic arena made of acrylic with a transparent wall transversally giving a triangular shape (20x23x35cm), (2) a square black floor covered with clean and fresh wood chip bedding (3) dim red light (< 5 Lux), (4) minimal background noise and (5) 1% acetic acid as cleaning solution and olfactory cue. After two minutes of exploring the novel environment, the used tone during the conditioning was played for 2 additional minutes. The specificity of the contextual memory and retest of auditory fear memory were performed in a third environment (altered context) using the same procedure as in the first cued test. The altered context consisted of a transparent acrylic home cage-shaped arena with clean and fresh wood chip bedding, dim red light (< 5 Lux), minimal background noise and 1% acetic acid as cleaning solution and olfactory cue.

Protocol 2 (3xCS-US, Figure 61e): This protocol was used for testing contextual fear extinction. The conditioning and contextual fear tests were performed under the same conditions for context as described in protocol 1. The mice were allowed to explore the chamber for 2 min and received three footshocks (2 s, 0.5 mA) with 60 s inter trial intervals. The mice remained in the chamber for an additional minute and returned to their home cage. For assessing contextual fear extinction, the mice were tested daily in the conditioning environment for 5 minutes during 6 consecutive days.

Protocol 3 (5xCS-US, Figure 61f): The conditioning context consisted of a rectangular prismatic arena with 3 opaque walls, dim red light (< 5 Lux), constant background noise was emitted from the fans (28 dB) and 70% ethanol as a cleaning solution and olfactory cue. The mice were allowed to explore the chamber for 2 min and received five temporally overlapped tone-footshock pairs (15 s, 2000 Hz, 98 dB)/shock (2 s, 0.25 mA) with 215 s inter trial intervals. After the last pair of tone-shock, the mice remained in the chamber for an additional minute and returned to their home cage. Contextual fear memory was tested at different time points placing the mice back to the original conditioning context for 2 min. Auditory fear memory was tested an hour later in a novel context consisting of a clear triangular prismatic arena made of acrylic with a square black floor (20x23x35 cm) covered with clean and fresh wood chip bedding, the chamber was illuminated with a white bright light (>50 Lux), minimal background noise and 1% acetic acid as cleaning solution and olfactory cue. After 1 minute of exploring the novel environment, the used tone during the conditioning was played for 1 additional minute.

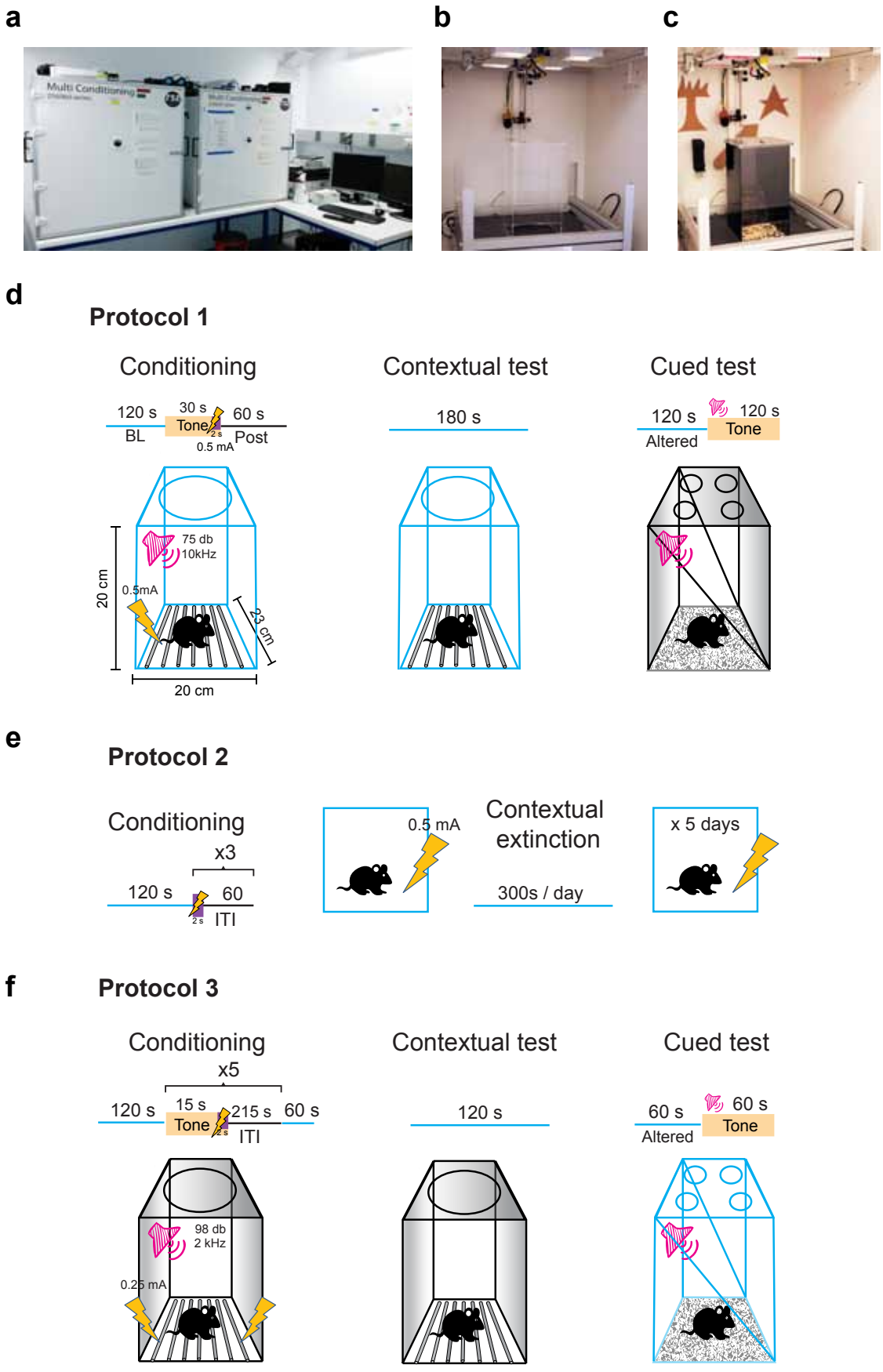

Figure 61. Fear conditioning and extinction protocols
a. TSE Multi-Conditioning System used for fear conditioning experiments. **b.** Conditioning context used in protocols 1 and 3. **c.** Representative photograph of altered context used for cued test in protocols 1. **d.** Schematic representation of fear conditioning protocol 1. **e.** Schematic representation of fear conditioning protocol 2. **f.** Schematic representation of fear conditioning protocol 3.

8.7.9. Three-chamber sociability and social novelty test

Rodents are social beings engaged in high-level reciprocal social interactions, sociability and novelty to social stimuli can be evaluated by using simple paradigms that are based on the normal preference of mice to spend more time with peers and explore novel intruders over familiar mice. The three-chamber sociability test was developed by Crawley *et al* (Moy *et al* 2004b) and consisted of a rectangular, three-chambered arena constructed with white forex plates (60x40x22cm) exposed to diffuse room light (4 X 40W bulbs). Side chambers had dimensions of 40x20x22cm each. Dividing walls were made of Plexiglas with an open middle section of 3.5 cm that allows free access to each chamber. Two identical transparent cylindrical plastic containers (8.5 x 12 cm) with removable lid and small holes in the walls were glued to the floor of both side chambers at the same position (Figure 62a-b).

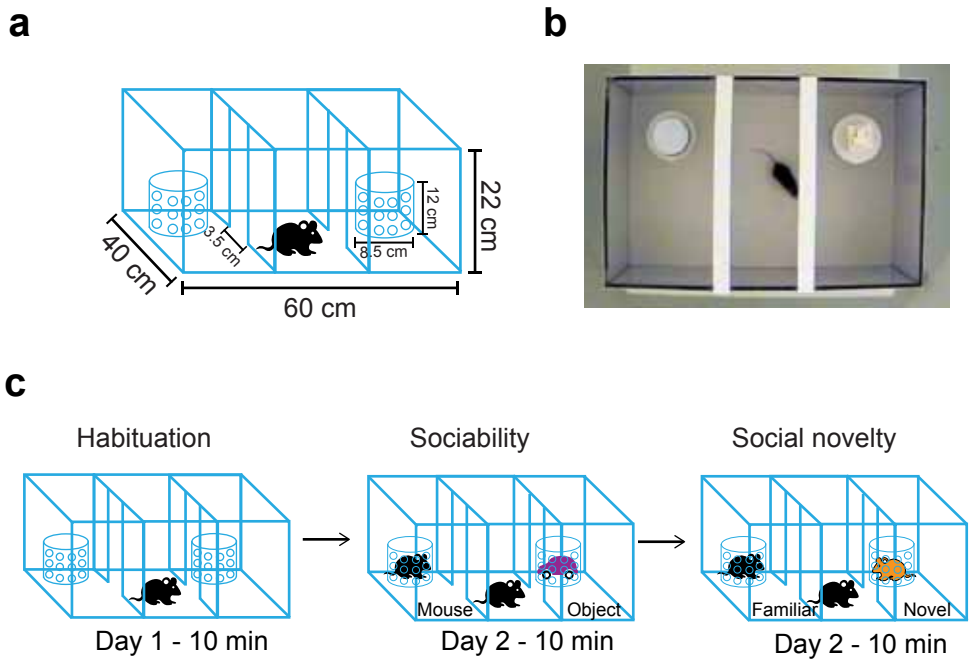

Figure 62. Three-chamber sociability and social novelty test
a. Schematic representation and dimension of the three-chambered box. **b.** Representative photograph. **c.** Schematic representation of three-chamber sociability and social novelty test protocol.

On the first day during the habituation phase, the mouse was placed in the middle chamber and allowed to explore the arena for 10 min. On the next day in the sociability phase, an unfamiliar gender-matched C57BL/6J mouse that had no prior contact with the tested mouse was introduced in one of the cylindrical containers; a black object was placed in the opposite container. The subject mouse was introduced in the middle chamber and allowed to explore for 10 min, after which it was placed back into its home change. Shortly after the sociability phase, the black object was exchanged for a second novel and unfamiliar mouse, after which the tested mouse was reintroduced to the middle chamber and allowed to explore for another 10 min.

Females and males were tested in separate sections to avoid gender and olfactory interferences. The location of the stranger and novel mice was always alternated between trials for avoiding placement biases. Time spent in each chamber, entries into each chamber and close interrelation time with each container (2 cm around each container) were recorded and analyzed by Ethovision XT video-tracking program (Noldus Information Technology, Wageningen, Netherlands). 70% ethanol was used to clean the arena between subjects.

8.7.10. Kainate-induced seizures

To induce maximal expression of neuronal activity-regulated genes (e.*g*. Arc/Arg3.1, c-fos) convulsive seizures were induced by the systemic application of kainate. Adult C57BL/6J mice (20-30 gr, 3 to 6 months of age) were injected intraperitoneally with kainate (Abcam, Cambridge, UK) with a dose of 14.8 mg/kg b.w. prepared in sterile PBS. Seizures were scored as using the scale by Yang DD *et al* (Yang *et al* 1997), as follows:

Table 51. Score scale to classify kainate-induced seizures

Seizure scale	Clinical signs
Grade 1	Arrest of motion
Grade 2	Myoclonic jerks of the head and neck, with brief twitching movements
Grade 3	Unilateral clonic activity
Grade 4	Bilateral forelimb tonic and clonic activity
Grade 5	Generalized tonic–clonic activity with loss of postural tone
Grade 6	Death from continuous convulsions

Onset of generalized tonic-clonic activity frequently occurred 25-40 min after the kainic acid injection. Mice were euthanized 90-120 min after generalized tonic-clonic activity onset and brain tissues were processed for biochemical or histological examinations.

8.8. Multichannel electrophysiology

Multichannel electrophysiology was performed by Jasper Grendel (Ph.D. student IMCC-ZMNH-UKE) under the supervision and assistance of Prof.Dr. Dirk Isbrandt (German Center for Neurodegenerative Diseases – DZNE, Universitätsklinikum Köln). Adult male mice were anesthetized with 0.8 g/kg b.w. urethane (10% w/v; NaCl 0.9%, Sigma-Aldrich, St. Louis, USA) and 0.05 µg/g b.w. of buprenorphine (Temgesic, Reckitt Benckiser, Slough, UK). Anesthesia was induced with 4% of isoflurane and during surgery maintained with 1.0–1.5% isoflurane in 100% water-saturated

oxygen. Animals were placed in a stereotaxic apparatus (Stoelting, Wood Dale, USA) and body temperature was maintained at 36.5 °C using a homeothermic heating pad and rectal thermometer (WPI, Sarasota, USA) throughout the experiment. A midline skin incision was made on the top of the skull. For a common ground and reference electrode, a hole was drilled and a stainless steel screw connected to the ground were was inserted above the cerebellum (lambda –1.5 mm, 1.0 mm lateral). Isoflurane anesthesia was discontinued after surgery, after which recording was started and lasted at least 2 hours. After drilling 0.8 mm wide craniotomies, two linear 16-site silicon probes with a distance of 100 µm between the recording sites and 177 μm^2 electrode surface (a1x16–5 mm-100–177; NeuroNexus Technologies, Michigan, USA) were vertically lowered into the right hemisphere: one into the dorsal hippocampus along the CA1–dentate gyrus axis (bregma -2 mm, lateral 1.4 mm, depth 2.1 mm), the other into the PFC (bregma 1.54 mm, lateral 0.3 mm, depth 2.8 mm). Prior to insertion, probes were dipped in a DiI-solution (Vybrant®, ThermoFisher scientific, Waltham, USA), for post-experimental probe position verification. Both probes were connected to a 1x preamplifier (Neuralynx, Bozeman, USA) mounted to the stereotaxic instrument. Animal breathing rate was detected by a piezoelectric sensor placed under the animal's thorax. When probes and sensor were in place, isoflurane anesthesia was discontinued. The recording was immediately started and lasted for at least 2 hours.

Data from both probes and the sensor were digitally filtered (0.5–9000 Hz bandpass) and digitized as 16-bit integers with a sampling rate of 32 kHz using a Digital Lynx 4SX data acquisition system (Neuralynx, Bozeman, USA). During the recording, anesthetic depth was observed from breathing rates, twitching, rear foot reflexes and electrophysiological activity. If requwered, additional 0.2 g/kg b.w. urethane doses were given. After the experiment, mice were deeply anesthetized with 4% isoflurane for 5 mins, before quick decapitation and excision of the brain, which was placed into 4% PFA. Probe positions were verified in NeuroTrace fluorescent Nissl-stained (Invitrogen, Waltham, USA) coronal slices (figure 63 a and b), which were used in combination with the local field potential (LFP) depth profile for layer identification (Buzsaki *et al* 2003).

All *in vivo* data were analyzed and visualized in MATLAB (Mathworks, Natick, MA, USA) or NeuroScope (Hazan *et al* 2006). LFPs were downsampled to 1.28 kHz from raw traces. Multitaper was computed using Chronux (www.chronux.org). Current source density (CSD) for hippocampal signal calculation was based on the inversion of the electrostatic forward solution, using the spline method, assuming a 0.5 mm source diameter and 0.3 S tissue conductivity (Pettersen *et al* 2006). Power between 0.2-1.2 Hz was used to mark Slow Wave Sleep (SWS)-like periods (Figure 63 a).

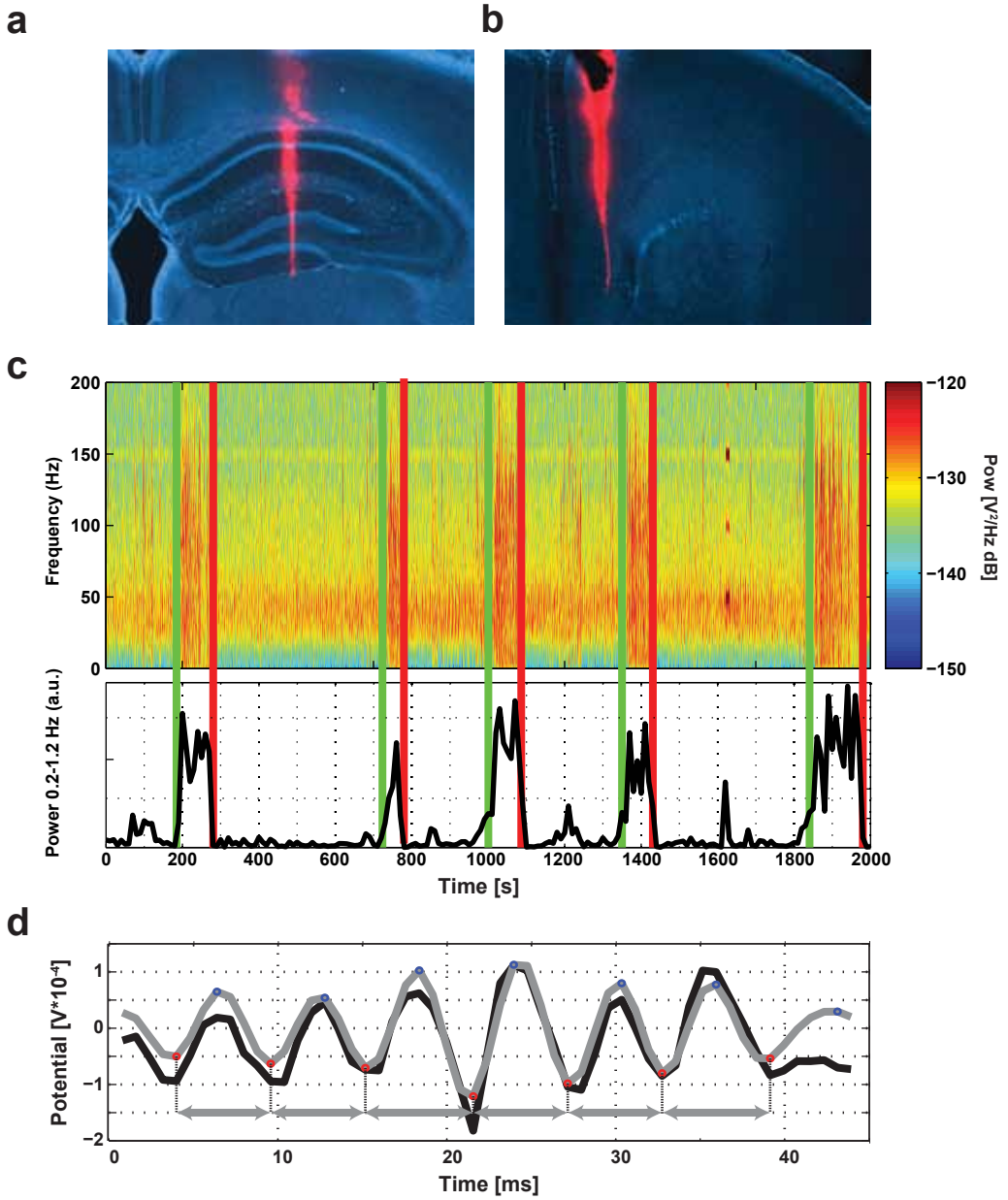

Figure 63. Multichannel electrophysiology and Local Field Potential (LFPs) analysis
a. Histological verification of DiI-coated probes for dorsal hippocampus and **b.** mPFC with DAPI staining shown in blue and DiI in magenta. **c.** Spectrogram excerpts from a recording show intermittent high frequency bursts (top). Low frequency (0.2 – 1.2 Hz) polr, indicative for putative SWS epochs, shows an increase in polr, during these intermittent bursts (bottom). SWS epochs in this example are marked with start (green) and stop (red) borders. **d.** Parameters from single ripples lre calculated as follows. The raw trace (black) was bandpass filtered (Butterwoth, 14th order, 100-250 Hz, grey). The ripple's amplitude was calculated by subtracting the average voltage of all local minima (red) from the average voltage of all local maxima (blue). The ripple's frequency was calculated by taking the average distances betlen local minima, i.e. the average of all grey arrows. (Courtesy of Jasper Grendel)

For automatic ripple detection during these periods, recordings were band filtered (Butterworth; 14th order, 100–250 Hz). Ripples were defined as events during which the instantaneous amplitudes, calculated by the absolute of the Hilbert transform, exceeded four times the SD above the mean. The left and right borders of detected ripple events were defined as the time points where the instantaneous polr dropped <1.75 SDs above the mean. Events shorter than 25 ms were excluded. For each individual ripple, its amplitude and estimated its frequency were calculated

(Figure 63 d). Ripple amplitude was obtained by measuring the average peak-to-peak amplitude per ripple on the band filtered signal. Ripple frequency was obtained by calculating the mean inverse distance between subsequent troughs. To obtain the ripple amplitude and frequency per animal, a mean was calculated for all detected ripples throughout a recording. Ripple occurrence was defined as the number of ripples per second of SWS-like brain states.

Paradoxical/Rapid Eye Movements (REM)-like epochs were manually selected and defined by the absence of slow wave power and the presence of continuous ϑ (3.8–6 Hz) oscillations. ϑ and γ power was calculated for the selected REM-like epochs by integrating the area below the ϑ and γ ranges (nFFT = 4096 points, sliding window 2048 points).

8.9. Magnetic resonance imaging

Magnetic resonance imaging (MRI) was performed in the department of Diagnostics and Interventional Neuroradiology – University Medical Center Hamburg-Eppendorf (UKE) under the supervision and assistance Dr. Jan Sedlacik. Mice aged 36-48 weeks were place in a 7 tesla (T) / 40 cm horizontal super conducting Magnetic Resonator (RM) for small animal imaging system (ClinScan, Bruker, Rheinstetten, Germany) and scanned with a tightly fitting mouse head array coil (rat body transmission coil, 2x2 phased array mouse head reception coil) while breathing a mixture of air and isoflurane (0.8-1.2%). Breathing rate was detected by a piezoelectric sensor placed under the animal's thorax and was maintained at a range of 90-110/min by changing isoflurane levels (figure 64a). Shimming was performed on a 16 mm x 16 mm region, using a 3D Fieldmap shimming 1st and 2nd order shimm currents.

8.9.1. Anatomical imaginig acquisition and analysis

MRI anaylsis was performed with the help of Jasper Grendel (Ph.D. student IMCC-ZMNH-UKE) under the supervision and assistance of Dr. Ora Ohana and Prof. Christian Büchel (Institute of Systems Neuroscience - UKE). High-resolution anatomical images were acquired with constructive interference steady state (CISS) sequence for 3D acquisition at a transversal orientation with the following parameters: repetition time (TR) / echo time (TE) 7.74 / 3.87 ms, matrix 128x128x120, field of view 16 x16 x 14.4mm3, elliptical K-space sampling, every image was an averages of 4 scans (or number of excitations (NEX)=4), flip angle 50°, readout bandwidth 200 Hz per pixel and scan time 12 min and 25 s. T2 weighted coronal slice images were obtained (32) with 125 x 125 x 120mm3 voxel, 0.12 mm per slice with an area of 1.6 x 1.6 mm.

Image preprocessing consisted of (i) the DICOM images were converted to the NIfTI format. (ii), Images were manually reoriented, co-registered, realigned to a T1 template, resliced and finally the realignment to template was manually verified (figure 64). (iii), brain segmentation into grey, white matter and CSF was performed by means of the Brain Extraction Tool (BET) (Smith 2002). (iv) A DARTEL normalization procedure was applied (on the gray matter-segmented file). For morphometric analysis, DARTEL normalized images were smoothed with a Gaussian kernel of 0.8 mm for anatomical and 0.5mm for Blood-oxygen-level dependent signal (BOLD) images, respectively. Voxels in anatomical images were compared between KO, cKO mice and their respective WT-controls littermates.

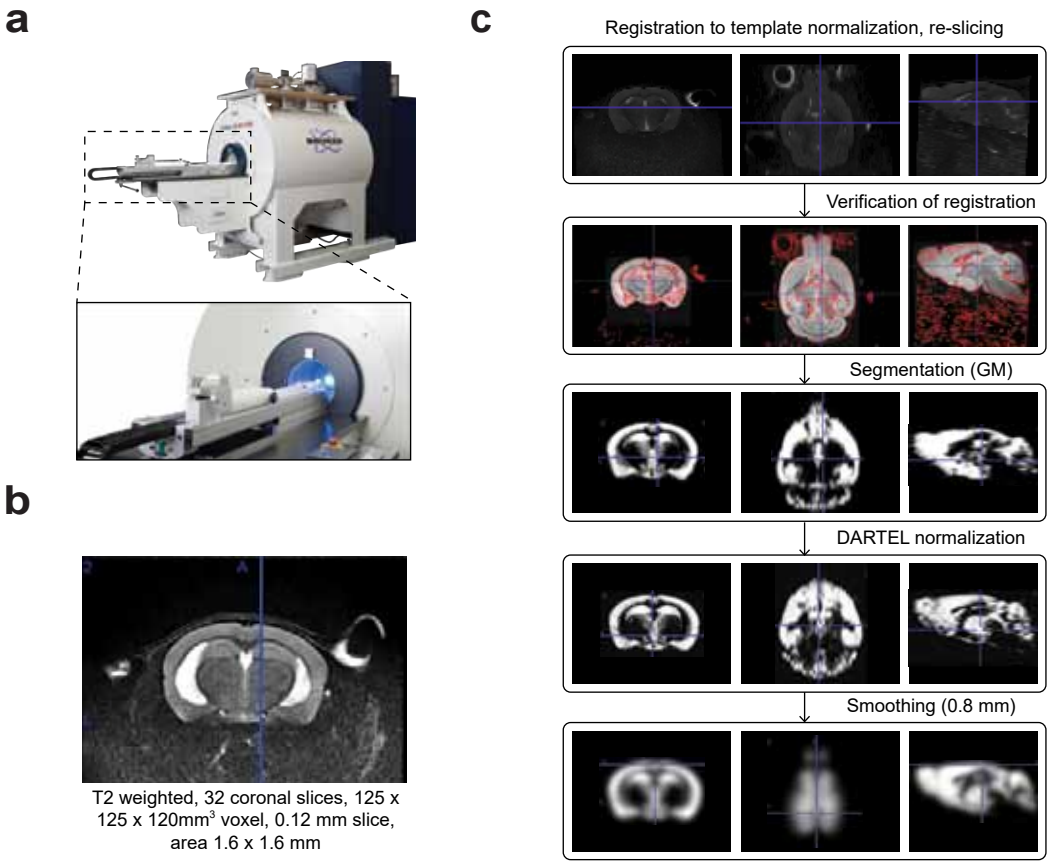

Figure 64. Magnetic resonance imaging acquisition and common image preprocessing
a. Representative image of the 7 tesla Magnetic Resonator (RM) for small animal imaging system (ClinScan, Bruker, Rheinstetten, Germany). **b.** Example of acquired T2 weighted image. Processing of acquired images.

8.9.2. Resting state functional magnetic resonance analysis

BOLD rsfMRI time series were acquired using an echo planar imaging EPI-FID sequence (free induction decay EPI) with the following parameters: TR/TE 2500/9 ms, flip angle 90°, matrix 64 × 64, field of view 20 x 20 mm, 24 coronal slices, slice thickness 0.3 mm, slice gap 0.1 mm, 360

volumes, partial fourier K-space sampling factor 6/8, fat-saturation, Bandwidth 3126 Hz/pixel, 150 repetitions and a total rsfMRI acquisition time of 6 min 20 s.

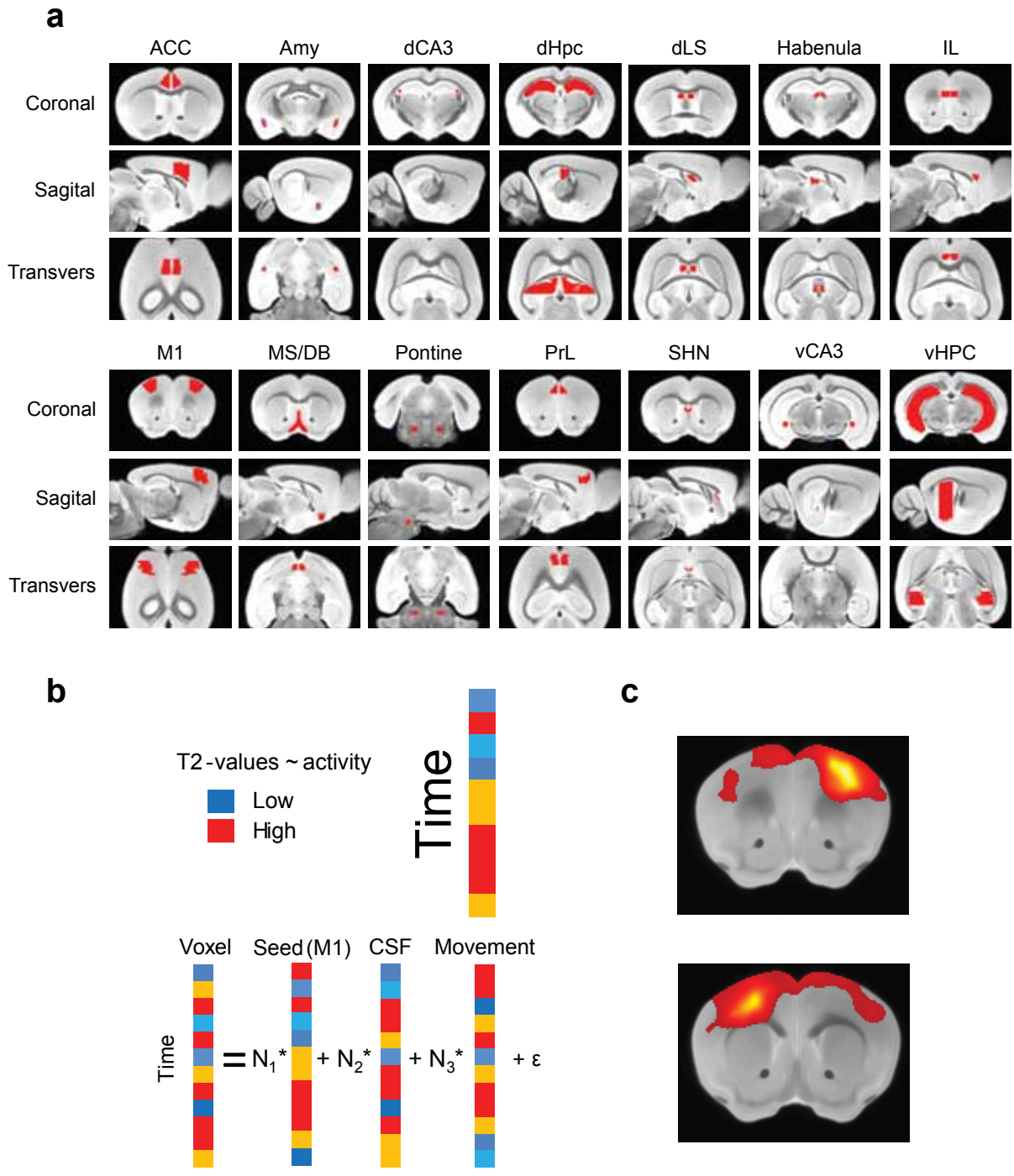

Figure 65. Resting state functional MRI (rsfMRI) analysis
a. Volume of interest (VOI). **b.** Summary and processing of acquired BOLD signals. **c.** Example of functional connectivity in M1 bilaterally as sanity test in Wild-type mice.

Anatomical regions of interest (ROIs) were based on the Paxinos and Franklin's Mouse Brain atlas and created using MRIcron freeware software (University of South Carolina, Columbia, SC, USA) on the template. I manually drew the following ROIs: Anterior Cingulate Cortex (ACC),

Amygdala (Amy), dorsal CA3 (dCA3), entire dorsal hippocampus (dHpc), dorsal Lateral Septum (dLS), Habenula, Infralimbic subregion of the medial Prefrontal Cortex (IL), primary motor cortex (M1), Medial Septal Nucleus (MB/DB), Pontine nuecleus (Pontine), Prelimbic subregion of the medial Prefrontal Cortex (PrL), Septal hippocampal nucleus (SHN), ventral CA3 (vCA3) and the entire ventral hippocampus (vHpc) (Figure 65a).

For the rsfMRI analysis, after preprocessing images were smoothed with a Gaussian kernel, Blood-oxygen-level dependent signal (BOLD) images, a generalized linear model was used to estimate the influence of drifts (through direct cosine transform) and movement. The mean time series of volumes of interest were extracted from the BOLD images, taking into account the slow drifts previously estimated. The generalized linear model was again applied to correlate each and every pixels's time course to the time course of the respective volume of interest (VOI), with movement and the mean time course of a hand drawn VOI of the Cerebral Spinal Fluid (CSF) as nuisance regressors. Differences in connectivity betwen mutants and WT-control littermates were thresholded where individual pixel p-values are below 0.001 (uncorrected) and cluster size was set such that its p-value was below 0.05.

8.10. Statistics

Two-tailed Student's t-tests were used when the data were normally distributed for comparing phenotypes in one variable. In the novel object recognition test, preference index was compared to the chance level performance (50%) with one sample t-test. In the open field, elevated plus maze, contextual fear conditioning, two sample t-tests were used to make comparisons betlen genotypes. When the data were not normally distributed, Mann-Whitney or Kruskal-Wallis-Test tests were performed. For the acquisition phase of the Morris water maze, conditioning taste aversion, time bin analysis in open field, contextual fear conditioning and extinction, two-way repeated measurement ANOVA (2way-RM ANOVA) was applied within subjects following time, trials or minute bins, and Fisher's LSD post hoc test was used if a significant difference was found from the analysis of variance. For the probe tests of the water maze, Elevated-plus maze and Light-dark box experiments, regular 2-way or 3-way ANOVAs were performed. All statistical analysis was done with IBM SPSS software (Version 19, IBM, New York City, NY, USA). $P < 0.05$ was considered as significant. All graphs were generated with GraphPad Prism 5 (GraphPad Software, La Jolla, USA), Adobe Illustrator CS5 version 15 (Adobe Systems, Mountain View, USA) and MATLAB (Mathworks, Natick, MA, USA). Numerical values in the figures are presented as mean ± SEM. For electrophysiological parameters, a non-parametric Mann-Whit-

ney-Wilcoxon (MWW) test was used. If the number of combinations to obtain the exact MWW distribution is less than 20000, the exact ranks distribution was calculated; otherwise a normal distribution approximation was used.

9. References

Adams JP, Robinson RA, Hudgins ED, Wissink EM, Dudek SM. **2009.** NMDA receptor-independent control of transcription factors and gene expression. *Neuroreport* 20: 1429-33

Adhikari A, Lerner TN, Finkelstein J, Pak S, Jennings JH, *et al*. **2015.** Basomedial amygdala mediates top-down control of anxiety and fear. *Nature* 527: 179-85

Adhikari A, Topiwala MA, Gordon JA. **2010.** Synchronized activity between the ventral hippocampus and the medial prefrontal cortex during anxiety. *Neuron* 65: 257-69

Adhikari A, Topiwala MA, Gordon JA. **2011.** Single units in the medial prefrontal cortex with anxiety-related firing patterns are preferentially influenced by ventral hippocampal activity. *Neuron* 71: 898-910

Akers KG, Candelaria-Cook FT, Rice JP, Johnson TE, Hamilton DA. **2009.** Delayed development of place navigation compared to directional responding in young rats. *Behavioral neuroscience* 123: 267-75

Akers KG, Martinez-Canabal A, Restivo L, Yiu AP, De Cristofaro A, *et al*. **2014.** Hippocampal neurogenesis regulates forgetting during adulthood and infancy. *Science* 344: 598-602

Alhowikan AM. **2016.** Activity-Regulated Cytoskeleton-Associated Protein Dysfunction May Contribute to Memory Disorder and Earlier Detection of Autism Spectrum Disorders. *Medical principles and practice : international journal of the Kuwait University, Health Science Centre*

Allin JT, Banks EM. **1972.** Functional aspects of ultrasound production by infant albino rats (Rattus norvegicus). *Animal behaviour* 20: 175-85

Anthony TE, Dee N, Bernard A, Lerchner W, Heintz N, Anderson DJ. **2014.** Control of stress-induced persistent anxiety by an extra-amygdala septohypothalamic circuit. *Cell* 156: 522-36

Antunes M, Biala G. **2012.** The novel object recognition memory: neurobiology, test procedure, and its modifications. *Cognitive processing* 13: 93-110

APA. **2013.** *Diagnostic and Statistical Manual of Mental Disorders 5th edn.* Washington, DC

London, England: *American Psychiatric Publishing*. 947 pp.

Ashby MC, Isaac JT. **2011.** Maturation of a recurrent excitatory neocortical circuit by experience-dependent unsilencing of newly formed dendritic spines. *Neuron* 70: 510-21

Bailey CH, Bartsch D, Kandel ER. **1996.** Toward a molecular definition of long-term memory storage. *Proceedings of the National Academy of Sciences of the United States of America* 93: 13445-52

Banbury C. **1997.** Mutant mice and neuroscience: recommendations concerning genetic background. Banbury Conference on genetic background in mice. *Neuron* 19: 755-9

Bandelow B, Michaelis S. **2015.** Epidemiology of anxiety disorders in the 21st century. *Dialogues in clinical neuroscience* 17: 327-35

Bannerman DM, Rawlins JN, McHugh SB, Deacon RM, Yee BK, *et al*. **2004.** Regional dissociations within the hippocampus-memory and anxiety. *Neuroscience and biobehavioral reviews* 28: 273-83

Barkus C, McHugh SB, Sprengel R, Seeburg PH, Rawlins JN, Bannerman DM. **2010.** Hippocampal NMDA receptors and anxiety: at the interface between cognition and emotion. *European journal of pharmacology* 626: 49-56

Beique JC, Na Y, Kuhl D, Worley PF, Huganir RL. **2011.** Arc-dependent synapse-specific homeostatic plasticity. *Proceedings of the National Academy of Sciences of the United States of America* 108: 816-21

Benes FM, Taylor JB, Cunningham MC. **2000.** Convergence and plasticity of monoaminergic systems in the medial prefrontal cortex during the postnatal period implications for the development of psychopathology. *Cerebral cortex* 10: 1014-27

Bersani FS, Minichino A, Fojanesi M, Gallo M, Maglio G, *et al*. **2014.** Cingulate Cortex in Schizophrenia: its relation with negative symptoms and psychotic onset. A review study. *European review for medical and pharmacological sciences* 18: 3354-67

Beveridge TJ, Mechan AO, Sprakes M, Pei Q, Zetterstrom TS, *et al*. **2004.** Effect of 5-HT depletion by MDMA on hyperthermia and Arc mRNA induction in rat brain. *Psychopharmacology* 173: 346-52

Bhagat SM, Butler SS, Taylor JR, McEwen BS, Strittmatter SM. **2015.** Erasure of fear memories is prevented by Nogo Receptor 1 in adulthood. *Molecular psychiatry*

Bianco IH, Wilson SW. **2009.** The habenular nuclei: a conserved asymmetric relay station in the ver-

tebrate brain. *Philosophical transactions of the Royal Society of London. Series B, Biological sciences* 364: 1005-20

Bick-Sander A. **2002.** Modifikation des genomischen Arg3.1 Lokus. Doktorarbeit thesis. *Universität Hamburg*, Hamburg. 117 pp.

Bicks LK, Koike H, Akbarian S, Morishita H. **2015.** Prefrontal Cortex and Social Cognition in Mouse and Man. *Frontiers in psychology* 6: 1805

Binkle L. **2014.** Untersuchugen zur Rolle von Arc/Arg3.1 in synpatischer Plastizität und endosomaler Sortierung. *Universität Hamburg*, Hamburg. 133 pp.

Bissiere S, Plachta N, Hoyer D, McAllister KH, Olpe HR, *et al*. **2008.** The rostral anterior cingulate cortex modulates the efficiency of amygdala-dependent fear learning. *Biological psychiatry* 63: 821-31

Bliss TV, Lomo T. **1973.** Long-lasting potentiation of synaptic transmission in the dentate area of the anaesthetized rabbit following stimulation of the perforant path. *The Journal of physiology* 232: 331-56

Blum S, Hebert AE, Dash PK. **2006.** A role for the prefrontal cortex in recall of recent and remote memories. *Neuroreport* 17: 341-4

Borre YE, O'Keeffe GW, Clarke G, Stanton C, Dinan TG, Cryan JF. **2014.** Microbiota and neurodevelopmental windows: implications for brain disorders. *Trends in molecular medicine* 20: 509-18

Botta P, Demmou L, Kasugai Y, Markovic M, Xu C, *et al*. **2015.** Regulating anxiety with extrasynaptic inhibition. *Nature neuroscience* 18: 1493-500

Bourgeron T. **2015.** From the genetic architecture to synaptic plasticity in autism spectrum disorder. Nature reviews. *Neuroscience* 16: 551-63

Boyce R, Glasgow SD, Williams S, Adamantidis A. **2016.** Causal evidence for the role of REM sleep theta rhythm in contextual memory consolidation. *Science* 352: 812-6

Brackmann M, Zhao C, Kuhl D, Manahan-Vaughan D, Braunewell KH. **2004.** MGluRs regulate the expression of neuronal calcium sensor proteins NCS-1 and VILIP-1 and the immediate early gene arg3.1/arc in the hippocampus *in vivo*. *Biochemical and biophysical research communications* 322: 1073-9

Bramham CR, Alme MN, Bittins M, Kuipers SD, Nair RR, *et al*. **2010.** The Arc of synaptic memory. *Experimental brain research* 200: 125-40

Brockmann MD, Poschel B, Cichon N, Hanganu-Opatz IL. **2011.** Coupled oscillations mediate directed interactions between prefrontal cortex and hippocampus of the neonatal rat. *Neuron* 71: 332-47

Bucy PC, Kluver H. **1955.** An anatomical investigation of the temporal lobe in the monkey (Macaca mulatta). *The Journal of comparative neurology* 103: 151-251

Budson AE, Price BH. **2001.** Memory: Clinical Disorders In *ENCYCLOPEDIA OF LIFE SCIENCES*

Buhl DL, Buzsaki G. **2005.** Developmental emergence of hippocampal fast-field "ripple" oscillations in the behaving rat pups. *Neuroscience* 134: 1423-30

Buzsaki G, Buhl DL, Harris KD, Csicsvari J, Czeh B, Morozov A. **2003.** Hippocampal network patterns of activity in the mouse. *Neuroscience* 116: 201-11

Buzsaki G, Moser EI. **2013.** Memory, navigation and theta rhythm in the hippocampal-entorhinal system. *Nature neuroscience* 16: 130-8

Caley DW, Maxwell DS. **1968a**. An electron microscopic study of neurons during postnatal development of the rat cerebral cortex. *The Journal of comparative neurology* 133: 17-44

Caley DW, Maxwell DS. **1968b.** An electron microscopic study of the neuroglia during postnatal development of the rat cerebrum. *The Journal of comparative neurology* 133: 45-70

Caley DW, Maxwell DS. **1970.** Development of the blood vessels and extracellular spaces during postnatal maturation of rat cerebral cortex. *The Journal of comparative neurology* 138: 31-47

Callaghan BL, Richardson R. **2012.** The effect of adverse rearing environments on persistent memories in young rats: removing the brakes on infant fear memories. *Translational psychiatry* 2: e138

Cao VY, Ye Y, Mastwal S, Ren M, Coon M, *et al*. **2015.** Motor Learning Consolidates Arc-Expressing Neuronal Ensembles in Secondary Motor Cortex. *Neuron* 86: 1385-92

Casanova E, Fehsenfeld S, Mantamadiotis T, Lemberger T, Greiner E, *et al*. **2001.** A CamKIIalpha iCre BAC allows brain-specific gene inactivation. *Genesis* 31: 37-42

Cetin A, Komai S, Eliava M, Seeburg PH, Osten P. **2006.** Stereotaxic gene delivery in the rodent brain. *Nature protocols* 1: 3166-73

Chee SS, Menard JL, Dringenberg HC. **2015.** The lateral septum as a regulator of hippocampal theta

oscillations and defensive behavior in rats. *Journal of neurophysiology* 113: 1831-41
Chen DY, Stern SA, Garcia-Osta A, Saunier-Rebori B, Pollonini G, *et al*. **2011.** A critical role for IGF-II in memory consolidation and enhancement. *Nature* 469: 491-7
Chia C, Otto T. **2013.** Hippocampal Arc (Arg3.1) expression is induced by memory recall and required for memory reconsolidation in trace fear conditioning. *Neurobiol Learn Mem* 106: 48-55
Choudhury SR, Hudry E, Maguire CA, Sena-Esteves M, Breakefield XO, Grandi P. **2016.** Viral vectors for therapy of neurologic diseases. *Neuropharmacology*
Chowdhury S, Shepherd JD, Okuno H, Lyford G, Petralia RS, *et al*. **2006.** Arc/Arg3.1 interacts with the endocytic machinery to regulate AMPA receptor trafficking. *Neuron* 52: 445-59
Christensen A, Dewing P, Micevych P. **2015.** Immediate early gene activity-regulated cytoskeletal-associated protein regulates estradiol-induced lordosis behavior in female rats. *Journal of neuroscience research* 93: 67-74
Chung K, Wallace J, Kim SY, Kalyanasundaram S, Andalman AS, *et al*. **2013.** Structural and molecular interrogation of intact biological systems. *Nature* 497: 332-7
Ciocchi S, Herry C, Grenier F, Wolff SB, Letzkus JJ, *et al*. **2010.** Encoding of conditioned fear in central amygdala inhibitory circuits. *Nature* 468: 277-82
Clemens Z, Molle M, Eross L, Barsi P, Halasz P, Born J. **2007.** Temporal coupling of parahippocampal ripples, sleep spindles and slow oscillations in humans. *Brain: a journal of neurology* 130: 2868-78
Colgin LL. **2013.** Mechanisms and functions of theta rhythms. *Annual review of neuroscience* 36: 295-312
Courtin J, Chaudun F, Rozeske RR, Karalis N, Gonzalez-Campo C, *et al*. **2014.** Prefrontal parvalbumin interneurons shape neuronal activity to drive fear expression. *Nature* 505: 92-6
Crawley J, Goodwin FK. **1980.** Preliminary report of a simple animal behavior model for the anxiolytic effects of benzodiazepines. *Pharmacology, biochemistry, and behavior* 13: 167-70
Cryan JF, Holmes A. **2005.** The ascent of mouse: advances in modelling human depression and anxiety. Nature reviews. *Drug discovery* 4: 775-90
Czerniawski J, Ree F, Chia C, Ramamoorthi K, Kumata Y, Otto TA. **2011.** The importance of having Arc: expression of the immediate-early gene Arc is required for hippocampus-dependent fear conditioning and blocked by NMDA receptor antagonism. *The Journal of neuroscience : the official journal of the Society for Neuroscience* 31: 11200-7
Damasio A, Carvalho GB. **2013.** The nature of feelings: evolutionary and neurobiological origins. Nature reviews. *Neuroscience* 14: 143-52
Dammermann B. **1999.** Herstellung und Charakterisierung einer arg3.1-Knockout-Maus. Doctoral thesis thesis. *Universität Hamburg*, Berlin. 164 pp.
Damsa C, Kosel M, Moussally J. **2009.** Current status of brain imaging in anxiety disorders. *Current opinion in psychiatry* 22: 96-110
Davidson BL, Stein CS, Heth JA, Martins I, Kotin RM, *et al*. **2000.** Recombinant adeno-associated virus type 2, 4, and 5 vectors: transduction of variant cell types and regions in the mammalian central nervous system. *Proceedings of the National Academy of Sciences of the United States of America* 97: 3428-32
Davis M, Walker DL, Miles L, Grillon C. **2010.** Phasic vs sustained fear in rats and humans: role of the extended amygdala in fear vs anxiety. *Neuropsychopharmacology : official publication of the American College of Neuropsychopharmacology* 35: 105-35
de Felipe P, Luke GA, Hughes LE, Gani D, Halpin C, Ryan MD. **2006.** E unum pluribus: multiple proteins from a self-processing polyprotein. T*rends in biotechnology* 24: 68-75
de Solis CA, Holehonnur R, Banerjee A, Luong JA, Lella SK, *et al*. **2015.** Viral delivery of shRNA to amygdala neurons leads to neurotoxicity and deficits in Pavlovian fear conditioning. *Neurobiol Learn Mem* 124: 34-47
Decker MW, Curzon P, Brioni JD. **1995.** Influence of separate and combined septal and amygdala lesions on memory, acoustic startle, anxiety, and locomotor activity in rats. *Neurobiol Learn Mem* 64: 156-68
Denny CA, Kheirbek MA, Alba EL, Tanaka KF, Brachman RA, *et al*. **2014.** Hippocampal memory traces are differentially modulated by experience, time, and adult neurogenesis. *Neuron* 83: 189-201
Diba K, Buzsaki G. **2007.** Forward and reverse hippocampal place-cell sequences during ripples. *Nature neuroscience* 10: 1241-2

DiMasi JA, Hansen RW, Grabowski HG. **2003.** The price of innovation: new estimates of drug development costs. *Journal of Health Economics* 22: 151-85

Dittgen T, Nimmerjahn A, Komai S, Licznerski P, Waters J, *et al*. **2004.** Lentivirus-based genetic manipulations of cortical neurons and their optical and electrophysiological monitoring *in vivo*. *Proceedings of the National Academy of Sciences of the United States of America* 101: 18206-11

Dudai Y. **2012.** The restless engram: consolidations never end. *Annual review of neuroscience* 35: 227-47

Dudai Y, Karni A, Born J. **2015.** The Consolidation and Transformation of Memory. *Neuron* 88: 20-32

Dudek SM, Bear MF. **1992.** Homosynaptic long-term depression in area CA1 of hippocampus and effects of N-methyl D-aspartate receptor blockade. *Proceedings of the National Academy of Sciences of the United States of America* 89: 4363-67

Dutta A, McKie S, Deakin JF. **2014.** Resting state networks in major depressive disorder. *Psychiatry research* 224: 139-51

Eberle AB, Visa N. **2014.** Quality control of mRNP biogenesis: networking at the transcription site. *Seminars in cell & developmental biology* 32: 37-46

Ego-Stengel V, Wilson MA. **2010.** Disruption of ripple-associated hippocampal activity during rest impairs spatial learning in the rat. *Hippocampus* 20: 1-10

Eluvathingal TJ, Chugani HT, Behen ME, Juhasz C, Muzik O, *et al*. **2006.** Abnormal brain connectivity in children after early severe socioemotional deprivation: a diffusion tensor imaging study. *Pediatrics* 117: 2093-100

Ennaceur A, Delacour J. **1988.** A new one-trial test for neurobiological studies of memory in rats. 1: Behavioral data. *Behavioural brain research* 31: 47-59

Etkin A, Egner T, Kalisch R. **2011.** Emotional processing in anterior cingulate and medial prefrontal cortex. *Trends Cogn Sci* 15: 85-93

Evans WO. **1961.** A comparison of the analgetic potency of some opiates as measured by the "flinch-jump" procedure. Report. *Army Medical Research Laboratory*: 1-5

Fagiolini M, Katagiri H, Miyamoto H, Mori H, Grant SG, *et al*. **2003.** Separable features of visual cortical plasticity revealed by N-methyl-D-aspartate receptor 2A signaling. *Proceedings of the National Academy of Sciences of the United States of America* 100: 2854-9

Feil R. **1996.** Ligand-activated site-specific recombination in mice. *Proceedings of the National Academy of Sciences of the United States of America* 93: 10887-90

Felix-Ortiz AC, Beyeler A, Seo C, Leppla CA, Wildes CP, Tye KM. **2013.** BLA to vHPC inputs modulate anxiety-related behaviors. *Neuron* 79: 658-64

Forni PE, Scuoppo C, Imayoshi I, Taulli R, Dastru W, *et al*. **2006.** High levels of Cre expression in neuronal progenitors cause defects in brain development leading to microencephaly and hydrocephaly. *The Journal of neuroscience : the official journal of the Society for Neuroscience* 26: 9593-602

Frankland PW, Bontempi B. **2005.** The organization of recent and remote memories. *Nature reviews. Neuroscience* 6: 119-30

Frey U, Huang YY, Kandel ER. **1993.** Effects of cAMP simulate a late stage of LTP in hippocampal CA1 neurons. *Science* 260: 1661-4

Fromer M, Pocklington AJ, Kavanagh DH, Williams HJ, Dwyer S, *et al*. **2014.** *De novo* mutations in schizophrenia implicate synaptic networks. *Nature* 506: 179-84

Frysztak RJ, Neafsey EJ. **1991.** The effect of medial frontal cortex lesions on respiration, freezing, and ultrasonic vocalizations during conditioned emotional responses in rats. *Cerebral cortex* 1: 418-25

Fukazawa' Y, Saitoh Y, Ozawa F, Ohta Y, Mizuno K, Inokuchi K. **2003.** Hippocampal LTP is accompanied by enhanced F-actin content within the dendritic spine that is essential for late LTP maintenance *in vivo*. *Neuron* 38: 447-60

Galef BG, Jr., Kaner HC. **1980.** Establishment and maintenance of preference for natural and artificial olfactory stimuli in juvenile rats. *Journal of comparative and physiological psychology* 94: 588-95

Gama Sosa MA, De Gasperi R, Elder GA. **2010.** Animal transgenesis: an overview. *Brain structure & function* 214: 91-109

Gao M, Sossa K, Song L, Errington L, Cummings L, *et al*. **2010.** A specific requirement of Arc/Arg3.1 for visual experience-induced homeostatic synaptic plasticity in mouse primary visual cortex. The *Journal of neuroscience : the official journal of the Society for Neuroscience* 30: 7168-78

Gao Y, Tatavarty V, Korza G, Levin MK, Carson JH. **2008.** Multiplexed dendritic targeting of alpha

calcium calmodulin-dependent protein kinase II, neurogranin, and activity-regulated cytoskeleton-associated protein RNAs by the A2 pathway. *Molecular biology of the cell* 19: 2311-27

García Márquez G. **1967.** Cien años de soledad. Editorial Sudamericana. 471 pp.

Gilmartin MR, Helmstetter FJ. **2010.** Trace and contextual fear conditioning require neural activity and NMDA receptor-dependent transmission in the medial prefrontal cortex. *Learning & memory* 17: 289-96

Giorgi C, Yeo GW, Stone ME, Katz DB, Burge C, *et al*. **2007.** The EJC factor eIF4AIII modulates synaptic strength and neuronal protein expression. *Cell* 130: 179-91

Girardeau G, Benchenane K, Wiener SI, Buzsaki G, Zugaro MB. **2009.** Selective suppression of hippocampal ripples impairs spatial memory. *Nature neuroscience* 12: 1222-3

Gogolla N, Caroni P, Luthi A, Herry C. **2009.** Perineuronal nets protect fear memories from erasure. Science 325: 1258-61

Gonzalez-Burgos G, Cho RY, Lewis DA. **2015.** Alterations in cortical network oscillations and parvalbumin neurons in schizophrenia. *Biological psychiatry* 77: 1031-40

Gonzalez MC, Villar ME, Igaz LM, Viola H, Medina JH. **2015.** Dorsal medial prefrontal cortex contributes to conditioned taste aversion memory consolidation and retrieval. *Neurobiology of Learning and Memory 126*: 1-6

Goshen I, Brodsky M, Prakash R, Wallace J, Gradinaru V, *et al*. **2011.** Dynamics of retrieval strategies for remote memories. *Cell* 147: 678-89

Goutagny R, Loureiro M, Jackson J, Chaumont J, Williams S, *et al*. **2013.** Interactions between the lateral habenula and the hippocampus: implication for spatial memory processes. *Neuropsychopharmacology : official publication of the American College of Neuropsychopharmacology* 38: 2418-26

Gouty-Colomer LA, Hosseini B, Marcelo IM, Schreiber J, Slump DE, *et al*. **2016.** Arc expression identifies the lateral amygdala fear memory trace. *Molecular psychiatry 21*: 364-75

Gozzi A, Schwarz AJ. **2016.** Large-scale functional connectivity networks in the rodent brain. *NeuroImage* 127: 496-509

Graham FL, Smiley J, Russell WC, Nairn R. **1977.** Characteristics of a human cell line transformed by DNA from human adenovirus type 5. *The Journal of general virology* 36: 59-74

Greer PL, Hanayama R, Bloodgood BL, Mardinly AR, Lipton DM, *et al*. **2010.** The Angelman Syndrome protein Ube3A regulates synapse development by ubiquitinating arc. *Cell* 140: 704-16

Grieger JC, Choi VW, Samulski RJ. **2006.** Production and characterization of adeno-associated viral vectors. *Nature protocols* 1: 1412-28

Grimm. **1998.** Novel tools for production and purification of recombinant adenoassociated virus vectors. *Human gene therapy* 9: 2745-60

Gruest N, Richer P, Hars B. 2004a. Emergence of long-term memory for conditioned aversion in the rat fetus. Developmental psychobiology 44: 189-98

Gruest N, Richer P, Hars B. 2004b. Memory consolidation and reconsolidation in the rat pup require protein synthesis. *The Journal of neuroscience : the official journal of the Society for Neuroscience* 24: 10488-92

Gu H. **2013.** Independent control of immunoglobulin switch recombination at individual switch regions evidenced through Cre-loxP-mediated gene targeting. *J Immunol* 191: 7-16

Guilfoyle DN, Gerum SV, Sanchez JL, Balla A, Sershen H, *et al*. **2013.** Functional connectivity fMRI in mouse brain at 7T using isoflurane. *Journal of neuroscience methods* 214: 144-8

Guillozet-Bongaarts AL, Hyde TM, Dalley RA, Hawrylycz MJ, Henry A, *et al*. **2014.** Altered gene expression in the dorsolateral prefrontal cortex of individuals with schizophrenia. *Molecular psychiatry* 19: 478-85

Guthrie K, Rayhanabad J, Kuhl D, Gall C. **2000.** Odors regulate Arc expression in neuronal ensembles engaged in odor processing. *Neuroreport* 11: 1809-13

Guzowski JF, Lyford GL, Stevenson GD, Houston FP, McGaugh JL, *et al*. **2000a**. Inhibition of activity-dependent arc protein expression in the rat hippocampus impairs the maintenance of long-term potentiation and the consolidation of long-term memory. *The Journal of neuroscience : the official journal of the Society for Neuroscience* 20: 3993-4001

Guzowski JF, Lyford GL, Stevenson GD, Houston FP, McGaugh JL, *et al*. **2000b**. Inhibition of Arc Protein Expression in the Rat Hippocampus Impairs the Maintenance of Long-Term Potentiation and

the Consolidation of Long-Term Memory. *The Journal of neuroscience : the official journal of the Society for Neuroscience* 20: 3993-4001

Hammond RS, Tull LE, Stackman RW. **2004.** On the delay-dependent involvement of the hippocampus in object recognition memory. *Neurobiol Learn Mem* 82: 26-34

Han Y, Chang QA, Virag T, West NC, George D, *et al*. **2010.** Lack of humoral immune response to the tetracycline (Tet) activator in rats injected intracranially with Tet-off rAAV vectors. *Gene therapy* 17: 616-25

Hannigan JH, Jr., Springer JE, Isaacson RL. **1984.** Differentiation of basal ganglia dopaminergic involvement in behavior after hippocampectomy. *Brain research* 291: 83-91

Harris EW, Ganong AH, Cotman CW. **1984.** Long-term potentiation in the hippocampus involves activation of N-methyl-D-aspartate receptors. *Brain research* 323: 132-7

Hazan L, Zugaro M, Buzsaki G. **2006.** Klusters, NeuroScope, NDManager: a free software suite for neurophysiological data processing and visualization. *Journal of neuroscience methods* 155: 207-16

Hearing MC, Schwendt M, McGinty JF. **2011.** Suppression of activity-regulated cytoskeleton-associated gene expression in the dorsal striatum attenuates extinction of cocaine-seeking. *The international journal of neuropsychopharmacology / official scientific journal of the Collegium Internationale Neuropsychopharmacologicum* 14: 784-95

Heidbreder CA, Groenewegen HJ. **2003.** The medial prefrontal cortex in the rat: evidence for a dorso-ventral distinction based upon functional and anatomical characteristics. *Neuroscience & Biobehavioral Reviews* 27: 555-79

Hellstrom M, Ruitenberg MJ, Pollett MA, Ehlert EM, Twisk J, *et al*. **2009.** Cellular tropism and transduction properties of seven adeno-associated viral vector serotypes in adult retina after intravitreal injection. *Gene therapy* 16: 521-32

Henke K. **2010.** A model for memory systems based on processing modes rather than consciousness. *Nature Reviews Neuroscience* 11: 523-32

Hirata RK, Russell DW. **2000.** Design and Packaging of Adeno-Associated Virus Gene Targeting Vectors. *Journal of virology* 74: 4612-20

Holloway CM, McIntyre CK. **2011.** Post-training disruption of Arc protein expression in the anterior cingulate cortex impairs long-term memory for inhibitory avoidance training. *Neurobiol Learn Mem* 95: 425-32

Huentelman MJ, Muppana L, Corneveaux JJ, Dinu V, Pruzin JJ, *et al*. **2015.** Association of SNPs in EGR3 and ARC with Schizophrenia Supports a Biological Pathway for Schizophrenia Risk. *PloS one* 10: e0135076

Hunter J, Rivero-Arias O, Angelov A, Kim E, Fotheringham I, Leal J. **2014.** Epidemiology of fragile X syndrome: a systematic review and meta-analysis. *American journal of medical genetics*. Part A 164A: 1648-58

Husi H, Ward MA, Choudhary JS, Blackstock WP, Grant SG. **2000.** Proteomic analysis of NMDA receptor-adhesion protein signaling complexes. *Nature neuroscience* 3: 661-9

Huttenlocher PR, Dabholkar AS. **1997.** Regional differences in synaptogenesis in human cerebral cortex. *The Journal of comparative neurology* 387: 167-78

Izquierdo I, Furini CR, Myskiw JC. **2016.** Fear Memory. *Physiological reviews* 96: 695-750

Janak PH, Tye KM. **2015.** From circuits to behaviour in the amygdala. *Nature* 517: 284-92

Jiang YH, Armstrong D, Albrecht U, Atkins CM, Noebels JL, *et al*. **1998.** Mutation of the Angelman Ubiquitin Ligase in Mice Causes Increased Cytoplasmic p53 and Deficits of Contextual Learning and Long-Term Potentiation. *Neuron* 21: 799-811

Jitsuki S, Takemoto K, Kawasaki T, Tada H, Takahashi A, *et al*. **2011.** Serotonin mediates cross-modal reorganization of cortical circuits. *Neuron* 69: 780-92

Kauderer BS, Kandel ER. **2000.** Capture of a protein synthesis-dependent component of long-term depression. *Proceedings of the National Academy of Sciences of the United States of America* 97: 13342-7

Kawashima T, Okuno H, Nonaka M, Adachi-Morishima A, Kyo N, *et al*. **2009.** Synaptic activity-responsive element in the Arc/Arg3.1 promoter essential for synapse-to-nucleus signaling in activated neurons. *Proceedings of the National Academy of Sciences of the United States of America* 106: 316-21

Kelly PT, Vernon P. **1985.** Changes in the subcellular distribution of calmodulin-kinase II during brain development. *Brain research* 350: 211-24

Kemp A, Tischmeyer W, Manahan-Vaughan D. **2013.** Learning-facilitated long-term depression requires activation of the immediate early gene, c-fos, and is transcription dependent. *Behavioural brain research* 254: 83-91

Kim J, Kwon JT, Kim HS, Josselyn SA, Han JH. **2014.** Memory recall and modifications by activating neurons with elevated CREB. *Nature neuroscience* 17: 65-72

Kim J, Matney CJ, Roth RH, Brown SP. **2016.** Synaptic Organization of the Neuronal Circuits of the Claustrum. *The Journal of neuroscience : the official journal of the Society for Neuroscience* 36: 773-84

Kim SS, Wang H, Li XY, Chen T, Mercaldo V, *et al*. **2011.** Neurabin in the anterior cingulate cortex regulates anxiety-like behavior in adult mice. *Molecular brain* 4: 6

Kim SY, Adhikari A, Lee SY, Marshel JH, Kim CK, *et al*. **2013.** Diverging neural pathways assemble a behavioural state from separable features in anxiety. *Nature* 496: 219-23

Kim Y, Venkataraju KU, Pradhan K, Mende C, Taranda J, *et al*. **2015.** Mapping social behavior-induced brain activation at cellular resolution in the mouse. *Cell reports* 10: 292-305

Kirov G, Pocklington AJ, Holmans P, Ivanov D, Ikeda M, *et al*. **2012.** *De novo* CNV analysis implicates specific abnormalities of postsynaptic signalling complexes in the pathogenesis of schizophrenia. *Molecular psychiatry* 17: 142-53

Kjelstrup KG, Tuvnes FA, Steffenach HA, Murison R, Moser EI, Moser MB. **2002.** Reduced fear expression after lesions of the ventral hippocampus. *Proceedings of the National Academy of Sciences of the United States of America* 99: 10825-30

Kobayashi H, Yamamoto S, Maruo T, Murakami F. **2005.** Identification of a cis-acting element required for dendritic targeting of activity-regulated cytoskeleton-associated protein mRNA. *The European journal of neuroscience* 22: 2977-84

Koga K, Descalzi G, Chen T, Ko HG, Lu J, *et al*. **2015.** Coexistence of two forms of LTP in ACC provides a synaptic mechanism for the interactions between anxiety and chronic pain. *Neuron* 85: 377-89

Korb E, Wilkinson CL, Delgado RN, Lovero KL, Finkbeiner S. **2013.** Arc in the nucleus regulates PML-dependent GluA1 transcription and homeostatic plasticity. *Nature neuroscience* 16: 874-83

Kosofsky BE, Genova LM, Hyman SE. **1995.** Postnatal age defines specificity of immediate early gene induction by cocaine in developing rat brain. *The Journal of comparative neurology* 351: 27-40

Kotterman MA, Schaffer DV. **2014.** Engineering adeno-associated viruses for clinical gene therapy. Nature reviews. *Genetics* 15: 445-51

Krakauer JW, Shadmehr R. **2006.** Consolidation of motor memory. *Trends Neurosci* 29: 58-64

Kreitzer AC, Malenka RC. **2008.** Striatal plasticity and basal ganglia circuit function. *Neuron* 60: 543-54

Kudrimoti HS, Barnes CA, McNaughton BL. **1999.** Reactivation of hippocampal cell assemblies: effects of behavioral state, experience, and EEG dynamics. T*he Journal of neuroscience : the official journal of the Society for Neuroscience* 19: 4090-101

Kugler S, Kilic E, Bahr M. **2003.** Human synapsin 1 gene promoter confers highly neuron-specific long-term transgene expression from an adenoviral vector in the adult rat brain depending on the transduced area. *Gene therapy* 10: 337-47

Kuhl PK. **2010.** Brain mechanisms in early language acquisition. *Neuron* 67: 713-27

Kuipers SD, Trentani A, Tiron A, Mao X, Kuhl D, Bramham CR. **2016.** BDNF-induced LTP is associated with rapid Arc/Arg3.1-dependent enhancement in adult hippocampal neurogenesis. *Scientific reports* 6: 21222

Kumar V, Fahey PG, Jong YJ, Ramanan N, O'Malley KL. **2012.** Activation of intracellular metabotropic glutamate receptor 5 in striatal neurons leads to up-regulation of genes associated with sustained synaptic transmission including Arc/Arg3.1 protein. *The Journal of biological chemistry* 287: 5412-25

Kwapis JL, Jarome TJ, Helmstetter FJ. **2014.** The role of the medial prefrontal cortex in trace fear extinction. *Learning & memory* 22: 39-46

Lacroix L, Spinelli S, Heidbreder CA, Feldon J. **2000.** Differential role of the medial and lateral prefrontal cortices in fear and anxiety. *Behavioral neuroscience* 114: 1119-30

Lahtinen H, Palva JM, Sumanen S, Voipio J, Kaila K, Taira T. **2002.** Postnatal development of rat hippocampal gamma rhythm *in vivo*. *Journal of neurophysiology* 88: 1469-74

Lamprea MR, Cardenas FP, Silveira R, Morato S, Walsh TJ. **2000.** Dissociation of memory and anxiety in a repeated elevated plus maze. *Behavioural brain research* 117: 97-105

Larson-Prior LJ, Ju YE, Galvin JE. **2014.** Cortical-subcortical interactions in hypersomnia disorders: mechanisms underlying cognitive and behavioral aspects of the sleep-wake cycle. *Front Neurol* 5: 165

LeDoux J. **2000.** Emotion circuits in the brain. *Annual review of neuroscience* 23: 155-84

LeDoux JE. **2014.** Coming to terms with fear. *Proceedings of the National Academy of Sciences of the United States of America* 111: 2871-8

Leone P, Shera D, McPhee SW, Francis JS, Kolodny EH, *et al*. **2012.** Long-Term Follow-Up After Gene Therapy for Canavan Disease. *Science translational medicine* 4: 165ra63

Levine S, Alpert M, Lewis GW. **1957.** Infantile experience and the maturation of the pituitary adrenal axis. *Science* 126: 1347

Li Y, Pehrson AL, Waller JA, Dale E, Sanchez C, Gulinello M. **2015.** A critical evaluation of the activity-regulated cytoskeleton-associated protein (Arc/Arg3.1)'s putative role in regulating dendritic plasticity, cognitive processes, and mood in animal models of depression. *Frontiers in neuroscience* 9: 279

Liao D, Malinow R. **1996.** Deficiency in Induction but not expression of LTP in hippocampal slices from young rats. *Learning & memory* 3: 138-49

Likhtik E, Stujenske JM, Topiwala MA, Harris AZ, Gordon JA. **2014.** Prefrontal entrainment of amygdala activity signals safety in learned fear and innate anxiety. *Nature neuroscience* 17: 106-13

Link W, Konietzko U, Kauselmann G, Krug M, Schwanke B, *et al*. **1995.** Somatodendritic expression of an immediate early gene is regulated by synaptic activity. *Proceedings of the National Academy of Sciences of the United States of America* 92: 5734-38

Lisman J, Yasuda R, Raghavachari S. **2012.** Mechanisms of CaMKII action in long-term potentiation. Nature reviews. *Neuroscience* 13: 169-82

Lisman JE, Jensen O. **2013.** The theta-gamma neural code. *Neuron* 77: 1002-16

Lister RG. **1987.** The use of a plus-maze to measure anxiety in the mouse. *Psychopharmacology* 92: 180-5

Liu Y, Zhou QX, Hou YY, Lu B, Yu C, *et al*. **2012.** Actin polymerization-dependent increase in synaptic Arc/Arg3.1 expression in the amygdala is crucial for the expression of aversive memory associated with drug withdrawal. *The Journal of neuroscience : the official journal of the Society for Neuroscience* 32: 12005-17

Logan DW, Brunet LJ, Webb WR, Cutforth T, Ngai J, Stowers L. **2012.** Learned recognition of maternal signature odors mediates the first suckling episode in mice. *Current biology* : CB 22: 1998-2007

Lohmann C, Kessels HW. **2014.** The developmental stages of synaptic plasticity. *The Journal of physiology* 592: 13-31

Loonstra A, Vooijs M, Beverloo HB, Allak BA, van Drunen E, *et al*. **2001.** Growth inhibition and DNA damage induced by Cre recombinase in mammalian cells. *Proceedings of the National Academy of Sciences of the United States of America* 98: 9209-14

Lorenz K. **1935.** Der Kumpan in der Umwelt des Vogels – Der Artgenosse als auslösendes Moment sozialer Verhaltensweisen. *Journal für Ornithologie* 83: 137-213

Lv XF, Xu Y, Han JS, Cui CL. **2011.** Expression of activity-regulated cytoskeleton-associated protein (Arc/Arg3.1) in the nucleus accumbens is critical for the acquisition, expression and reinstatement of morphine-induced conditioned place preference. *Behavioural brain research* 223: 182-91

Lyford GL, Yamagata K, Kaufmann WE, Barnes CA, Sanders LK, *et al*. **1995.** Arc, a Growth-Factor and Activity-Regulated Gene, Encodes a Novel Cytoskeleton-Associated Protein That Is Enriched in Neuronal Dendrites. *Neuron* 14: 433-45

Lynn DA, Brown GR. **2010.** The ontogeny of anxiety-like behavior in rats from adolescence to adulthood. *Developmental psychobiology* 52: 731-9

Macrì S, Adriani W, Chiarotti F, Laviola G. **2002.** Risk taking during exploration of a plus-maze is greater in adolescent than in juvenile or adult mice. *Animal behaviour* 64: 541-46

Maddox SA, Schafe GE. **2011.** The activity-regulated cytoskeletal-associated protein (Arc/Arg3.1) is required for reconsolidation of a Pavlovian fear memory. *The Journal of neuroscience : the official journal of the Society for Neuroscience* 31: 7073-82

Malenka RC, Bear MF. **2004.** LTP and LTD: an embarrassment of riches. *Neuron* 44: 5-21

Maren S, Holt WG. **2004.** Hippocampus and Pavlovian fear conditioning in rats: muscimol infusions into the ventral, but not dorsal, hippocampus impair the acquisition of conditional freezing to an auditory conditional stimulus. *Behavioral neuroscience* 118: 97-110

Margolis SS, Sell GL, Zbinden MA, Bird LM. **2015.** Angelman Syndrome. *Neurotherapeutics : the journal of the American Society for Experimental NeuroTherapeutics* 12: 641-50

Marin O, Rubenstein JL. **2003.** Cell migration in the forebrain. Annual review of neuroscience 26: 441-83

Maroun M, Wagner S. **2016.** Oxytocin and Memory of Emotional Stimuli: Some Dance to Remember, Some Dance to Forget. *Biological psychiatry* 79: 203-12

Martin SJ, Grimwood PD, Morris RG. **2000.** Synaptic Plasticity and Memory: An Evaluation of the Hypothesis. *Annual review of neuroscience* 23: 649-711

Martinez MC, Alen N, Ballarini F, Moncada D, Viola H. **2012.** Memory traces compete under regimes of limited Arc protein synthesis: implications for memory interference. *Neurobiol Learn Mem* 98: 165-73

Matsuda T, Cepko CL. **2007.** Controlled expression of transgenes introduced by *in vivo* electroporation. *Proceedings of the National Academy of Sciences of the United States of America* 104: 1027-32

Matsuoka M, Yoshida-Matsuoka J, Sugiura H, Yamagata K, Ichikawa M, Norita M. **2002.** Mating behavior induces differential Arc expression in the main and accessory olfactory bulbs of adult rats. *Neuroscience letters* 335: 111-4

Matsutani S, Yamamoto N. **2004.** Postnatal development of dendritic spines on olfactory bulb granule cells in rats. *The Journal of comparative neurology* 473: 553-61

Maurer D, Lewis TL, Brent HP, Levin AV. **1999.** Rapid improvement in the acuity of infants after visual input. *Science* 286: 108-10

Mayford M, Bach ME, Huang YY, Wang L, Hawkins RD, Kandel ER. **1996.** Control of memory formation through regulated expression of a CaMKII transgene. *Science* 274: 1678-83

McCarty DM, Young SM, Jr., Samulski RJ. **2004.** Integration of adeno-associated virus (AAV) and recombinant AAV vectors. *Annual review of genetics* 38: 819-45

McCurry CL, Shepherd JD, Tropea D, Wang KH, Bear MF, Sur M. **2010.** Loss of Arc renders the visual cortex impervious to the effects of sensory experience or deprivation. *Nature neuroscience* 13: 450-7

McDonald AJ. **1982.** Neurons of the lateral and basolateral amygdaloid nuclei: a Golgi study in the rat. *The Journal of comparative neurology* 212: 293-312

McDonald AJ. **1998.** CORTICAL PATHWAYS TO THE MAMMALIAN AMYGDALA. *Progress in neurobiology* 55: 257-332

McHugh TJ, Jones MW, Quinn JJ, Balthasar N, Coppari R, *et al*. **2007.** Dentate gyrus NMDA receptors mediate rapid pattern separation in the hippocampal network. *Science* 317: 94-9

McReynolds JR, Holloway-Erickson CM, Parmar TU, McIntyre CK. **2014.** Corticosterone-induced enhancement of memory and synaptic Arc protein in the medial prefrontal cortex. *Neurobiol Learn Mem* 112: 148-57

Meier ID, Bernreuther C, Tilling T, Neidhardt J, Wong YW, *et al*. **2010.** Short DNA sequences inserted for gene targeting can accidentally interfere with off-target gene expression. *FASEB journal : official publication of the Federation of American Societies for Experimental Biology* 24: 1714-24

Messaoudi E, Kanhema T, Soule J, Tiron A, Dagyte G, *et al*. **2007.** Sustained Arc/Arg3.1 synthesis controls long-term potentiation consolidation through regulation of local actin polymerization in the dentate gyrus *in vivo*. *The Journal of neuroscience : the official journal of the Society for Neuroscience* 27: 10445-55

Mikuni T, Uesaka N, Okuno H, Hirai H, Deisseroth K, *et al*. **2013.** Arc/Arg3.1 is a postsynaptic mediator of activity-dependent synapse elimination in the developing cerebellum. *Neuron* 78: 1024-35

Miller JA. **1991.** The calibration of 35S or 32P with 14C-labeled brain paste or 14C-plastic standards for quantitative autoradiography using LKB Ultrofilm or Amersham Hyperfilm. *Neuroscience letters* 121: 211-4

Mochcovitch MD, da Rocha Freire RC, Garcia RF, Nardi AE. **2014.** A systematic review of fMRI studies in generalized anxiety disorder: evaluating its neural and cognitive basis. *Journal of affective disorders* 167: 336-42

Mohns EJ, Blumberg MS. **2008.** Synchronous Bursts of Neuronal Activity in the Developing Hippocampus: Modulation by Active Sleep and Association with Emerging Gamma and Theta Rhythms.

Journal of Neuroscience 28: 10134-44

Molteni R, Chourbaji S, Brandwein C, Racagni G, Gass P, Riva M. **2008.** Depression-prone mice with reduced glucocorticoid receptor expression display an altered stress-dependent regulation of brain-derived neurotrophic factor and activity-regulated cytoskeleton-associated protein. *Journal of Psychopharmacology* 24: 595-603

Monteggia LM, Barrot M, Powell CM, Berton O, Galanis V, *et al*. **2004.** Essential role of brain-derived neurotrophic factor in adult hippocampal function. *Proceedings of the National Academy of Sciences of the United States of America* 101: 10827-32

Morgan MA, LeDoux JE. **1995.** Differential contribution of dorsal and ventral medial prefrontal cortex to the acquisition and extinction of conditioned fear in rats. Behavioral neuroscience 109: 681-8

Moriceau S, Roth TL, Okotoghaide T, Sullivan RM. **2004.** Corticosterone controls the developmental emergence of fear and amygdala function to predator odors in infant rat pups. *International journal of developmental neuroscience : the official journal of the International Society for Developmental Neuroscience* 22: 415-22

Moriceau S, Sullivan RM. **2006.** Maternal presence serves as a switch between learning fear and attraction in infancy. *Nature neuroscience* 9: 1004-6

Morris R. **1984.** Developments of a water-maze procedure for studying spatial learning in the rat. *Journal of neuroscience methods* 11: 47-60

Morris RG, Garrud P, Rawlins JN, O'Keefe J. **1982.** Place navigation impaired in rats with hippocampal lesions. *Nature* 297: 681-3

Moscarello JM, LeDoux J. **2014.** Diverse Effects of Conditioned Threat Stimuli on Behavior. *Cold Spring Harbor symposia on quantitative biology* 79: 11-9

Moy SS, Nadler JJ, Perez A, Barbaro RP, Johns JM, *et al*. 2004a. Sociability and preference for social novelty in five inbred strains. *Genes Brain and Behavior* 3: 287-302

Moy SS, Nadler JJ, Perez A, Barbaro RP, Johns JM, *et al*. 2004b. Sociability and preference for social novelty in five inbred strains: an approach to assess autistic-like behavior in mice. *Genes, brain, and behavior* 3: 287-302

Mulkey RM, Malenka RC. **1992.** Mechanisms underlying induction of homosynaptic long-term depression in area CA1 of the hippocampus. *Neuron* 9: 967-75

Murrough JW, Yaqubi S, Sayed S, Charney DS. **2015.** Emerging drugs for the treatment of anxiety. *Expert opinion on emerging drugs* 20: 393-406

Nabavi S, Fox R, Proulx CD, Lin JY, Tsien RY, Malinow R. **2014.** Engineering a memory with LTD and LTP. *Nature* 511: 348-52

Nabel EM, Morishita H. **2013.** Regulating critical period plasticity: insight from the visual system to fear circuitry for therapeutic interventions. *Frontiers in psychiatry* 4: 146

Nakashiba T, Buhl DL, McHugh TJ, Tonegawa S. **2009.** Hippocampal CA3 output is crucial for ripple-associated reactivation and consolidation of memory. *Neuron* 62: 781-7

Nakashiba T, Young JZ, McHugh TJ, Buhl DL, Tonegawa S. **2008.** Transgenic inhibition of synaptic transmission reveals role of CA3 output in hippocampal learning. *Science* 319: 1260-4

Nakayama D, Hashikawa-Yamasaki Y, Ikegaya Y, Matsuki N, Nomura H. **2016.** Late Arc/Arg3.1 expression in the basolateral amygdala is essential for persistence of newly-acquired and reactivated contextual fear memories. *Scientific reports* 6: 21007

Nakayama D, Iwata H, Teshirogi C, Ikegaya Y, Matsuki N, Nomura H. **2015.** Long-delayed expression of the immediate early gene Arc/Arg3.1 refines neuronal circuits to perpetuate fear memory. *The Journal of neuroscience : the official journal of the Society for Neuroscience* 35: 819-30

Nassi JJ, Cepko CL, Born RT, Beier KT. **2015.** Neuroanatomy goes viral! *Frontiers in neuroanatomy* 9: 80

Niere F, Wilkerson JR, Huber KM. **2012.** Evidence for a fragile X mental retardation protein-mediated translational switch in metabotropic glutamate receptor-triggered Arc translation and long-term depression. *The Journal of neuroscience : the official journal of the Society for Neuroscience* 32: 5924-36

Okuno H, Akashi K, Ishii Y, Yagishita-Kyo N, Suzuki K, *et al*. **2012.** Inverse Synaptic Tagging of Inactive Synapses via Dynamic Interaction of Arc/Arg3.1 with CaMKIIβ. *Cell* 149: 886-98

Olmsted JB, Carlson K, Klebe R, Ruddle F, Rosenbaum J. **1970.** Isolation of microtubule protein from cultured mouse neuroblastoma cells. *Proceedings of the National Academy of Sciences of the*

United States of America 65: 129-36

Onoue K, Nakayama D, Ikegaya Y, Matsuki N, Nomura H. **2014.** Fear extinction requires Arc/Arg3.1 expression in the basolateral amygdala. *Molecular brain* 7: 30

Orsini CA, Maren S. **2012.** Neural and cellular mechanisms of fear and extinction memory formation. *Neuroscience and biobehavioral reviews* 36: 1773-802

Oudman E, Nijboer TC, Postma A, Wijnia JW, Van der Stigchel S. **2015.** Procedural Learning and Memory Rehabilitation in Korsakoff's Syndrome - a Review of the Literature. *Neuropsychology review* 25: 134-48

ozeske RR, Valerio S, Chaudun F, Herry C. **2015.** Prefrontal neuronal circuits of contextual fear conditioning. *Genes, brain, and behavior* 14: 22-36

Padilla-Coreano N, Bolkan SS, Pierce GM, Blackman DR, Hardin WD, *et al*. **2016.** Direct Ventral Hippocampal-Prefrontal Input Is Required for Anxiety-Related Neural Activity and Behavior. *Neuron* 89: 857-66

Panksepp J. **2005.** Affective consciousness: Core emotional feelings in animals and humans. *Consciousness and cognition* 14: 30-80

Pape HC, Pare D. **2010.** Plastic synaptic networks of the amygdala for the acquisition, expression, and extinction of conditioned fear. *Physiological reviews* 90: 419-63

Park S, Park JM, Kim S, Kim JA, Shepherd JD, *et al*. **2008.** Elongation factor 2 and fragile X mental retardation protein control the dynamic translation of Arc/Arg3.1 essential for mGluR-LTD. *Neuron* 59: 70-83

Peebles CL, Yoo J, Thwin MT, Palop JJ, Noebels JL, Finkbeiner S. **2010.** Arc regulates spine morphology and maintains network stability *in vivo*. *Proceedings of the National Academy of Sciences of the United States of America* 107: 18173-8

Pei Q, Sprakes M, Millan MJ, Rochat C, Sharp T. 2004a. The novel monoamine reuptake inhibitor and potential antidepressant, S33005, induces Arc gene expression in cerebral cortex. *European journal of pharmacology* 489: 179-85

Pei Q, Tordera R, Sprakes M, Sharp T. 2004b. Glutamate receptor activation is involved in 5-HT2 agonist-induced Arc gene expression in the rat cortex. *Neuropharmacology* 46: 331-9

Pellow S, Chopin P, File SE, Briley M. **1985.** Validation of open:closed arm entries in an elevated plus-maze as a measure of anxiety in the rat. *Journal of neuroscience methods* 14: 149-67

Pettersen KH, Devor A, Ulbert I, Dale AM, Einevoll GT. **2006.** Current-source density estimation based on inversion of electrostatic forward solution: effects of finite extent of neuronal activity and conductivity discontinuities. *Journal of neuroscience methods* 154: 116-33

Pintchovski SA, Peebles CL, Kim HJ, Verdin E, Finkbeiner S. **2009.** The serum response factor and a putative novel transcription factor regulate expression of the immediate-early gene Arc/Arg3.1 in neurons. *The Journal of neuroscience : the official journal of the Society for Neuroscience* 29: 1525-37

Plath N. **2004.** Funktionelle Charackterisierung des aktivitätsregulierten Gens Arg3.1. Doctoral thesis thesis. *Free University of Berlin*, Belin. 154 pp.

Plath N, Ohana O, Dammermann B, Errington ML, Schmitz D, *et al*. **2006.** Arc/Arg3.1 is essential for the consolidation of synaptic plasticity and memories. *Neuron* 52: 437-44

Ploski JE, Pierre VJ, Smucny J, Park K, Monsey MS, *et al*. **2008.** The activity-regulated cytoskeletal-associated protein (Arc/Arg3.1) is required for memory consolidation of pavlovian fear conditioning in the lateral amygdala. *The Journal of neuroscience : the official journal of the Society for Neuroscience* 28: 12383-95

Popa D, Duvarci S, Popescu AT, Lena C, Pare D. **2010.** Coherent amygdalocortical theta promotes fear memory consolidation during paradoxical sleep. *Proceedings of the National Academy of Sciences of the United States of America* 107: 6516-9

Pratt HD, Tsitsika AK. **2007.** Fetal, childhood, and adolescence interventions leading to adult disease prevention. *Primary care* 34: 203-17

Purcell SM, Moran JL, Fromer M, Ruderfer D, Solovieff N, *et al*. **2014.** A polygenic burden of rare disruptive mutations in schizophrenia. *Nature* 506: 185-90

Raineki C, Shionoya K, Sander K, Sullivan RM. **2009.** Ontogeny of odor-LiCl vs. odor-shock learning: similar behaviors but divergent ages of functional amygdala emergence. *Learning & memory* 16: 114-21

Rasch B, Born J. **2013.** About sleep's role in memory. *Physiological reviews* 93: 681-766

Ren M, Cao V, Ye Y, Manji HK, Wang KH. **2014.** Arc regulates experience-dependent persistent firing patterns in frontal cortex. *The Journal of neuroscience : the official journal of the Society for Neuroscience* 34: 6583-95

Rescorla RA, Wagner AR. **1972.** "A theory of Pavlovian conditioning: Variations in the effectiveness of reinforcement and nonreinforcement" in *Classical Conditioning II: Current Research and Theory*. pp. 64–99. New York, NY: Appleton-Century-Crofts.

Ribeiro S. **2012.** Sleep and plasticity. Pflugers Archiv : *European journal of physiology* 463: 111-20

Rodenas-Ruano A, Chavez AE, Cossio MJ, Castillo PE, Zukin RS. **2012.** REST-dependent epigenetic remodeling promotes the developmental switch in synaptic NMDA receptors. *Nature neuroscience* 15: 1382-90

Rodriguez Parkitna J, Engblom D. **2012.** Addictive drugs and plasticity of glutamatergic synapses on dopaminergic neurons: what have we learned from genetic mouse models? *Frontiers in molecular neuroscience* 5:89

Rolls ET. **2000.** Precis of The brain and emotion. *The Behavioral and brain sciences* 23: 177-91; discussion 92-233

Rosenblum K, Meiri N, Dudai Y. **1993.** Taste memory: the role of protein synthesis in gustatory cortex. *Behavioral and neural biology* 59: 49-56

Saldarriaga W, Tassone F, Gonzalez-Teshima LY, Forero-Forero JV, Ayala-Zapata S, Hagerman R. **2014.** Fragile X syndrome. *Colombia médica* 45: 190-8

Sanders JD, Happe HK, Bylund DB, Murrin LC. **2008.** Differential effects of neonatal norepinephrine lesions on immediate early gene expression in developing and adult rat brain. *Neuroscience* 157: 821-32

Sanger F. **1981.** Determination of nucleotide sequences in DNA. *Science* 214: 1205-10

Schenk F. **1985.** Development of place navigation in rats from weaning to puberty. *Behavioral and neural biology* 43: 69-85

Schoch. **1996.** Neuron-specific Gene Expression of Synapsin I. *The Journal of biological chemistry* 271: 3317-23

Schubert D, Martens GJ, Kolk SM. **2015.** Molecular underpinnings of prefrontal cortex development in rodents provide insights into the etiology of neurodevelopmental disorders. *Molecular psychiatry* 20: 795-809

Schuster S. **2009.** Arc/Arg3.1, kortikale Plastizität und sensorisches Lernen. Diplomarbeit thesis. *Frei Universität Berlin*, Berlin. 91 pp.

Scott KM. **2014.** Depression, anxiety and incident cardiometabolic diseases. *Current opinion in psychiatry* 27: 289-93

Scoville WB, Milner B. **1957.** Loss of recent memory after bilateral hippocampal lesions. *Journal of neurology, neurosurgery, and psychiatry* 20: 11-21

Seamans JK, Lapish CC, Durstewitz D. **2008.** Comparing the Prefrontal Cortex of Rats and Primates. *Neurotoxicity research* 14: 249-62

Seidenbecher T, Laxmi TR, Stork O, Pape HC. **2003.** Amygdalar and hippocampal theta rhythm synchronization during fear memory retrieval. *Science* 301: 846-50

Selemon LD, Zecevic N. **2015.** Schizophrenia: a tale of two critical periods for prefrontal cortical development. *Translational psychiatry* 5: e623

Shepherd JD, Bear MF. **2011.** New views of Arc, a master regulator of synaptic plasticity. *Nature neuroscience* 14: 279-84

Shepherd JD, Rumbaugh G, Wu J, Chowdhury S, Plath N, *et al*. **2006.** Arc/Arg3.1 mediates homeostatic synaptic scaling of AMPA receptors. *Neuron* 52: 475-84

Shiba Y, Santangelo AM, Roberts AC. **2016.** Beyond the Medial Regions of Prefrontal Cortex in the Regulation of Fear and Anxiety. *Frontiers in systems neuroscience* 10: 12

Shimshek DR, Kim J, Hubner MR, Spergel DJ, Buchholz F, *et al*. **2002.** Codon-improved Cre recombinase (iCre) expression in the mouse. *Genesis* 32: 19-26

Sierra-Mercado D, Padilla-Coreano N, Quirk GJ. **2011.** Dissociable roles of prelimbic and infralimbic cortices, ventral hippocampus, and basolateral amygdala in the expression and extinction of conditioned fear. *Neuropsychopharmacology : official publication of the American College of Neuropsychopharmacology* 36: 529-38

Smith-Hicks C, Xiao B, Deng R, Ji Y, Zhao X, *et al*. **2010.** SRF binding to SRE 6.9 in the Arc promoter is essential for LTD in cultured Purkinje cells. *Nature neuroscience* 13: 1082-9

Smith SM. **2002.** Fast robust automated brain extraction. *Human brain mapping* 17: 143-55

Soriano P. **1999.** Generalized lacZ expression with the ROSA26 Cre reporter strain. *Nature genetics* 21: 70-1

Sotres-Bayon F, Quirk GJ. **2010.** Prefrontal control of fear: more than just extinction. *Current opinion in neurobiology* 20: 231-5

Sotres-Bayon F, Sierra-Mercado D, Pardilla-Delgado E, Quirk GJ. **2012.** Gating of fear in prelimbic cortex by hippocampal and amygdala inputs. *Neuron* 76: 804-12

Squire LR, Dede AJ. **2015.** Conscious and unconscious memory systems. *Cold Spring Harbor perspectives in biology* 7: a021667

Stanton PK, Sarvey JM. **1984.** Blockade of long-term potentiation in rat hippocampal CA1 region by inhibitors of protein synthesis. *The Journal of neuroscience : the official journal of the Society for Neuroscience* 4: 3080-8

Stent GS. **1973.** A Physiological Mechanism for Hebb's Postulate of Learning. *Proceedings of the National Academy of Sciences of the United States of America* 70: 997-1001

Stevens FL, Hurley RA, Taber KH. **2011.** Anterior Cingulate Cortex Unique Role in Cognition and Emotion. *The Journal of neuropsychiatry and clinical neurosciences* 23: 121-5

Steward O, Falk PM. **1991.** Selective localization of polyribosomes beneath developing synapses a quantitative analysis of the relationships between polyribosomes and developing synapses in the hippocampus and dentate gyrus. *Journal of Comparative Neurology* 314: 545-57

Steward O, Worley PF. **2001.** Selective targeting of newly synthesized Arc mRNA to active synapses requires NMDA receptor activation. *Neuron* 30: 227-40

Swanson LW, Petrovich GD. **1998.** What is the amygdala? *Trends Neurosci* 21: 323-31

Sweatt JD. **2016.** Neural Plasticity & Behavior - Sixty Years of Conceptual Advances. *J Neurochem*

Tagawa Y, Kanold PO, Majdan M, Shatz CJ. **2005.** Multiple periods of functional ocular dominance plasticity in mouse visual cortex. *Nature neuroscience* 8: 380-8

Takesian AE, Hensch TK. **2013.** Balancing plasticity/stability across brain development. *Progress in brain research* 207: 3-34

Tambini A, Ketz N, Davachi L. **2010.** Enhanced brain correlations during rest are related to memory for recent experiences. *Neuron* 65: 280-90

Tanaka KZ, Pevzner A, Hamidi AB, Nakazawa Y, Graham J, Wiltgen BJ. **2014.** Cortical representations are reinstated by the hippocampus during memory retrieval. *Neuron* 84: 347-54

Tang J, Ko S, Ding HK, Qiu CS, Calejesan AA, Zhuo M. **2005.** Pavlovian fear memory induced by activation in the anterior cingulate cortex. *Molecular pain* 1: 6

Tang W, Ehrlich I, Wolff SB, Michalski AM, Wolfl S, *et al*. **2009.** Faithful expression of multiple proteins via 2A-peptide self-processing: a versatile and reliable method for manipulating brain circuits. *The Journal of neuroscience : the official journal of the Society for Neuroscience* 29: 8621-9

Teixeira CM, Pomedli SR, Maei HR, Kee N, Frankland PW. **2006.** Involvement of the anterior cingulate cortex in the expression of remote spatial memory. *The Journal of neuroscience : the official journal of the Society for Neuroscience* 26: 7555-64

Tepper JM, Sharpe NA, Koos TZ, Trent F. **1998.** Postnatal Development of the Rat Neostriatum: Electrophysiological, Light- and Electron-Microscopic Studies. *Developmental neuroscience* 20: 125-45

Thompson JV, Sullivan RM, Wilson DA. **2008.** Developmental emergence of fear learning corresponds with changes in amygdala synaptic plasticity. *Brain research* 1200: 58-65

Thorne RG, Nicholson C. **2006.** In vivo diffusion analysis with quantum dots and dextrans predicts the width of brain extracellular space. *Proceedings of the National Academy of Sciences of the United States of America* 103: 5567-72

Thyagarajan B, Guimaraes MJ, Groth AC, Calos MP. **2000.** Mammalian genomes contain active recombinase recognition sites. *Gene* 244: 47-54

Tian D, Stoppel LJ, Heynen AJ, Lindemann L, Jaeschke G, *et al*. **2015.** Contribution of mGluR5 to pathophysiology in a mouse model of human chromosome 16p11.2 microdeletion. *Nature neuroscience* 18: 182-4

Tomaiuolo M, Katche C, Viola H, Medina JH. **2015.** Evidence of Maintenance Tagging in the Hippocampus for the Persistence of Long-Lasting Memory Storage. *Neural plasticity* 2015: 603672

Tovote P, Fadok JP, Luthi A. **2015.** Neuronal circuits for fear and anxiety. *Nature reviews. Neuroscience* 16: 317-31

Treit D, Menard J. **1997.** Dissociations among the anxiolytic effects of septal, hippocampal, and amygdaloid lesions. *Behavioral neuroscience* 111: 653-8

Turrigiano G. **2012.** Homeostatic synaptic plasticity: local and global mechanisms for stabilizing neuronal function. *Cold Spring Harbor perspectives in biology* 4: a005736

Tye KM, Prakash R, Kim SY, Fenno LE, Grosenick L, *et al*. **2011.** Amygdala circuitry mediating reversible and bidirectional control of anxiety. *Nature* 471: 358-62

Uematsu A, Kitamura A, Iwatsuki K, Uneyama H, Tsurugizawa T. **2015.** Correlation Between Activation of the Prelimbic Cortex, Basolateral Amygdala, and Agranular Insular Cortex During Taste Memory Formation. *Cerebral cortex* 25: 2719-28

van Eden CG, Kros JM, Uylings HBM. **1991.** Chapter 8 The development of the rat prefrontal cortex : Its size and development of connections with thalamus, spinal cord and other cortical areas. 85: 169-83

Van Eden CG, Uylings HB. **1985.** Cytoarchitectonic development of the prefrontal cortex in the rat. The *Journal of comparative neurology* 241: 253-67

Vazdarjanova A, Ramirez-Amaya V, Insel N, Plummer TK, Rosi S, *et al*. **2006.** Spatial exploration induces ARC, a plasticity-related immediate-early gene, only in calcium/calmodulin-dependent protein kinase II-positive principal excitatory and inhibitory neurons of the rat forebrain. *The Journal of comparative neurology* 498: 317-29

Vertes RP. **2006.** Interactions among the medial prefrontal cortex, hippocampus and midline thalamus in emotional and cognitive processing in the rat. *Neuroscience* 142: 1-20

Vogt MA, Chourbaji S, Brandwein C, Dormann C, Sprengel R, Gass P. **2008.** Suitability of tamoxifen-induced mutagenesis for behavioral phenotyping. *Experimental neurology* 211: 25-33

Vorhees CV, Williams MT. **2006.** Morris water maze: procedures for assessing spatial and related forms of learning and memory. *Nature protocols* 1: 848-58

Vousden DA, Epp J, Okuno H, Nieman BJ, van Eede M, *et al*. **2015.** Whole-brain mapping of behaviourally induced neural activation in mice. *Brain structure & function* 220: 2043-57

Waghorn G, Chant D, White P, Whiteford H. **2005.** Disability, employment and work performance among people with ICD-10 anxiety disorders. *Aust Nz J Psychiat* 39: 55-66

Walf AA, Frye CA. **2007.** The use of the elevated plus maze as an assay of anxiety-related behavior in rodents. *Nature protocols* 2: 322-8

Waltereit R, Dammermann B, Wulff P, Scafidi J, Staubli U, *et al*. **2001.** Arg3.1/Arc mRNA induction by Ca2+ and cAMP requires protein kinase A and mitogen-activated protein kinase/extracellular regulated kinase activation. *The Journal of neuroscience : the official journal of the Society for Neuroscience* 21: 5484-93

Wang H, Ardiles AO, Yang S, Tran T, Posada-Duque R, *et al*. **2016.** Metabotropic Glutamate Receptors Induce a Form of LTP Controlled by Translation and Arc Signaling in the Hippocampus. T*he Journal of neuroscience : the official journal of the Society for Neuroscience* 36: 1723-9

Wang JH, Stelzer A. **1996.** Shared calcium signaling pathways in the induction of long-term potentiation and synaptic disinhibition in CA1 pyramidal cell dendrites. *Journal of neurophysiology* 75: 1687-702

Wang KH, Majewska A, Schummers J, Farley B, Hu C, *et al*. **2006.** *In vivo* two-photon imaging reveals a role of arc in enhancing orientation specificity in visual cortex. *Cell* 126: 389-402

Waung MW, Pfeiffer BE, Nosyreva ED, Ronesi JA, Huber KM. **2008.** Rapid translation of Arc/Arg3.1 selectively mediates mGluR-dependent LTD through persistent increases in AMPAR endocytosis rate. *Neuron* 59: 84-97

Weber M, Richardson R. **2001.** Centrally administered corticotropin-releasing hormone and peripheral injections of strychnine hydrochloride potentiate the acoustic startle response in preweanling rats. *Behavioral neuroscience* 115: 1273-82

Welzl H, D'Adamo P, Lipp HP. **2001.** Conditioned taste aversion as a learning and memory paradigm. *Behavioural brain research* 125: 205-13

Whitesell L, Geselowitz D, Chavany C, Fahmy B, Walbridge S, *et al*. **1993.** Stability, clearance, and disposition of intraventricularly administered oligodeoxynucleotides: implications for therapeutic application within the central nervous system. *Proceedings of the National Academy of Sciences*

of the United States of America 90: 4665-9

Wiesel T. **1982.** Postnatal development of the visual cortex and the influence of environment. *Nature* 299

Williams LM, Gordon E. **2007.** Dynamic Organization of the Emotional Brain: Responsivity, Stability, and Instability. *Neuroscientist* 13: 349-70

Wiltgen BJ, Zhou M, Cai Y, Balaji J, Karlsson MG, *et al*. **2010.** The hippocampus plays a selective role in the retrieval of detailed contextual memories. *Current biology* : CB 20: 1336-44

Winslow JT, Insel TR. **2004.** Neuroendocrine basis of social recognition. *Current opinion in neurobiology* 14: 248-53

Witter MP. **2007.** Intrinsic and extrinsic wiring of CA3: indications for connectional heterogeneity. *Learning & memory* 14: 705-13

Wu J, Petralia RS, Kurushima H, Patel H, Jung MY, *et al*. **2011.** Arc/Arg3.1 regulates an endosomal pathway essential for activity-dependent beta-amyloid generation. *Cell* 147: 615-28

Xie Q, Bu W, Bhatia S, Hare J, Somasundaram T, *et al*. **2002.** The atomic structure of adeno-associated virus (AAV-2), a vector for human gene therapy. *Proceedings of the National Academy of Sciences of the United States of America* 99: 10405-10

Yamada K, Homma C, Tanemura K, Ikeda T, Itohara S, Nagaoka Y. **2011.** Analyses of fear memory in Arc/Arg3.1-deficient mice: intact short-term memory and impaired long-term and remote memory. *World Journal of Neuroscience* 01: 1-8

Yamaguchi T, Danjo T, Pastan I, Hikida T, Nakanishi S. **2013.** Distinct roles of segregated transmission of the septo-habenular pathway in anxiety and fear. *Neuron* 78: 537-44

Yamamoto T. **2007.** Brain regions responsible for the expression of conditioned taste aversion in rats. *Chemical senses* 32: 105-9

Yang DD, Kuan CY, Whitmarsh AJ, Rincon M, Zheng TS, *et al*. **1997.** Absence of excitotoxicity-induced apoptosis in the hippocampus of mice lacking the Jnk3 gene. *Nature* 389: 865-70

Yap K, Makeyev EV. **2013.** Regulation of gene expression in mammalian nervous system through alternative pre-mRNA splicing coupled with RNA quality control mechanisms. *Molecular and cellular neurosciences* 56: 420-8

Yashiro K, Riday TT, Condon KH, Roberts AC, Bernardo DR, *et al*. **2009.** Ube3a is required for experience-dependent maturation of the neocortex. *Nature neuroscience* 12: 777-83

Yasuda H, Barth AL, Stellwagen D, Malenka RC. **2003.** A developmental switch in the signaling cascades for LTP induction. *Nature neuroscience* 6: 15-6

Yizhar O, Fenno LE, Prigge M, Schneider F, Davidson TJ, *et al*. **2011.** Neocortical excitation/inhibition balance in information processing and social dysfunction. *Nature* 477: 171-8

Zalfa F, Giorgi M, Primerano B, Moro A, Di Penta A, *et al*. **2003.** The Fragile X Syndrome Protein FMRP Associates with BC1 RNA and Regulates the Translation of Specific mRNAs at Synapses. *Cell* 112: 317-27

Zhang W, Wu J, Ward MD, Yang S, Chuang YA, *et al*. **2015.** Structural basis of arc binding to synaptic proteins: implications for cognitive disease. *Neuron* 86: 490-500

Zhuo M. **2016.** Neural Mechanisms Underlying Anxiety-Chronic Pain Interactions. *Trends Neurosci* 39: 136-45

Zolotukhin. **1999.** Recombinant adeno-associated virus purification using novel methods improves infectious titer and yield. *Gene therapy* 6: 973-85

10. Statement of contribution

The conception and funding of these projects were provided by Dr. Ora Ohana and Prof. Dietmar Kuhl (Institute for Molecular and Cellular Cognition, UKE). Dr. Ora Ohana performed initial experiments, oversaw and directed all experiments. Dr. Mario Sergio Castro Gómez and Xiaoyan Gao designed experimental procedures, performed and analyzed all behavioral, biochemical and histology experiments. Sabine Graf conducted immunohistochemistry, rISH experiments and genotyping of the lines. Jasper Grendel performed and analyzed all LFP recordings with the assistance and supervision of Prof. Dirk Isbrandt (Group for Experimental Neurophysiology, German Center for Neurodegenerative Diseases -DZNE- Universitätsklinikum Köln). MRI was performed by Dr. Mario Sergio Castro Gómez, Xiaoyan Gao and Dr. Ora Ohana with the assistance and supervision of Dr. Jan Sedlacik at the department of Neuroradiological Diagnostics and Intervention – UKE. MRI data was analyzed by Jasper Grendel with the assistance of Prof. Christian Büchel (Institute of Systems Neuroscience - UKE). Dr. Lars Binkle designed rISH plasmid. Dr. Daniel Menshing assisted the cloning of rAAV-Syn1-Cre2AP-Venus and rAAV-CaMKIIα-CreER^{T2}2AP-venus viral vectors. Steffen Schuster cloned the prAAV-CaMKIIα-Cre under the supervision of Dr. Claudia Mahlke. The mouse lines were previously generated by Dr. Björn Dammermann (Dammermann, 1999), Dr. Anika Bick-Sander (Bick-Sander, 2002) and Eric Therstappen under the supervision of Prof. Dr. Dietmar Kuhl and Dr. Michael Bösl in the ZMNH-facility for transgenic animals. Technical assistance with animal breeding and caring was provided by Eva Kronenberg.

The study was supported by a DFG grant SFB 936 to project B4 in the years 2011-2014 and by the grant "Molekulare Mechanismen der Netzlrkmodifizierung" from the Federal State of Hamburg.

Some results from this thesis were used in the paper:
"Arc/Arg3.1 Regulates a Critical Period for Learning and Memory Networks"
Authors: Xiaoyan Gao[#], **Sergio Castro-Gomez**[#], Jasper Grendel[#], Sabine Graf, Lars Binkle, Daniel Mensching, Dirk Isbrandt, Dietmar Kuhl, Ora Ohana.
[#]Contributed to an equal extent. Currently under submission.

11. Acknowledgments

I would like to express my sincere gratitude to the entire Institute of Molecular and Cellular Cognition and the Center of Molecular Neurobiology of Hamburg, especially to Prof. Dietmar Kuhl and Dr. Ora Ohana for offering me the opportunity to join the Institute and conduct these projects with them, for their excellent supervision, guidance and all the discussions during the course of this research. I am also immensely grateful to have worked together with Xiaoyan Gao and Sabine Graf, who had a strong commitment with this work, patience, collegiality and true friendship during these years. I am very grateful with Mary Muhia for discussions and advice on behavioral experiments

I would also like to thank Prof. Markus Glatzel and Prof. Stefan Kindler for agreeing to be my committee and reviewers of this thesis, for the helpful advice and time during the MD/PhD program, to Dr. Günther Schutz for providing CamKIIα-Cre mice; Dr. Rolf Sprengel and Dr. Wannan Tang for sharing a Syn-iCre2AP-Venus plasmid; Dr. Ingke Braren at the Hamburg Center for Experimental Therapy Research (HEXT) vector facility of the UKE for overtaking virus production and purification; Dr. Sabine Hoffmeister-Ullerich for sequencing and CNV services; Dr. Irm Hermanns-Borgmeyer for advice on animal breeding and Eva Kronberg for animal care. Further, I feel very thankful for the great collaborators in other institutions: Dr. Dirk Isbrandt and his group for Experimental Neurophysiology at the German Center for Neurodegenerative Diseases -DZNE- Universitätsklinikum Köln; Dr. Jan Sedlacik at the department of Neuroradiological Diagnostics and Intervention – UKE, and Prof. Christian Büchel and his Institute of Systems Neuroscience – UKE. I learnt immensely from all of you!

I would like to thank very much all the former and current members of the Institute of Molecular and Cellular Cognition who helped with the work in these projects: Xioyan Gao, Sabine Graf, Jasper Grendel, Dörthe Carstesen, Andrea Zaisser, Ute Süsens, Nina Feller, Dr. Lars Binkle, Dr. Daniel Mensching, Dr. Xiaosong Mao and Dr. Claudia Mahlke; and all the other members who share with me the amazing time and fruitful discussions.

Many thanks to the „Nerds-GoT group"; Anne, Brennita, Iris, Lars, Danielo, Paul, Andree and Mauro for their friendship, support, happy meals, parties and GoT nights, and to the other PhDs and postdocs of the ZMNH that made this experience more enjoyable; Kay, Anna, Andrea, Rita, Aida, Nagammal, Abuzar, Franco, André, Jasper, Francesca, Daniel, Stephan, Mary, Shu-Ting, Urban, Jerome, Sandra, Tiemo, Karin, Lili, Jakob, Sina, and our excellent master students Chrisi and Helia. Thanks for supporting the "DoSe" and all the funny discussions about science and life.

This experience would have been much harder without the support of my friends Jorge, Caro, Ana, Álvaro, el profe Marco, Saris, Julia, Emi, Joaco, Dani, Manuel, Fede, Tamy, Markus, Paul, Zay, Sanna; and without the unconditional care and affection of my entire family, to whom I dedicate this thesis: to Marti, Herma, Luzma and Papá.

12. Eidesstattliche Versicherung

Ich versichere ausdrücklich, dass ich die Arbeit selbständig und ohne fremde Hilfe verfasst, andere als die von mir angegebenen Quellen und Hilfsmittel nicht benutzt und die aus den benutzten Irken wörtlich oder inhaltlich entnommenen Stellen einzeln nach Ausgabe (Auflage und Jahr des Erscheinens), Band und Seite des benutzten Irkes kenntlich gemacht habe.
Ferner versichere ich, dass ich die Dissertation bisher nicht einem Fachvertreter an einer anderen Hochschule zur Überprüfung vorgelegt oder mich anderlitig um Zulassung zur Promotion beworben habe.
Ich erkläre mich einverstanden, dass meine Dissertation vom Dekanat der Medizinischen Fakultät mit einer gängigen Software zur Erkennung von Plagiaten überprüft Irden kann.

Unterschrift: